NASA CR 135403

NATIONAL AERONAUTICS AND
SPACE ADMINISTRATION

EVALUATION OF FLAWED COMPOSITE STRUCTURAL COMPONENTS UNDER STATIC AND CYCLIC LOADING

BY

T. R. PORTER

Boeing Aerospace Company
A Division of The Boeing Company
Seattle, Washington

Prepared for

NATIONAL AERONAUTICS AND SPACE ADMINISTRATION

NASA Lewis Research Center
Contract NAS3-19709
Gordon T. Smith, Project Engineer

1. Report No. NASA CR-135403	2. Government Accession No.	3. Recipient's Catalog No.
4. Title and Subtitle Evaluation of Flawed Composite Structural Components Under Static and Cyclic Loading		5. Report Date February 1979
		6. Performing Organization Code
7. Author(s) T. R. Porter		8. Performing Organization Report No.
		10. Work Unit No.
9. Performing Organization Name and Address Boeing Aerospace Company P.O. Box 3999 Seattle, Washington 98124		11. Contract or Grant No. NAS 3-19709
		13. Type of Report and Period Covered
12. Sponsoring Agency Name and Address National Aeronautics and Space Administration Lewis Research Center 21000 Brookpark Road Cleveland, Ohio 44135		14. Sponsoring Agency Code
15. Supplementary Notes Project Manager, Gordon T. Smith Materials and Structures Division NASA Lewis Research Center Cleveland, Ohio 44135		

16. Abstract

This report presents the results of a program investigating the effects of initial defects on the fatigue and fracture response of composite laminates. The structural lamiantes investigated were a typical angle ply laminate, a polar/hoop wound pressure vessel laminate, and a typical engine fan blade laminate. Defects investigated were full and half penetration circular holes, full and half penetration slits, and countersink holes. Results are presented showing the effects of the defect size and type on the static fracture strength, fatigue performance, and residual static strength. The results of inspection procedures are shown, describing the effect of cyclic and static loadings on damage propagation in composite laminates. The data in this study were used to define proof test levels as a qualification procedure in composite structure subjected to cyclic loading.

17. Key Words (Suggested by Author(s))		18. Distribution Statement	
Composite Materials Graphite/Epoxy Fracture Fatigue Proof Test Flaw		Unclassified - Unlimited	
19. Security Classif. (of this report) Unclassified	20. Security Classif. (of this page) Unclassified	21. No. of Pages 265	22. Price*

* For sale by the National Technical Information Service, Springfield, Virginia 22161

NASA-C-168 (Rev. 10-75)

N80-71692

Page intentionally left blank

FOREWORD

This report summarizes the work accomplished on NASA Contract NAS3-19709, "Evaluation of Flawed Composite Structural Components Under Static and Cyclic Loading."

The program was sponsored by the National Aeronautics and Space Administration, Lewis Research Center, Cleveland, Ohio. Mr. G. T. Smith, NASA Lewis Research Center, was Project Manager.

Performance of this contract was under the direction of the Boeing Military Airplane Development (BMAD) organization of Boeing Aerospace Company. Dr. R. R. June, reporting to Mr. D. E. Strand who heads the Structures/Materials Technology organization, was the Program Leader. Mr. T. R. Porter was the Technical Leader, C. R. Speelmon coordinated specimen fabrication, C. C. Kissler provided testing support and L. R. Hause was responsible for ultrasonic inspection support.

Page intentionally left blank

TABLE OF CONTENTS

Page intentionally left blank

LIST OF FIGURES

Figure	Title	Page

Figure	Title	Page

LIST OF TABLES

INTRODUCTION

The objective of this program was to derive data for evaluating the integrity of fiber composite components. In particular, the static and cyclic performance of three potential composite laminate designs containing inadvertent flaws and natural defects was investigated. The results address the following topics:

1) Effect of defect type and size on static fracture.

2) Effect of defect type and size on fatigue.

3) Descriptions of the effects of static and cyclic loadings on damage accumulation in material surrounding the various stress concentrations.

4) The effect of preloads on damage growth, static strength, and cyclic load behavior.

5) The viability of proof loading as a qualification method for advanced composite structure, and the development of approaches to application of proof testing.

Data were obtained on the effects of six different types of stress concentrations or flaws (full and half penetration circular holes, full and half penetration sharp slits, excessive voids,and delaminations) on the static strength and fatigue lives of three different graphite/epoxy composite materials. The test panels were fabricated from T-300/934 0.3 m (12 in) wide prepreg tape. Three different 20-ply laminates were tested. These included a typical angle ply laminate $((0/\pm45/0/90)_S)_2$, a laminate that is representative of polar/hoop wound pressure vessels $((0_3/\pm80)_2)_S$, and a laminate that is representative of fan blades for turbine propulsion systems $((0/+30/0*/-30/0)_2)_S$ The fan blade laminate contains four plies of S-glass (denoted by *) to improve the fracture performance. Both static and cyclic

tests were conducted on specimens containing one of three different sizes of each type of defect. Comparison specimens were preloaded to 90% of their ultimate load capacity, prior to static and cyclic testing, to assess the potential effects of proof loading. Intermittent nondestructive inspection was used to detect changes in defect geometry, and other structural changes occurring in the region immediately surrounding the defects. The test data were evaluated, using current composite fracture and fatigue analysis concepts. The effectiveness of using proof test procedures for quality assurance of composite components was evaluated.

The program was divided into six tasks. Task I defined the materials, layups, fabrication and processing steps, defect fabrication methods, and design and fabrication of test specimens. Tasks II, III, and IV consisted of static, tension/tension, and tension/compression cyclic testing, while Task V included data analysis and Task VI reporting.

The report contains a presentation of the specimen preparation, test procedures, static and cyclic test results, and a potential proof test method. All the test data, ultrasonic inspection data, crack opening displacement data, and photographs of the test specimens are included in the appendices.

SPECIMEN DESIGN AND MANUFACTURE

The test specimen materials, design, and fabrication procedures were selected to permit the generation of data for evaluation of flawed structural components. The components considered were a general purpose laminate structure, a polar/hoop wound pressure vessel, and a turbine engine fan blade.

Materials

The materials used for the program were Thornel T-300 graphite fiber, 901 S-glass fiber, and Fiberite 934 epoxy resin. Intermediate stiffness graphite/epoxy was selected as the basic material for the program, because of its wide usage, moderate cost, and established structural performance. The Thornel T-300 graphite fibers were selected since they can be supplied with a twist making them suitable for general purpose structure as well as filament winding pressure vessels. The fiberite 934 resin system satisfied the requirements of a general purpose epoxy and has a wide range of applications in aerospace structures. In the turbine engine fan blade layup 901 S-glass fiber plies were interspersed with the T-300 fiber plies to improve impact damage resistance of the laminate. This S-glass/graphite hybrid was selected on the basis of prior work (References 1 through 3) demonstrating significantly improved impact damage tolerance.

Layups and Stacking Sequences

Three different layups were used in the fabrication of test specimens, as shown in Figure 1. The first layup (L1) was a 20-ply balanced layup representative of a practical aerospace application. This layup is moderately directional, and would be used to support biaxial loads having about a 2:1 ratio. The second layup (L2) is representative of spacecraft pressure vessels, fabricated using both polar and hoop wraps. The third layup (L3) is representative of turbine fan blades or, possibly, tubular support struts. The S-glass fiber was included as zero degree plies.

The stacking sequence for layup L1 was selected based on symmetry and load transfer requirements. The stacking sequence was $((0/\underline{+}45/0/90)_S)_2$ and has distributed (0) plies throughout the thickness.

The stacking sequence for layup L2 is representative of a typical pressure vessel layup. There are two basic approaches to polar/hoop wrapping of aerospace pressure vessels. If the hoop thickness is thin, all the polar wraps can be applied at once followed by all the hoop wraps. When the hoop thickness is too large to prevent slippage of the hoop wraps at the end of the cylinder, the polar and hoop wraps are interspersed. This would typically be accomplished by applying one revolution (2 plies) of polar wrap followed by three plies of hoop wrap. The resulting stacking sequence is (0/0/0/+80/-80). Hence, stacking sequence for laminate L2 was $((0/0/0/+80/-80)_2)_S$.

The stacking sequence for layup L3 was representative of those used in composite turbine engine blades. Two possible approaches are the dispersed ply approach and the core-shell approach. The dispersed ply approach was used because such layups are less subject to delamination due to foreign object impact. A representative stacking sequence then becomes $((0/+30/0^*/-30/0)_2)_S$. The asterisks indicate the plies that are replaced with S-glass to increase fracture toughness of the laminate. Replacement of the middle ply results in an even distribution of the hybridizing material throughout the panel.

Test Specimen Configuration

The test specimen configuration is shown in Figure 2. The 76 mm (3.0 in) width was chosen to provide specimens large ~~enought~~ enough to preclude significant interaction between the stress concentration and stress-free specimen boundaries. The specimen was designed so that the stress concentration factor for the largest defect would be within five percent of the corresponding stress concentration factor for an infinitely wide plate. The test section was selected as twice the specimen width to ensure representative load distribution around the imposed defect. The zero degree laminate direction

corresponds to the axial direction of the specimen. Woven fiberglass grip tabs were bonded to the specimen.

Test Specimen Fabrication and Processing

Specimen fabrication and processing steps are illustrated in Figure 3. Laminates were laid up and cured in 81 cm (32 in) wide panels having lengths ranging up to 244 cm (100 in). Specimens for laminates L2 and L3 were cut from a single panel. Two panels were requred for L1 specimens. The fiberglass end tabs were bonded to the basic laminates. Finally, the panels were sawcut into specimen blanks. The panel fabrication steps were as follows:

1) Remove material from freezer and allow it to come to room temperature before unwrapping.

2) Unwrap material and cut tape to length. Use a template to cut angle plies to size. (Allow excess on all edges.)

3) Lay up plies.

4) Debulk after 4th, 8th, 12th, 16th, and 20th ply by holding the laminate under vacuum for 15 to 20 minutes.

5) Cover laminate with perforated FEP, one ply of 1581 fiberglass bleeder for each four plies of laminate, a layer of nonperforated FEP, a metal caul sheet, two layers of 1581 fiberglass breather, and a vacuum bag.

6) Cure laminate in an autoclave using the following cure cycle:

   o Apply vacuum.

   o Increase autoclave temperature so that laminate temperature increases at a rate of 0.5 to 2.8°C (1 to 5°F) per minute.

- Hold 60 min at (121°C $\pm$5.5°C) (250°F $\pm$20°F).

- Apply 689 kPa (100 psi) pressure 15 minutes after the laminate reaches temperature.

- Increase laminate temperature to 177°C $\pm$5.5°C (350°F $\pm$10°F) at a rate of 0.5 to 2.8°C (1 to 5°F) per minute.

- Hold at temperature for 120 min $\pm$5 min., then cool under pressure.

7) Cut laminate panels to length of test specimens.

8) Lay up fiberglass/epoxy grips on the panel edges.

9) Vacuum bag and cure in an autoclave at 121°C (250°F).

10) Remove panels from autoclave and cut specimens from the panels.

Specimen Defect Geometry

A number of defects can occur in composite laminates due to either manufacturing, handling, or inservice damage. Defects that can be found in the basic laminates are:

1) Excessive porosity or voids due to contamination of the prepreg materials, geometrical restrictions that prevent the escape of volatiles during cure, or low curing pressure.

2) Wrinkled or nonaligned fibers due to improper layup, thickness changes, etc.

3) Resin-rich and resin-starved areas.

4) Impacted damaged surface areas, resulting in delaminations or broken fibers.

5) Scratched or gouged surfaces caused by mishandling during manufacture or inservice damage.

There are also a number of defects associated with the use of fasteners in composite structure. Some of these are:

1) Delaminations near the exit side of drilled holes due to inadequate backing or excessive drill pressure.

2) Overly deep countersinks.

3) Local damage due to excessive fastener torque.

4) Resin starved bearing surfaces, resulting from excessive heat from drilling.

5) Relocated holes where mislocated holes have been redrilled.

The potential effects of several of these defects were assessed by testing laminates containing defects simulated by stress concentrations. These defect types can be categorized as (1) sharp defects that break or cut filaments, (2) blunt defects that cut or break filaments, (3) delaminations, and (4) poor resin properties. The defect categories that include cut or broken filaments were represented by holes and sharp slits. Both full penetration (FP) and half penetration (HP) holes and slits were tested, as shown in Figure 4. The delaminations were produced by inducing a disbond into the laminate during cure. In addition to these stress concentrations, potential natural defects typical of the particular laminate application were also tested, as shown in Figure 5.

For laminate L1, specimens were tested that had holes containing overly deep countersinks. Deep countersinks are often unavoidable due to the lack of thickness of laminate skins. This condition was simulated by countersinking holes so that the countersink extended through the laminate thickness and left a sharp edge at the exit side of the hole.

For filament-wound pressure vessels, great care must be taken to provide the correct pressure during cure. Hence, it is appropriate to investigate the effects of low pressure on fracture and fatigue strength of laminate L2. Three variations of curing pressure were used, 345 kPa (50 psi), 172 kPa (25 psi), and 86 kPa (12.5 psi). The normal curing pressure is 689 kPa (100 psi).

For laminate L3, tests were conducted in a 20-ply layup that contained no S-glass. These tests were conducted to allow an evaluation of the effectiveness of the S-glass in increasing the fracture toughness of the laminates.

The hole and slit sizes selected for test were 3.18 mm (0.125 in), 9.52 mm (0.375 in), and 15.87 mm (0.625 in). These sizes cover the range of most practical fastener diameters. They are also at the threshold of detectable damage sizes for many common inspection procedures. The same sizes were used for the surface length of the half penetration defects, since when partial penetration damage exists in structure, the most obvious dimension is the length of the damage on the surface.

The type and size codes used to identify each of the defects are given in Table I.

All slits were perpendicular to the primary load carrying direction of each laminate. This means that they were perpendicular to the zero degree fibers. The zero degree fibers correspond to the hoop direction of a cylindrical filament-wound pressure vessel for laminate L3.

The slits were fabricated by means of ultrasonic machining. Ultrasonic machining is typically used to produce cuts of difficult configuration in nonconductive materials. Circular cutter tips were machined with a thickness of 0.06 inch and a sharp radius. The ultrasonic vibrations of the cutter produce a lapping action in an abrasive slurry that carries away the excess material as the cutter penetrates the part. The slit radius in the composite laminate was typically about 0.127 mm (0.005 in) with a smooth surface.

Figure 6 shows a typical partial penetration flaw that has been sectioned to illustrate the root geometry.

The full penetration circular holes were drilled, and the half penetration circular holes were end milled.

Page intentionally left blank

TEST PROCEDURES

The test program had the following objectives for each layup and defect:

1) Evaluate the initial static strength.
2) Establish maximum cyclic stresses for given cyclic lives.
3) Monitor the residual static tensile strength during cyclic loading.
4) Evaluate the effects of proof loading on cyclic and static behavior.

These objectives were satisfied by following the test load sequences shown in Figure 7. The numbers of test specimens and test conditions are defined in Tables II, III, and IV.

The first specimen in each series was static loaded to failure. The second specimen was preloaded to 90% of the failure load, unloaded, and then residual static loaded to failure. The remaining specimens were cyclic tested. However, one-half of these remaining specimens were statically preloaded to 90% of the first specimen failure load prior to cyclic test.

The cyclic testing included specimens that were "fatigue to failure" tests and "fatigue/residual static" tests. The maximum fatigue load was limited in most cases to 90% of the static preload (81% of the estimated static strength). This was established as an upper limit for use in structural applications. The cyclic loading in each test was limited to a maximum predetermined number, as defined in Tables III and IV. In the cyclic tests where failure did not occur after 10^3, 10^5, or 1.5×10^6 cycles as appropriate, the specimens were loaded to failure to obtain the residual static strength.

In this manner, fatigue life data were defined for stress levels up to 81% of the static strength, and cyclic lives to 1.5×10^6 cycles. For test specimen configurations that had fatigue behavior that exceeded these conditions (i.e., no fatigue failures at 81% of static strength and 1.5×10^6 cycles), these conditions were considered to be the minimum

performance. However, this minimum fatigue performance would exceed nearly all practical requirements.

Both the baseline static and the residual static test specimens were loaded to failure, using a loading rate of about 1100 N/s. This loading rate resulted in failure in about one minute after the onset of loading. This loading rate was also used for applying the preload.

The majority of the cyclic testing was performed using tension/tension loading (R = 0.05). Comparison cyclic testing was performed on laminate L1 test specimens with tension/compression loading. Two cyclic stress ratio values of R = -1.0 and R = -0.5 were included in these tests. The compression loaded test specimens were supported with two plates covering the specimen faces between the grips. The face plates were constructed of 13 mm (0.5 in) aluminum and faced with Teflon to minimize surface friction. The plates were clamped to the specimen using finger-tight bolts at the plate edge. A 51 mm (2.0 in) diameter central cutout in both plates was placed over the defect for instrumentation and inspection access, and to allow out of plane displacements around the defect. The edges of the specimen were fully supported since the specimen width is greater than the hole size. The 51 mm (2.0 in) diameter circular portion of the test specimen would be stable for panel buckling.

All flawed specimens were continuously instrumented throughout each test to detect both the time, at which and the manner in which, structural changes occur in the region immediately surrounding the defect. This was accomplished by continuous monitoring of the displacement across the stress concentrations using clip gages. Clip gages were spring-loaded against knife edges bonded to the specimen surface at the specimen centerline. For all but the 5/8 FP holes, the knife edges were located immediately above and below the stress concentration, as illustrated in Figure 8. For the test specimens containing the largest full penetration holes, knife edged supports were placed against the hole surfaces. In static tests, both clip gage and load cell were connected to an X-Y recorder to produce a recording of load versus clip gage

displacement. In the cyclic tests, the clip gage was connected to a strip chart recorder to obtain a recording of deflection amplitude versus cycles.

The fatigue test specimens were cycled at a maximum frequency of 10 Hz. The cyclic frequency was reduced to 1 Hz for the first cycles, and again when reading the instrumentation.

The tests were performed in room temperature laboratory air. These ambient conditions were nominally 20°C (70°F) and 40% relative humidity.

Page intentionally left blank

STATIC FRACTURE TEST BEHAVIOR

The static testing is discussed in this section. All test data are tabulated in Appendix A of this report. Figures 9 through 14 present static failure stresses and residual static stresses, after preloading, for all the test laminates and defect types.

The results for the half penetration slit tests show less effect of slit surface length on strength degradation. A comparison betwen the static (NPL) and residual static after preload (PL) specimens can also be made from these figures. The residual static results for the laminate L1 specimens show a slight increase over the NPL specimens. This trend was not consistent with the L2 and L3 laminate specimen results. In all three laminates, a hole and a slit of equal transverse size had essentially the same effect on static strength. It can also be seen from the results shown in Figure 9 that the full depth countersink hole has a strength that corresponds to a hole size equal to the average diamater.

The low cure pressures used in laminate L2 static specimens did not have an effect on static strength. This result is consistent with the conclusion that the static tension properties are fiber dominated in these layups, and are not influenced by the changes in matrix properties associated with the low curing pressures investigated. These data do not support the need for tight control of cure pressures in pressure vessels.

A comparison of the fracture stress of laminate L3 panels for the S-glass hybrid and the all-graphite layups is given in Figure 14. These results show an improvement in fracture stress for the hybrid laminate.

Examination of the failure faces and crack opening displacement (COD) records reveals a difference in the fracture behavior of the three laminates. Sample crack opening displacement records from testing of each of the three laminates with a full penetration hole are shown in Figures 15, 16, and 17. All the crack opening data records are included in Appendix C. The tests for one

specimen configuration are included on one figure. The first recording in each figure is from the static fracture test, followed by the preload record, the residual static fracture record, and the preloaded fatigue specimen records. Laminate L1 had nearly a linear COD record to failure as shown in Figure 15. In some cases there is an indication of damage growth just prior to failure that is [are] manifested by sudden small increases in the crack opening. Laminate L1 failure faces showed transverse fracture with a relatively small amount of delamination. Laminate L2 (Figure 16) demonstrated a nonlinear load-COD relationship with an indication of some specimens having a larger amount of sudden damage growth prior to failure. The fracture face of laminate L2 specimens displayed delamination and splitting. The delaminations occur in the plane of ±80 degree plies. The load-COD records for laminate L3 specimens (Figure 17) were initially linear, with sudden occurrences of damage growth prior to maximum load. There was a sudden drop in maximum load when the graphite fibers failed in the test panel. The test panel had not separated into two pieces, because all the glass fibers had not failed. There was extensive damage to the panel, however, in the form of fractures and delamination. Continued loading of the panel resulted in separation of the panel at a much lower load than that which caused the initial fracture of the graphite fibers. The failed test specimen has extensive delamination in the planes of the S-glass. Final separation of the panel resulted in fiber pull-out of the S-glass giving a "broom like" appearance. The COD records obtained during preloading of the fatigue specimens of each of the laminates followed the trends for the static fracture specimens. The linear behavior of the L1 laminates resulted in a single load/unload curve. The COD records show that laminates L2 and L3 experienced damage around the stress concentration due to the application of the preload.

The static data developed for the three laminates were examined for a consistent trend between failure stress and defect size. Figure 18 presents the static data for the full penetration holes and slits, as a function of defect size. As a comparison in this figure, the inherent flaw analysis prepared by Waddoups, et al (Reference 4), was applied to the data. In this analysis, an inherent flaw is assumed to control the static strength of the

undamaged laminate, and is assumed to exist at the edge of holes and slits. This condition results in the following expressions for fracture toughness parameters.

For slits (through center cracks)

$$K_c = \sigma_c [\ \pi (a+a_o)\ ]^{\frac{1}{2}}$$

For holes

$$K_c = \sigma_c [\ \pi\ a_o\ ]^{\frac{1}{2}}\ F(a_o/R)$$

For static unnotched strength

$$K_c = \sigma_c [\ \pi\ a_o]^{\frac{1}{2}}$$

where:

a_o = inherent flaw size
σ_c = fracture stress
K_c = critical stress intensity factor
a = one-half slit length (for through center cracks)
R = hole radius
$F(\ )$ = Bowie function for cracks emanating from a hole

In preparing the curves presented in Figure 18, the data for the unnotched tests and the 15.8 mm (0.625 in) slits were utilized to evaluate the two dependent quantities a and K . As shown in the figure, constant values of the a and K provide trends that are quite good for laminates L1 and L3. For L2, the smallest damage size is more severe than predicted. Also, the inherent flaw size computed for laminate L2 is much larger than for other laminates. Similar analyses are presented in Figure 19 for the average stress failure criteria , and in Figure 20 for the point stress criteria . As shown, the three fracture prediction methods yield comparable results.

Page intentionally left blank

CYCLIC LOAD BEHAVIOR

Figures 21 through 52 present the tension/tension cyclic test data for the three laminates. The figures present the applied gross area stress as a function of the number of applied load cycles. Triangle symbols represent static fracture tests, and circles represent cyclic tests. The closed symbols indicate specimens that have been previously preloaded (PL). An arrow indicates a cyclic test that did not result in a fatigue failure.

A review of the data confirms the high resistance of all the laminates to tension/tension fatigue, which is characteristic of such composite laminates. Only the laminates L2 and L3, containing half penetration defects or no defect had a consistent tendency to develope fatigue failures in less than 1.5×10^6 cycles. This is illustrated by the data in Figures 40, 42, and 49 through 52. In the remaining cases, the majority of the cyclic tests were terminated at the targeted number of cycles.

A beneficial effect of preload was noted for the residual static fracture test for laminate L1. The application of a preload to a laminate L1 specimen resulted in a subsequent increase in the preloaded specimen residual static strength when compared to the nonpreloaded static test result. However, the fatigue data do not show such an effect from preloading.

Results of the laminate L1 tension/compression fatigue tests are presented in Figures 53 through 62. The data are presented as applied load cycles against the maximum tension load. Two tension/compression stress ratios R(R = min load/max load) were tested, (1) fully reversed, R = -1 and (2) R = -0.5. All test specimens were the general purpose 20-ply laminate L1. This laminate is T-300/934 graphite/epoxy with a $((0/\pm45/0/90)_S)_2$ stacking. On the figures, the circles represent the R = -1.0 fatigue data, the squares represent the R = -0.5 fatigue data, and the triangles represent the residual static tests of the specimens that did not fail during cycling. The closed symbols represent test specimens that had been preloaded (PL) to 90% of the estimated static strength prior to cyclic test.

In general, the test data indicate a significant influence of the compression loading on cyclic life. This was in contrast to the small effect found for the tension loads.

When comparing the effects of the various types of defects, it was noted that increasing the notch severity had a greater effect on static than on the fatigue properties. This is illustrated by the relative fatigue performance comparison between the specimens containing holes and the unnotched specimens presented in Figure 63. As shown, the relative fatigue strength of the notched specimens is greater than that of the unnotched specimens.

The test results of disbond defects developed in this program were found to be no different than for unnotched specimens, as illustrated in Figure 64.

A visual comparison of the test specimens after cyclic loadings illustrated the effect of layup on damage propagation. The test specimens constructed from laminate L1, $((0/\pm45/0/90)_S)_2$, showed only minimal or no visual damage. The appearance of damage was evidenced by a fine craze or split running parallel to the loading direction of the outer 0^o plies. Laminate L2 $((0_3/\pm80)_2)_S$ generally displayed greater splitting than found in laminate L1. The splits in laminate L2 penetrated the outer plies, and were up to several centimeters in length. An example of splitting in laminate L2 is shown in Figure 65 for a fatigue specimen with only 1,000 cycles. A photograph of a similar specimen from laminate L3 $((0/+30/0/-30/0)_2)_S$ in Figure 66 showed only minimal damage. Visual examinations of laminte L1 specimens displayed even less damage. It was concluded that the cyclic fatigue characteristics are influenced by the clustering or dispersion of the (0) plies in the laminate.

These visual observations were extended by the use of ultrasonic records. These records are traces of through transmission scans of the test specimens made with a Holosonics Model 200 unit. Both signal attenuation and a time gate were used, resulting in light areas for delaminations as well as for the edges and initial defects. The inspection records from a half penetration hole are presented in Figure 67. In this case delamination occurs, and is

shown to extend from the defect in a direction parallel to the loading, with the greatest extent of delamination progressing along the center line of the panel. A similar record for a full penetration hole is shown in Figure 68. As shown in this figure, there is no apparent damage extension from the defect, even though the number of load cycles applied is much greater. Records for a full penetration hole specimen from laminate L2 $((0_3/\underline{+}80)_2)_S$ are shown in Figure 69. The extent of delamination was greater for laminate L2 specimens than for L1.

Similar results were found for the tension/compression test data. Several examples are shown in Figures 70 and 71. Results for a half penetration slit are shown in Figure 70. For this type of defect, the damage propagates above and below the initial slit. The development of edge delaminations can also be seen in this specimen. The edge delaminations developed in specimens with small or no initial defects that were cycled at relatively high stress levels. Figure 71 presents the records for a specimen containing a half penetration hole where the delaminations above and below the defect can be seen. The delamination in this specimen was the result of only 1,000 fatigue cycles.

Appendix B of this report contains all the ultrasonic C-scan records. These records were made for a range of defect types and loading conditions.

The damage growth during cyclic loading was also monitored, using a crack opening displacement gage that was recorded during the cyclic test. These results from the cyclic testing identified the time of damage growth during the testing. Appendix D contains the results of these measurements.

Page intentionally left blank

PROOF TEST PROCEDURES FOR COMPOSITE STRUCTURE

The development of data for establishing proof loading techniques for composite structure was a major objective of this program. For illustration, typical requirements for proof loading are shown in Figure 72. A key element is whether the initial strength and the cyclic life or residual strength distribution are controlled in the same manner by an initial defect; i.e., is there a relationship between initial static strength and the fatigue performance.

A second requirement is that the application of the proof load either (1) does not have a detrimental effect on the subsequent structural performance, or (2) the effects on the fatigue behavior can be accurately assessed. The application of the preload had a beneficial effect on only the laminate L1 static test behavior. All other comparisons including the fatigue and the residual static strength after cyclic loading, did not reveal any difference between preloaded and non-preloaded test specimens. Therefore, the application of a proof load was not considered to affect the subsequent performance of the structure.

As a first step in the development of a proof test method, the cyclic test data developed for each flaw type were reviewed to determine the minimum cyclic life associated with given cyclic stress levels. It was recognized that the number of test data points developed for each specimen configuration was limited (six to eight specimens). However, there is a systematic variation in defect type and size in the test program. For this reason, the collective data demonstrate the consistent trend of a sharp transition between stress levels that produce early fatigue failures, and stress levels below which no failures occur. Because of this result, it is possible to construct, from the available data base, S/N curves that represent the maximum allowed cyclic stress for given cyclic lives. Since the maximum demonstrated cyclic stress was used when constructing the curves, further testing could result in higher allowable cyclic stresses. However, because of the curve shape and the

relatively high cyclic stress test results, there could be only a slight increase in the result.

As the next step in the evaluation of proof loading methods, potential relationships between initial static strength and cyclic behavior were investigated. The quantitative evaluation of such a potential relationship is an integral part of developing a useful proof test method. A number of techniques have been proposed (Reference 6 for example), using analytical models. Some were extensions of metallic fracture analysis procedures. Because of the large flaw type and flaw size data base developed in this program, a direct experimental approach was used. As a step in this approach the minimum cyclic data (S/N) curves found for each of the defects were defined. The initial static strength found for test specimens that contained the same defect geometry was used to identify the curves. As illustrated in Figure 73 for the laminate L1 data, these curves present a systematic relationship between fatigue performance and the initial static strength for all types of defects tested. This result is amplified in Figure 74 which defines the cyclic stress level for the selected cyclic lives of 1, 10^2, 10^4, and 10^6 as a function of the initial static strength.

Since a relationship exists between initial static strength and fatigue behavior, these curves then define the proof loading requirements to meet defined life and operating stress levels.

Similar analyses were performed for laminates L2 and L3. The results were normalized (to the undamaged static strength) for all laminates at 10^6 cycles, and are presented in Figure 75. As can be seen, laminates L1 and L3 display nearly identical behavior, while laminate L2 shows a slightly different response. However, the variation between all three is only slight, indicating that this result is applicable to a wide variety of composite laminates.

CONCLUSIONS

Three composite 20-ply laminates representative of general structure, pressure vessels and turbo engine fan blades were studied to develop data on their static and fatigue behavior. The test results presented apply specifically to the laminates and test conditions evaluated. However the trends define general behavior for a wide range of laminate configurations. Some general conclusions that are discussed in detail in the report are presented below:

1) Initial defects of the type that cut filaments can significantly reduce the static tension strength of composite structure.

2) Graphite fiber composite materials are relatively insensitive to tension/tension fatigue, and may be cycled at high percentages of their static strength. In tension/compression fatigue, however, these composite materials exhibit increased sensitivity.

3) Half penetration defects are less severe than full penetration defects with the same surface length.

4) There is little difference between the performance of laminates with circular holes or with sharp slits in the sizes tested.

5) For a wide range of flaw types, there is a relationship between initial static strength and cyclic life. This relationship was found for the three laminates tested, and was used to develop proof load requirements for the types of composites tested. It is expected that this approach will be applicable to other graphite fiber composites as well.

6) No detrimental effect on the subsequent fatigue or static strength was found as a result of the application of a proof load.

Page intentionally left blank

REFERENCES

1. Hoggatt, J. T. and Dobyns, A. L., "Evaluation of Hybrid Composites," Boeing contract with AFML, F33615-74-C-5074.

2. Friedrich, L. D. and Preston, J. L. Jr., "Impact Resistance of Fiber Composite Blades Used in Aircraft Turbine Engines," NASA CR-134052.

3. "Battle Damage Tolerant Wing Structure Development," Navy Contract N00019-75-C-0178 with The Boeing Aerospace Company, in progress.

4. Waddoups, M. E., Eisenmann, J. R., and Kamminski, B. E., "Microscopic Fracture Mechanics of Advanced Composite Materials," Journal of Composite Materials, Vol. 5, October 1971.

5. Whitney, J. M., and Nuismer, R. J., "Stress Fracture Criteria for Laminated Composites Containing Stress Concentrations," Journal of Composite Materials, Vol. 8, July 1974.

6. Halpin, J. C., Jerina, K. L. and Johnson, T. E., "Characterization of Composites for the Purpose of Reliability Evaluation," Analysis of Test Methods for High Modulus Fibers and Composites, Air Force Materials Laboratory Presentation to Industry, February 1975.

Page intentionally left blank

Table 1. Defect Type and Size Code

Defect type \ Approximate diameter or surface length mm (in)	3.18 (0.125)	9.52 (0.375)	15.9 (0.625)
Full-penetration hole	1/8 FP hole	3/8 FP hole	5/8 FP hole
Half-penetration hole	1/8 HP hole	3/8 HP hole	5/8 HP hole
Full-penetration slit	1/8 FP slit	3/8 FP slit	5/8 FP slit
Half-penetration slit	1/8 HP slit	3/8 HP slit	5/8 HP slit
100-degree full-depth countersink hole	1/8 CSK hole	3/8 CSK hole	5/8 CSK hole
Circular disbond defect between 15th and 16th plies	–	–	5/8 disbond

Table 2. Static Test Matrix

Laminate	Proof load (% σ_{ult})	Number of tests															
			Circular holes						Sharp slits						Natural defects		
			S_1		S_2		S_3		S_1		S_2		S_3				
		Unflawed Specimens	FP	HP	FP	HP	FP	HP	FP	HP	FP	HP	FP	HP	S_1	S_2	S_3
L_1	0	1	1	1	1	1	1	1	1	1	1	1	1	1	1	1	1
	90	1	1	1	1	1	1	1	1	1	1	1	1	1	1	1	1
L_2	0	1	1		1		1		1	1	1	1	1	1	1	1	1
	90	1	1		1		1		1	1	1	1	1	1	1	1	1
L_3	0	1	1		1		1		1	1	1	1	1	1	1	1	1
	90	1	1		1		1		1	1	1	1	1	1	1	1	1

S_1, S_2, S_3 depict defect sizes

FP = full penetration of thickness

HP = half penetration of thickness

Table 3. Tension/Tension Load Test Matrix

Laminate	Proof load (%σ_{ult})	Cyclic stress	Number of tests																
			Unflawed	Circular holes						Sharp slits						Natural defects		
				S_1		S_2		S_3		S_1		S_2		S_3				
				FP	HP	FP	HP	FP	HP	FP	HP	FP	HP	FP	HP	S_1	S_2	S_3
L_1	0	σ_1	1	1	1	1		1	1	1	1	1		1	1	1		1
		σ_2	1	1	1	1		1	1	1	1	1		1	1			
		σ_3	1	1	1	1		1	1	1	1	1		1	1	1		1
	90	σ_1	1	1	1	1		1	1	1	1	1		1	1	1		1
		σ_2	1	1	1	1		1	1	1	1	1		1	1			
		σ_3	1	1	1	1		1	1	1	1	1		1	1	1		1
L_2	0	σ_1	1	1				1		1	1			1	1	1		1
		σ_3	1	1				1		1	1			1	1	1		1
	90	σ_1	1	1				1		1	1			1	1	1		1
		σ_3	1	1				1		1	1			1	1	1		1
L_3	0	σ_1	1	1		1		1		1	1	1	1	1	1			
		σ_3	1	1		1		1		1	1	1	1	1	1			
	90	σ_1	1	1		1		1		1	1	1	1	1	1			
		σ_3	1	1		1		1		1	1	1	1	1	1			

$\sigma_1, \sigma_2, \sigma_2$ σ_3 = stress levels corresponding to cyclic lives of 500, 50,000, and 10^6 cycles, respectively

S_1, S_2, S_3 depict different defect sizes

FP = full penetration HP = half penetration

Table 4. Tension/Compression Cyclic Load Test Matrix

Laminate	Proof load (5 UH)	Cyclic stress	Number of tests																
			Unflawed		Circular holes					Sharp slits						Counter-sink holes	Disbond defect		
					S_1 FP	S_3 FP		S_3 HP		S_1 FP	S_1 HP	S_3 FP		S_3 HP		S_3 FP	5/8-in circular		
			R -0.5	R -1.0	R -1.0	R -0.5	R -1.0	R -0.5	R -1.0	R -1.0	R -1.0	R -0.5	R -1.0	R -0.5	R -1.0	R -1.0	R -0.5	R -1.0	R +0.1
L_1	0	σ_1	1	1	1	1	1	1	1	1	1	1	1	1	1	1	1	1	1
		σ_3	1	1	1	1	1	1	1	1	1	1	1	1	1	1	1	1	1
	90	σ_1	0	1	0	1	1	0	0	0	0	0	1	0	0	1	0	1	0

σ_1, σ_3 = stress levels corresponding to cyclic lives of 500 and 10^6 cycles, respectively.

S_1, S_3 depict different defect sizes

FP = full penetration HP = half penetration

DESIGNATION	MATERIAL	LAYUP	APPLICATION
L1	THORNEL 300/FIBERITE 934 (T300/934)	$\left[(0/\pm 45/0/90)_S\right]_2$	GENERAL STRUCTURE
L2	T300/934	$\left[(0_3/\pm 80)_2\right]_S$	PRESSURE VESSELS
L3	T300/934 with 901-S	$\left[(0/+30/0^*/-30/0)_2\right]_S$	TURBINE ENGINE FAN BLADES OR SUPPORT STRUTS

* PLIES THAT ARE REPLACED WITH S-glass

Figure 1. Structural Laminates Evaluated

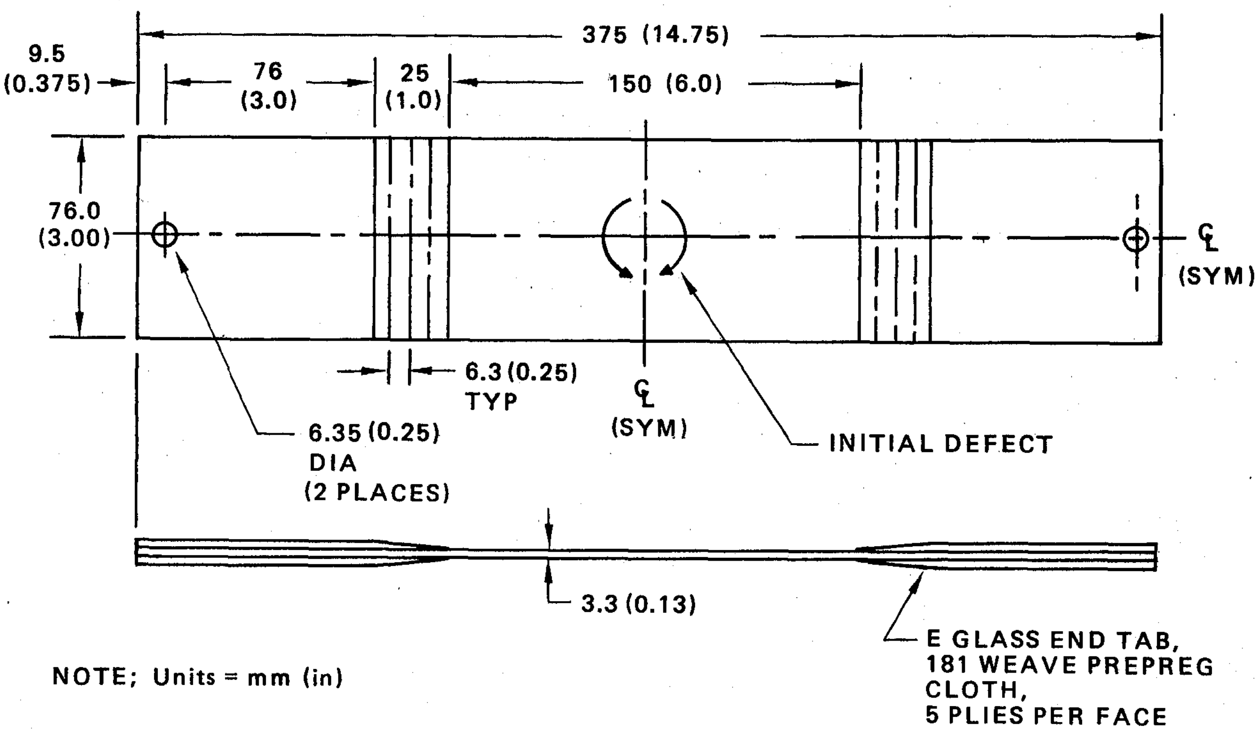

Figure 2. Test Specimen Configuration

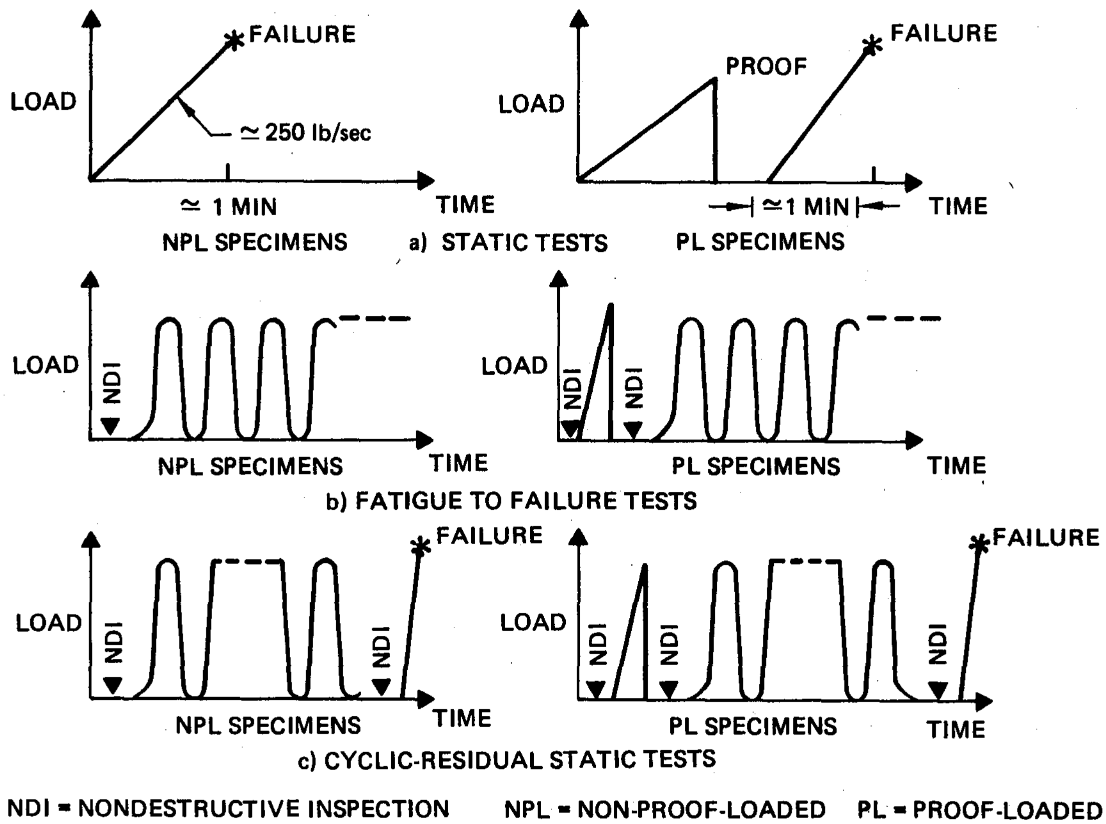

Figure 3. Test Program Load Sequences

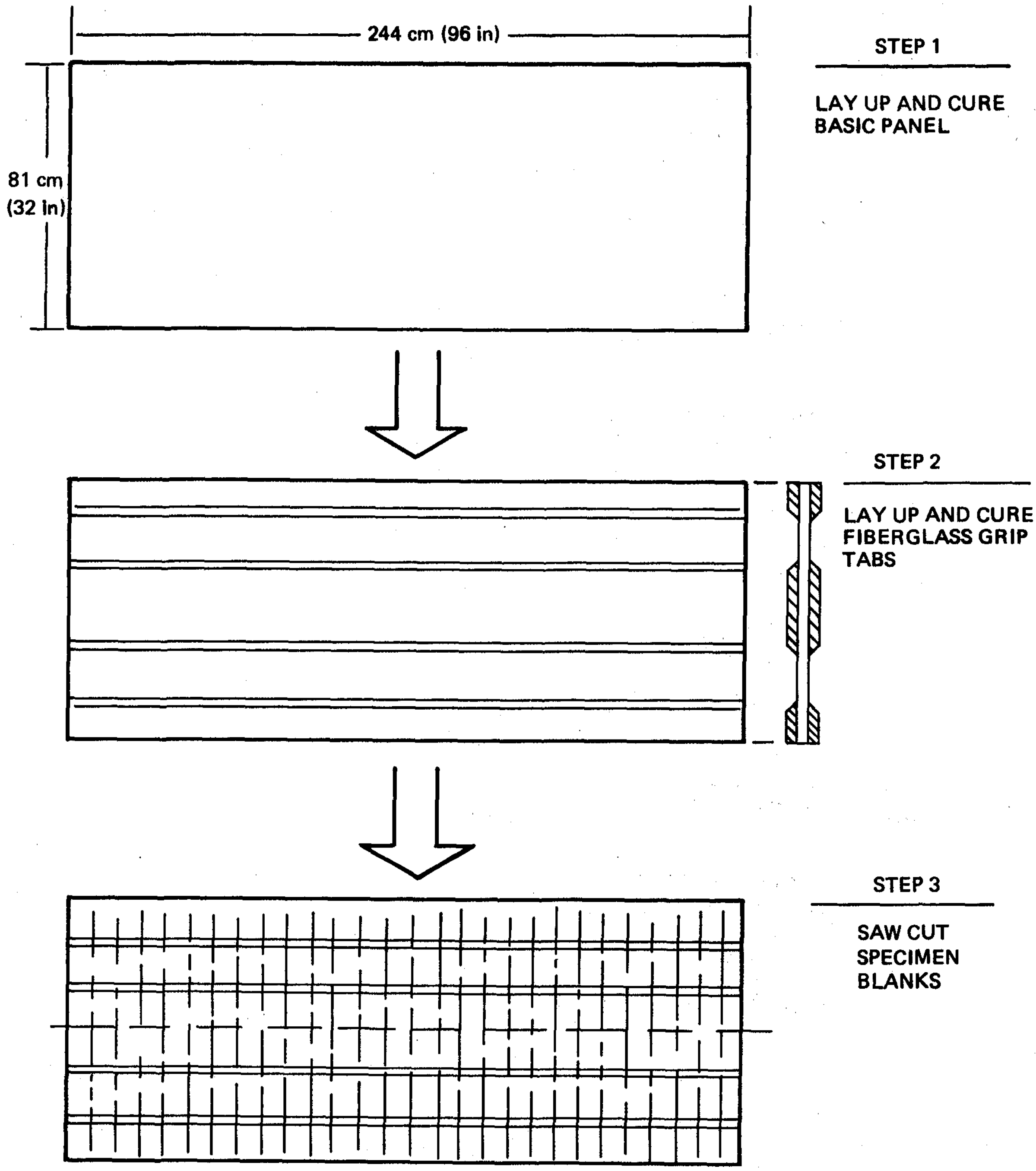

Figure 4. Test Specimen Fabrication Sequence

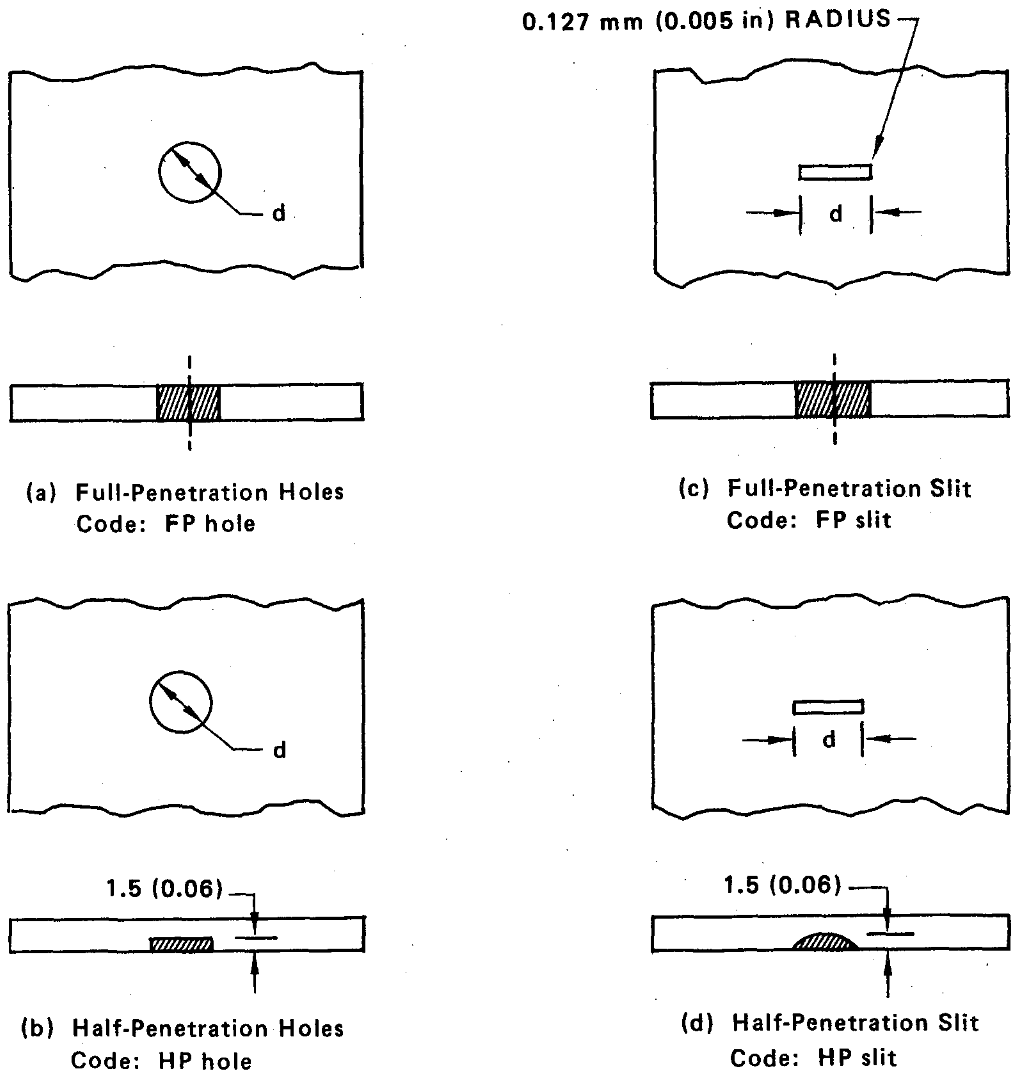

Figure 5. Stress Concentration Configurations Tested

LAMINATE	DEFECT
L1	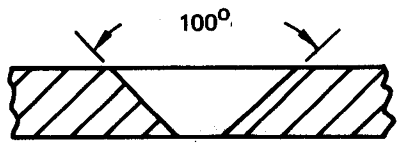 DEEP COUNTERSINK
L2	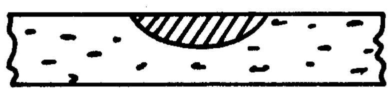 VOIDS
L3	 NO HYBRID FIBERS

Figure 6. Natural Defect Configurations Tested for Each Laminate Type

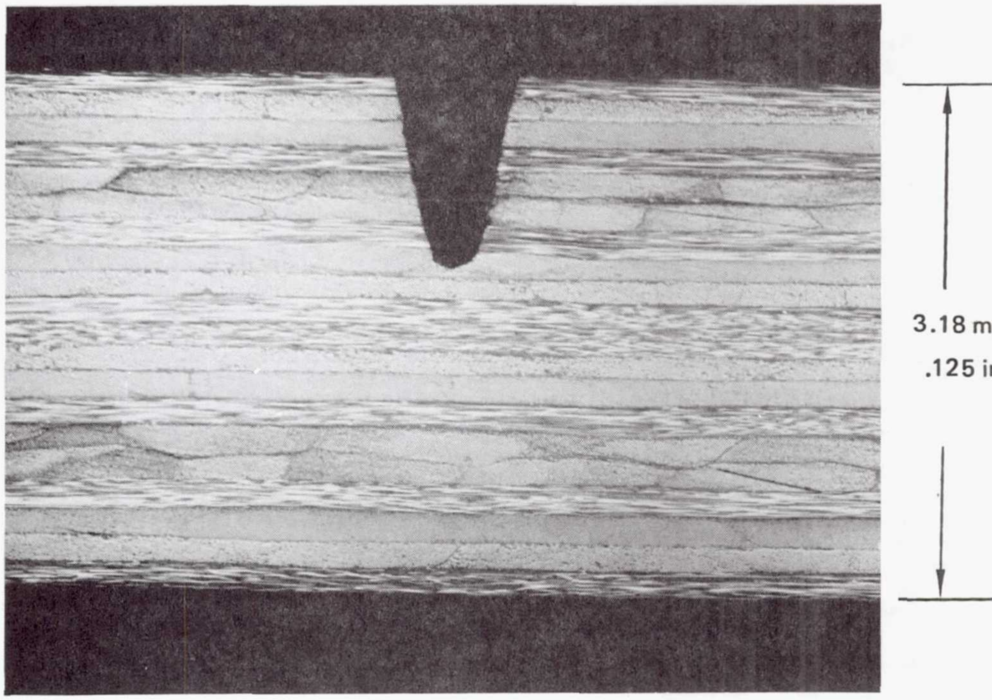

Figure 7. Photomicrograph Showing Root of Ultrasonic Flaw

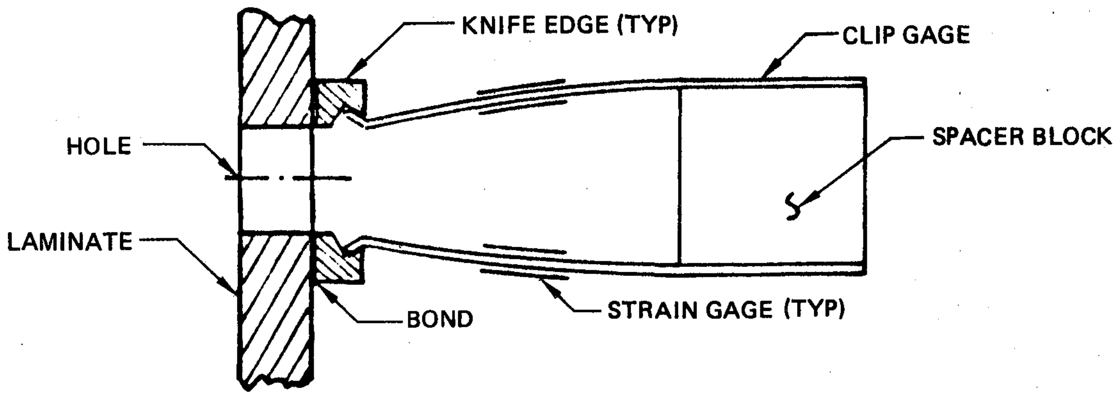

SECTION A-A FOR CIRCULAR HOLES

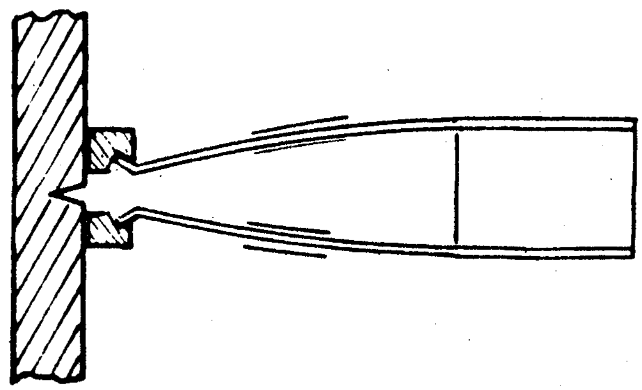

SECTION A-A FOR SLITS

Figure 8. Clip Gage Installation on Test Specimens Containing Defects

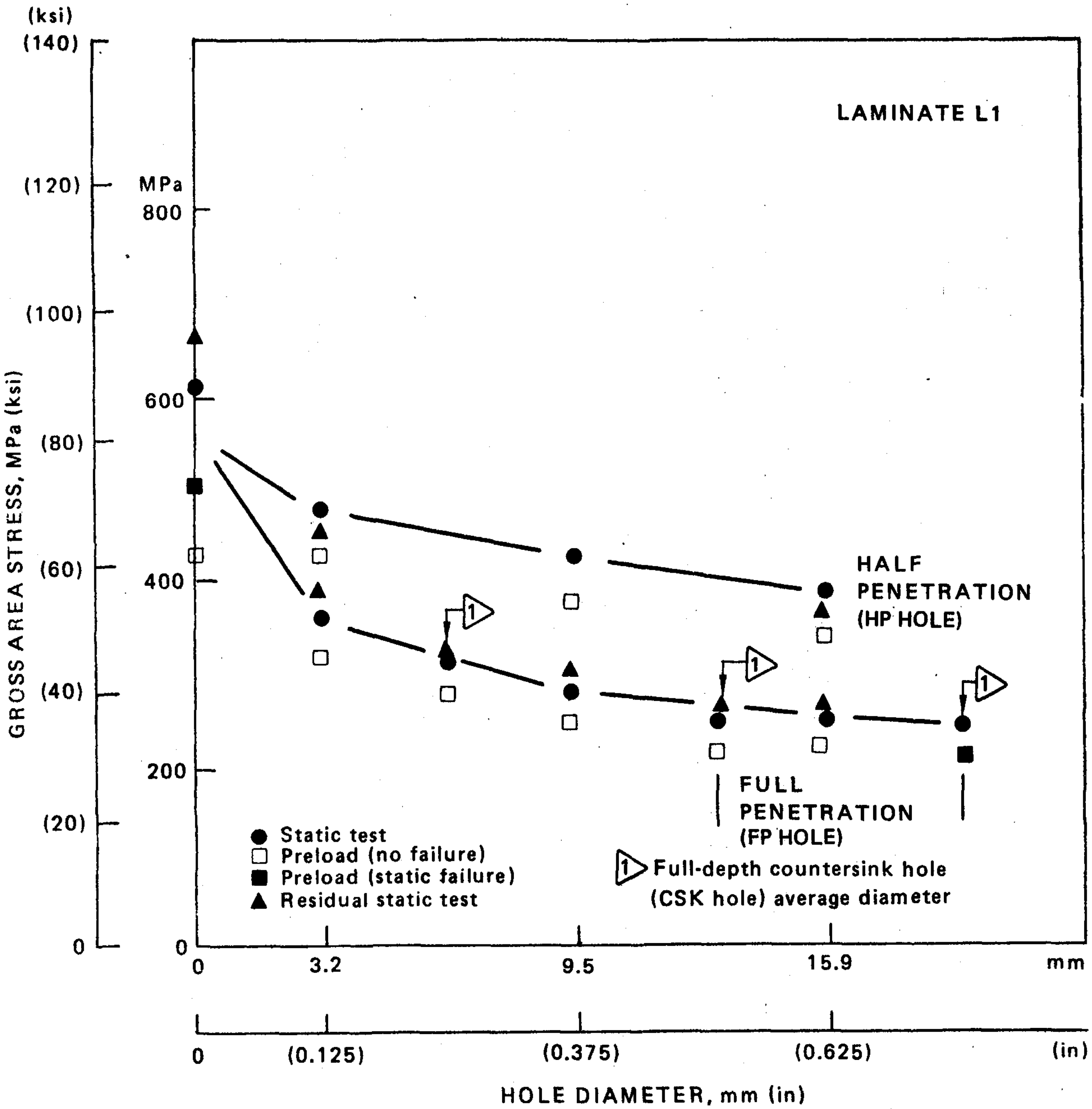

Figure 9. Static Test Results for Laminate L1 Specimens With Holes

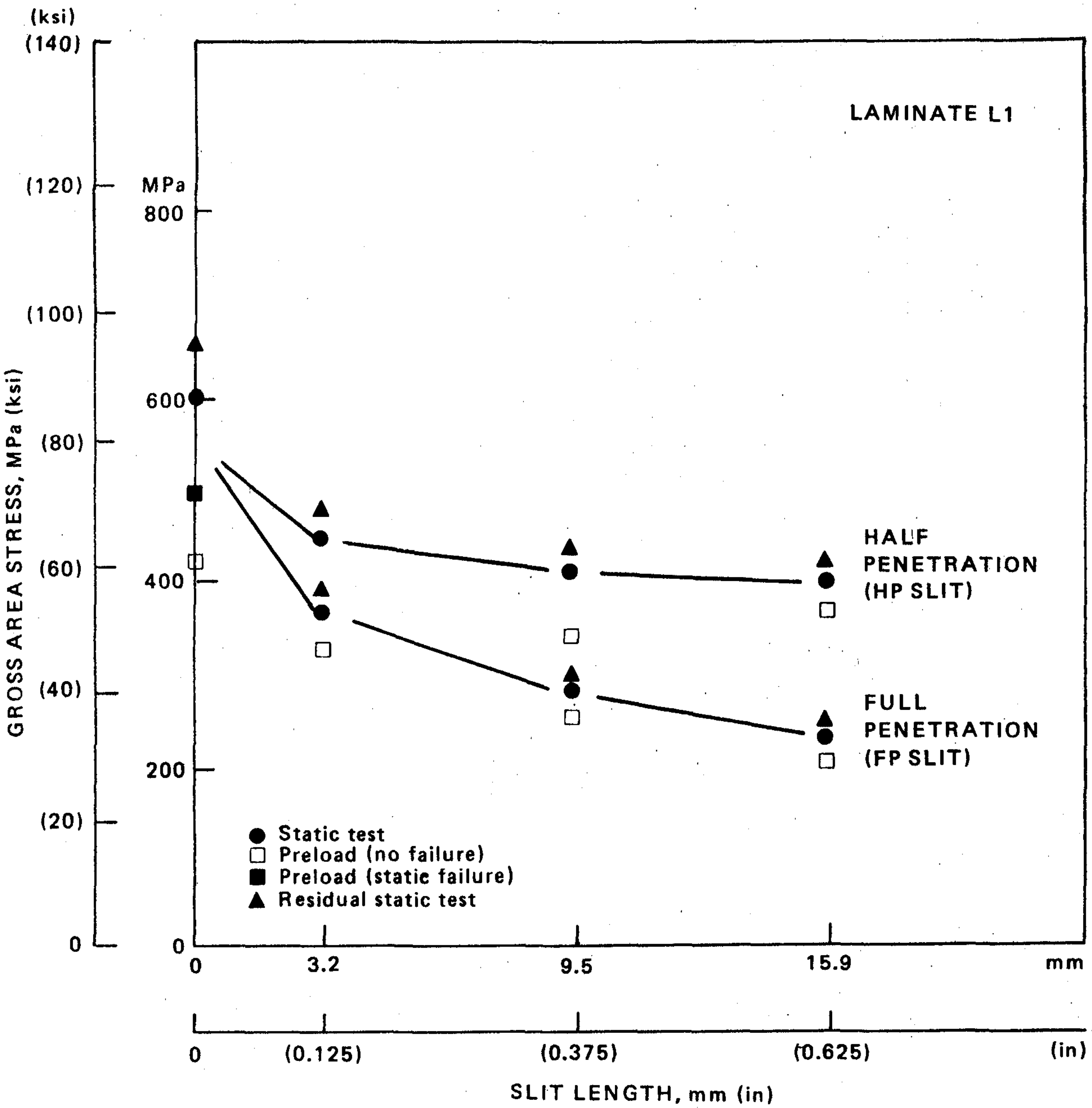

Figure 10. Static Test Results for Laminate L1 Specimens With Slits

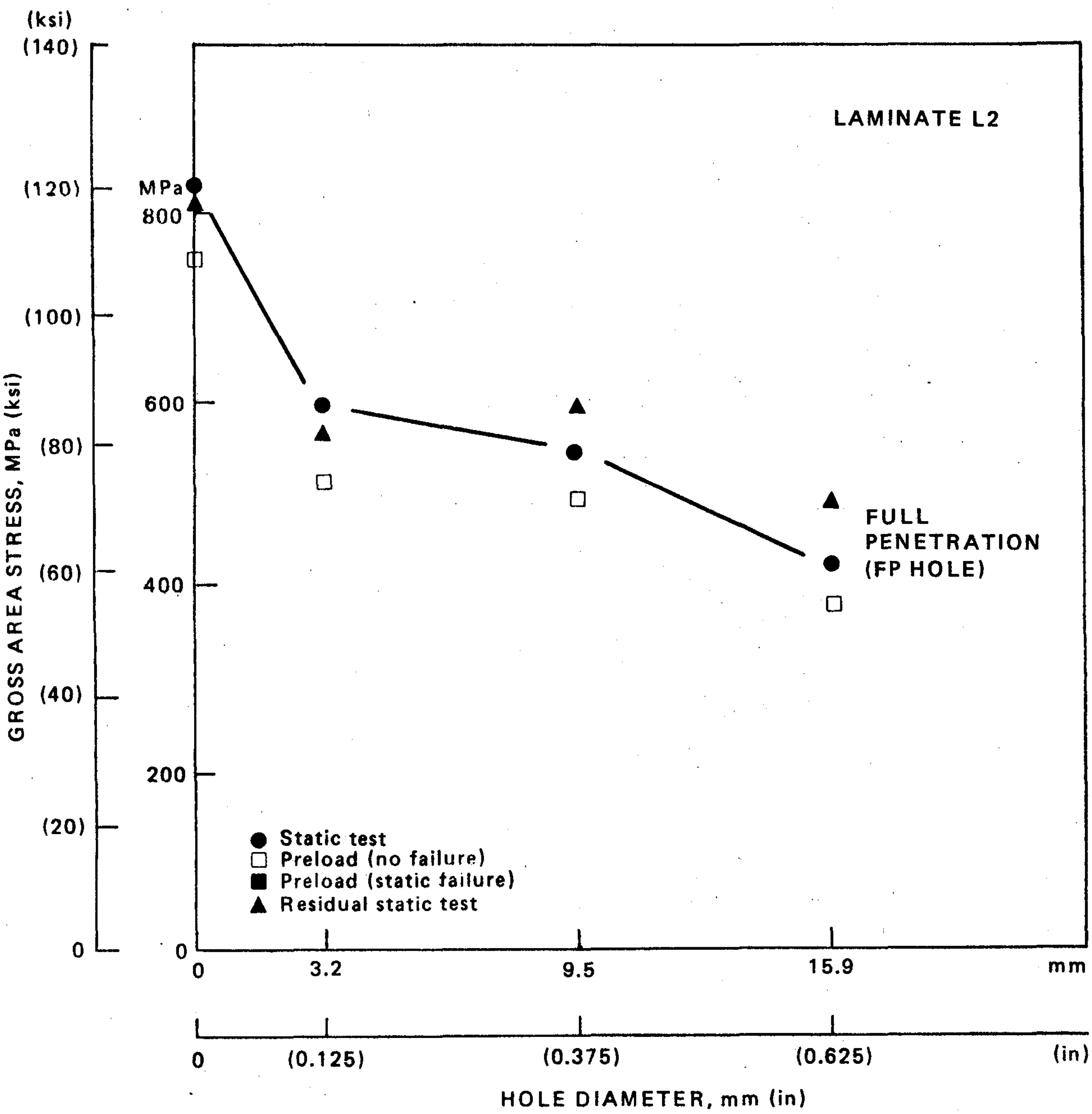

Figure 11. Static Test Results for Laminate L2 Specimens With Holes

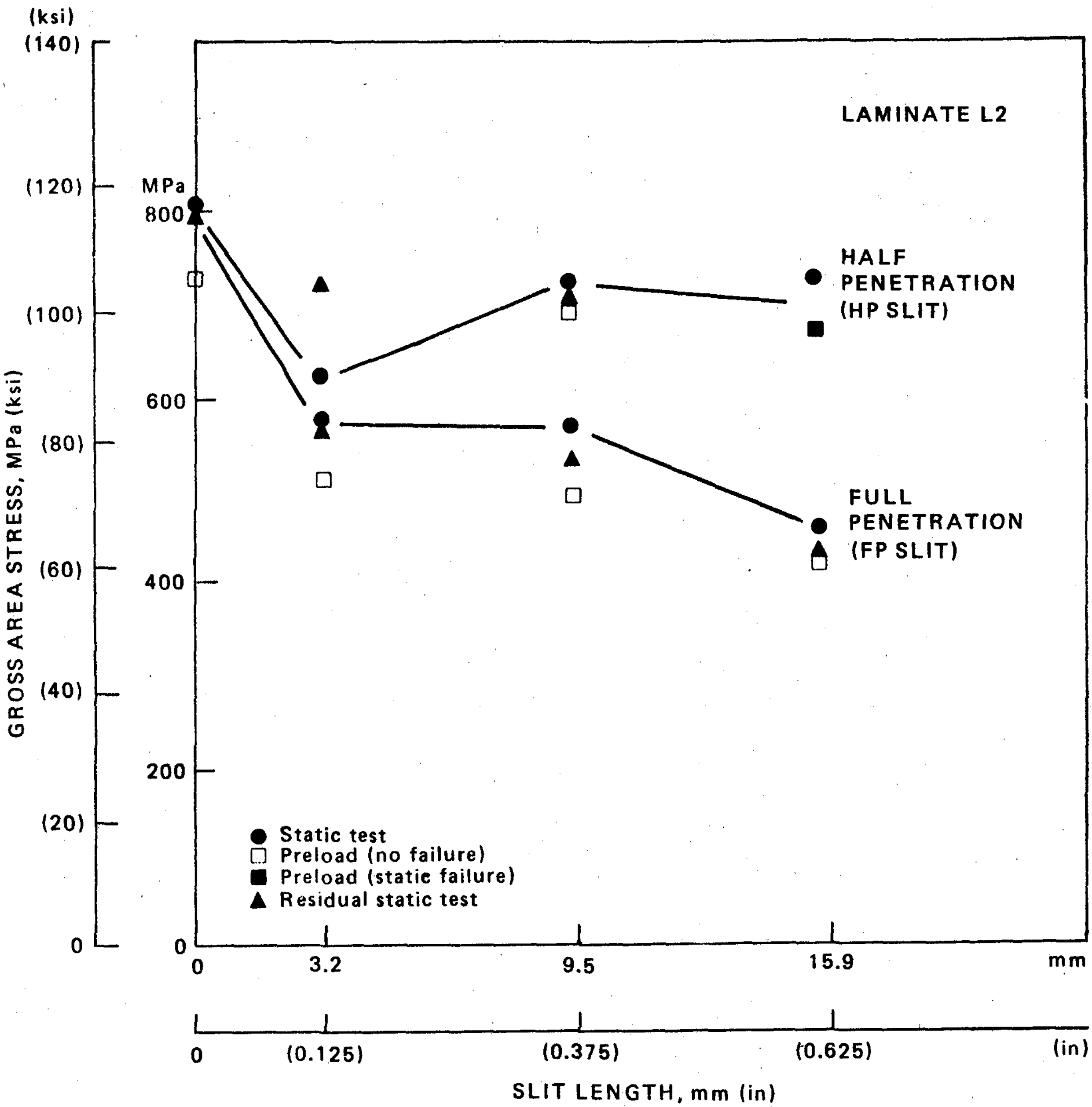

Figure 12. Static Test Data for Laminate L2 Specimens With Slits

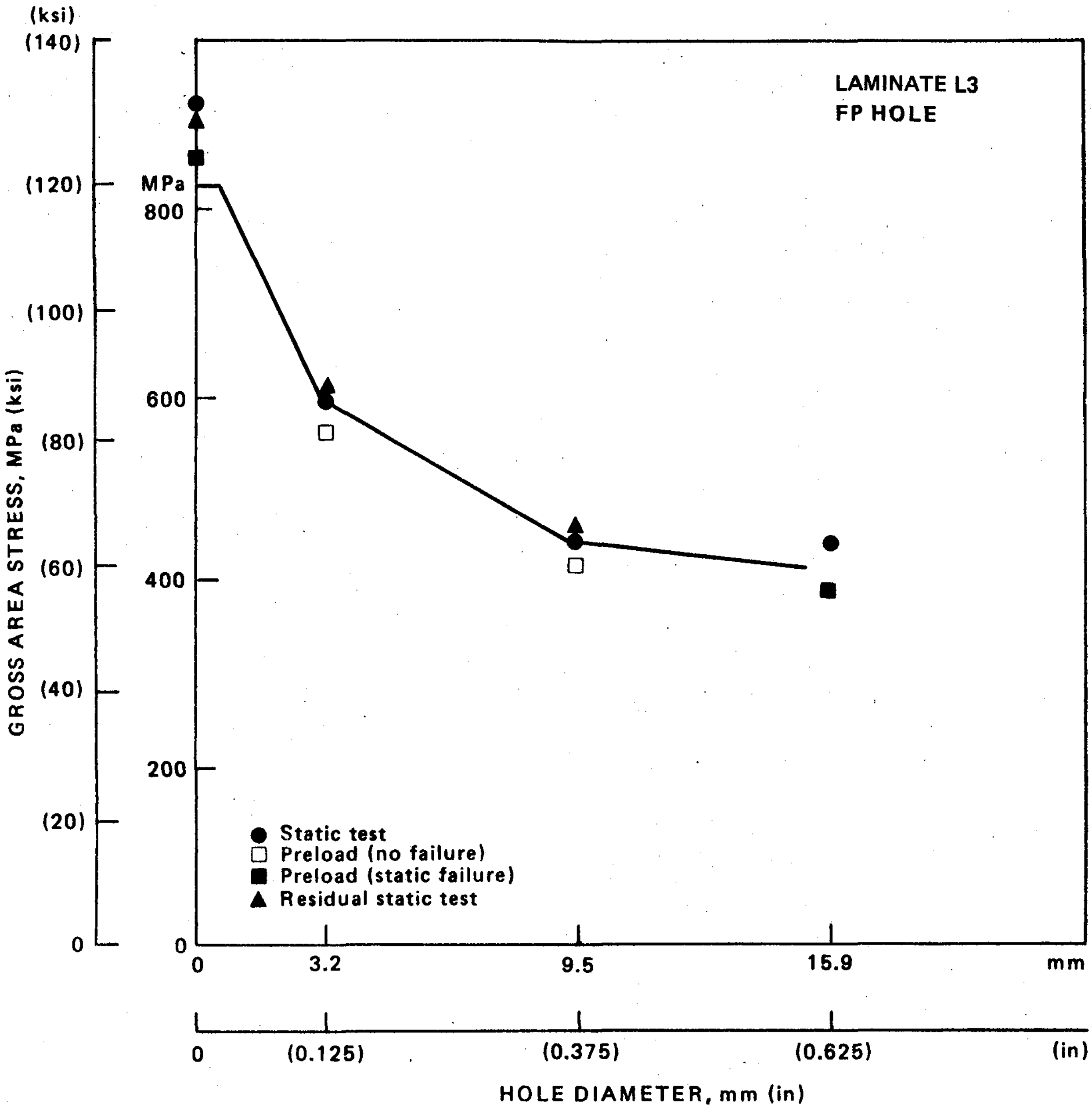

Figure 13. Static Test Results for Laminate L3 Specimens With Holes

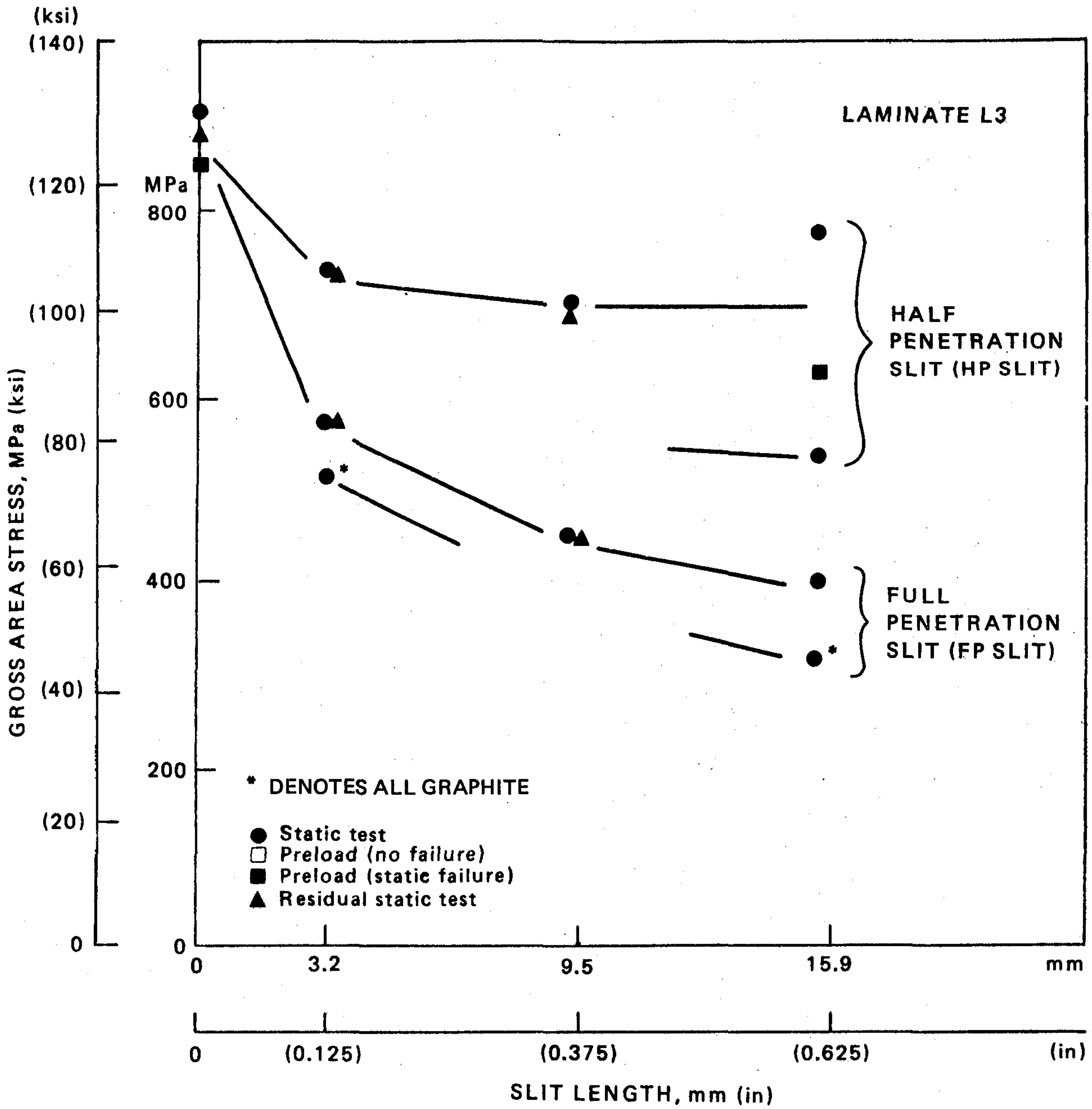

Figure 14. Static Test Results for Laminate L3 Specimens With Slits

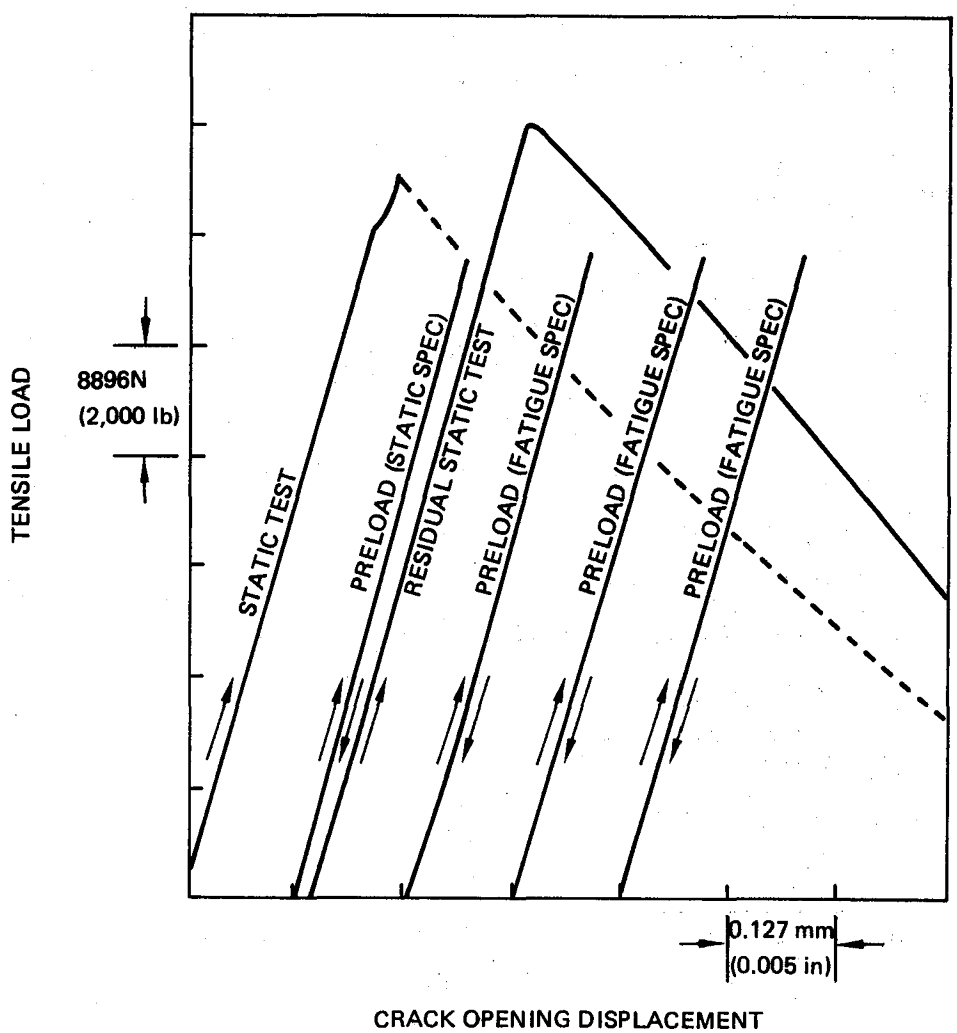

Figure 15. Crack Opening Displacement Records for Laminate L1 Specimens With Full-Penetration Hole

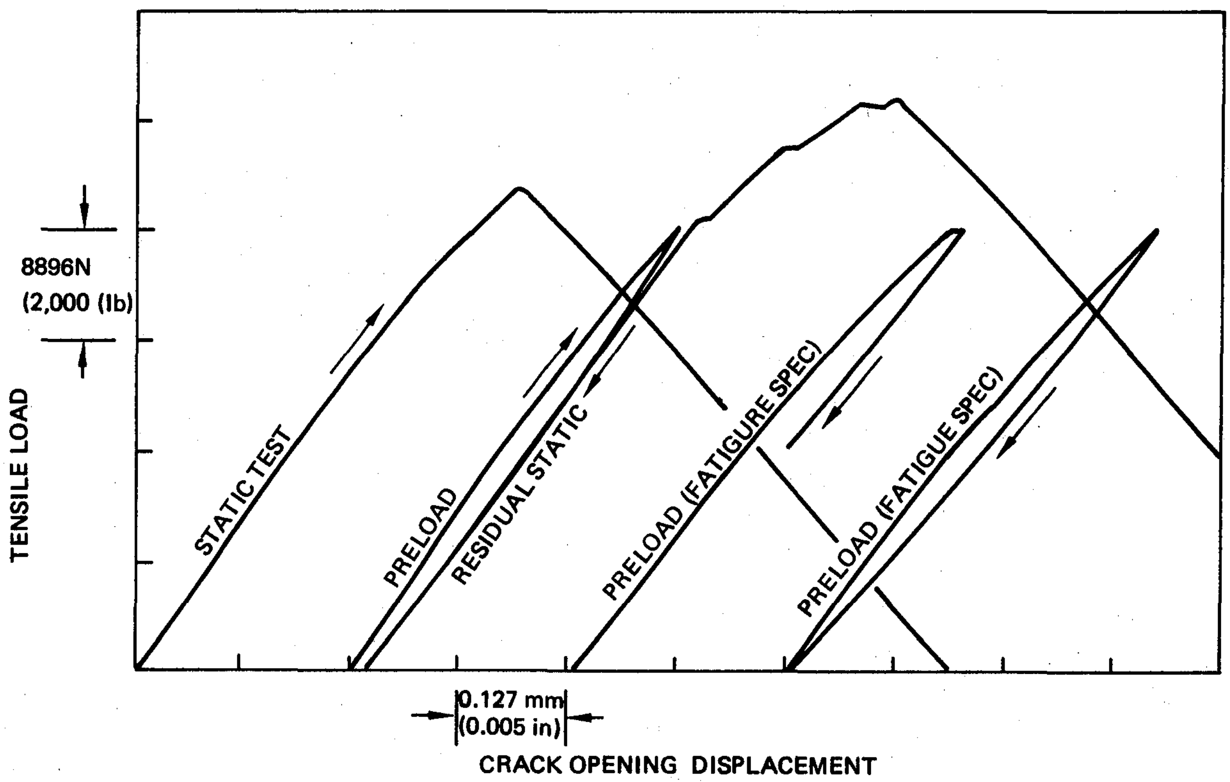

Figure 16. Crack Opening Displacement Records for Laminate L2 Specimens With Full-Penetration Hole

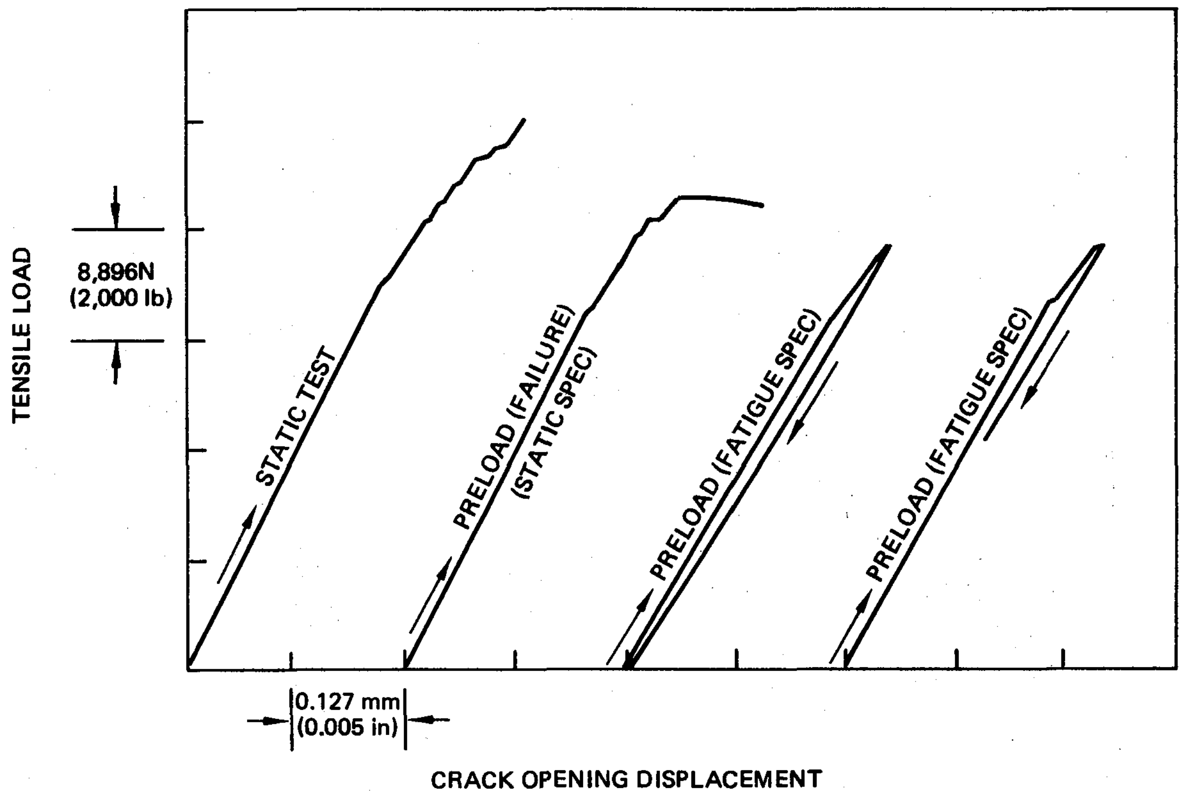

Figure 17. Crack Opening Displacement Records for Laminate L3 Specimens With Full-Penetration Hole

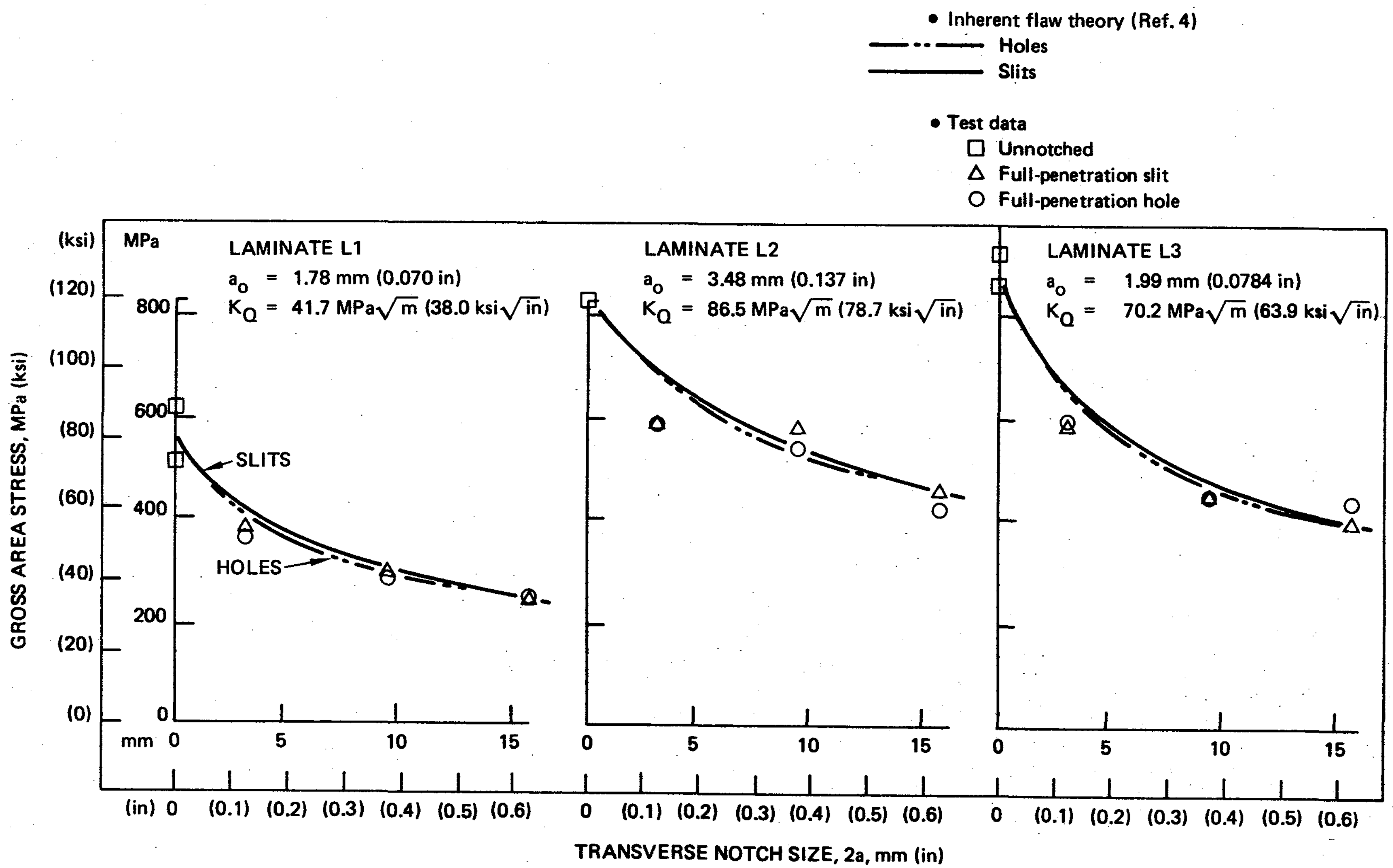

Figure 18. Comparison of Inherent Flaw Analysis and Static Test Data

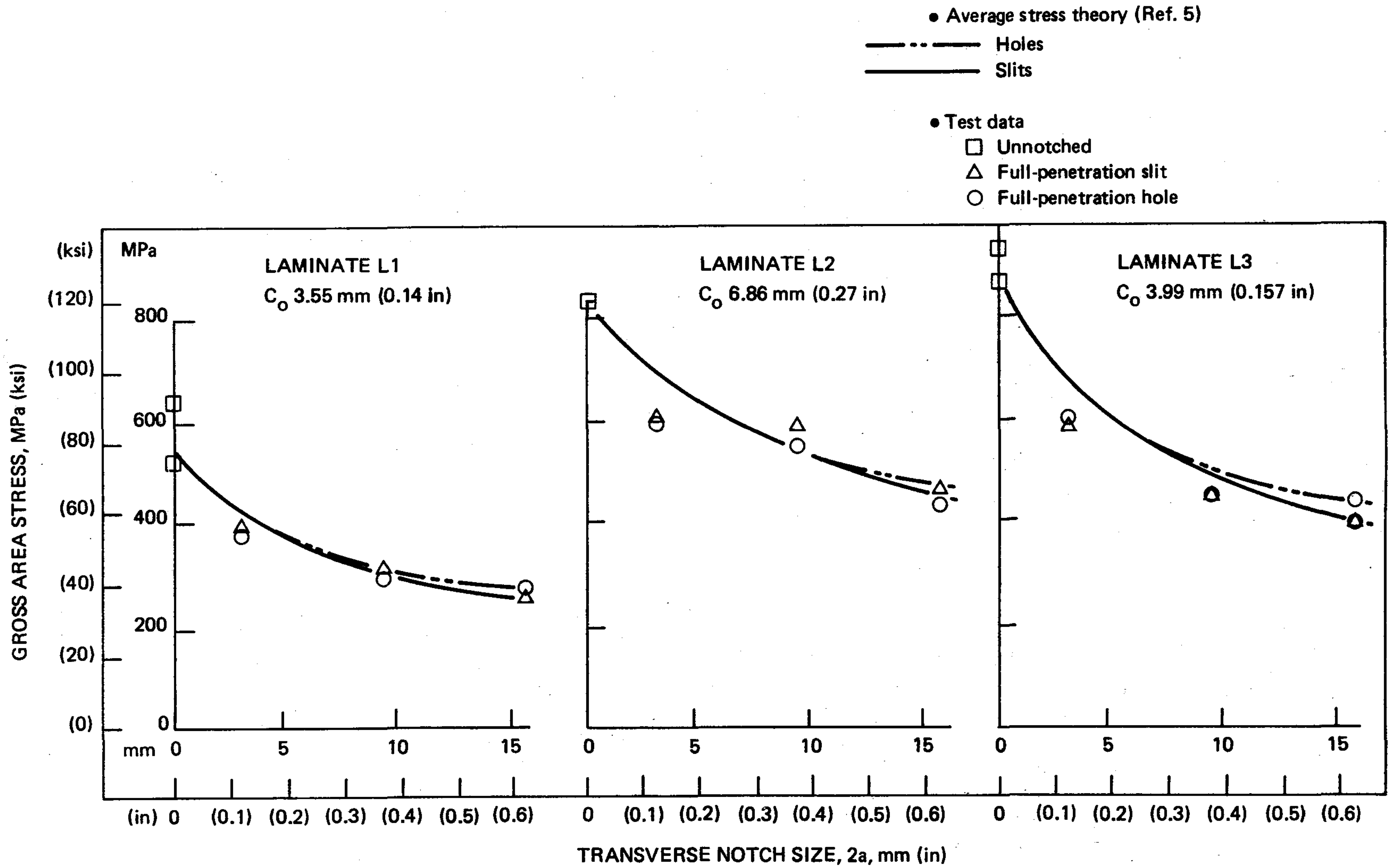

Figure 19. Comparison of Average Stress Analysis and Static Test Data

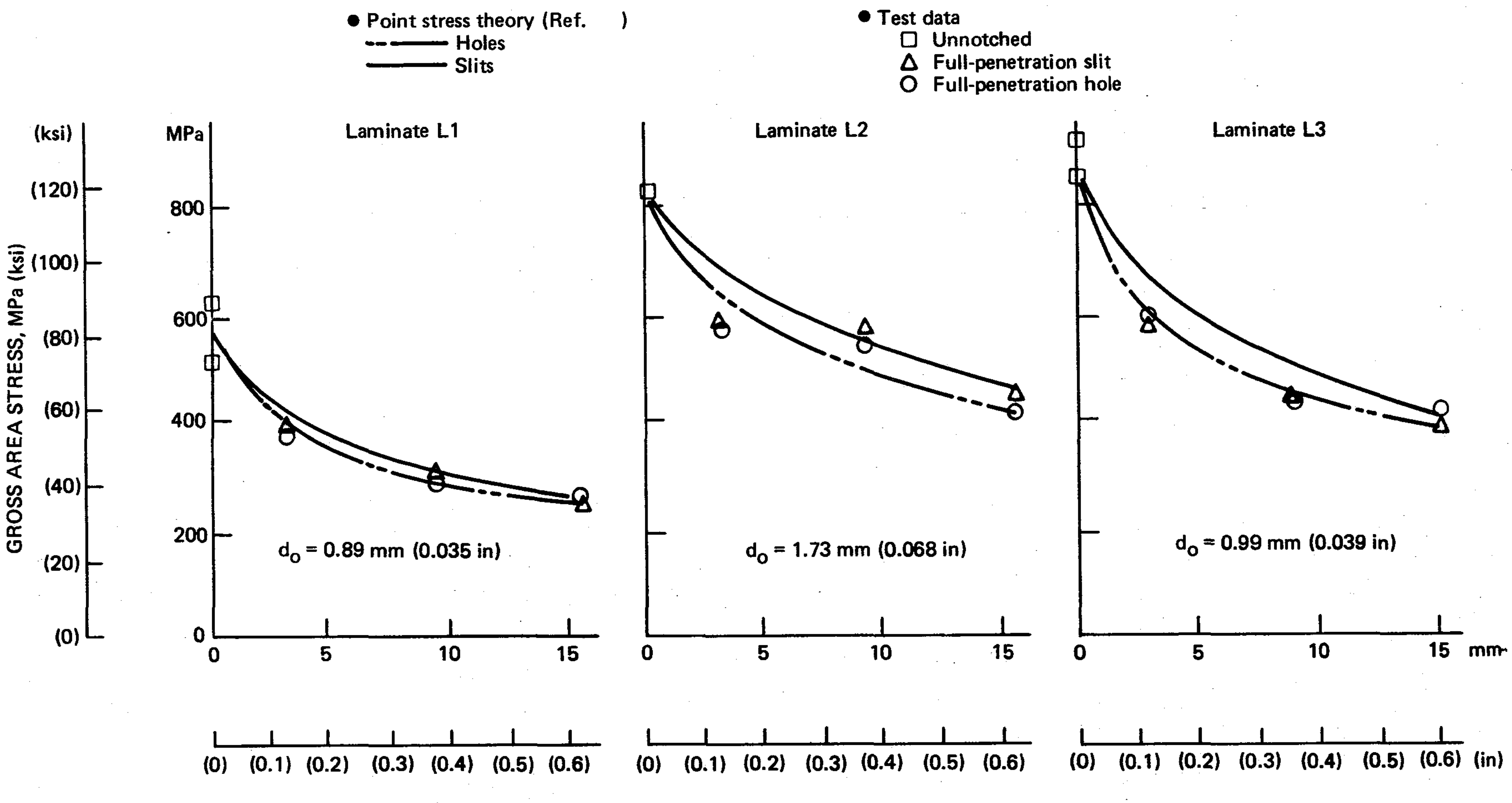

Figure 20. Comparison of Point Stress Analysis and Static Test Data

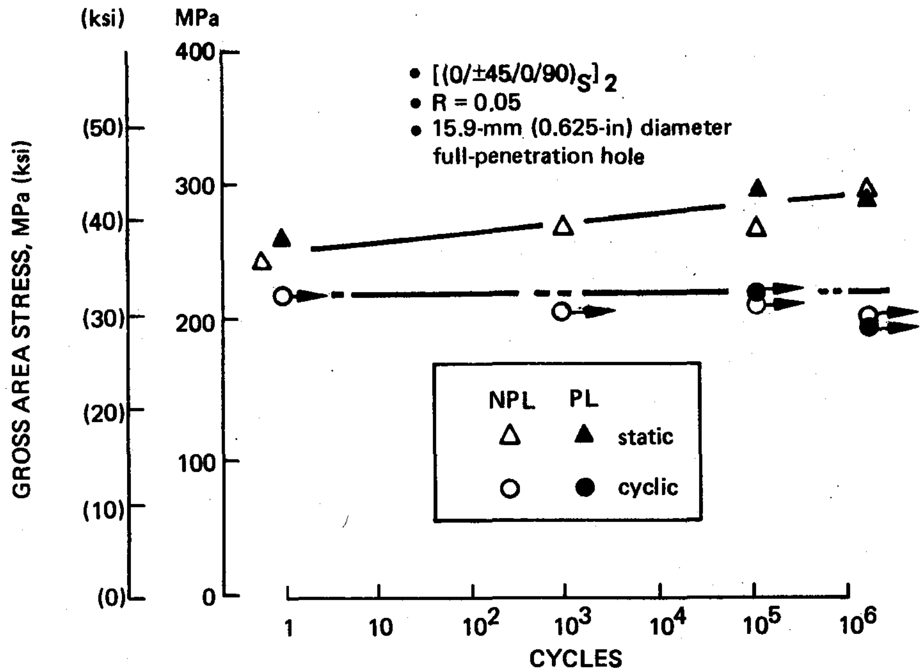

Figure 21. Fatigue Data for Laminate L1 5/8 FP Hole

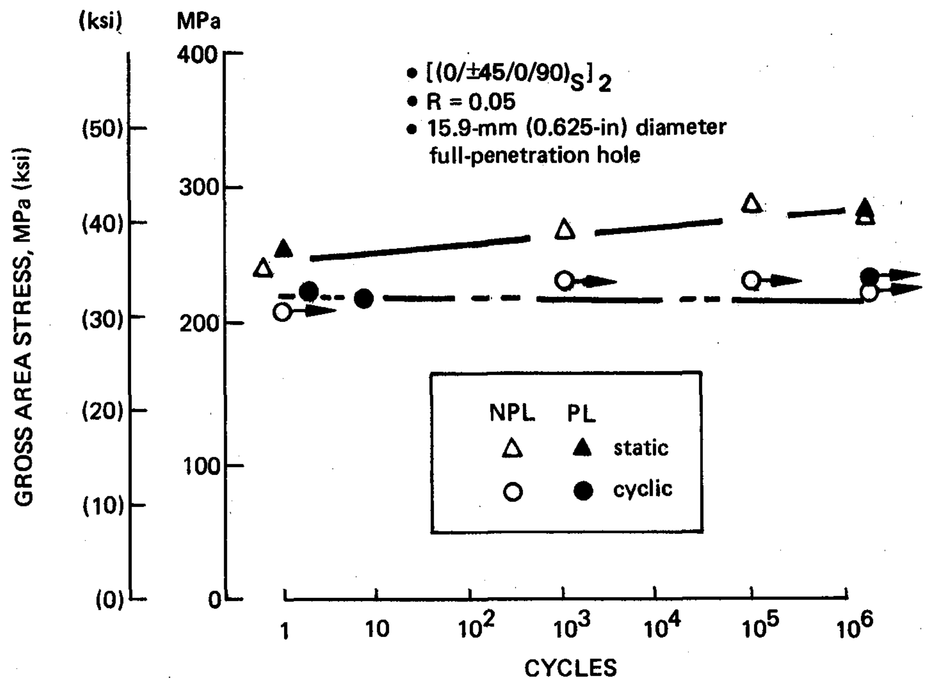

Figure 22. Fatigue Data for Laminate L1 5/8 FP Slit

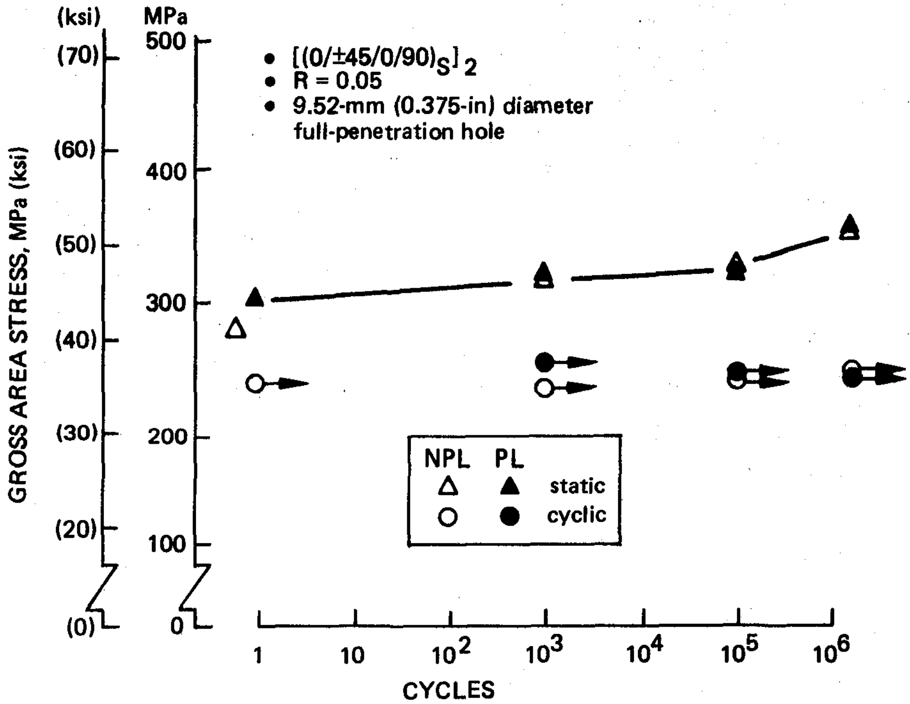

Figure 23. Fatigue Data for Laminate L1 3/8 FP Hole

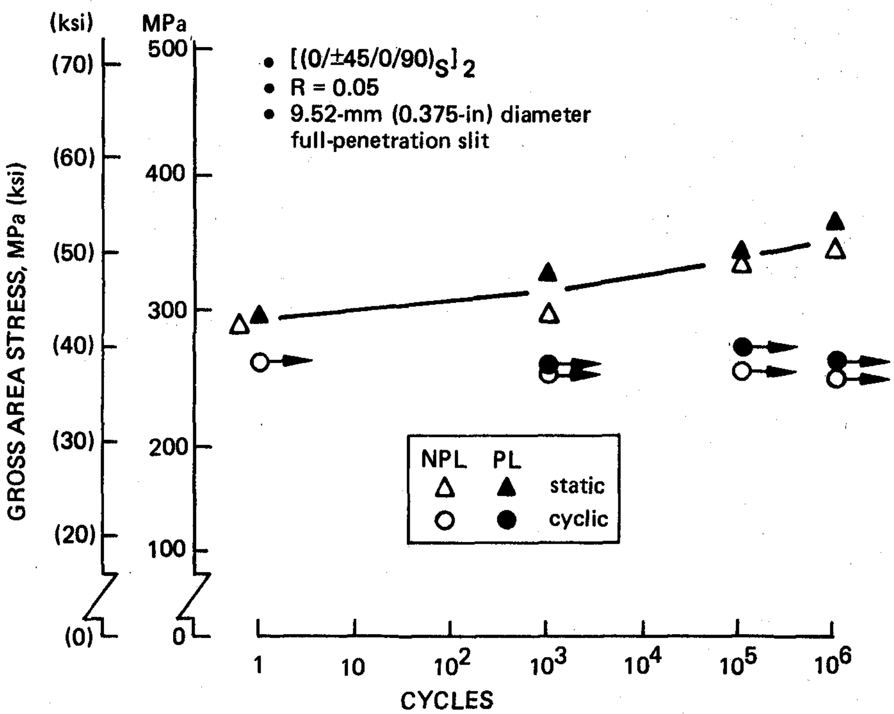

Figure 24. Fatigue Data for Laminate L1 3/8 FP Slit

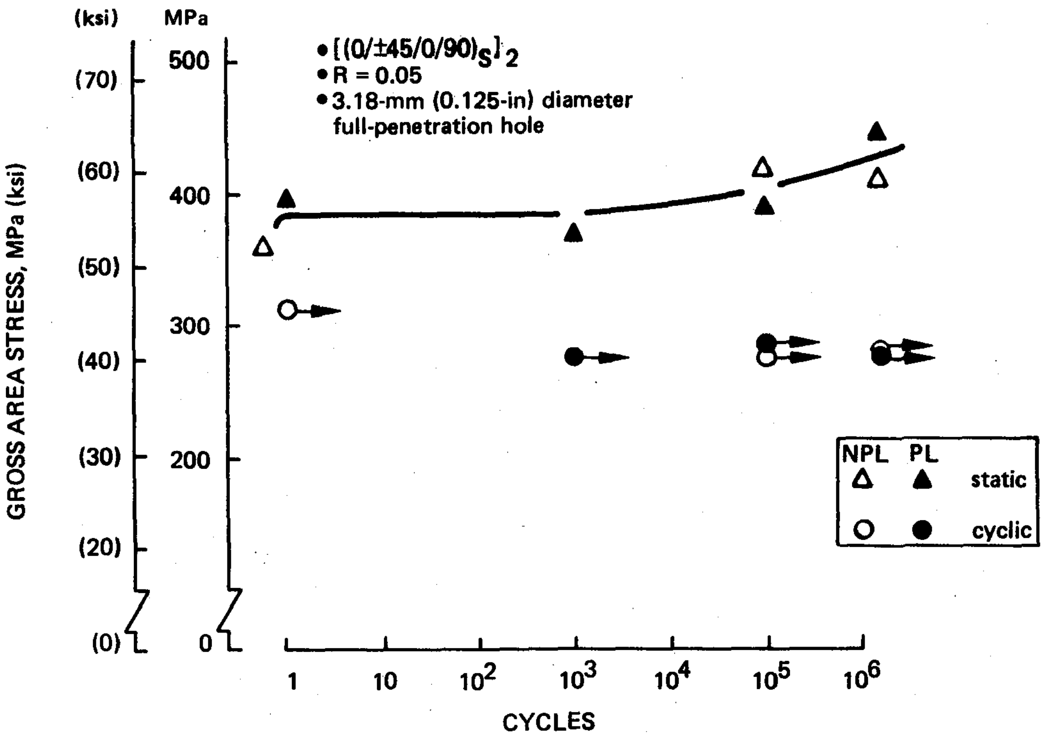

Figure 25. Fatigue Data for Laminate L1 1/8 FP Hole

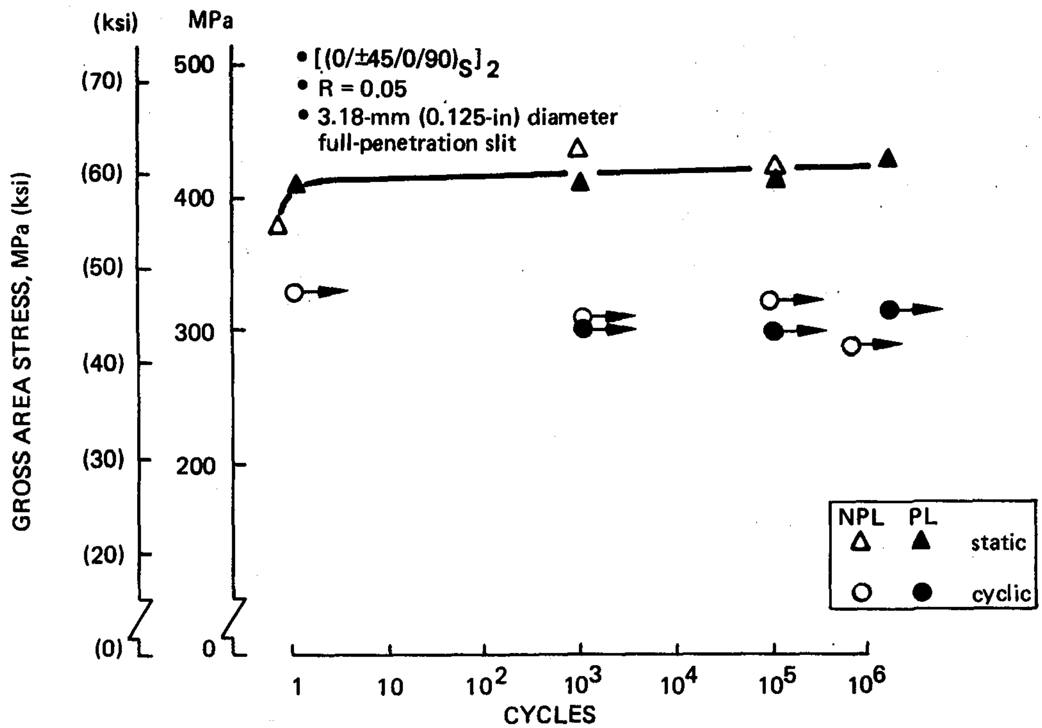

Figure 26. Fatigue Data for Laminate L1 1/8 FP Slit

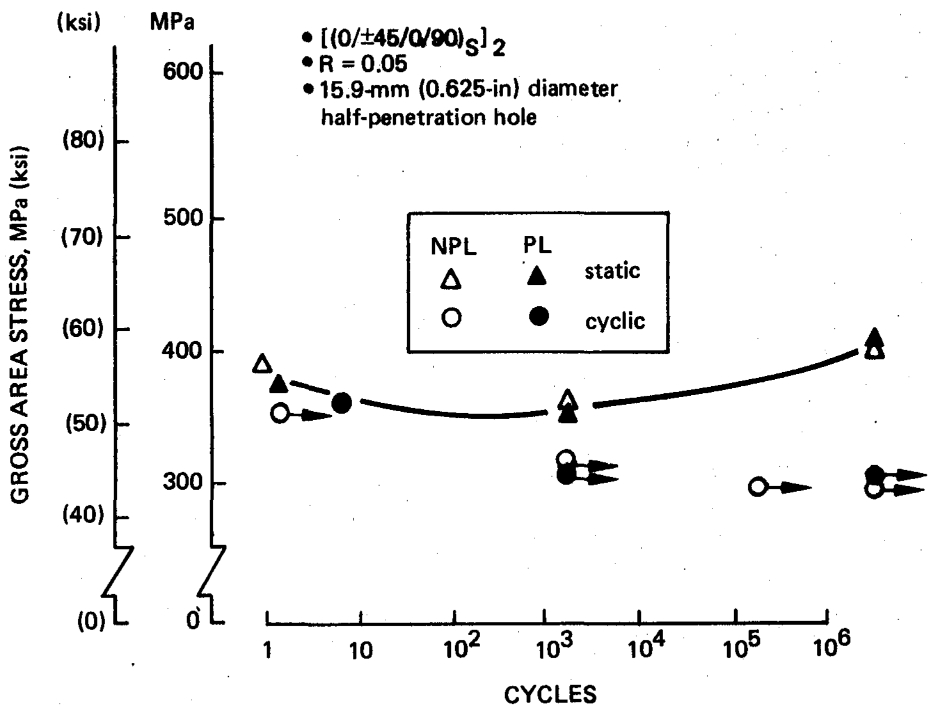

Figure 27. Fatigue Data for Laminate L1 5/8 HP Hole

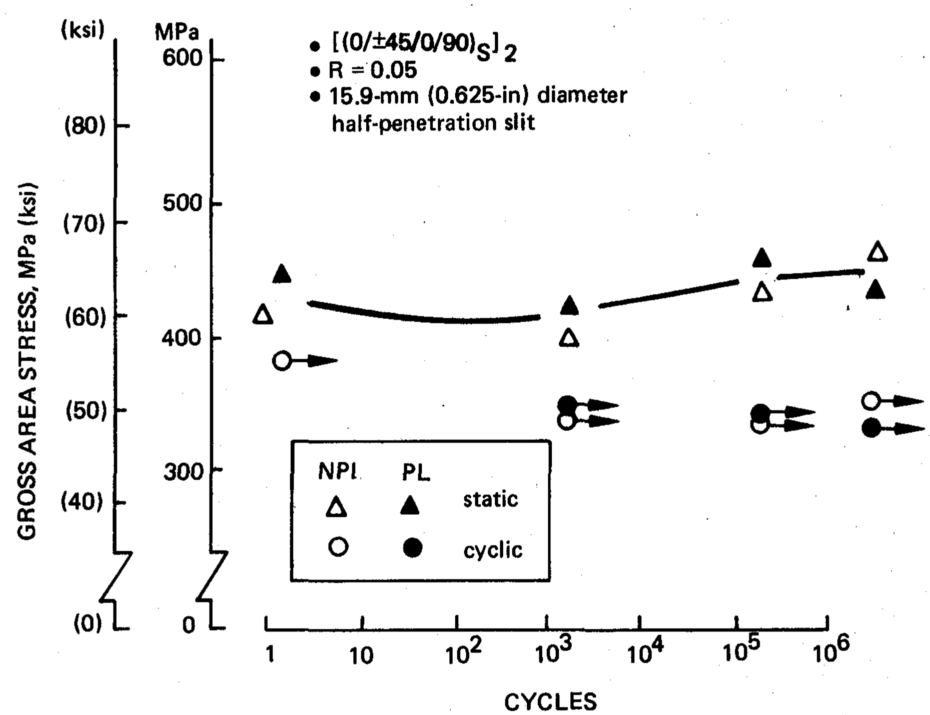

Figure 28. Fatigue Data for Laminate L1 5/8 HP Slit

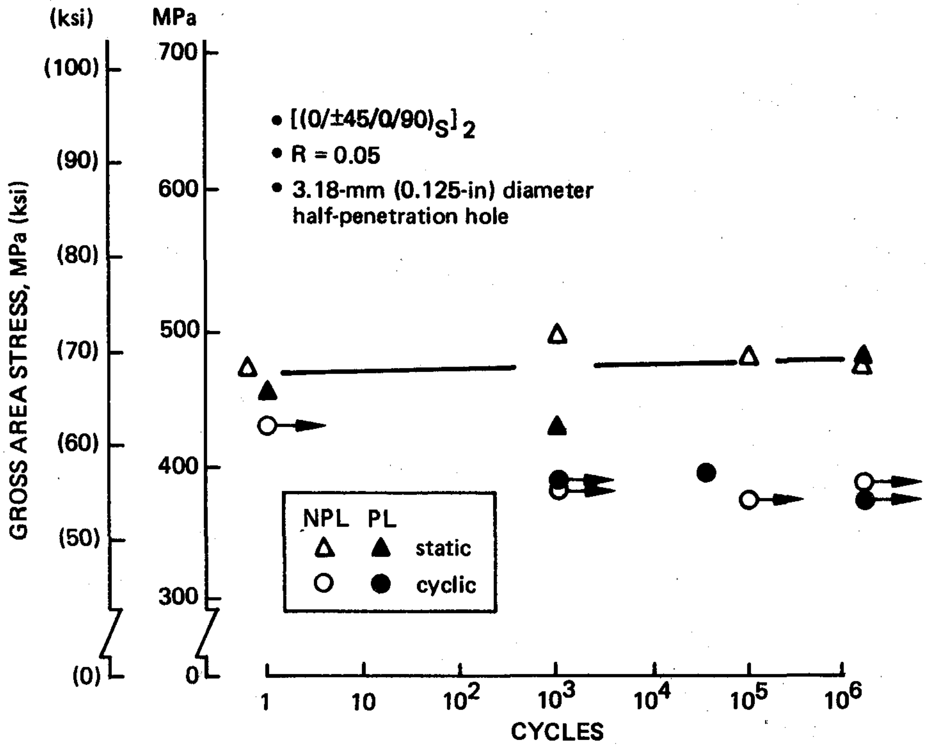

Figure 29. Fatigue Data for Laminate L1 1/8 HP Hole

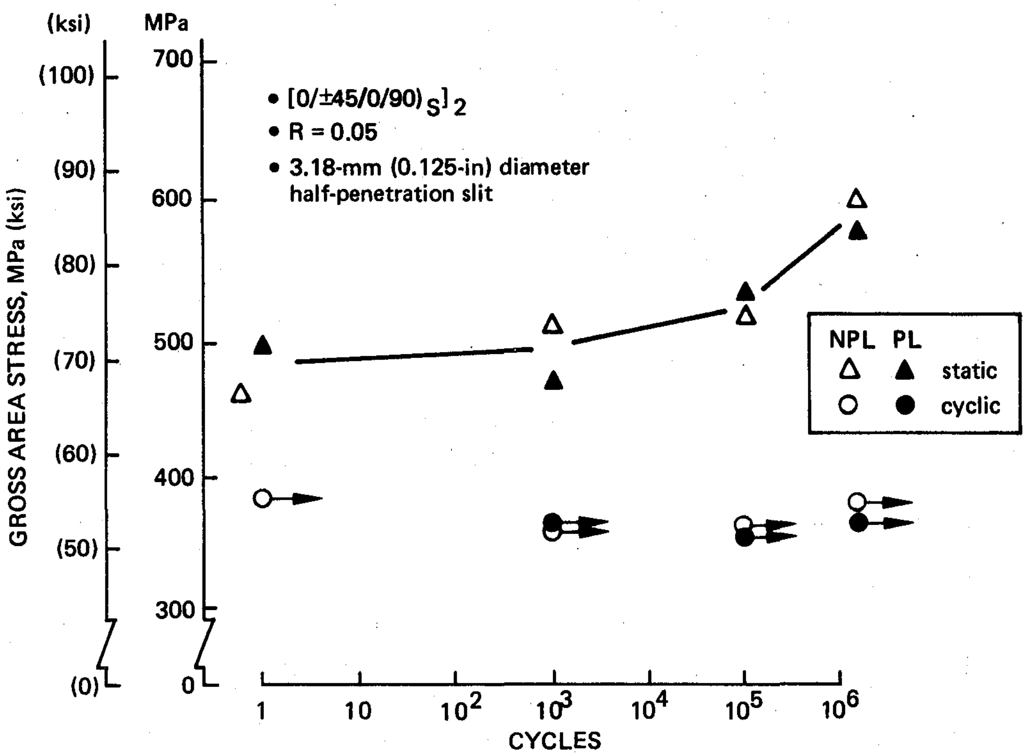

Figure 30. Fatigue Data for Laminate L1 1/8 HP Slit

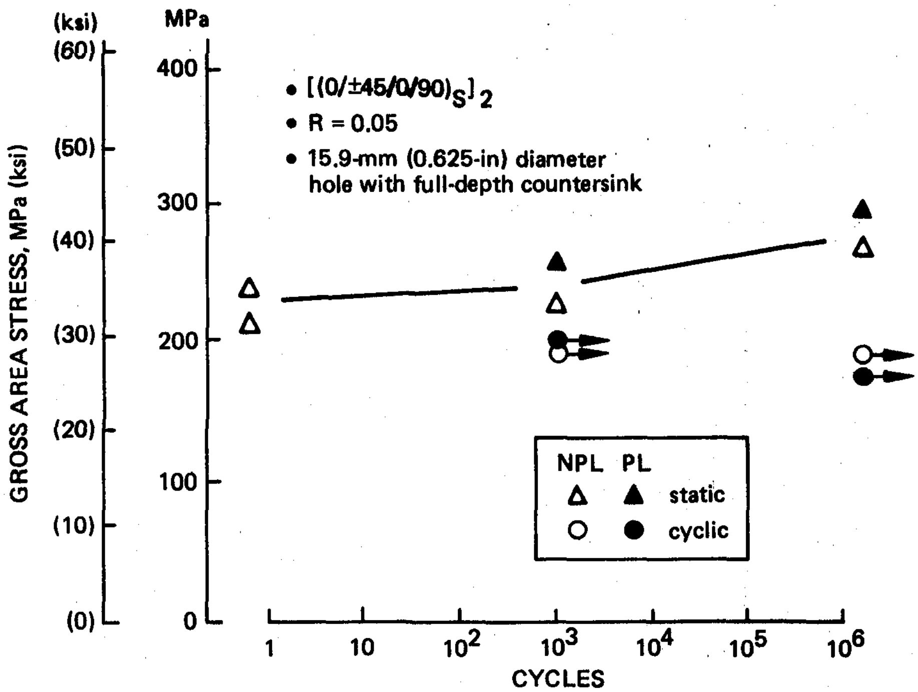

Figure 31. Fatigue Data for Laminate L1 5/8 CSK Hole

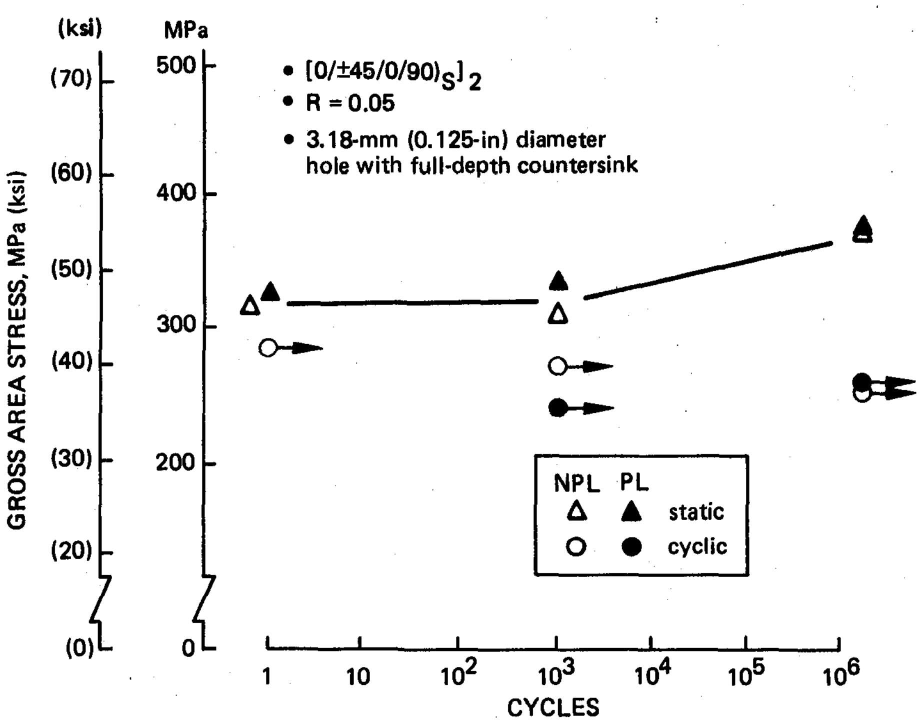

Figure 32. Fatigue Data for Laminate L1 1/8 CSK Hole

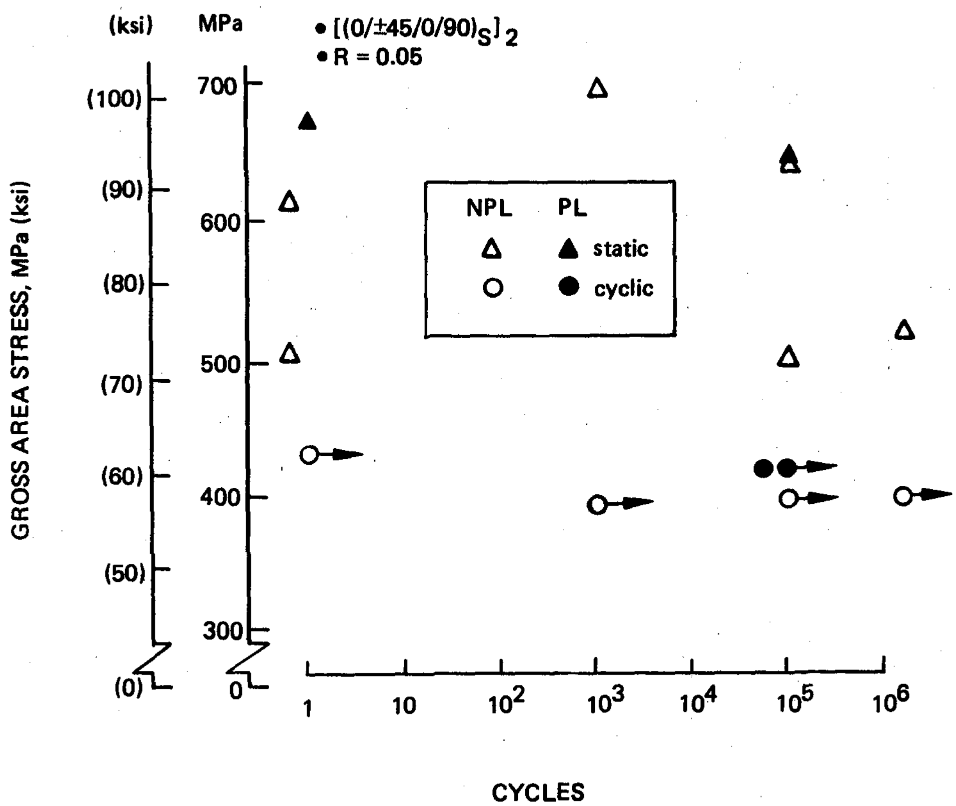

Figure 33. Fatigue Data for Laminate L1 No Initial Defect

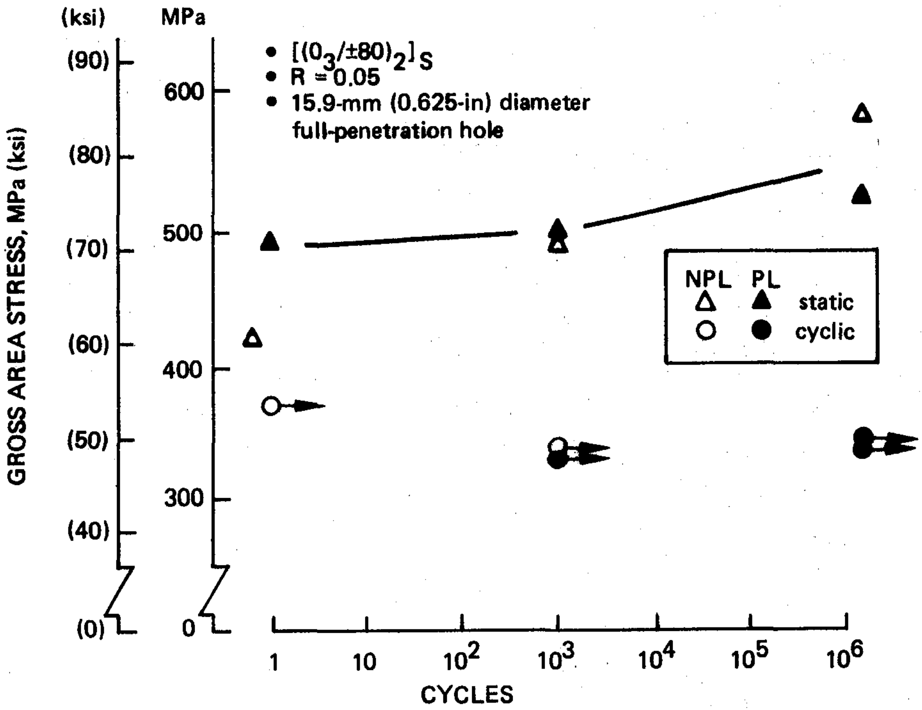

Figure 34. Fatigue Data for Laminate L2 5/8 FP Hole

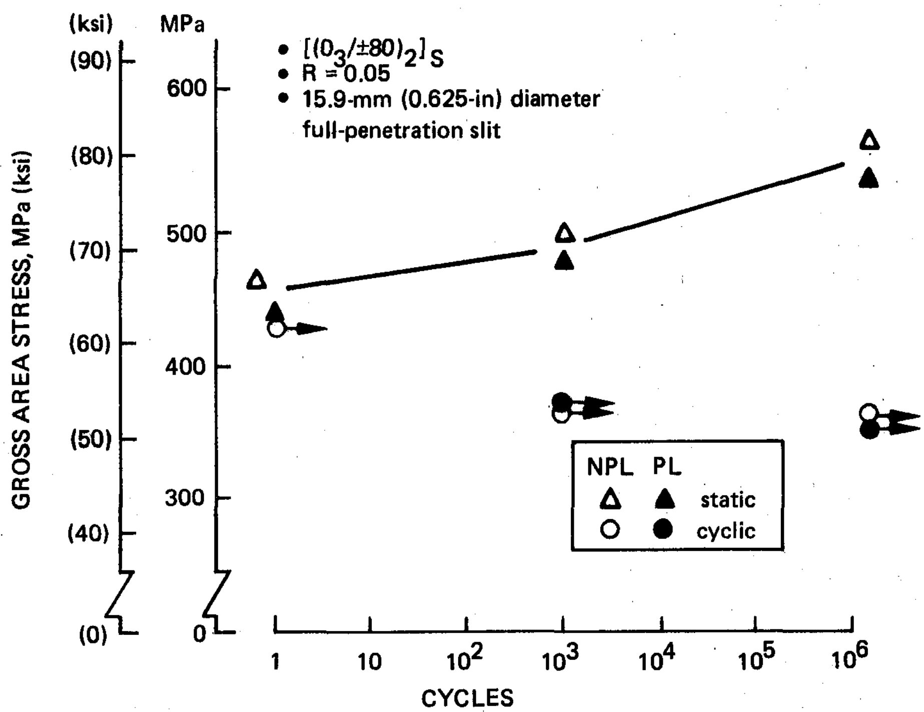

Figure 35. Fatigue Data for Laminate L2 5/8 FP Slit

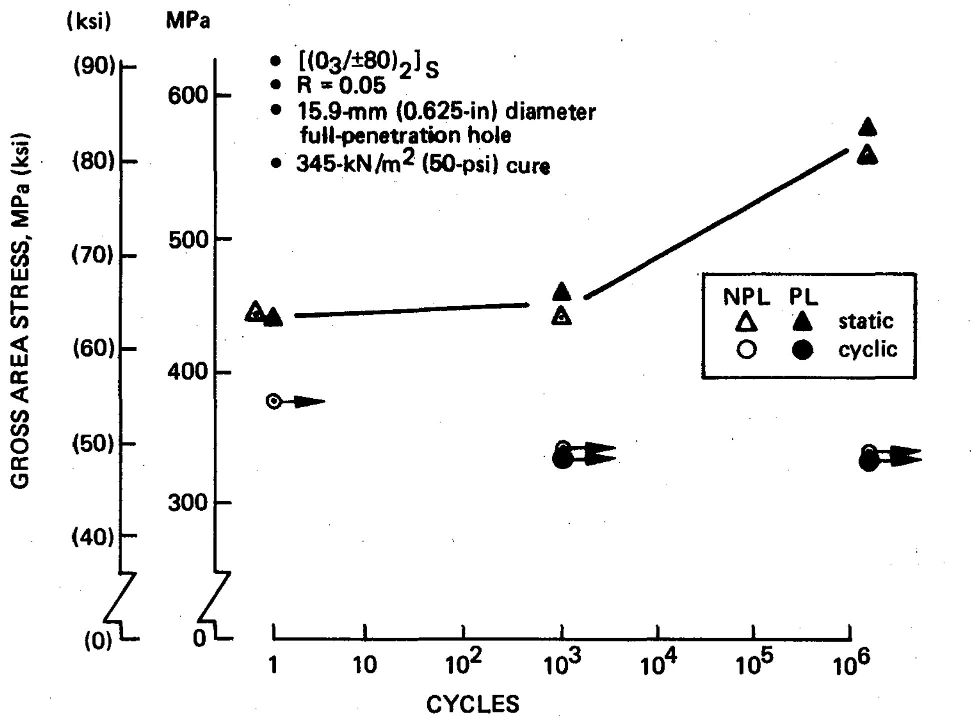

Figure 36. Fatigue Data for Laminate L2 With Low Cure Pressure and 5/8 FP Hole

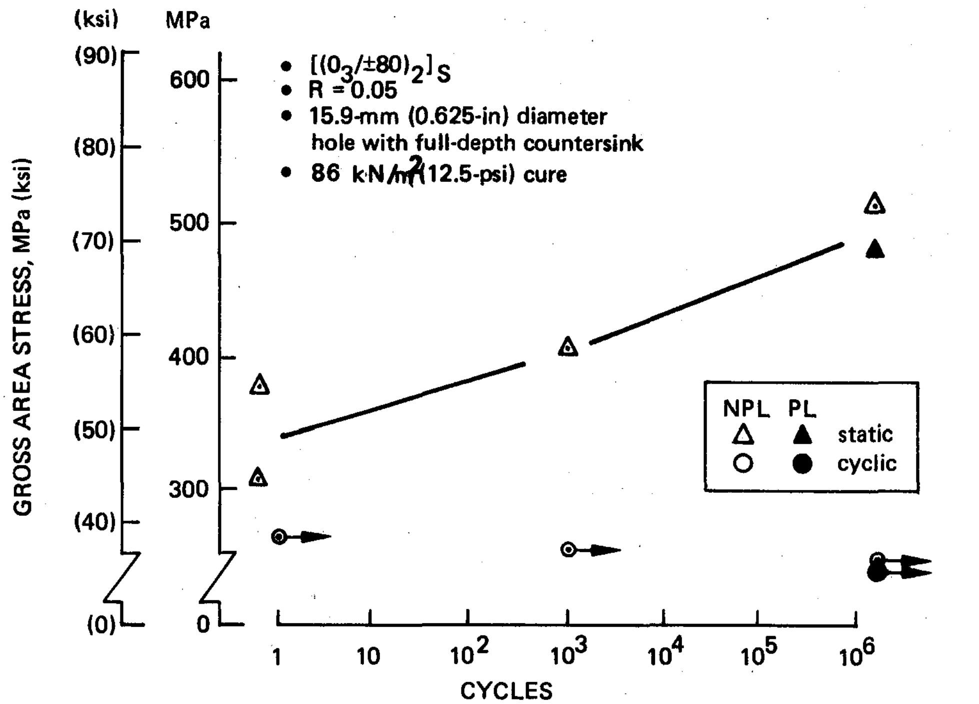

Figure 37. Fatigue Data for Laminate L2 With Low Cure Pressure and 5/8 CSK Hole

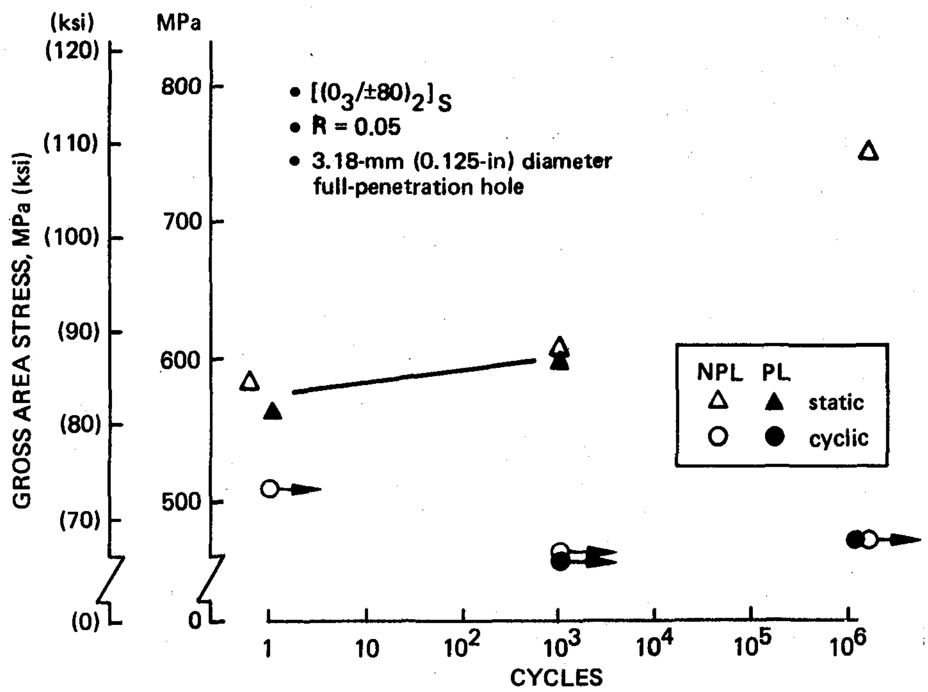

Figure 38. Fatigue Data for Laminate L2 1/8 FP Hole

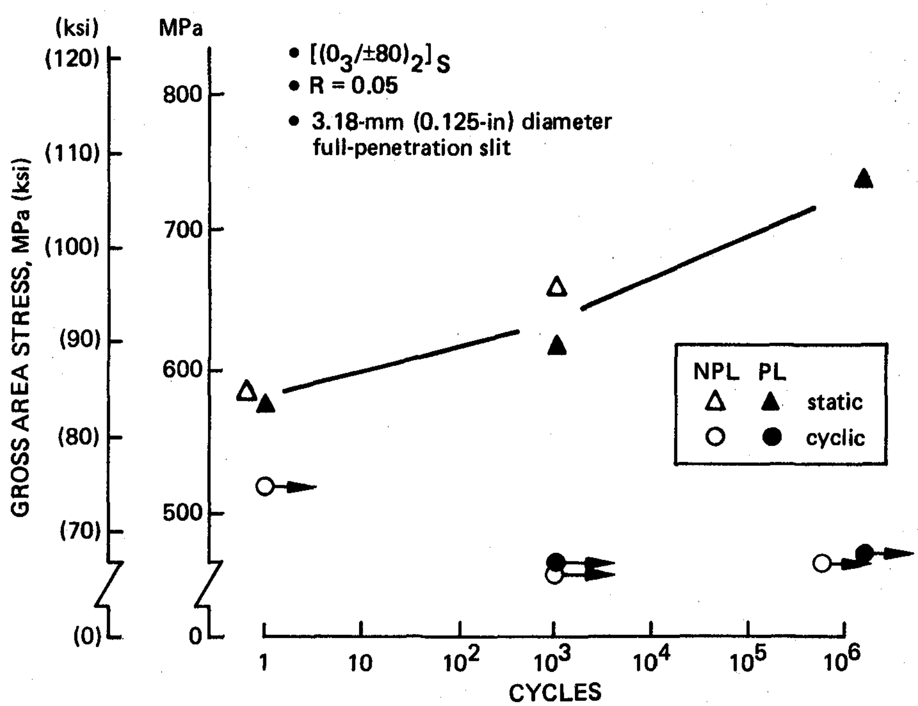

Figure 39. Fatigue Data for Laminate L2 1/8 FP Slit

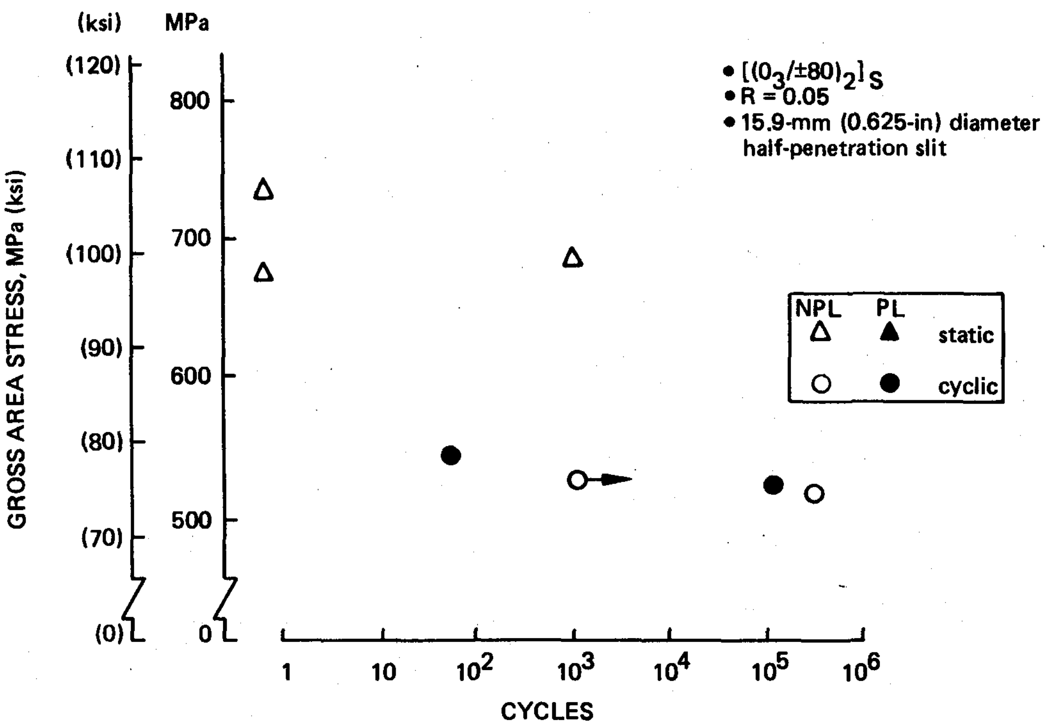

Figure 40. Fatigue Data for Laminate L2 5/8 HP Slit

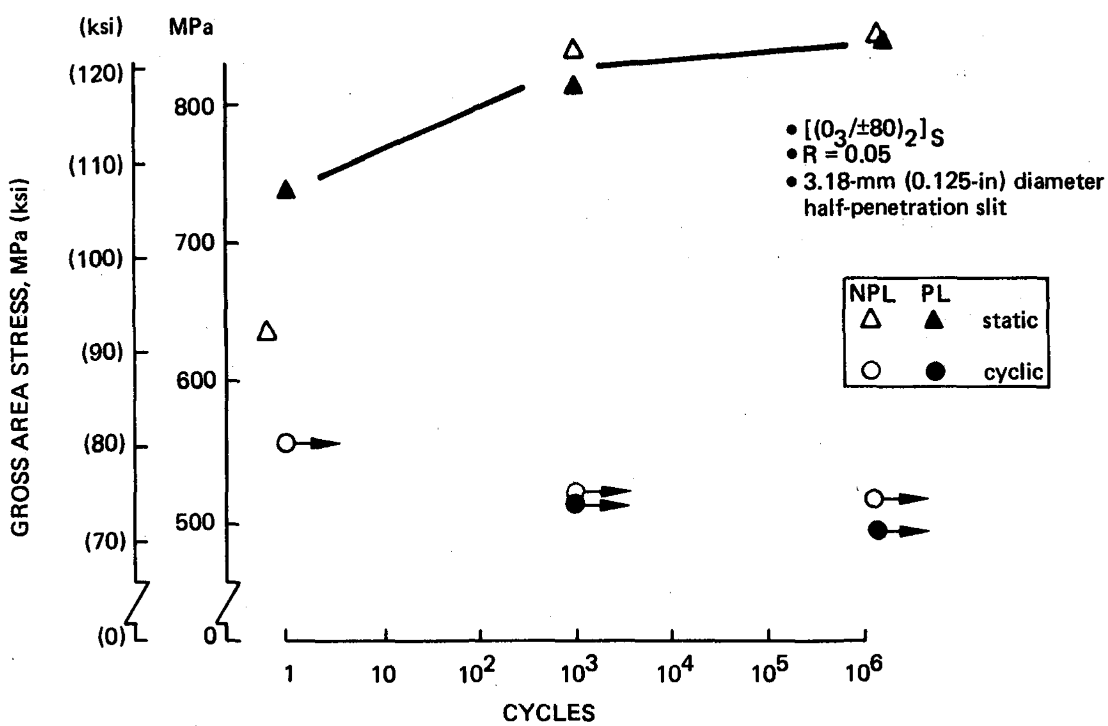

Figure 41. Fatigue Data for Laminate L2 1/8 HP Slit

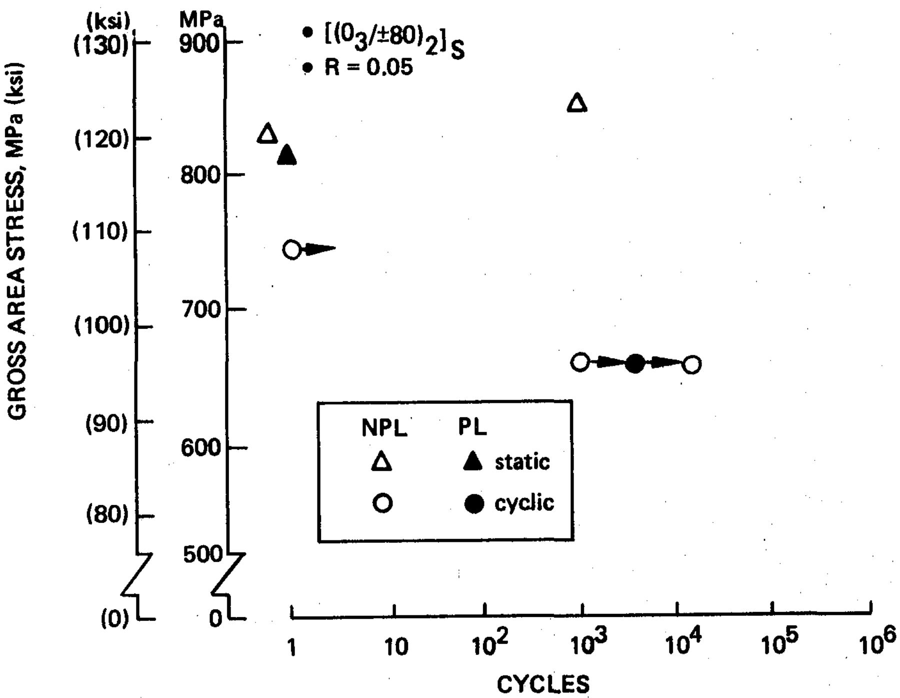

Figure 42. Fatigue Data for Laminate L2 Specimens With No Initial Defect

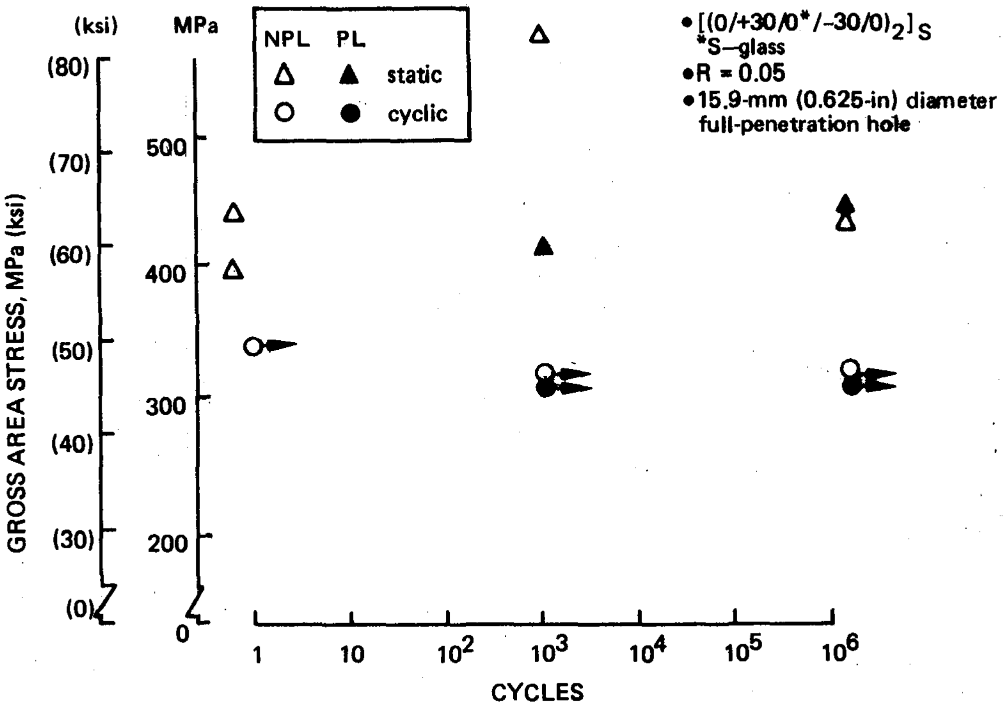

Figure 43. Fatigue Data for Laminate L3 5/8 FP Hole

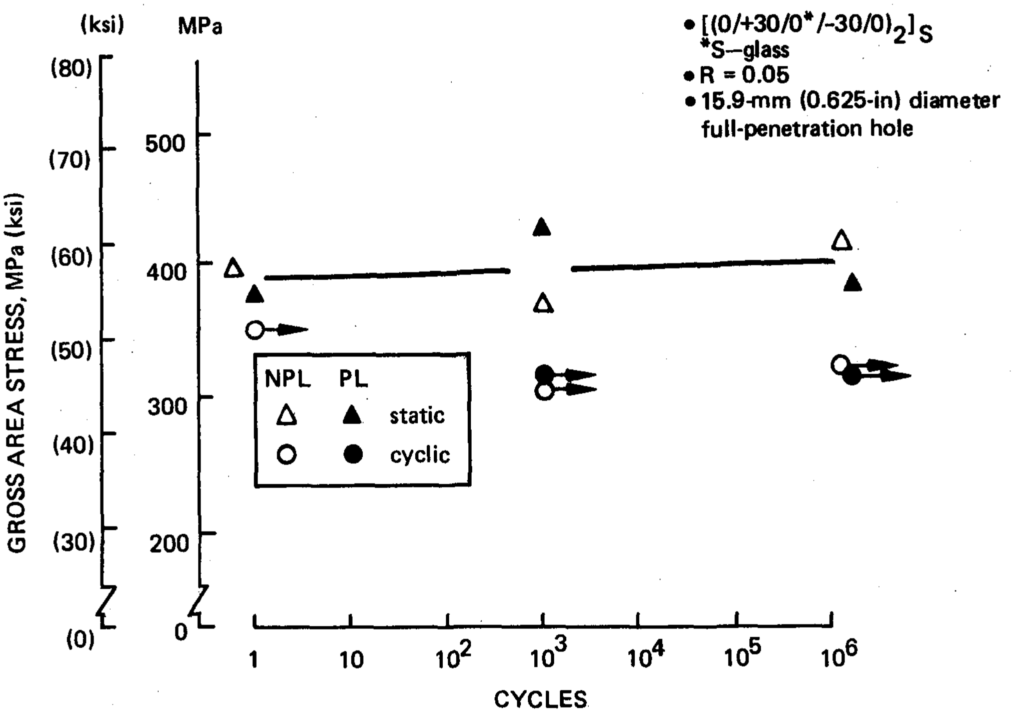

Figure 44. Fatigue Data for Laminate L3 5/8 FP Slit

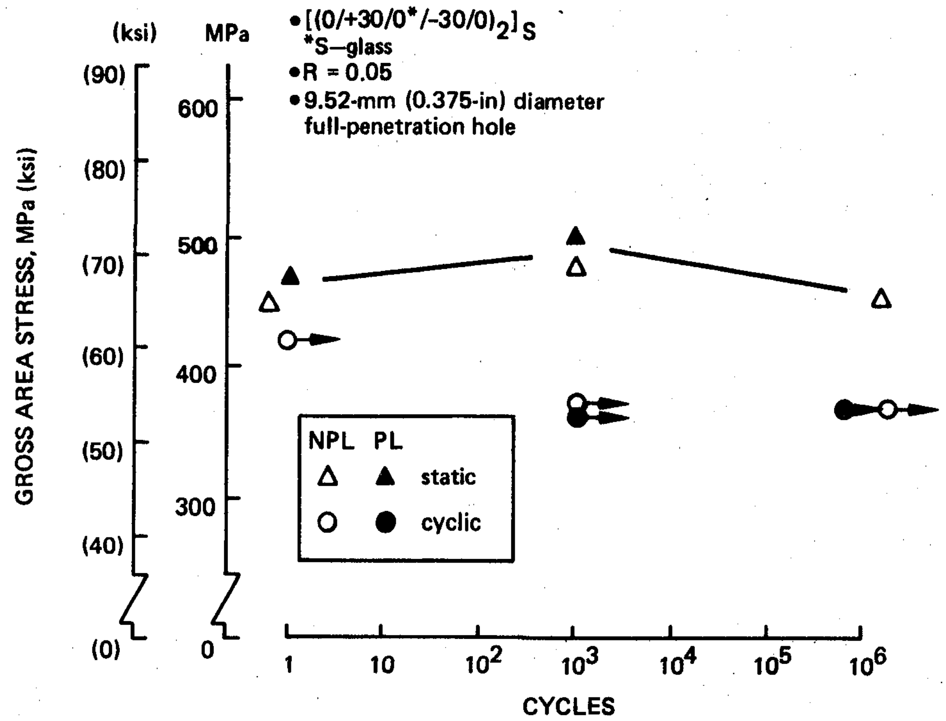

Figure 45. Fatigue Data for Laminate L3 3/8 FP Hole

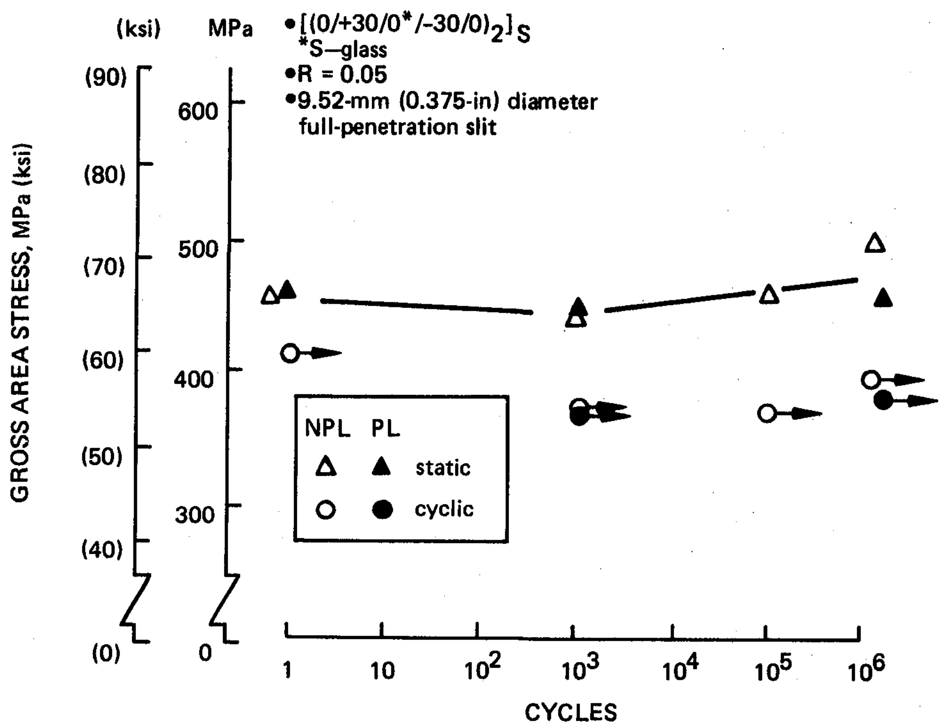

Figure 46. Fatigue Data for Laminate L3 3/8 FP Slit

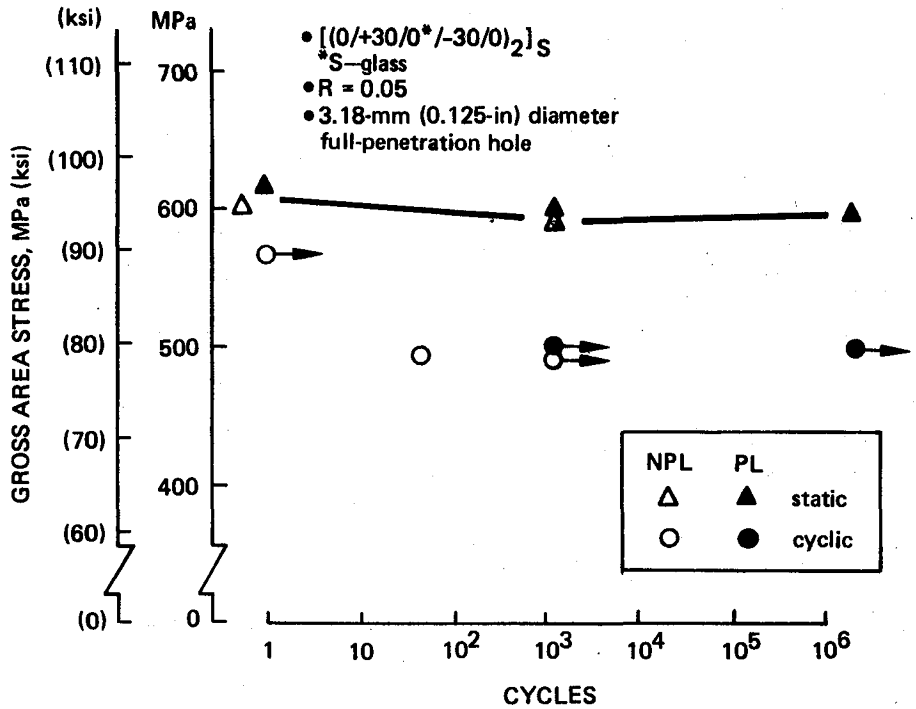

Figure 47. Fatigue Data for Laminate L3 1/8 FP Hole

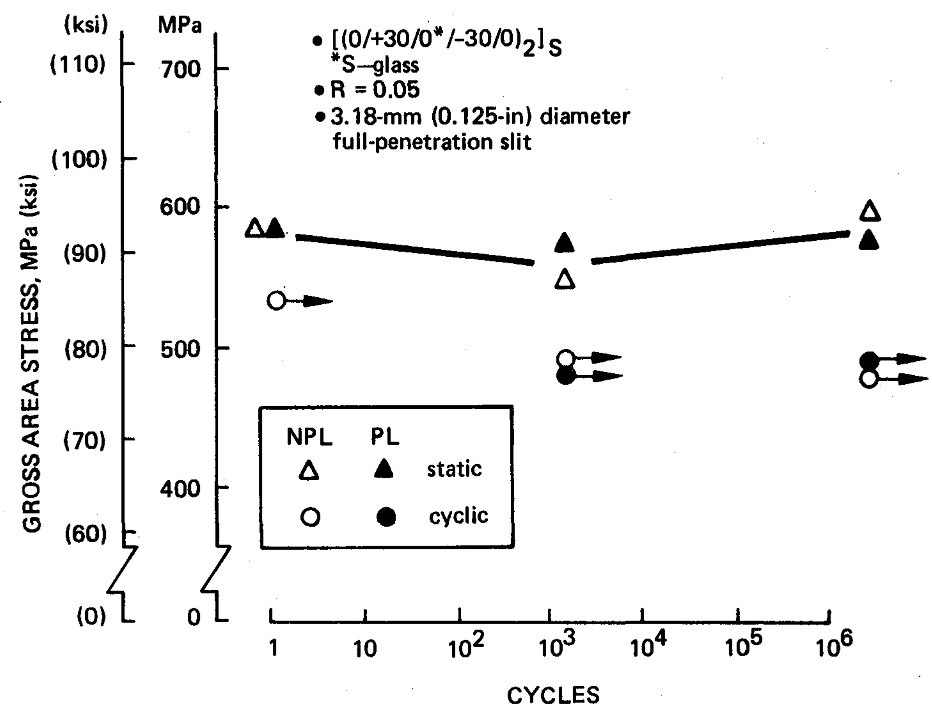

Figure 48. Fatigue Data for Laminate L3 1/8 FP Slit

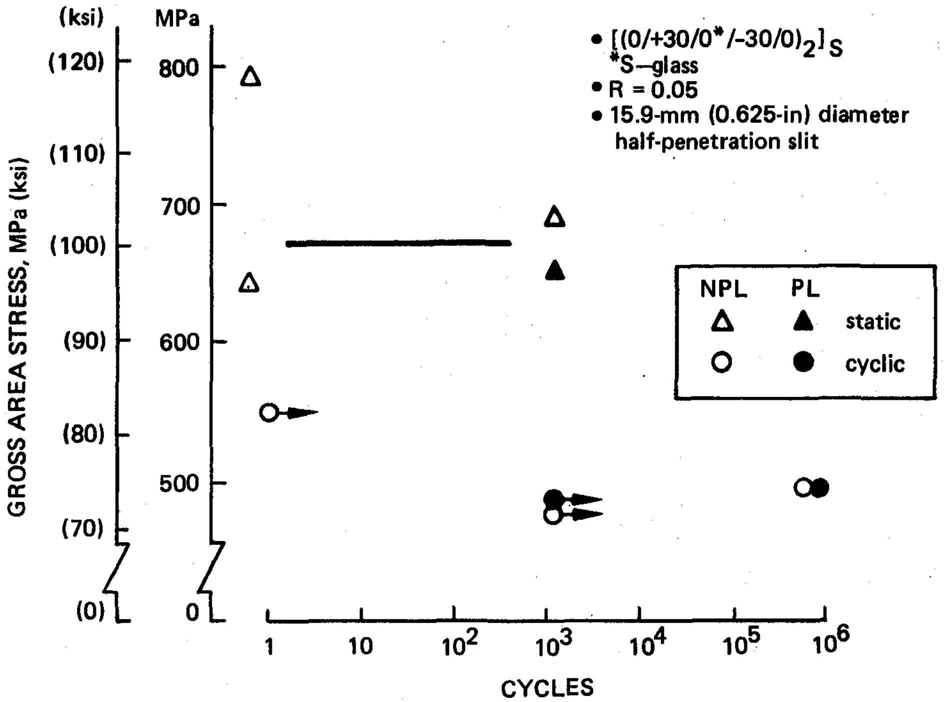

Figure 49. Fatigue Data for Laminate L3 5/8 HP Slit

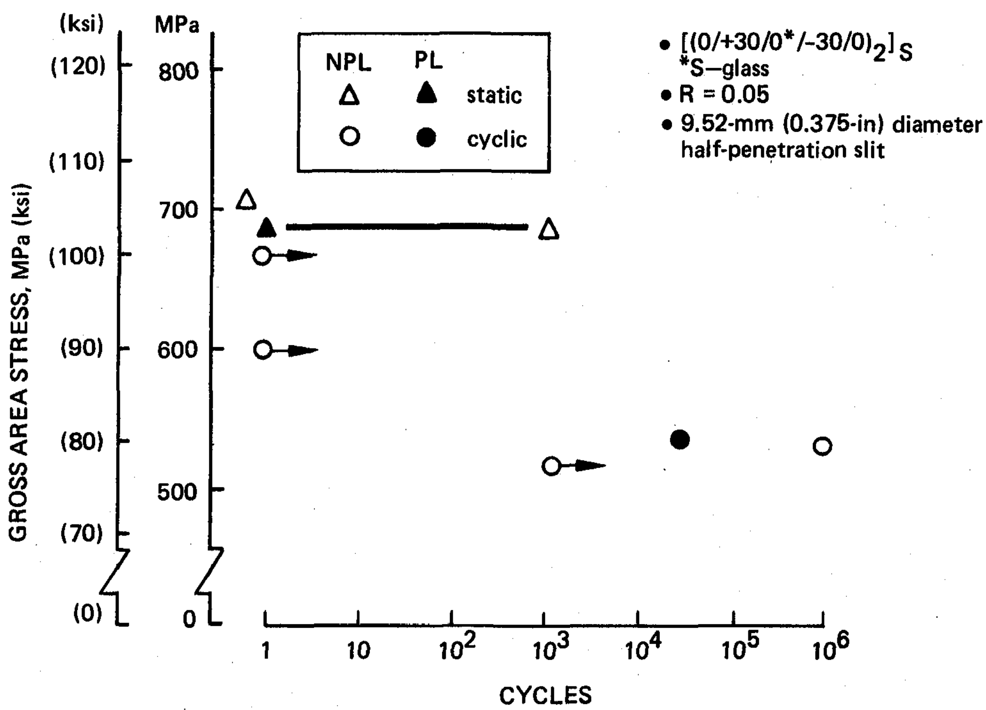

Figure 50. Fatigue Data for Laminate L3 3/8 HP Slit

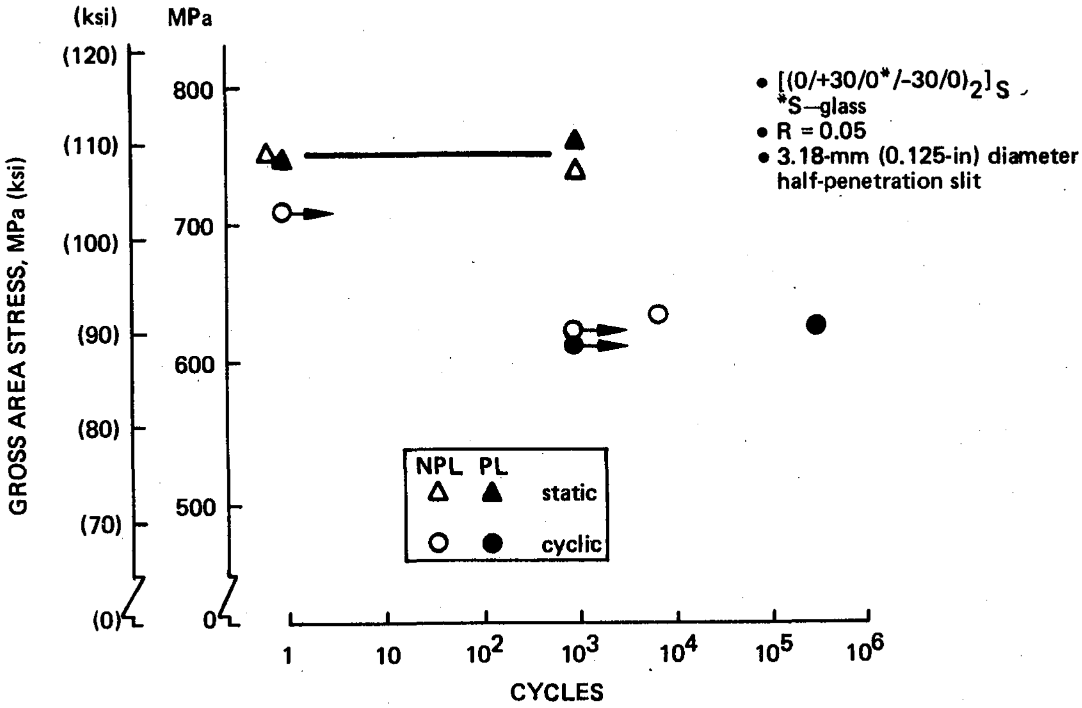

Figure 51. Fatigue Data for Laminate L3 1/8 HP Slit

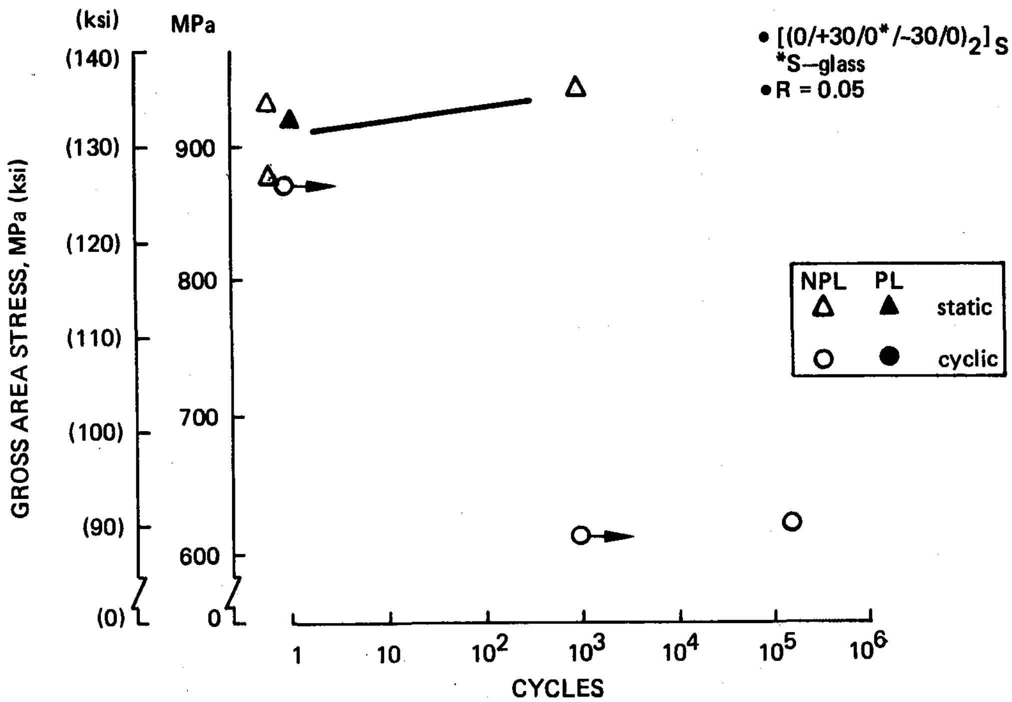

Figure 52. Fatigue Data for Laminate L3 With No Initial Defect

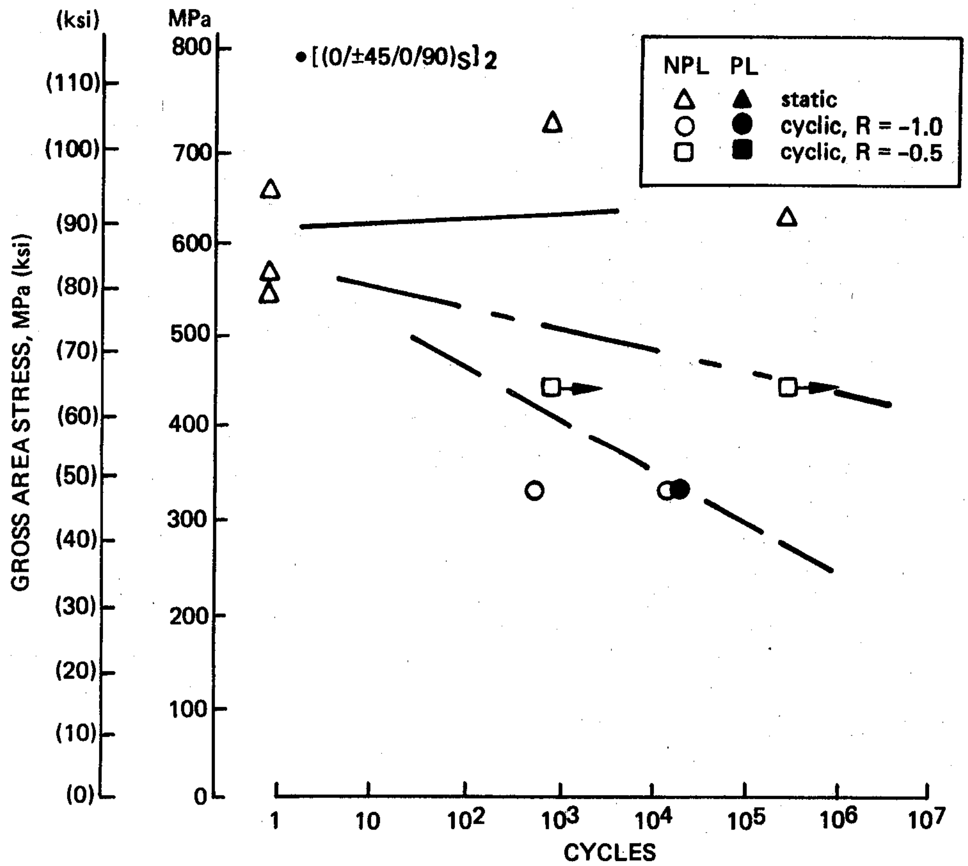

Figure 53. Tension Compression Fatigue Data for Laminate L1, No Initial Defect

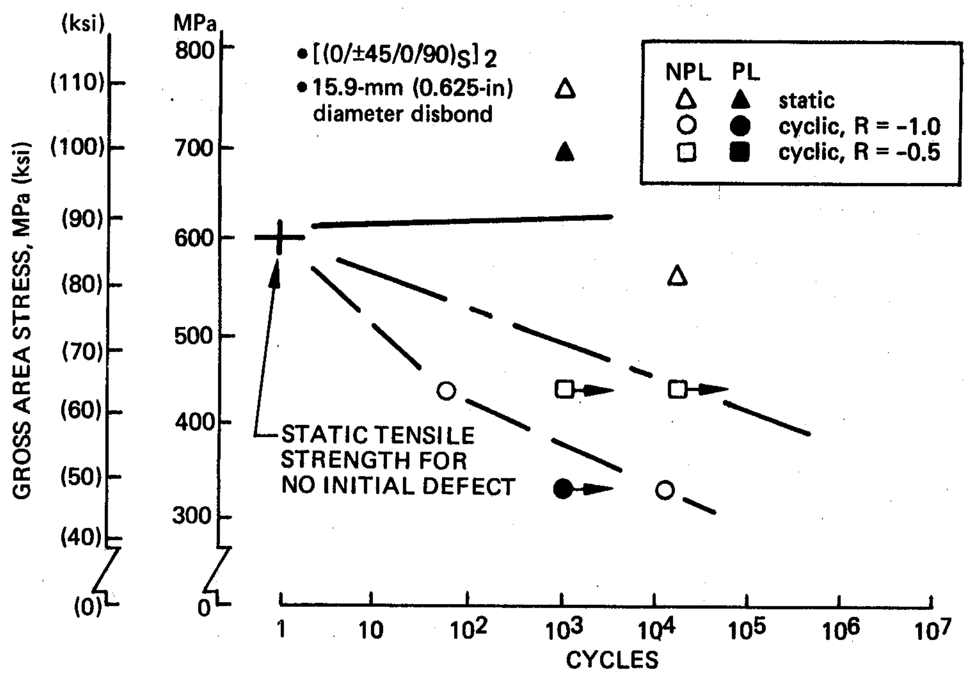

Figure 54. Tension Compression Fatigue Data for Laminate L1, Disbond Defect

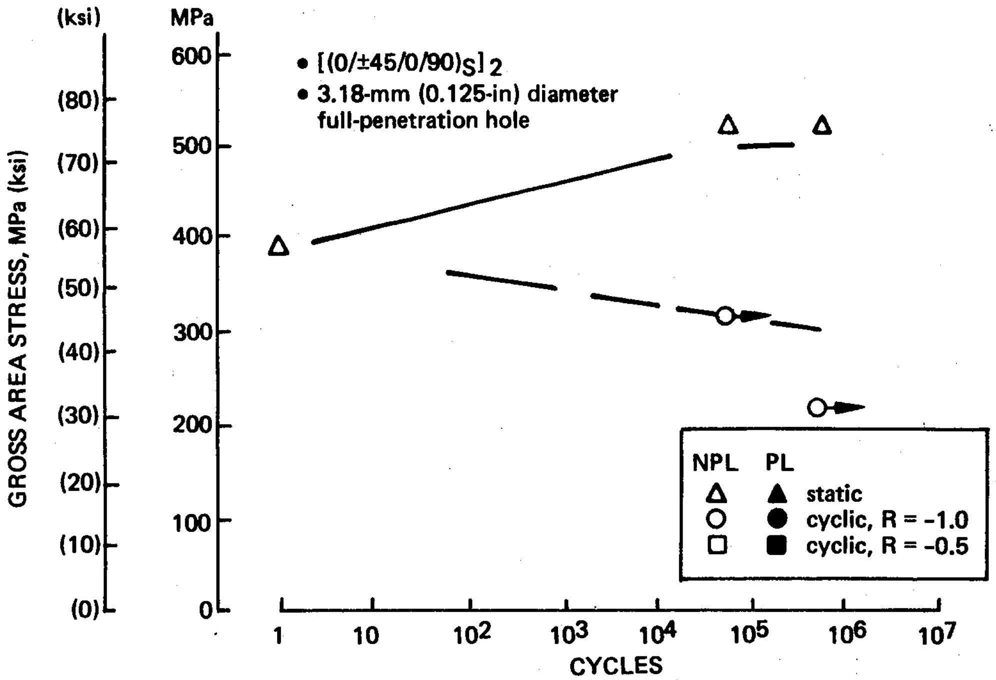

Figure 55. Tension Compression Fatigue Data for Laminate L1,1/8 FP Hole

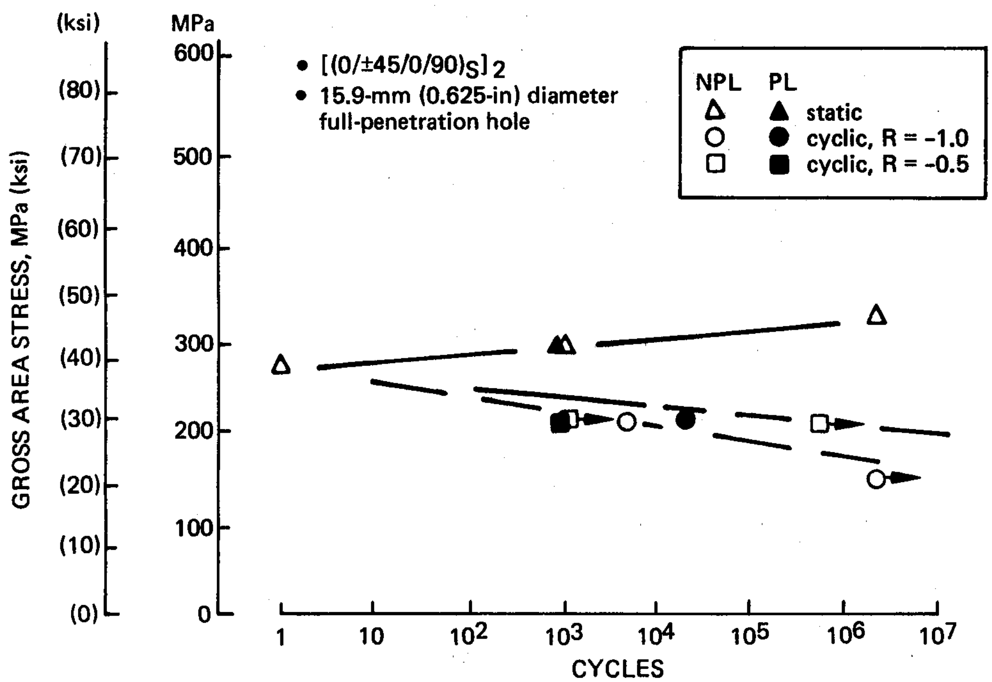

Figure 56. Tension Compression Fatigue Data for Laminate L1,5/8 FP Hole

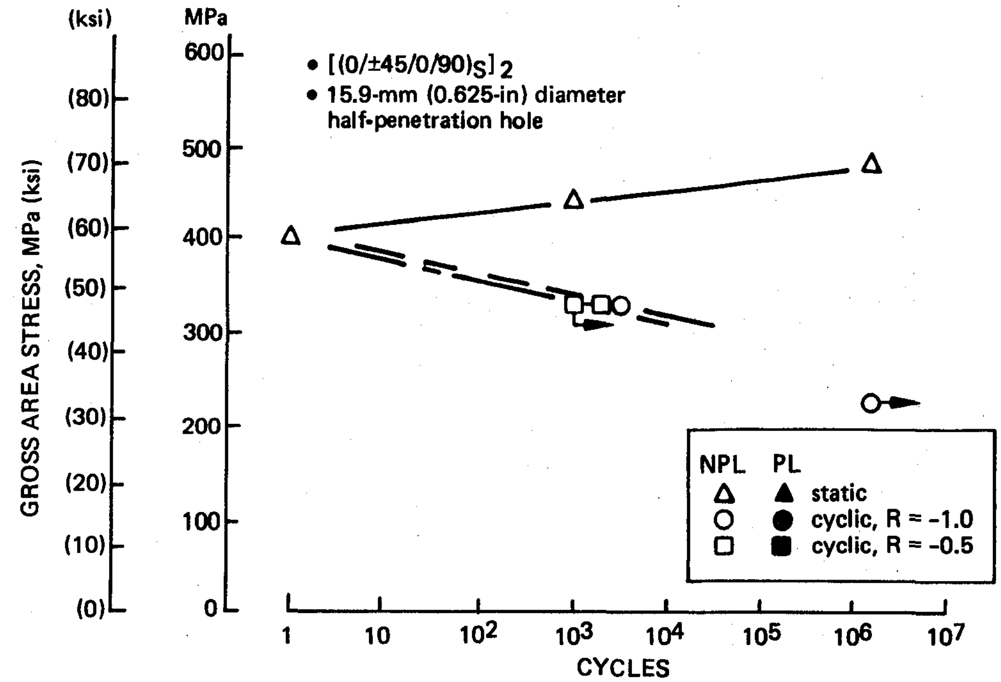

Figure 57. Tension Compression Fatigue Data for Laminate L1, 5/8 HP Hole

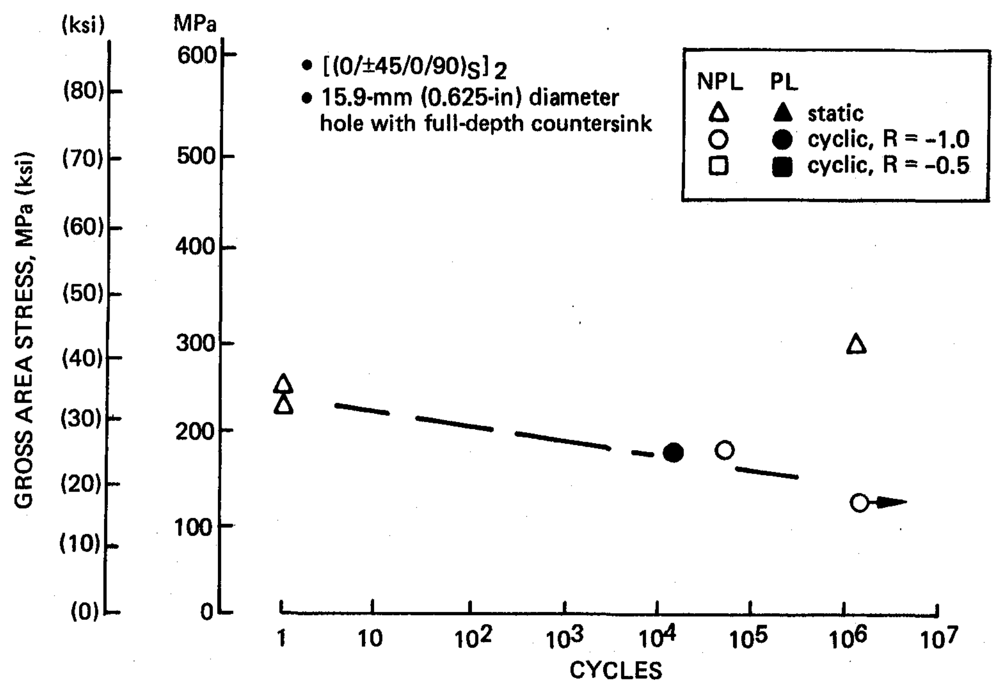

Figure 58. Tension Compression Fatigue Data for Laminate L1,5/8 CSK Hole

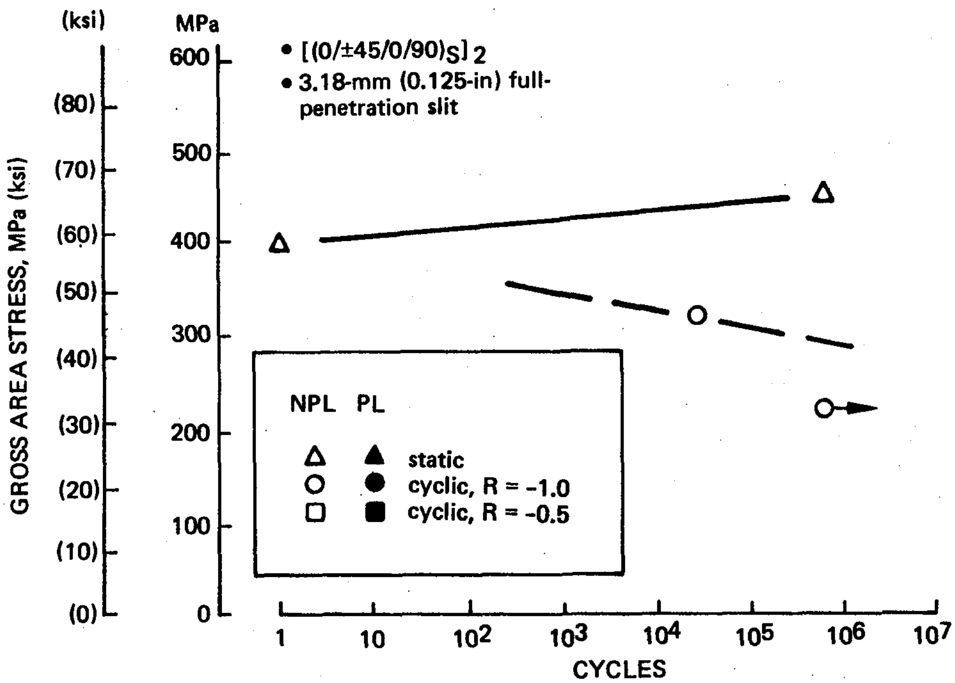

Figure 59. Tension Compression Fatigue Data for Laminate L1,1/8 FP Slit

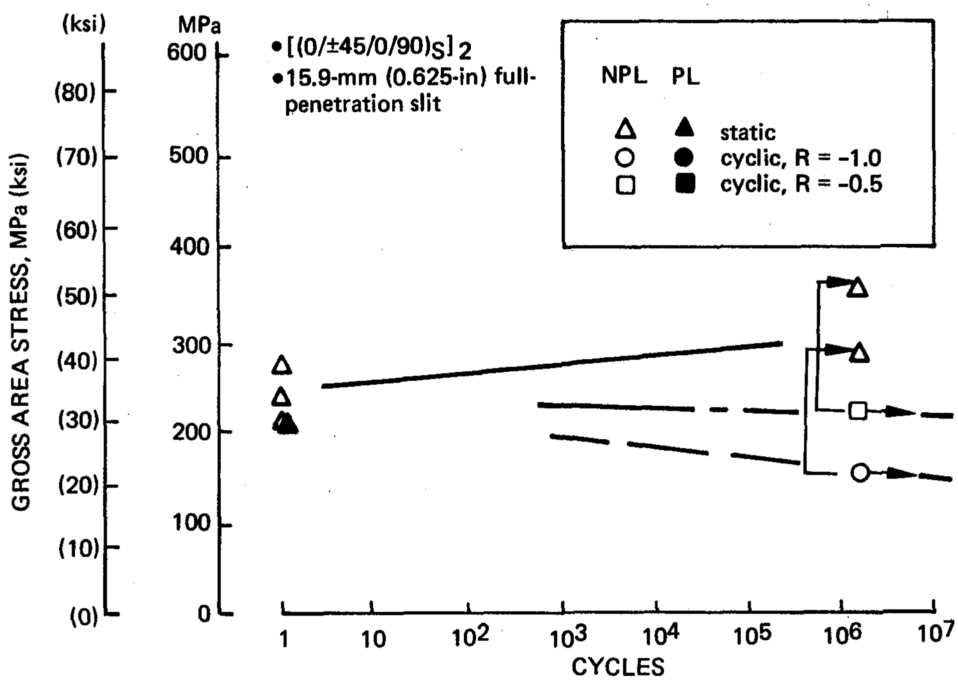

Figure 60. Tension Compression Fatigue Data for Laminate L1, 5/8 FP Slit

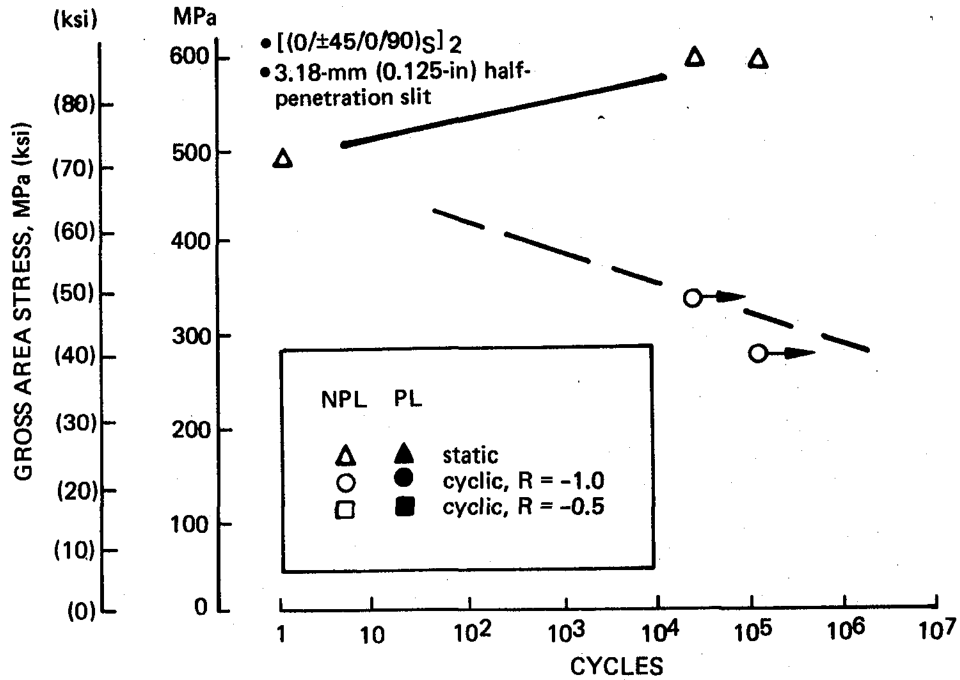

Figure 61. Tension Compression Fatigue Data for Laminate L1, 1/8 HP Slit

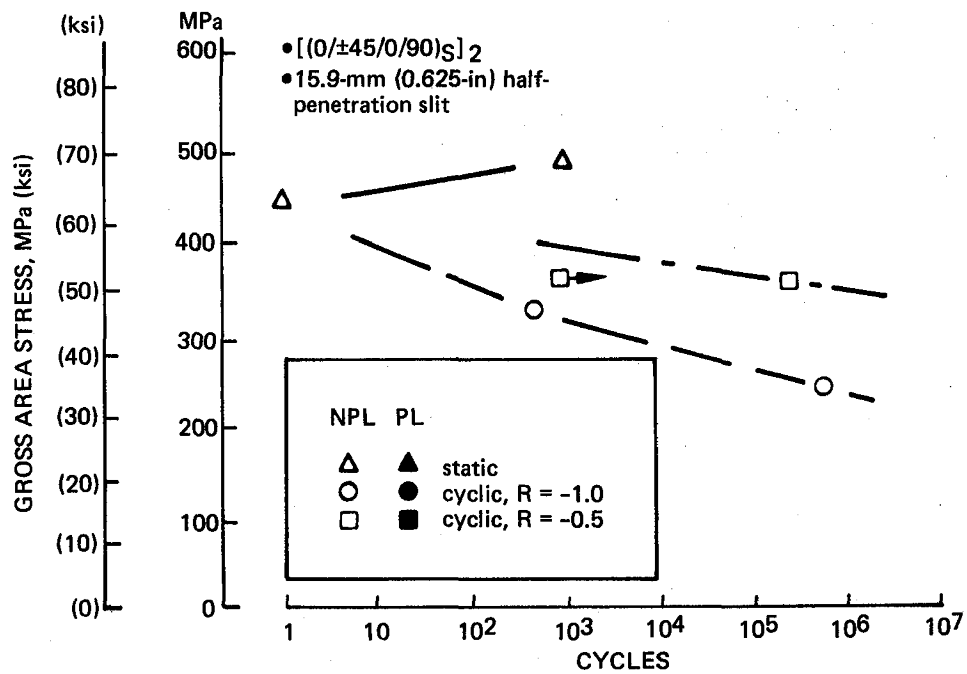

Figure 62. Tension Compression Fatigue Data for Laminate L1, 5/8 HP Slit

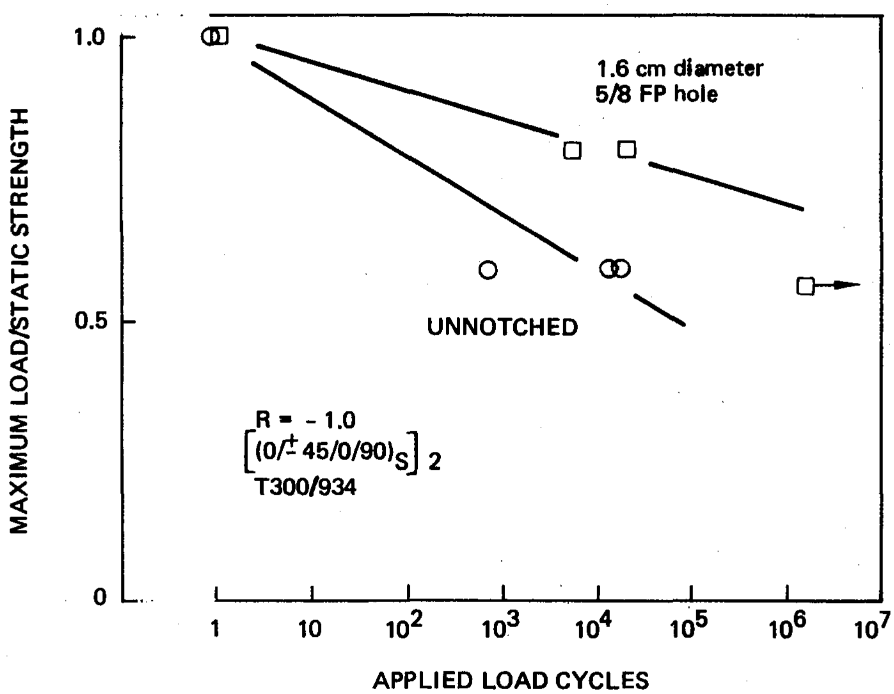

Figure 63. Relative Fatigue Behavior of Unnotched and Circular Hole Flawed Specimens

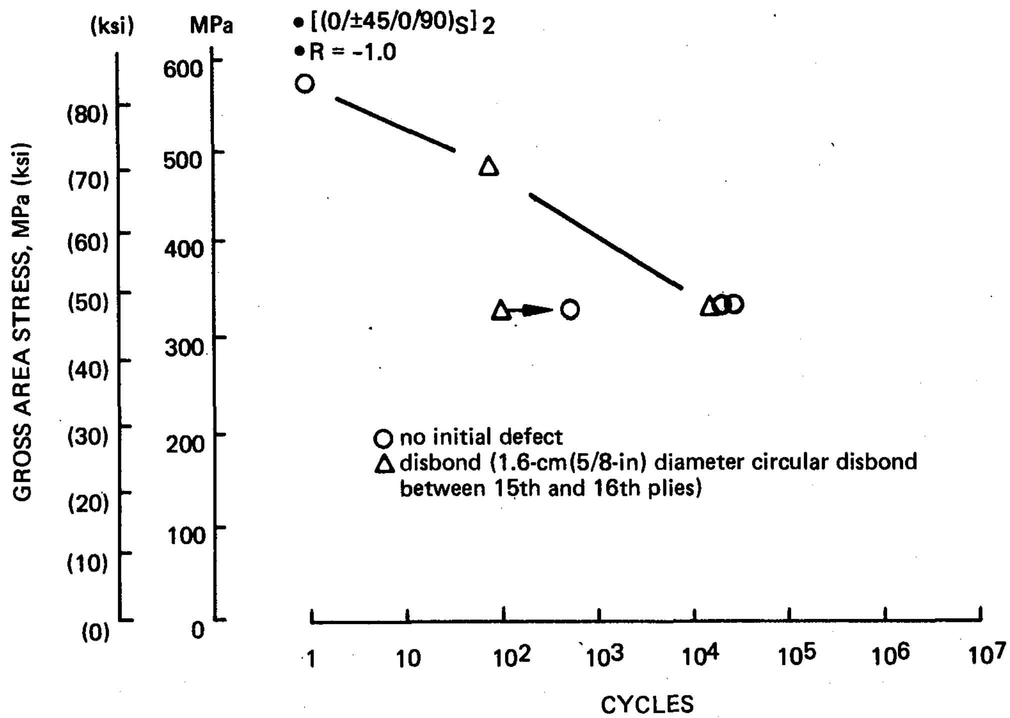

Figure 64. Comparison of Circular Disbond and No Initial Defects

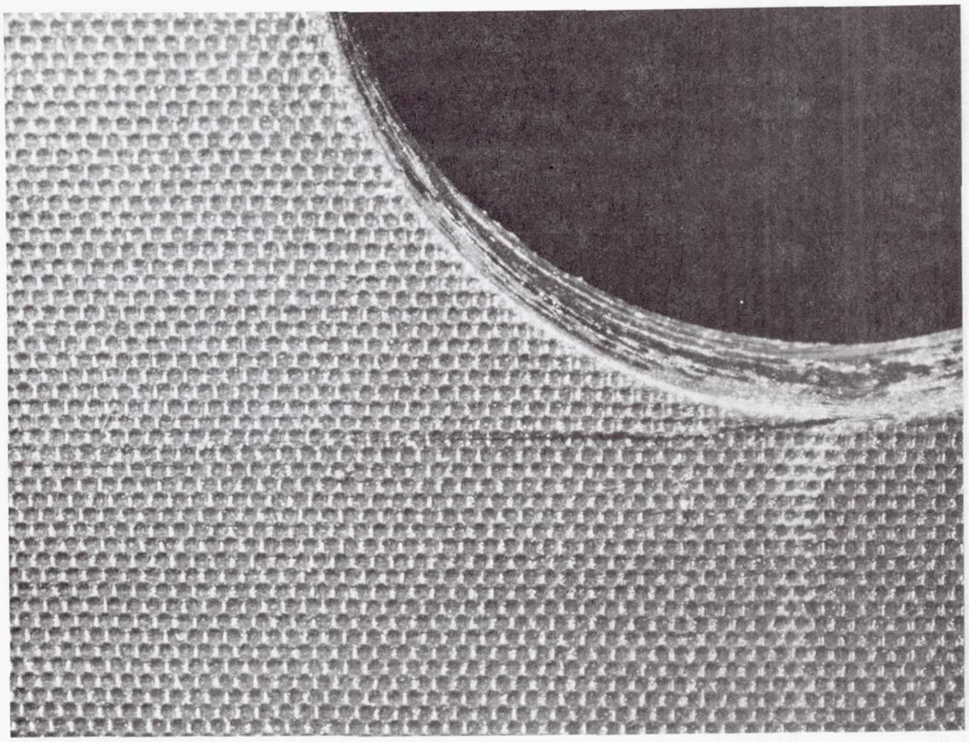

Figure 65. Laminate L2 Fatigue Test Specimen – 5/8 FP Hole, 10^3 Cycles

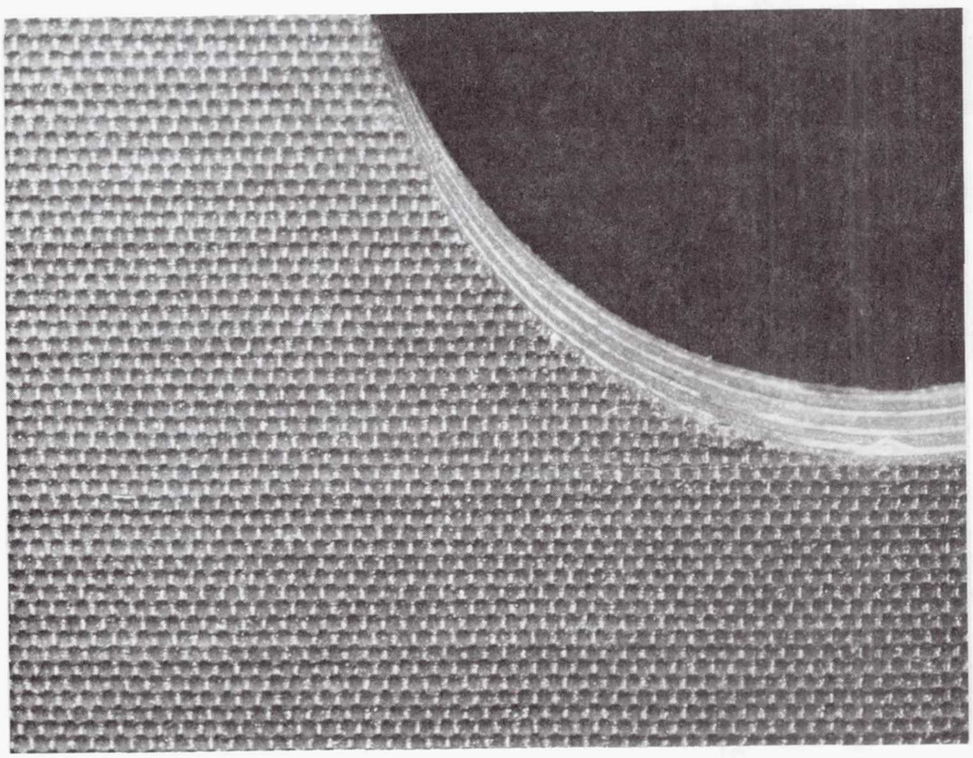

Figure 66. Laminate L3 Fatigue Test Specimen – 5/8 FP Hole, 1.5×10^6 Cycles

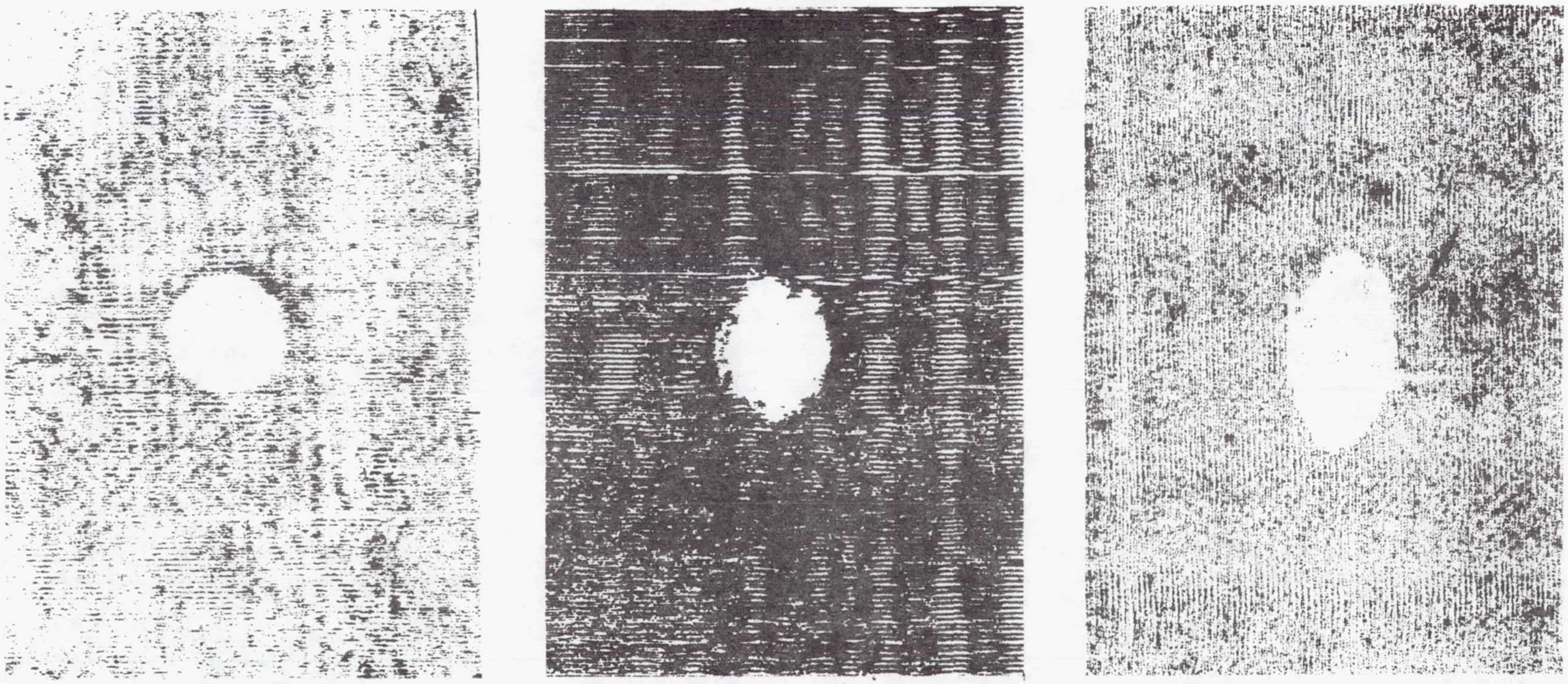

- Specimen L1- 6 · 3
- 15.8-mm (0.625-in)-dia half-penetration hole

Figure 67. Ultrasonic Scan Records of Laminate L1 Specimen Containing 5/8 HP Hole

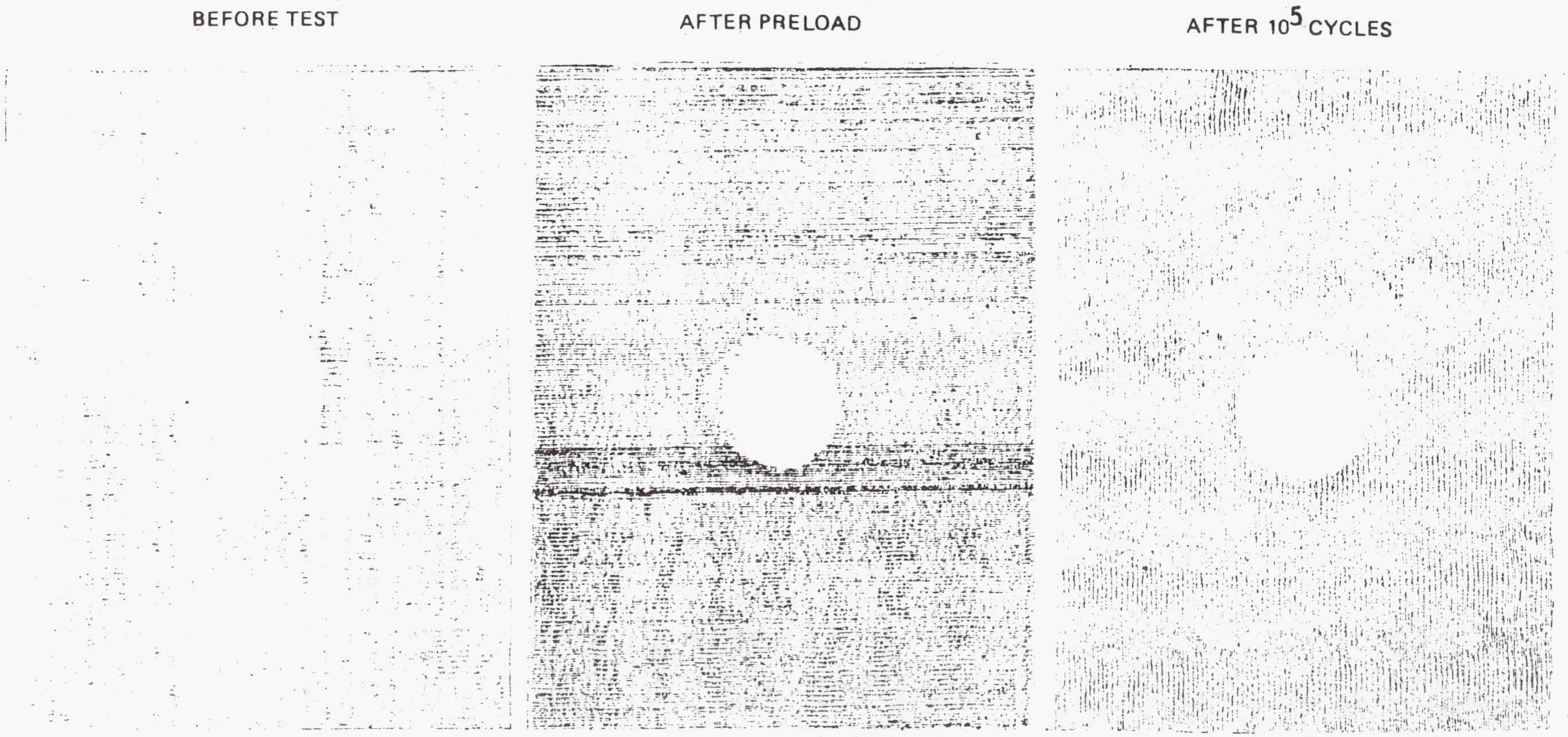

- Specimen L1-5-9
- 15.8-mm (0.625-in)-dia half-penetration hole

Figure 68. Ultrasonic Scan Records of Laminate L1 Specimen Containing 5/8 FP Hole

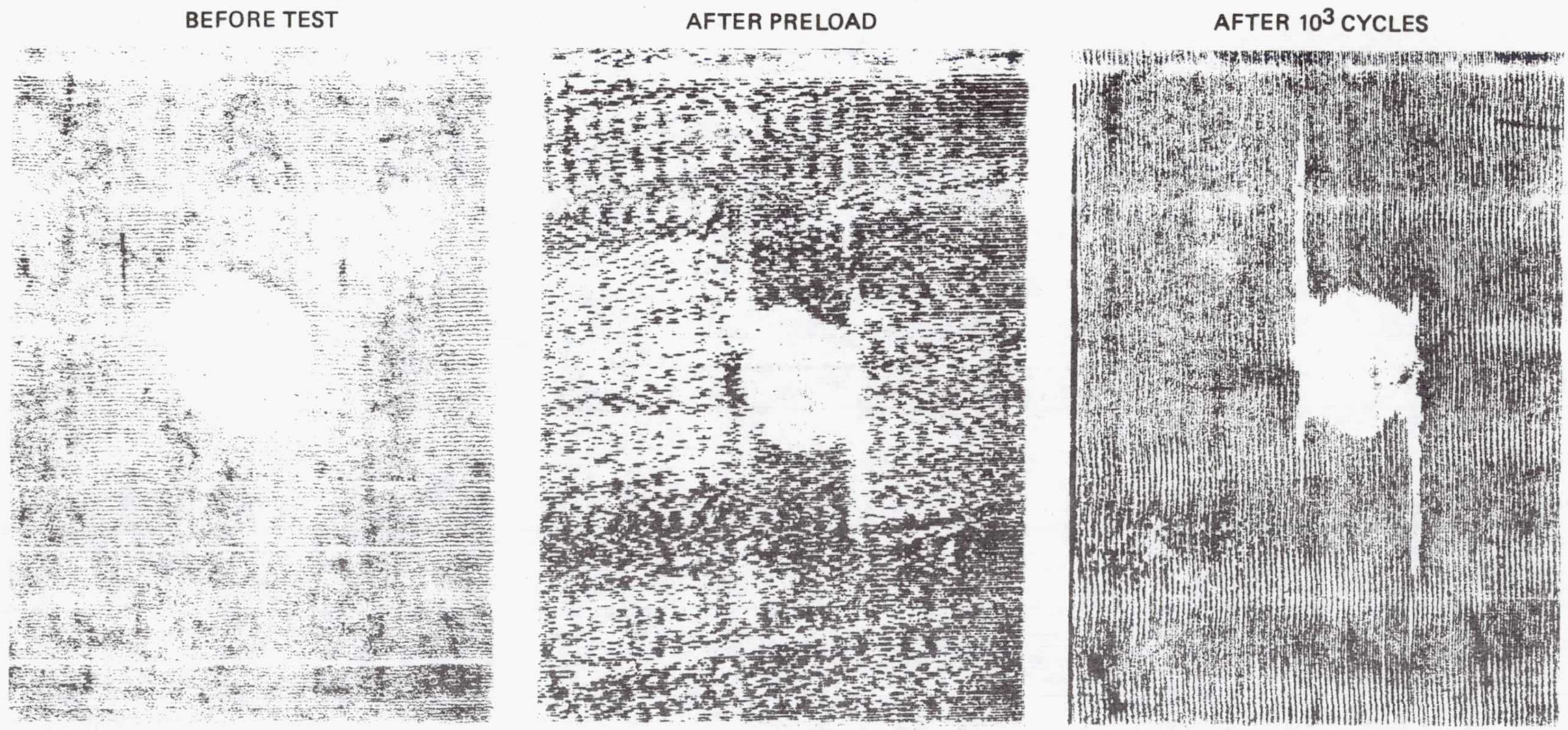

- Specimen L2-1-32
- 15.8-mm (0.625-in)-dia full-penetration hole

Figure 69. Ultrasonic Scan Records of Laminate L2 Specimen Containing 5/8 FP Hole

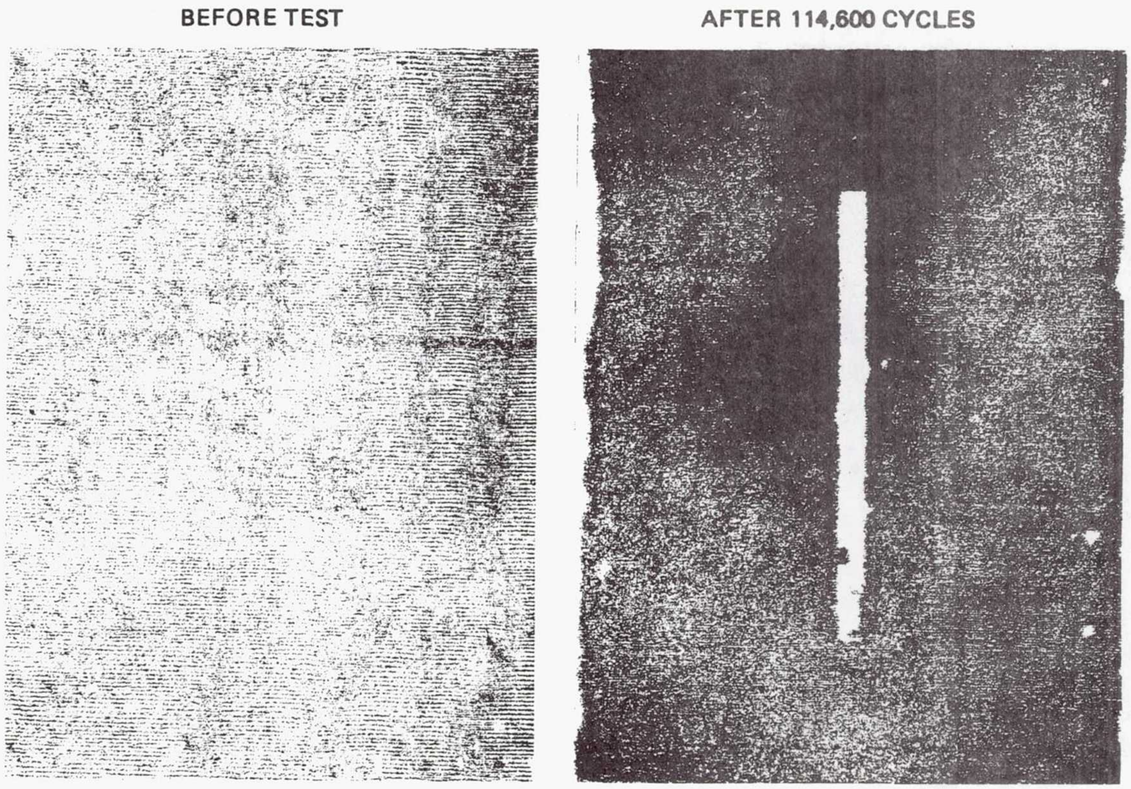

- Specimen L1-10-27
- 3.18 mm(0.125-in) half-penetration slit

Figure 70. Ultrasonic Scan Record for Laminate L1 Tension-Compression Fatigue Test Specimen 1/8 HP Slit

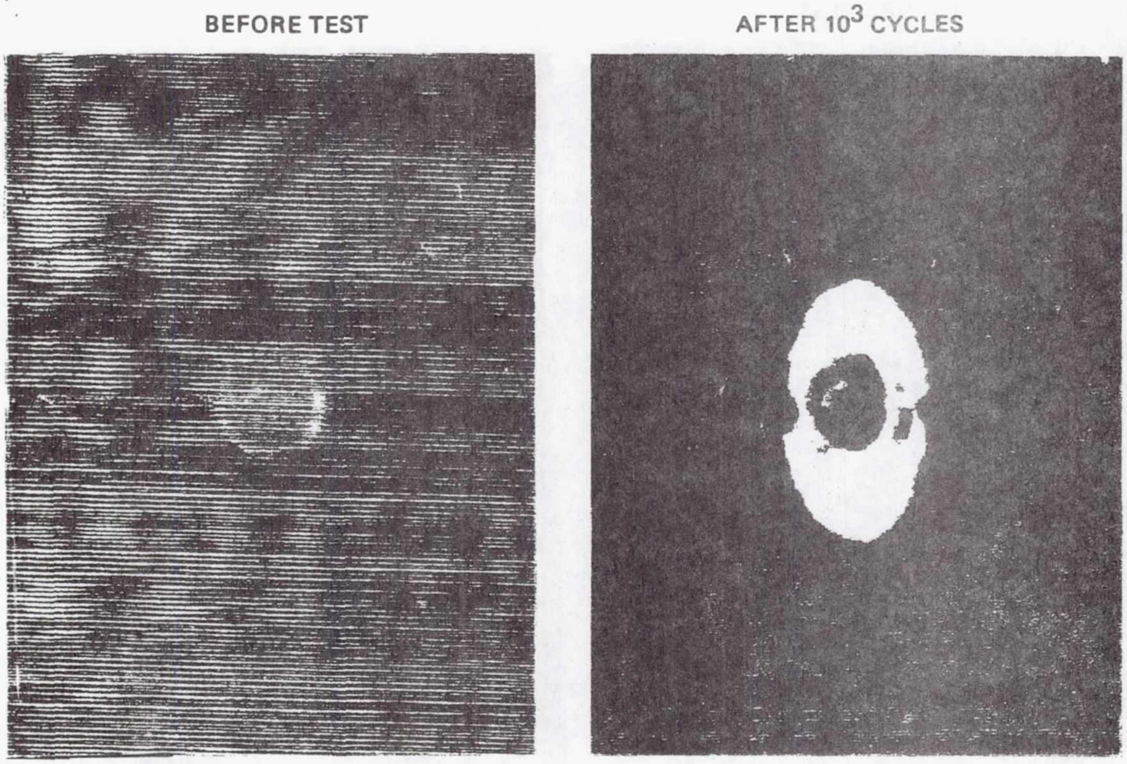

- Specimen L1-10-15
- 15.8-mm (0.625-in) half-penetration hole

Figure 71. Ultrasonic Scan Record for Laminate L1 Tension-Compression Fatigue Test Specimen 5/8 HP Hole

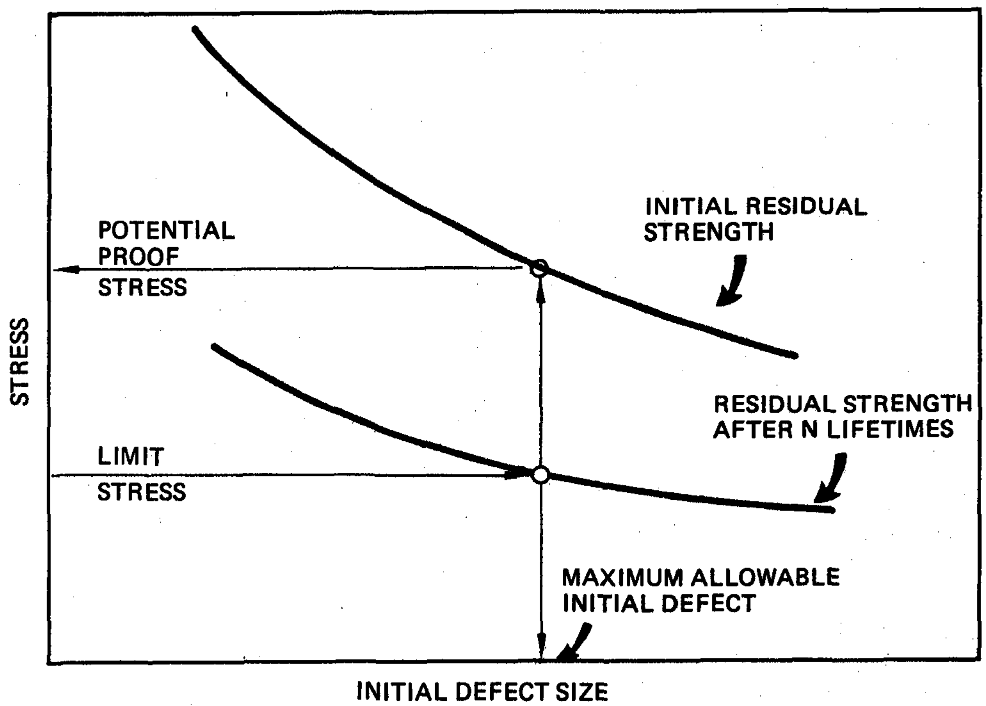

Figure 72. Potential Proof Test Method

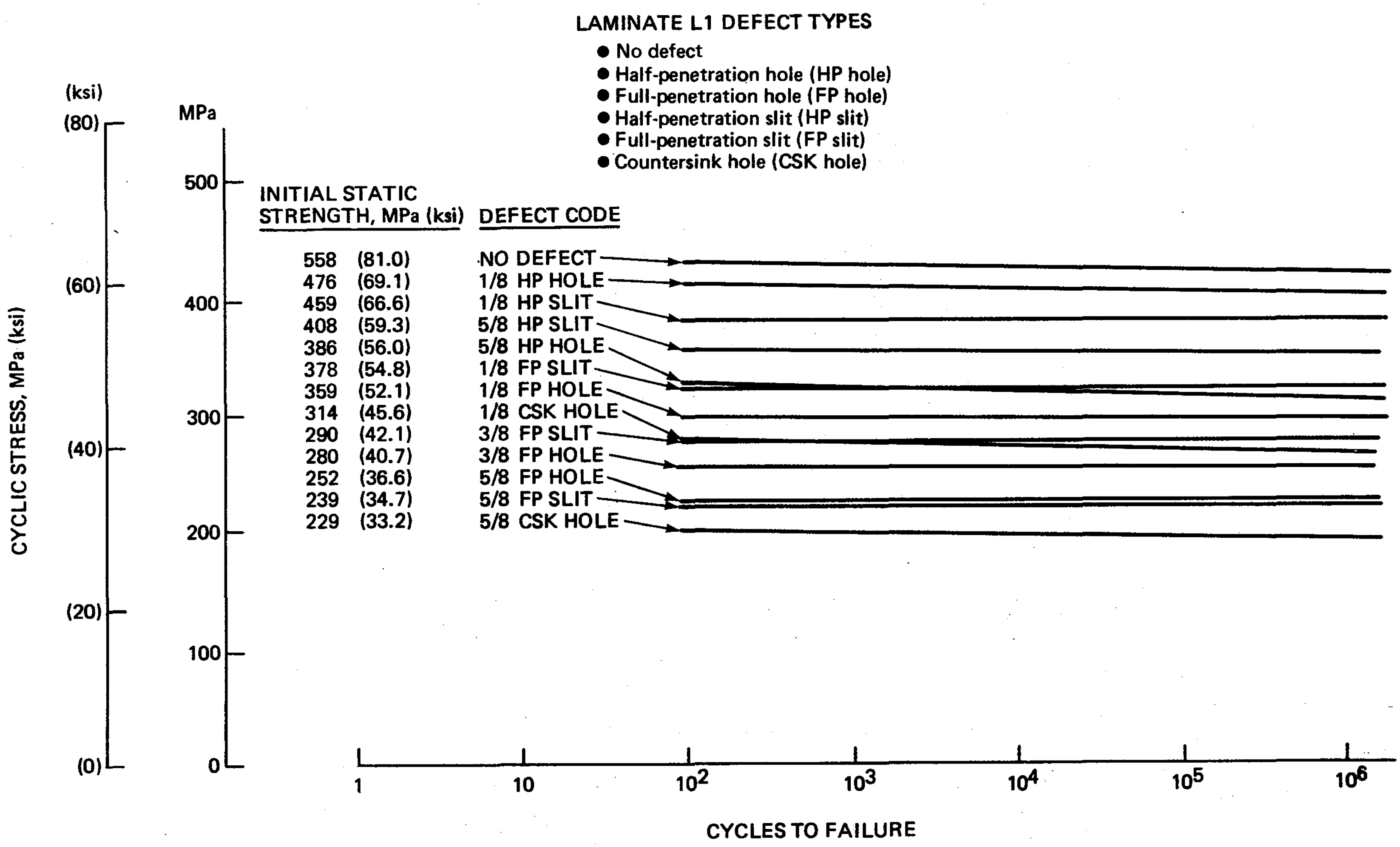

Figure 73. Minimum Fatigue Behavior for L1 Laminate Test Specimens Having Various Defects

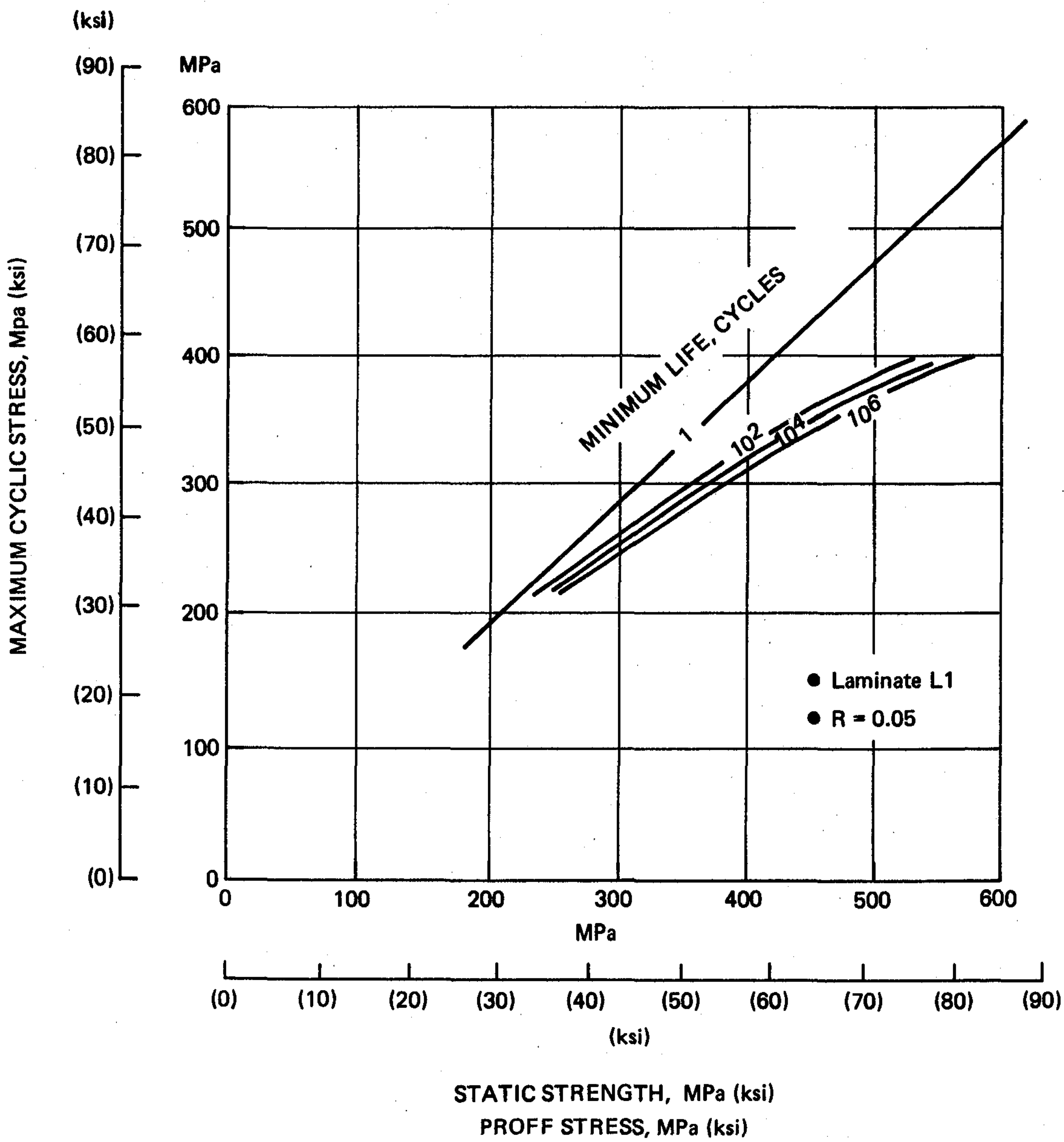

Figure 74. Proof Stress Requirements for Life Assurance of Laminate L1

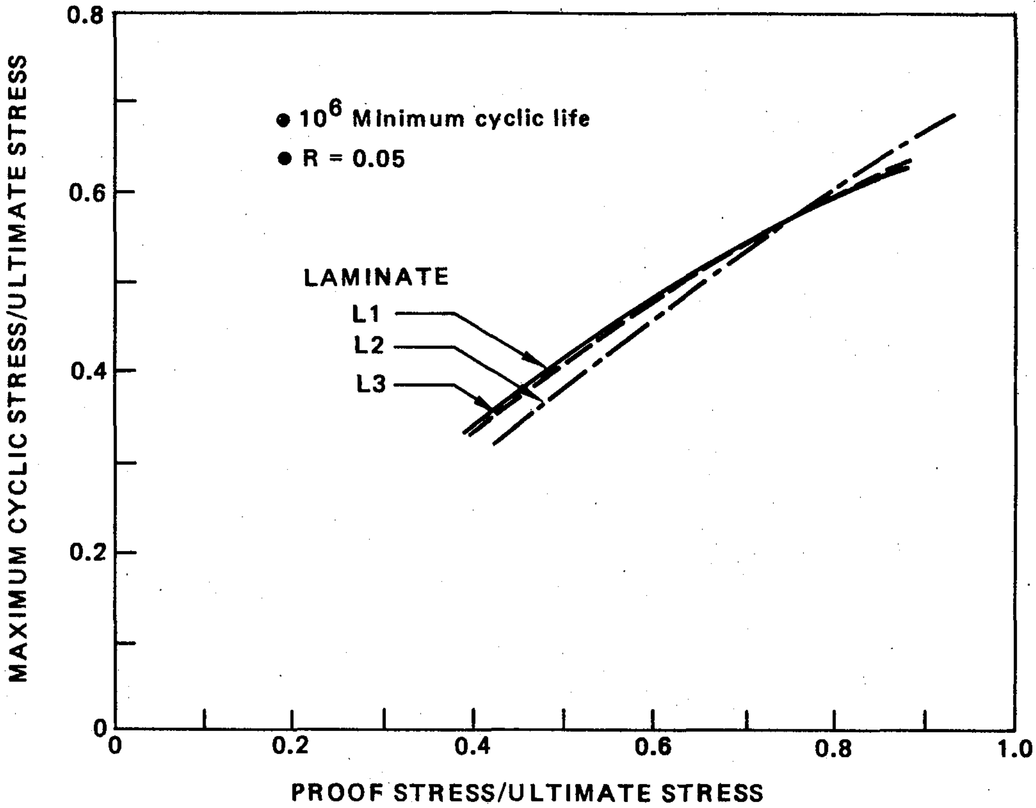

Figure 75. Comparison of Proof Stress Requirements of Tested Laminates at 10^6 Cyclic Life

APPENDIX A

STATIC AND CYCLIC TEST DATA

This appendix contains the static and cyclic test data for all specimens. The reported data include specimen geometry, loadings and test parameters. The gross section stresses have been reported for all the critical test conditions.

SPEC. NO.	LAYUP	THICK-NESS mm (INCH)	WIDTH mm (INCH)	FLAW TYPE	FLAW LENGTH FRONT mm (INCH)	FLAW LENGTH BACK mm (INCH)	FLAW DEPTH mm (INCH)	TEST TYPE	TEST TEMP. °K (°F)	PRELOAD LOAD N (16)	PRELOAD STRESS [2] MN/m² (KSI)	CYCLIC LOADING MAX LOAD N (16)	CYCLIC LOADING MAX STRESS [2] MN/m² (KSI)	CYCLIC LOADING R	CYCLIC LOADING CYCLES	RESIDUAL STATIC LOAD N (16)	RESIDUAL STATIC STRESS [2] MN/m² (KSI)	REMARKS
L1-1-11	L1 [1]	3.05 (0.120)	75.7 (2.981)	5/8 FP HOLE	15.7 (0.62)		–	STATIC	RT	0	–	NONE	–	–	–	58 300 (13 100)	252 (36.6)	
L1-1-12		3.15 (0.124)	75.9 (2.990)		15.8 (0.625)		–	PRELOAD STATIC		52 600 (11 820)	220 (31.9)	NONE	–	–	–	63 200 (14 200)	264 (38.3)	
L1-5-6		3.25 (0.128)	77.7 (3.059)		15.7 (0.620)		–	CYCLIC		0	–	52 500 (11 800)	207 (30.1)	0.05	10^3	68 000 (15 300)	270 (39.1)	
L1-5-5		3.18 (0.125)	76.5 (3.011)		15.8 (0.624)		–			0	–	52 500 (11 800)	216 (31.3)		10^5	64 500 (14 500)	265 (38.5)	
L1-5-4		3.05 (0.120)	75.6 (2.977)		15.8 (0.623)		–			0	–	46 600 (10 480)	202 (29.3)		1.5×10^6	68 900 (15 500)	299 (43.4)	
L1-5-8		3.05 (0.120)	75.8 (2.984)		15.8 (0.621)		–	PRELOAD CYCLIC		52 500 (11 810)	228 (33.0)	–	–		1	–	–	OVERLOAD DURING CYCLIC TEST
L1-5-9		3.18 (0.125)	75.8 (2.984)		15.7 (0.62)		–			52 500 (11 810)	218 (31.7)	52 500 (11 800)	218 (31.6)		10^5	71 400 (16 050)	296 (43.0)	
L1-5-7		3.20 (0.126)	75.4 (2.970)		15.8 (0.622)		–			52 500 (11 810)	218 (31.6)	46 600 (10 480)	193 (28.0)		1.5×10^6	[illegible]0700 (15 900)	293 (42.5)	
L1-2-9	L1	3.28 (0.129)	76.0 (2.994)	5/8 FP SLIT	15.7 (0.62)		–	STATIC		0	—	NONE	—	—	—	59 600 (13 400)	239 (34.7)	
L1-2-10		3.25 (0.128)	75.5 (2.972)		16.0 (0.63)		–	PRELOAD STATIC		53 600 (12 060)	218 (31.7)	NONE	–	–	–	62 300 (14 000)	254 (36.8)	
L1-7-9		3.25 (0.128)	76.5 (3.012)		15.7 (0.62)		–	CYCLIC		0	–	53 400 (12 000)	214 (31.1)	.05	1.5×10^6	68 500 (15 400)	275 (39.9)	
L1-7-10		3.22 (0.127)	75.6 (2.977)		15.7 (0.62)		–			0	–	53 400 (12 000)	(31.7)		10^5	69 400 (15 600)	285 (41.3)	
L1-7-11		3.12 (0.123)	76.4 (3.008)		16.0 (0.63)		–			0	–	53 400 (12 000)	218 (32.4)		10^3	63 600 (14 300)	267 (38.7)	
L1-7-12		3.20 (0.126)	75.9 (2.987)		15.7 (0.62)		–	PRELOAD CYCLIC		53 600 (12 060)	221 (32.0)	53 400 (12 000)	220 (31.9)		7	–	–	FATIGUE FAILURE
L1-7-13		3.18 (0.125)	75.6 (2.977)		16.3 (0.64)		–			53 600 (12 060)	223 (32.4)	53 400 (12 000)	222 (32.2)		2	–	–	FATIGUE FAILURE
L1-7-14		3.22 (0.127)	75.8 (2.986)		15.2 (0.60)		–			53 600 (12 060)	219 (31.8)	53 400 (12 000)	218 (31.6)		1.5×10^6	67 600 (15 200)	276 (40.1)	

[1] LAMINATE L1 $[(0/\pm45/0/90)_s]_2$

[2] GROSS SECTION STRESS

SPEC. NO.	LAYUP	THICK-NESS mm (INCH)	WIDTH mm (INCH)	FLAW TYPE	FLAW LENGTH FRONT mm (INCH)	FLAW LENGTH BACK mm (INCH)	FLAW DEPTH mm (INCH)	TEST TYPE	TEST TEMP. °K (°F)	PRELOAD LOAD N (16)	PRELOAD STRESS [2] MN/m² (KSI)	CYCLIC LOADING MAX LOAD N (16)	CYCLIC LOADING MAX STRESS [2] MN/m² (KSI)	R	CYCLES	RESIDUAL STATIC LOAD N (16)	RESIDUAL STATIC STRESS [2] MN/m² (KSI)	REMARKS
L1-1-7	L1 [1]	3.07 (.121)	75.8 (2.986)	3/8 FP HOLE	9.4 (.37)		—	STATIC	RT	0	—	NONE	—	—	—	65400 (14700)	281 (40.1)	
L1-1-8		3.18 (.125)	75.6 (2.975)		9.4 (.37)		—	PRELOAD STATIC		58500 (13150)	244 (35.4)	NONE	—	—	—	72900 (16400)	304 (44.1)	
L1-4-11		3.22 (.127)	76.1 (2.996)		9.5 (.375)			CYCLIC		0	—	58900 (13250)	240 (34.8)	.05	10^3	77840 (17500)	317 (46.0)	
L1-4-12		3.12 (.123)	77.3 (3.042)		9.4 (.375)					0	—	58900 (13250)	244 (35.4)		106,320	78700 (17700)	326 (47.3)	
L1-5-1		3.07 (.121)	76.4 (3.009)		9.4 (.374)					0	—	58900 (13250)	251 (36.4)		1.5×10^6	83200 (18700)	354 (51.4)	
L1-9-1		3.05 (.120)	75.0 (2.952)		9.4 (.370)			PRELOAD CYCLIC		58700 (13250)	258 (37.4)	58900 (13250)	258 (37.4)		10^3	72900 (16400)	319 (46.3)	
L1-5-3		3.18 (.125)	75.9 (2.987)		9.4 (.370)					58700 (13250)	245 (35.5)	58900 (13250)	245 (35.5)		10^5	77840 (17500)	323 (46.9)	
L1-5-2		3.18 (.125)	75.9 (2.987)		9.5 (.375)					58700 (13250)	245 (35.5)	58900 (13250)	245 (35.5)		1.5×10^6	85400 (19200)	354 (51.4)	
[illegible]		3.25 (.128)	75.4 (2.970)	3/8 FP SLIT	9.1 (.36)		—	STATIC		0	—	NONE	—	—	—	71200 (16000)	290 (42.1)	
L1-2-3		3.18 (.125)	76.0 (2.991)		9.4 (.37)		—	PRELOAD STATIC		64100 (14400)	265 (38.5)	NONE	—	—	—	71600 (16100)	297 (43.1)	
L1-7-4		3.25 (.128)	76.5 (3.012)		9.4 (.37)			CYCLIC		0	—	64100 (14400)	257 (37.3)	.05	10^3	74300 (16700)	299 (43.3)	
L1-7-5		3.25 (.128)	76.4 (3.009)		9.4 (.37)					0	—	64100 (14400)	258 (37.4)		10^5	83200 (18700)	335 (48.6)	
L1-7-6		3.19 (.124)	76.3 (3.033)		9.4 (.37)					0	—	60900 (13700)	251 (36.4)		1.5×10^6	82700 (18600)	345 (50.0)	
L1-7-8		3.22 (.127)	76.0 (2.992)		9.4 (.37)			PRELOAD CYCLIC		64100 (14400)	261 (37.9)	64100 (14400)	261 (37.9)		10^3	80100 (18000)	327 (47.4)	
L1-7-7		3.10 (.122)	75.8 (2.986)		9.4 (.37)					64100 (14400)	272 (39.5)	64100 (14400)	272 (39.5)		10^5	80100 (18000)	341 (49.4)	
L1-9-2		3.05 (.120)	75.0 (2.954)		15.7 (.62)					64100 (14400)	280 (40.6)	60900 (13700)	266 (38.6)		1.5×10^6	83200 (18700)	363 (52.7)	

[1] LAMINATE L1 $[(0/\pm45/0/90)_s]_2$
[2] GROSS SECTION STRESS

SPEC. NO.	LAYUP	THICK-NESS mm (INCH)	WIDTH mm (INCH)	FLAW TYPE	FLAW LENGTH FRONT mm (INCH)	FLAW LENGTH BACK mm (INCH)	FLAW DEPTH mm (INCH)	TEST TYPE	TEST TEMP. °K (°F)	PRELOAD LOAD N (lb)	PRELOAD STRESS [2] MN/m² (KSI)	CYCLIC LOADING MAX LOAD N (lb)	CYCLIC LOADING MAX STRESS [2] MN/m² (KSI)	CYCLIC LOADING R	CYCLIC LOADING CYCLES	RESIDUAL STATIC LOAD N (lb)	RESIDUAL STATIC STRESS [2] MN/m² (KSI)	REMARKS
L1-1-3	L1 [1]	3.12 (.123)	76.1 (2.995)	1/8 FP HOLE	3.0 (.12)		–	STATIC	RT	0	—	NONE	–	–	–	85400 (19200)	359 (52.1)	
L1-1-4		3.22 (.127)	76.3 (3.003)		3.0 (.12)		–	PRELOAD STATIC		76900 (17300)	313 (45.4)	NONE	–	–	–	94300 (21200)	393 (57.0)	
L1-4-1		3.25 (.128)	76.1 (2.998)		3.0 (.12)		–	CYCLIC		0	—	68900 (15500)	278 (40.4)	.05	10^5	103200 (23200)	416 (60.4)	
L1-3-12		3.12 (.123)	76.0 (2.992)		3.0 (.12)		–			0	—	—	—		—	—	—	GRIP AREA FAILURE
L1-3-11		3.22 (.127)	76.1 (2.996)		3.0 (.12)		–			0	—	68900 (15500)	281 (40.7)		1.5×10^6	100100 (22500)	407 (59.1)	
L1-4-3		3.25 (.128)	75.9 (2.989)		3.0 (.12)		–	PRELOAD CYCLIC		76900 (17300)	312 (45.2)	68900 (15500)	279 (40.5)		1060	91600 (20600)	371 (53.8)	
L1-4-4		3.10 (.122)	75.9 (2.989)		3.0 (.12)		–			76900 (17300)	327 (47.4)	68900 (15500)	293 (42.5)		10^5	91200 (20500)	387 (56.2)	
L1-4-2		3.28 (.129)	75.5 (2.972)		3.0 (.12)		–			76900 (17300)	311 (45.1)	68900 (15500)	278 (40.4)		1.5×10^6	109400 (24600)	443 (64.2)	
L1-2-1		3.10 (.122)	76.0 (2.994)	1/8 FP SLIT	3.3 (.13)		–	STATIC		0	—	NONE	–	–	–	89000 (20000)	378 (54.8)	
L1-2-2		3.20 (.126)	75.9 (2.987)		3.3 (.13)		–	PRELOAD STATIC		80000 (18000)	329 (47.8)	NONE	–	–	–	98300 (22100)	406 (58.7)	
L1-6-4		3.05 (.120)	76.6 (3.018)		3.3 (.13)		–	CYCLIC		0	—	72000 (16200)	308 (44.7)	.05	10^3	100500 (22600)	430 (62.4)	
L1-6-5		2.94 (.116)	75.9 (2.988)		3.3 (.13)		–			0	–	72000 (16200)	322 (46.7)		10^5	93400 (21000)	418 (60.6)	
L1-6-6		3.18 (.125)	78.3 (3.083)		3.3 (.13)		–			0	–	72000 (16200)	290 (42.0)		819662	—	—	GRID FAILURE DUE TO ECCENTRIC LOAD
L1-6-7		3.15 (.124)	75.8 (2.983)		3.3 (.13)		–	PRELOAD CYCLIC		80000 (18000)	336 (48.7)	72000 (16200)	302 (43.8)		10^3	97000 (21800)	406 (58.9)	
L1-6-8		3.18 (.125)	75.8 (2.984)		3.0 (.12)		–			80000 (18000)	332 (48.2)	72000 (16200)	299 (43.4)		10^5	99200 (22300)	412 (59.8)	
L1-6-9		3.02 (.119)	75.8 (2.984)		3.3 (.13)		–			80000 (18000)	350 (50.7)	72000 (16200)	314 (45.6)		1.5×10^6	97800 (22000)	427 (62.0)	

[1] LAMINATE L1 $[(0/\pm45/0/90)_S]_2$

[2] GROSS SECTION STRESS

SPEC. NO.	LAYUP	THICKNESS mm (INCH)	WIDTH mm (INCH)	FLAW TYPE	FLAW LENGTH FRONT mm (INCH)	FLAW LENGTH BACK mm (INCH)	FLAW DEPTH mm (INCH)	TEST TYPE	TEST TEMP. °K (°F)	PRELOAD LOAD N (16)	PRELOAD STRESS [2] MN/m² (KSI)	CYCLIC LOADING MAX LOAD N (16)	CYCLIC LOADING MAX STRESS [2] MN/m² (KSI)	CYCLIC LOADING R	CYCLIC LOADING CYCLES	RESIDUAL STATIC LOAD N (16)	RESIDUAL STATIC STRESS [2] MN/m² (KSI)	REMARKS
L1-1-13	L1 [1]	3.07 (.121)	75.7 (2.980)	5/8 HP HOLE	15.7 (.62)	0	1.5 (0.06)	STATIC	RT	0	-	NONE	-	-	-	89800 (20200)	386 (56.0)	
L1-1-14		3.10 (.122)	75.4 (2.970)		15.7 (.62)			PRELOAD STATIC		80900 (18200)	346 (50.2)	NONE	-	-	-	86300 (19400)	369 (53.5)	
L1-5-10		3.18 (.125)	76.4 (3.008)		15.7 (.62)			CYCLIC		0	-	72900 (16400)	301 (43.6)	.05	1 502 000	95600 (21500)	394 (51.2)	
L1-5-11		3.20 (.126)	76.5 (3.010)		15.7 (.62)					0	-	72900 (16400)	298 (43.2)		10^5	-	-	OVERLOAD FAILURE AT CYCLIC TEST TERMINATION
L1-5-12		3.12 (.123)	74.4 (2.928)		15.7 (.62)					0	-	72900 (16400)	314 (45.5)		10^3	83600 (18800)	354 (51.3)	
L1-6-1		3.07 (.121)	75.9 (2.989)		15.7 (.62)			PRELOAD CYCLIC		80900 (18200)	347 (50.3)	80900 (18200)	347 (50.3)		6	-	-	FATIGUE FAILURE
L1-6-2		3.18 (.125)	75.6 (2.977)		15.7 (.62)					80900 (18200)	337 (48.9)	72900 (16400)	304 (44.1)		1 550 000	96500 (21700)	402 (58.3)	
L1-6-3		3.15 (.124)	75.9 (2.989)		15.7 (.62)					80900 (18200)	338 (49.1)	72900 (16400)	305 (44.2)		10^3	84500 (19000)	354 (51.3)	
L1-2-11		3.18 (.125)	76.1 (2.996)	5/8 HP SLIT	15.7 (.62)		1.5 (0.06)	STATIC		0	-	NONE	-	-	-	98800 (22200)	409 (59.3)	
L1-2-12		3.10 (.122)	76.4 (3.010)		16.2 (.64)			PRELOAD STATIC		89000 (20000)	376 (54.5)	NONE	-	-	-	103600 (23300)	437 (63.4)	
L1-8-1		3.00 (.118)	77.0 (3.030)		15.2 (.61)			CYCLIC		0	-	89000 (18000)	247 (80.3)	.05	1504 000	106300 (23900)	461 (66.8)	
L1-8-2		3.12 (.123)	76.6 (3.016)		14.5 (.57)					0	-	89000 (18000)	334 (48.5)		101 410	102700 (23100)	430 (62.3)	
L1-8-3		3.10 (.122)	76.9 (3.028)		16.5 (.65)					0	-	89000 (18000)	336 (48.7)		10^3	94300 (21200)	396 (57.4)	
L1-8-4		3.18 (.125)	75.9 (2.987)		16.0 (.63)			PRELOAD CYCLIC		89000 (20000)	369 (53.6)	89000 (18000)	332 (48.2)		1.5×10^6	104500 (23500)	434 (62.9)	
L1-8-5		3.12 (.123)	75.7 (2.980)		15.0 (.59)					89000 (20000)	376 (54.6)	89000 (18000)	339 (49.1)		10^5	106700 (24000)	452 (65.5)	
L1-8-6		3.10 (.122)	75.8 (2.985)		16.8 (.66)					89000 (20000)	378 (54.9)	89000 (18000)	341 (49.4)		10^3	97600 (22000)	416 (60.4)	

[1] LAMINATE L1 $[(0/\pm45/0/90)_s]_2$

[2] GROSS SECTION STRESS

SPEC. NO.	LAYUP	THICKNESS mm (INCH)	WIDTH mm (INCH)	FLAW TYPE	FLAW LENGTH FRONT mm (INCH)	FLAW LENGTH BACK mm (INCH)	FLAW DEPTH mm (INCH)	TEST TYPE	TEST TEMP. °K (°F)	PRELOAD LOAD N (LB)	PRELOAD STRESS [2] MN/m² (KSI)	CYCLIC LOADING MAX LOAD N (LB)	CYCLIC LOADING MAX STRESS [2] MN/m² (KSI)	R	CYCLES	RESIDUAL STATIC LOAD N (LB)	RESIDUAL STATIC STRESS [2] MN/m² (KSI)	REMARKS
L1-1-5	L1 [1]	3.18 (.125)	76.5 (3.011)	1/8 HP HOLE	3.0 (.12)	0	1.5 (.06)	STATIC	RT	0	—	NONE	-	-	-	115 700 (26000)	476 (69.1)	
L1-1-6		3.15 (.124)	76.3 (3.002)		3.0 (.12)			PRELOAD STATIC		104000 (23400)	434 (62.9)	NONE	-	-	-	109 900 (24700)	458 (66.4)	
L1-4-5		3.15 (.124)	75.9 (2.978)		3.0 (.12)			CYCLIC		0	—	93800 (21100)	394 (57.1)	.05	1.5x10^6	111200 (25600)	478 (69.3)	
L1-4-6		3.25 (.128)	76.3 (3.003)		3.0 (.12)					0	—	93800 (21 100)	378 (54.9)		10^5	120 100 (27000)	484 (70.2)	
L1-4-7		3.20 (.126)	75.8 (2.983)		3.0 (.12)					0	—	93 800 (21 100)	387 (56.1)		10^3	120500 (27 100)	497 (72.1)	TESTED FIRST AT 16,200 lb FOR 10^3 CYCLES
L1-4-8		3.22 (.127)	75.7 (2.982)		3.0 (.12)			PRELOAD CYCLIC		104 000 (23400)	426 (61.8)	93800 (21,100)	384 (55.7)		1.5x10^6	118 300 (26600)	484 (70.2)	
L1-4-9		3.10 (.122)	75.7 (2.979)		3.0 (.12)					104000 (23400)	444 (64.4)	93800 (21100)	400 (58.0)		32 545	—	—	FATIGUE FAILURE
L1-4-10		3.18 (.125)	75.3 (2.963)		3.0 (.12)					104 000 (23400)	436 (63.2)	93 800 (21 100)	393 (57.0)		10^3	104100 (23400)	436 (63.2)	
L1-2-3		3.15 (.124)	75.9 (2.989)	1/8 HP SLIT	3.3 (.13)		1.5 (.06)	STATIC		0	—	NONE	-	-	-	106 500 (23 950)	459 (66.6)	
L1-2-4		3.30 (.130)	75.4 (2.969)		3.3 (.13)			PRELOAD STATIC		95800 (21550)	385 (55.8)	NONE	-	-	-	122 800 (27600)	496 (71.9)	
L1-6-10		3.00 (.118)	75.9 (2.989)		3.0 (.12)			CYCLIC		0	—	86300 (19400)	379 (55.0)	.05	1500400	135200 (30 400)	594 (86.2)	
L1-6-11		3.12 (.123)	76.5 (3.011)		3.0 (.12)					0	—	86300 (19400)	361 (52.4)		10^5	122 800 (27600)	514 (74.5)	
L1-6-12		3.12 (.123)	76.3 (3.003)		3.0 (.12)					0	—	86300 (19400)	362 (52.5)		10^3	121000 ([illegible])	507 (73.6)	
L1-7-1		3.12 (.123)	75.8 (2.985)		3.0 (.12)			PRELOAD CYCLIC		95800 (21550)	405 (58.7)	86300 (19400)	364 (52.8)		1.5x10^6	136100 (30600)	574 (83.3)	
L1-7-2		3.20 (.126)	75.9 (2.990)		3.0 (.12)					95800 (21550)	394 (57.2)	86300 (19400)	355 (51.5)		10^5	129000 (29000)	531 (77.0)	
L1-7-3		3.15 (.124)	75.9 (2.987)		3.0 (.12)					95800 (21550)	401 (58.2)	86300 (19400)	361 (52.4)		10^3	112 100 (25 200)	469 (68.0)	

[1] LAMINATE L1 $[0/\pm45/0/90)_s]_2$
[2] GROSS SECTION STRESS

SPEC. NO.	LAYUP	THICK-NESS mm (INCH)	WIDTH mm (INCH)	FLAW TYPE	FLAW LENGTH FRONT mm (INCH)	FLAW LENGTH BACK mm (INCH)	FLAW DEPTH mm (INCH)	TEST TYPE	TEST TEMP. °K (°F)	PRELOAD LOAD N (16)	PRELOAD STRESS [2] MN/m² (KSI)	CYCLIC LOADING MAX LOAD N (16)	CYCLIC LOADING MAX STRESS [2] MN/m² (KSI)	CYCLIC LOADING R	CYCLIC LOADING CYCLES	RESIDUAL STATIC LOAD N (16)	RESIDUAL STATIC STRESS [2] MN/m² (KSI)	REMARKS
L1-3-3	L1 [1]	3.07 (.121)	75.2 (2.962)	5/8 CSK HOLE	22.9 (.90)	16.2 (.64)	—	STATIC	RT	0	—	NONE	—	—	—	56000 (12600)	242 (35.1)	
L1-3-4	↓	3.07 (.121)	75.3 (2.966)	↓	22.9 (.90)	15.7 (.62)	—	PRELOAD STATIC	↓	49800 (11200)	215 (31.2)	NONE	—	—	—	—	—	FAILURE DURING PRELOAD
L1-8-11	↓	3.07 (.121)	76.3 (3.005)	↓	22.9 (.90)	15.7 (.62)	—	CYCLIC	↓	0	—	44900 (10100)	192 (27.8)	.05	10^3	52900 (11900)	225 (32.7)	
L1-8-12	↓	3.05 (.120)	76.2 (3.001)	↓	22.9 (.90)	15.7 (.62)	—	↓	↓	0	—	40500 (9100)	174 (25.3)	↓	1502900	61400 (13800)	264 (38.3)	
L1-8-13	↓	3.05 (.120)	73.5 (2.894)	↓	22.9 (.90)	16.0 (.63)	—	PRELOAD STATIC	↓	44900 (10100)	201 (29.1)	44900 (10100)	201 (29.1)	↓	10^3	57400 (12900)	256 (37.1)	
L1-8-14	↓	3.10 (.122)	76.5 (3.011)	↓	22.9 (.90)	15.7 (.62)	—	↓	↓	44900 (10100)	190 (27.5)	40500 (9100)	171 (24.8)	↓	1.5×10^6	69400 (15600)	293 (42.5)	
L1-3-1	↓	3.10 (.122)	76.1 (2.997)	3/8 CSK HOLE	16.8 (.66)	9.6 (.38)	—	STATIC	↓	0	—	NONE	—	—	—	60500 (13600)	256 (37.2)	
L1-3-2	↓	3.22 (.127)	75.9 (2.989)	↓	16.8 (.66)	9.4 (.37)	—	PRELOAD STATIC	↓	54300 (12200)	221 (32.1)	NONE	—	—	—	66300 (14900)	271 (39.3)	
L1-2-13	↓	3.22 (.127)	75.6 (2.976)	1/8 CSK HOLE	10.9 (.43)	3.0 (.12)	—	STATIC	↓	0	—	NONE	—	—	—	76700 (17250)	314 (45.6)	
L1-2-14	↓	3.20 (.126)	76.1 (2.997)	↓	10.7 (.42)	3.0 (.12)	—	PRELOAD STATIC	↓	68900 (15500)	283 (41.0)	NONE	—	—	—	79200 (17800)	325 (47.1)	
L1-8-7	↓	2.95 (.116)	76.7 (3.021)	↓	9.6 (.38)	3.0 (.12)	—	CYCLIC	↓	0	—	61800 (13900)	274 (39.7)	.05	10^3	69800 (15700)	309 (44.8)	
L1-8-8	↓	3.18 (.125)	76.8 (3.024)	↓	10.4 (.41)	3.0 (.12)	—	↓	↓	0	-	61800 (13900)	254 (36.8)	↓	1.5×10^6	90300 (20300)	370 (53.7)	
L1-8-9	↓	3.15 (.124)	75.7 (2.982)	↓	10.2 (.40)	3.0 (.12)	—	PRELOAD CYCLIC	↓	68900 (15500)	289 (41.9)	57400 (12900)	241 (34.9)	↓	10^3	79200 (17800)	332 (48.1)	
L1-8-10	↓	3.18 (.125)	75.5 (2.972)	↓	10.4 (.41)	3.0 (.12)	—	↓	↓	68900 (15500)	288 (41.7)	61800 (13900)	258 (37.4)	↓	1.5×10^6	89000 (20000)	371 (53.8)	
L1-2-7	↓	3.02 (.119)	76.0 (2.994)	3/8 HP SLIT	9.4 (.37)	0	1.5 (.06)	STATIC	↓	0	—	NONE	—	—	—	96500 (21700)	420 (60.9)	
L1-2-8	↓	3.28 (.129)	75.9 (2.988)	↓	9.4 (.37)	0	↓	PRELOAD STATIC	↓	87000 (19550)	350 (50.7)	NONE	—	—	—	113000 (25400)	454 (65.9)	

[1] LAMINATE L1 $[(0/\pm45/0/90)_s]_2$

[2] GROSS SECTION STRESS

SPEC. NO.	LAYUP	THICK-NESS mm (INCH)	WIDTH mm (INCH)	FLAW TYPE	FLAW LENGTH FRONT mm (INCH)	FLAW LENGTH BACK mm (INCH)	FLAW DEPTH mm (INCH)	TEST TYPE	TEST TEMP. °K (°F)	PRELOAD LOAD N (lb)	PRELOAD STRESS [2] MN/m² (KSI)	CYCLIC LOADING MAX LOAD N (lb)	CYCLIC LOADING MAX STRESS [2] MN/m² (KSI)	CYCLIC LOADING R	CYCLIC LOADING CYCLES	RESIDUAL STATIC LOAD N (lb)	RESIDUAL STATIC STRESS [2] MN/m² (KSI)	REMARKS
L1-1-2	L1 [1]	3.12 (.123)	75.6 (2.977)	NONE	0	0	0	STATIC	RT	0	–	NONE	–	–	–	145 000 (32 600)	614 (89.0)	
L1-1-1		3.10 (.122)	76.8 (3.023)					PRELOAD STATIC		120 000 (27 000)	505 (73.2)	NONE	–	–	–	–	–	FAILURE DURING PRELOAD
L1-3-10		3.15 (.124)	75.6 (2.978)					PRELOAD STATIC		102 700 (23 100)	431 (62.5)	NONE	–	–	–	160 100 (36 000)	672 (97.5)	
L1-3-5		3.20 (.126)	76.1 (2.997)					CYCLIC		0	–	97400 (21900)	400 (58.0)	.05	1.3×10^6	126 800 (28 500)	520 (75.5)	
L1-3-6		3.25 (.128)	75.4 (2.967)							0	–	97400 (21 900)	398 (57.7)		10^5	151 500 (35 400)	643 (93.2)	
L1-3-7		3.23 (.127)	76.0 (2.993)							0	–	97400 (21 900)	397 (57.6)		10^3	169 900 (38 200)	692 (100.4)	
L1-3-8		3.10 (.122)	75.7 (2.979)					PRELOAD CYCLIC		108100 (24300)	462 (66.9)	97400 (21900)	416 (60.3)		51 056	–	–	FATIGUE FAILURE
L1-3-9		3.07 (.121)	75.7 (2.980)							108100 (24300)	465 (67.4)	97400 (21900)	419 (60.7)		10^5	149 900 (33 700)	645 (93.5)	

[1] LAMINATE L1 $[(0/\pm45/0/90)_s]_2$
[2] GROSS SECTION STRESS

SPEC. NO.	LAYUP	THICK-NESS mm (INCH)	WIDTH mm (INCH)	FLAW TYPE	FLAW LENGTH		FLAW DEPTH mm (INCH)	TEST TYPE	TEST TEMP. °K (°F)	PRELOAD		CYCLIC LOADING				RESIDUAL STATIC		REMARKS
					FRONT mm (INCH)	BACK mm (INCH)				LOAD N (lb)	STRESS MN/m² (KSI)	MAX LOAD N (lb)	MAX STRESS MN/m² (KSI)	R	CYCLES	LOAD N (lb)	STRESS MN/m² (KSI)	
L1-10-1	L1 ▷	2.87 (.113)	75.7 (2.980)	NONE	0	0	0	STATIC	RT	0	—	NONE	—	—	—	126 300 (28 400)	581 (84.3)	
L1-10-2		2.94 (.116)	75.6 (2.974)					CYCLIC		0	—	97400 (21 900)	438 (63.6)	-0.5	1000	161 000 (36 200)	723 (104.9)	
L1-10-3		2.84 (.112)	75.5 (2.973)							0	—	97400 (21 900)	454 (65.8)	-0.5	337700	137 900 (31 000)	642 (93.1)	
L1-10-4		2.87 (.113)	75.5 (2.973)							0	—	73 400 (16 500)	339 (49.1)	-1.0	13800	—	—	FATIGUE FAILURE
L1-10-5		2.94 (.116)	75.6 (2.974)							0	—	73 400 (16 500)	320 (47.8)	-1.0	700	—	—	FATIGUE FAILURE
L1-10-6		2.87 (.113)	75.6 (2.976)					PRELOAD CYCLIC		108 100 (24 300)	498 (72.3)	73 400 (16 500)	329 (49.1)	-1.0	15600	—	—	FATIGUE FAILURE
L1-10-7		3.02 (.119)	76.0 (2.994)	1/8 FP HOLE	3.0 (.12)			CYCLIC		0	—	68500 (15400)	298 (43.2)	-1.0	83900	114 800 (25 800)	499 (72.4)	
L1-10-8		2.79 (.110)	76.0 (2.992)		3.0 (.12)					0	—	47200 (10600)	222 (32.2)	-1.0	566600	108 100 (24 300)	509 (73.8)	
L1-10-9		2.97 (.117)	75.7 (2.980)	5/8 FP HOLE	15.7 (.62)			CYCLIC		0	—	46600 (10480)	208 (30.1)	-0.5	1000	64 100 (14 400)	285 (41.3)	
L1-10-10		2.87 (.113)	75.5 (2.972)		15.7 (.62)					0	—	46600 (10480)	215 (31.2)	-0.5	522850	80100 (18000)	370 (53.6)	STATIC COMPRESSIVE OVERLOAD
L1-10-11		2.94 (.116)	76.0 (2.993)		15.7 (.62)					0	—	46 600 (10 480)	208 (30.2)	-1.0	7300	—	—	FATIGUE FAILURE
L1-10-12		2.89 (.114)	75.7 (2.982)		15.7 (.62)					0	—	32 000 (7 200)	215 (21.2)	-1.0	1842500	72 100 (16 200)	329 (47.7)	
L1-10-13		3.00 (.118)	75.4 (2.968)		15.7 (.62)			PRELOAD CYCLIC		52500 (11 800)	232 (33.7)	46600 (10480)	206 (29.9)	-0.5	1000	63600 (14 300)	281 (40.8)	
L1-10-14		3.00 (.118)	76.0 (2.993)		15.7 (.62)			PRELOAD CYCLIC		52500 (11800)	230 (33.4)	46600 (10480)	205 (29.7)	-1.0	22800	—	—	FATIGUE FAILURE

▷ LAMINATE L1 $[(0/\pm 45/0/90)_s]_2$ T300/934 TAPE

SPEC. NO.	LAYUP	THICK-NESS mm (INCH)	WIDTH mm (INCH)	FLAW TYPE	FLAW LENGTH FRONT mm (INCH)	FLAW LENGTH BACK mm (INCH)	FLAW DEPTH mm (INCH)	TEST TYPE	TEST TEMP. °K (°F)	PRELOAD LOAD N (LB)	PRELOAD STRESS MN/m² (KSI)	CYCLIC LOADING MAX LOAD N (LB)	CYCLIC LOADING MAX STRESS MN/m² (KSI)	CYCLIC LOADING R	CYCLIC LOADING CYCLES	RESIDUAL STATIC LOAD N (LB)	RESIDUAL STATIC STRESS MN/m² (KSI)	REMARKS
L1-10-15	L1 ▷	2.97 (.117)	76.0 (2.992)	5/8 HP HOLE	15.7 (.62)			CYCLIC	RT	0	–	72900 (16400)	323 (46.8)	-0.5	1000	97400 (21900)	432 (62.6)	
L1-10-16		2.84 (.112)	75.7 (2.981)		15.7 (.62)					0	–	72900 (16400)	339 (49.1)	-0.5	1793	–	–	FATIGUE FAILURE
L1-10-17		3.00 (.118)	76.0 (2.992)		15.7 (.62)					0	–	72900 (16400)	321 (46.5)	-1.0	3100	–	–	FATIGUE FAILURE
L1-10-18		3.00 (.118)	76.0 (2.993)		15.7 (.62)					0	–	49400 (11100)	216 (31.4)	-1.0	1500000	105900 (23800)	465 (67.4)	
L1-10-19		3.02 (.119)	76.0 (2.994)	1/8 FP SLIT	3.0 (.12)			CYCLIC		0	–	71200 (16000)	310 (44.9)	-1.0	36100	–	–	FATIGUE FAILURE
L1-10-20		3.02 (.119)	75.6 (2.975)		3.0 (.12)					0	–	48900 (11000)	214 (31.1)	-1.0	741100	101000 (22700)	442 (64.1)	
L1-10-21		2.92 (.115)	76.1 (2.996)	5/8 FP SLIT	15.7 (.62)			CYCLIC		0	–	47100 (10580)	212 (30.7)	-0.5	1	–	–	STATIC FAILURE AT (10580 LBS)
L1-10-22		2.97 (.117)	76.1 (2.996)		15.7 (.62)					0	–	47600 (10700)	210 (30.5)	-0.5	1500000	76500 (17200)	338 (49.1)	
L1-10-23		2.87 (.113)	75.6 (2.976)		15.7 (.62)					0	–	46100 (10360)	212 (30.8)	-1.0	1	–	–	STATIC FAILURE AT (10360 LBS)
L1-10-24		2.87 (.113)	75.6 (2.976)		15.7 (.62)					0	–	32900 (7400)	152 (22.0)	-1.0	1500000	62300 (14000)	287 (41.6)	
L1-10-25		3.02 (.119)	76.1 (2.996)		15.7 (.62)			PRELOAD CYCLIC		51400 (11560)	223 (32.4)	–	–	–	–	–	–	FAILURE DURING PRELOAD
L1-10-26		3.02 (.119)	76.0 (2.993)	1/8 HP SLIT	3.0 (.12)	0		CYCLIC		0	–	73400 (16500)	319 (46.3)	-1.0	23800	132100 (29700)	575 (83.4)	
L1-10-27		2.94 (.116)	75.7 (2.981)		3.0 (.12)	0				0	–	58300 (13100)	261 (37.9)	-1.0	114600	129000 (29000)	578 (83.9)	

▷ LAMINATE L1 $[(0/\pm 45/0/90)_s]_2$ T300/434 TAPE

SPEC. NO.	LAYUP	THICKNESS mm (INCH)	WIDTH mm (INCH)	FLAW TYPE	FLAW LENGTH FRONT mm (INCH)	FLAW LENGTH BACK mm (INCH)	FLAW DEPTH mm (INCH)	TEST TYPE	TEST TEMP. °K (°F)	PRELOAD LOAD N (LB)	PRELOAD STRESS MN/m² (KSI)	CYCLIC LOADING MAX LOAD N (LB)	CYCLIC LOADING MAX STRESS MN/m² (KSI)	CYCLIC LOADING R	CYCLIC LOADING CYCLES	RESIDUAL STATIC LOAD N (LB)	RESIDUAL STATIC STRESS MN/m² (KSI)	REMARKS
L1-10-28	L1 ▷	2.94 (.116)	75.5 (2.972)	5/8 NP SLIT	16.8 (.66)	0		CYCLIC	RT	0	–	80100 (18000)	360 (52.2)	-0.5	1000	108 100 (24 300)	486 (70.5)	
L1-10-29		2.97 (.117)	76.0 (2.993)		16.8 (.66)	0				0	–	80100 (18000)	354 (51.4)	-0.5	272 400	–	–	FATIGUE FAILURE
L1-10-30		2.92 (.115)	76.0 (2.992)		16.8 (.66)	0				0	–	73400 (16500)	331 (48.0)	-1.0	400	–	–	FATIGUE FAILURE
L1-10-31		2.92 (.115)	76.0 (2.994)		16.8 (.66)	0				0	–	54300 (12200)	244 (35.4)	-1.0	742 400	–	–	FATIGUE FAILURE
L1-10-32		2.97 (.117)	76.0 (2.994)	5/8 CSK HOLE	22.3 (.88)	15.7 (.62)		CYCLIC		0	–	42300 (9500)	137 (27.1)	-1.0	50800	–	–	FATIGUE FAILURE
L1-10-33		2.89 (.114)	76.0 (2.992)		22.3 (.88)	15.7 (.62)				0	–	28900 (6500)	132 (19.1)	-1.0	1500000	66700 (15000)	303 (44.0)	
L1-10-34		3.00 (.118)	75.6 (2.975)		22.6 (.89)	15.7 (.62)		PRELOAD CYCLIC		52500 (11800)	232 (33.6)	42300 (9500)	187 (27.1)	-1.0	16600	–	–	FATIGUE FAILURE
L1-11-1		2.87 (.113)	75.5 (2.973)	5/8 DISBOND				CYCLIC		0	–	97400 (21900)	450 (65.2)	-0.5	1000	169000 (38000)	780 (113.1)	
L1-11-2		2.89 (.114)	75.7 (2.982)							0	–	97400 (21900)	444 (64.4)	-0.5	15780	124500 (28000)	568 (82.4)	
L1-11-3		2.94 (.116)	75.5 (2.973)							0	–	97400 (21900)	438 (63.5)	-1.0	77	–	–	FATIGUE FAILURE
L1-11-4		2.94 (.116)	75.3 (2.965)							0	–	73400 (16500)	331 (48.0)	-1.0	12560	–	–	FATIGUE FAILURE
L1-11-5		2.87 (.113)	75.3 (2.975)							0	–	97400 (21900)	449 (65.1)	+0.1	1000	150300 (33800)	693 (100.5)	
L1-11-6		2.82 (.111)	75.3 (2.975)							0	–	97400 (21900)	457 (66.3)	+0.1	1500000	117900 (26500)	553 (80.2)	
L1-11-7		2.92 (.115)	75.5 (2.973)					PRELOAD CYCLIC		108100 (24300)	490 (71.1)	73400 (16500)	333 (48.3)	-1.0	1000	154300 (34700)	700 (101.5)	

▷ LAMINATE L1 $[(0/\pm45/0/90)_s]$ T300/934 TAPE

SPEC. NO.	LAYUP	THICKNESS mm (INCH)	WIDTH mm (INCH)	FLAW TYPE	FLAW LENGTH FRONT mm (INCH)	FLAW LENGTH BACK mm (INCH)	FLAW DEPTH mm (INCH)	TEST TYPE	TEST TEMP. °K (°F)	PRELOAD LOAD N (16)	PRELOAD STRESS [2] MN/m² (KSI)	CYCLIC LOADING MAX LOAD N (16)	CYCLIC LOADING MAX STRESS [2] MN/m² (KSI)	R	CYCLES	RESIDUAL STATIC LOAD N (16)	RESIDUAL STATIC STRESS [2] MN/m² (KSI)	REMARKS
L2-1-7	L2 [1]	3.10 (.122)	76.4 (3.007)	5/8 FP HOLE	15.7 (.62)		-	STATIC	RT	0	-	NONE	-	-	-	99000 (22250)	418 (60.6)	
L2-1-8	↓	3.18 (.125)	76.2 (3.000)	↓	15.7 (.62)		-	PRELOAD STATIC	↓	89200 (20050)	369 (53.5)	NONE	-	-	-	117600 (26450)	486 (70.5)	
L2-1-30	↓	3.18 (.125)	76.1 (2.996)	↓	15.7 (.62)		-	CYCLIC	↓	0	-	80100 (18000)	332 (48.1)	.05	10^3	116500 (26200)	482 (70.0)	
L2-1-29	↓	3.12 (.123)	75.4 (2.969)	↓	15.7 (.62)		-	↓	↓	0	-	80100 (18000)	340 (49.3)	↓	$1.5X10^6$	135200 (30400)	574 (83.2)	
L2-1-32	↓	3.18 (.125)	75.9 (2.987)	↓	15.7 (.62)		-	PRELOAD CYCLIC	↓	89000 (20000)	370 (53.6)	80100 (18000)	332 (48.2)	↓	10^3	118800 (26700)	493 (71.5)	
L2-1-31	↓	3.12 (.123)	75.9 (2.988)	↓	15.7 (.62)		-	↓	↓	89000 (20000)	375 (54.4)	80100 (18000)	338 (49.0)	↓	$1.5X10^6$	121900 (27400)	514 (74.6)	
L2-1-5	↓	3.18 (.125)	74.4 (2.930)	3/8 FP HOLE	9.6 (.38)		-	STATIC	↓	0	-	NONE	-	-	-	127700 (28700)	540 (78.4)	
L2-1-6	↓	3.18 (.125)	74.6 (2.936)	↓	9.6 (.38)		-	PRELOAD STATIC	↓	115000 (25850)	485 (70.4)	NONE	-	-	-	139200 (31300)	588 (85.3)	
L2-1-3	↓	3.12 (.123)	74.6 (2.936)	1/8 FP HOLE	3.0 (.12)		-	STATIC	↓	0	-	NONE	-	-	-	136600 (30700)	586 (85.0)	
L2-1-4	↓	3.25 (.128)	74.4 (2.931)	↓	3.0 (.12)		-	PRELOAD STATIC	↓	122800 (27600)	507 (73.6)	NONE	-	-	-	136100 (30600)	563 (81.6)	
L2-1-26	↓	3.12 (.123)	76.4 (3.009)	↓	3.0 (.12)		-	CYCLIC	↓	0	-	110300 (24800)	462 (67.0)	.05	10^3	161500 (36300)	607 (88.1)	
L2-1-25	↓	3.10 (.122)	75.3 (2.963)	↓	3.0 (.12)		-	↓	↓	0	-	110300 (24800)	473 (68.6)	↓	$1.5X10^6$	175300 (39400)	751 (108.9)	
L2-1-28	↓	3.18 (.125)	75.9 (2.990)	↓	3.0 (.12)		-	PRELOAD CYCLIC	↓	122800 (27600)	509 (73.8)	110300 (24800)	457 (66.3)	↓	10^3	145000 (32600)	601 (87.2)	
L2-1-27	↓	3.05 (.120)	76.2 (3.001)	↓	3.0 (.12)		-	↓	↓	122800 (27600)	528 (76.6)	110300 (24800)	475 (68.9)	↓	1300000	—	—	FATIGUE FAILURE

[1] LAMINATE L2 $[(0_3/\pm 80)_2]_s$

[2] GROSS SECTION STRESS

SPEC. NO.	LAYUP	THICKNESS mm (INCH)	WIDTH mm (INCH)	FLAW TYPE	FLAW LENGTH FRONT mm (INCH)	FLAW LENGTH BACK mm (INCH)	FLAW DEPTH mm (INCH)	TEST TYPE	TEST TEMP. °K (°F)	PRELOAD LOAD N (lb)	PRELOAD STRESS [2] MN/m² (KSI)	CYCLIC LOADING MAX LOAD N (lb)	CYCLIC LOADING MAX STRESS [2] MN/m² (KSI)	CYCLIC LOADING R	CYCLIC LOADING CYCLES	RESIDUAL STATIC LOAD N (lb)	RESIDUAL STATIC STRESS [2] MN/m² (KSI)	REMARKS
L2-1-17	L2 [1]	3.20 (.126)	74.4 (2.931)	5/8 FP SLIT	15.2 (.60)		–	STATIC	RT	0	—	NONE	-	-	-	109 000 (24500)	457 (66.3)	
L2-1-18	↓	3.15 (.124)	73.8 (2.905)	↓	15.7 (.62)		–	PRELOAD STATIC	↓	98100 (22050)	422 (61.2)	NONE	-	-	-	100 500 (22600)	432 (62.7)	
L2-1-41	↓	3.22 (.127)	76.3 (3.004)	↓	16.0 (.63)		–	CYCLIC	↓	0	–	88100 (19800)	358 (51.9)	.05	1.5×10^6	137000 (30800)	556 (80.7)	
L2-1-42	↓	3.20 (.126)	75.9 (2.987)	↓	16.0 (.63)		–	↓	↓	0	—	88100 (19800)	363 (52.6)	↓	10^3	119200 (26800)	491 (71.2)	
L2-1-43	↓	3.25 (.128)	76.0 (2.993)	↓	16.0 (.63)		–	PRELOAD CYCLIC	↓	98100 (22050)	393 (57.6)	88100 (19800)	256 (51.7)	↓	1.5×10^6	130800 (29400)	529 (76.7)	
L2-1-44	↓	3.15 (.124)	76.4 (3.008)	↓	15.7 (.62)		–	↓	↓	98100 (22050)	407 (59.1)	88100 (19800)	366 (53.1)	↓	10^3	113900 (25600)	473 (68.6)	
L2-1-13	↓	3.12 (.123)	73.6 (2.898)	2/8 FP SLIT	9.4 (.37)		–	STATIC	↓	0	—	NONE	-	-	-	133 000 (29900)	578 83.9	
L2-1-14	↓	3.18 (.125)	75.1 (2.959)	↓	9.4 (.37)		–	PRELOAD STATIC	↓	119 600 (26900)	501 (72.7)	NONE	-	-	-	129 200 (29050)	591 (78.5)	
L2-1-9	↓	3.18 (.125)	74.4 (2.929)	1/8 FP SLIT	3.0 (.12)		–	STATIC	↓	0	—	NONE	–	-	-	138 800 (31200)	587 (85.2)	
L2-1-10	↓	3.23 (.127)	74.5 (2.932)	↓	3.3 (.13)		–	PRELOAD STATIC	↓	125000 (28100)	520 (75.5)	NONE	-	-	-	140 100 (31500)	583 (84.6)	
L2-1-33	↓	3.18 (.125)	75.9 (2.987)	↓	3.3 (.13)		–	CYCLIC	↓	0	—	112500 (25300)	467 (67.8)	.05	521 660	—	—	FAILURE DURING CYCLIC TEST DUE TO OVERLOAD
L2-1-34	↓	3.22 (.127)	76.3 (3.003)	↓	3.0 (.12)		–	↓	↓	0	—	112500 (25300)	457 (66.3)	↓	1 004	162 800 (36 600)	662 (96.0)	
L2-1-35	↓	3.12 (.123)	76.1 (2.998)	↓	3.3 (.13)		–	PRELOAD CYCLIC	↓	125000 (28100)	525 (76.2)	112500 (25300)	473 (68.6)	↓	1500150	176 100 (39600)	740 (107.4)	
L2-1-36	↓	3.20 (.126)	75.7 (2.980)	↓	3.3 (.13)		–	↓	↓	125000 (28100)	516 (74.8)	112500 (25300)	465 (67.4)	↓	1003	150300 (33 800)	620 (90.0)	

[1] LAMINATE L2 $[(0_3/\pm 80)_2]_S$

[2] GROSS SECTION STRESS

SPEC. NO.	LAYUP	THICKNESS mm (INCH)	WIDTH mm (INCH)	FLAW TYPE	FLAW LENGTH FRONT mm (INCH)	FLAW LENGTH BACK mm (INCH)	FLAW DEPTH mm (INCH)	TEST TYPE	TEST TEMP. °K (°F)	PRELOAD LOAD N (16)	PRELOAD STRESS [2] MN/m² (KSI)	CYCLIC LOADING MAX LOAD N (16)	CYCLIC LOADING MAX STRESS [2] MN/m² (KSI)	CYCLIC LOADING R	CYCLIC LOADING CYCLES	RESIDUAL STATIC LOAD N (16)	RESIDUAL STATIC STRESS [2] MN/m² (KSI)	REMARKS
L2-1-19	L2 [1]	3.18 (.125)	75.1 (2.956)	3/8 LF SLIT	15.2 (.6[illegible])	0	1.5 (.06)	STATIC	RT	0	-	NONE	-		-	176 100 (39600)	739 (107.2)	
L2-1-20	↓	3.07 (.121)	75.1 (2.958)	↓	15.2 (.60)	↓	↓	PRELOAD STATIC	↓	156 600 (35200)	678 (98.3)	NONE	-	-	-	-	-	FAILURE DURING PRELOAD
L2-1-45	↓	3.20 (.126)	76.5 (3.014)	↓	15.5 (.61)	↓	↓	CYCLIC	↓	0	-	126 800 (28 500)	517 (75.0)	.05	267 210	—	—	FATIGUE FAILURE
L2-1-46	↓	3.15 (.124)	76.3 (3.005)	↓	16.9 (.66)	↓	↓	↓	↓	0	-	126 800 (28 500)	527 (76.5)	↓	10^3	165 000 (37200)	688 (99.8)	
L2-1-47	↓	3.18 (.125)	76.6 (3.017)	↓	14.7 (.58)	↓	↓	PRELOAD CYCLIC	↓	141 000 (31700)	580 (84.1)	126 800 (28 500)	521 (75.6)	↓	105 295	-	-	FATIGUE FAILURE
L2-1-48	↓	3.02 (.119)	76.5 ([illegible])	↓	[illegible] (.62)	↓	↓	↓	↓	141 000 (31 700)	609 (88.4)	126 800 (28500)	548 (79.5)	↓	46	-	-	FATIGUE FAILURE
L2-1-15	↓	3.25 (.128)	75.0 (2.953)	3/8 HP SLIT	9.4 (.37)	↓	↓	STATIC	↓	0	-	NONE	—	—	—	179 700 (404[illegible])	737 (106.9)	
L2-1-16	↓	3.12 (.123)	73.4 (2.890)	↓	10.2 (.40)	↓	↓	PRELOAD STATIC	↓	161 900 (36400)	706 (102.4)	NONE	-	-	-	165 000 (37 100)	720 (104.4)	
L2-1-11	↓	3.15 (.124)	74.9 (2.950)	1/8 HP SLIT	3.0 (.12)	↓	↓	STATIC	↓	0	—	NONE	-	-	-	149 900 (33700)	635 (92.1)	
L2-1-12	↓	3.22 (.127)	75.1 (2.957)	↓	3.3 (.13)	↓	↓	PRELOAD STATIC	↓	135 000 (30 350)	557 (80.8)	NONE	-	-	-	178 800 (40200)	738 (107.0)	
L2-1-37	↓	3.07 (.121)	76.4 (3.007)	↓	3.0 (.12)	↓	↓	CYCLIC	↓	0	—	121 400 (27300)	517 (75.0)	.05	1 500 165	199 300 (44 800)	845 (123.1)	
L2-1-38	↓	3.10 (.122)	76.3 (3.003)	↓	3.0 (.12)	↓	↓	↓	↓	0	-	121 400 (27300)	514 (74.5)	↓	1004	197 900 (44500)	838 (121.5)	
L2-1-39	↓	3.22 (.127)	76.5 (3.012)	↓	3.0 (.12)	↓	↓	PRELOAD CYCLIC	↓	135 000 (30350)	547 (79.3)	121 400 (27300)	492 (71.4)	↓	1.5×10^6	209 500 (47100)	849 (123.1)	
L2-1-40	↓	3.10 (.122)	76.3 (3.006)	↓	3.0 (.12)	↓	↓	↓	↓	135 000 (30350)	571 (82.8)	121 400 (27 300)	513 (74.4)	↓	1421	192 100 (43 200)	812 (117.8)	

[1] LAMINATE L2 $[(0_3/\pm 80)_2]_s$

[2] GROSS SECTION STRESS

SPEC. NO.	LAYUP	THICK-NESS mm (INCH)	WIDTH mm (INCH)	FLAW TYPE	FLAW LENGTH FRONT mm (INCH)	FLAW LENGTH BACK mm (INCH)	FLAW DEPTH mm (INCH)	TEST TYPE	TEST TEMP. °K (°F)	PRELOAD LOAD N (16)	PRELOAD STRESS [2] MN/m² (KSI)	CYCLIC LOADING MAX LOAD N (16)	CYCLIC LOADING MAX STRESS [2] MN/m² (KSI)	CYCLIC LOADING R	CYCLIC LOADING CYCLES	RESIDUAL STATIC LOAD N (16)	RESIDUAL STATIC STRESS [2] MN/m² (KSI)	REMARKS
L2-1-1	L2 [1]	3.18 (.125)	74.5 (2.932)	NONE	0	0	0	STATIC	RT	0	—	NONE	—	—	—	195700 (44000)	827 (120.0)	
L2-1-2		3.17 (.125)	74.5 (2.932)					PRELOAD STATIC		176400 (39 650)	746 (108.2)	NONE	-	-	-	193 500 (43 500)	818 (118.6)	
L2-1-21		3.17 (.125)	76.2 (2.999)					CYCLIC		0	—	158800 (35700)	656 (95.2)	.05	10298	—	—	FATIGUE FAILURE
L2-1-22		3.15 (.124)	76.1 (2.998)							0	—	158 800 (35700)	662 (96.0)		1003	203100 (45800)	849 (123.2)	
L2-1-23		3.17 (.125)	75.7 (2.981)					PRELOAD CYCLIC		176400 (39650)	734 (106.4)	158 800 (35700)	661 (95.8)		4 599	—	—	FAILED DURING CYCLIC TEST FROM MACHINE FAILURE
L2-1-24		3.10 (.122)	76.1 (2.995)							176400 (39650)	748 (108.5)	—	-	—	—	—	—	STATIC OVERLOAD FAILURE DURING CYCLIC TEST...

[1] LAMINATE L2 $[(0_3/\pm 80)_2]_s$

[2] GROSS SECTION STRESS

SPEC. NO.	LAYUP	THICKNESS mm (INCH)	WIDTH mm (INCH)	FLAW TYPE	FLAW LENGTH FRONT mm (INCH)	FLAW LENGTH BACK mm (INCH)	FLAW DEPTH mm (INCH)	TEST TYPE	TEST TEMP. °K (°F)	PRELOAD LOAD N (lb)	PRELOAD STRESS [2] MN/m² (KSI)	CYCLIC LOADING MAX LOAD N (lb)	CYCLIC LOADING MAX STRESS [2] MN/m² (KSI)	CYCLIC LOADING R	CYCLIC LOADING CYCLES	RESIDUAL STATIC LOAD N (lb)	RESIDUAL STATIC STRESS [2] MN/m² (KSI)	REMARKS
L2-2-1	L2 [1]	3.00 (.118)	75.2 (2.960)	5/8 FP HOLE	15.7 (.62)		–	STATIC	RT	0	–	NONE	–	–	–	99200 (22300)	440 (63.8)	LOW AUTOCLAVE PRESSURE = 345 kN/m² (50 psi)
L2-2-2	↓	3.18 (.125)	75.1 (2.958)	↓	15.7 (.62)		–	PRELOAD STATIC	↓	89400 (20100)	375 (54.4)	NONE	–	–	–	104100 (23400)	436 (63.3)	↓
L2-2-3	↓	3.18 (.125)	75.2 (2.961)	↓	15.7 (.62)		–	CYCLIC	↓	0	–	80500 (18100)	337 (48.9)	.05	1.5×10^6	131700 (29600)	552 (80.0)	↓
L2-2-4	↓	3.15 (.124)	75.2 (2.961)	↓	15.7 (.62)		–	↓	↓	0	–	80500 (18100)	340 (49.3)	↓	10^3	102100 (23100)	434 (62.9)	↓
L2-2-5	↓	3.18 (.125)	75.3 (2.963)	↓	15.7 (.62)		–	PRELOAD CYCLIC	↓	89400 (20100)	374 (54.3)	80500 (18100)	337 (48.9)	↓	1.5×10^6	137000 (30800)	574 (83.2)	↓
L2-2-6	↓	3.20 (.126)	75.2 (2.961)	↓	15.7 (.62)		–	↓	↓	89400 (20100)	372 (53.9)	80500 (18100)	334 (48.5)	↓	10^3	109400 (24600)	454 (65.9)	↓
L2-3-1	↓	3.10 (.122)	74.9 (2.948)	5/8 FP HOLE	15.7 (.62)		–	STATIC	↓	0	–	NONE	–	–	–	101900 (22900)	439 (63.7)	LOW AUTOCLAVE PRESSURE = 172 kN/m² (25 psi)
L2-3-2	↓	3.12 (.123)	74.3 (2.927)	↓	15.7 (.62)		–	PRELOAD STATIC	↓	91000 (20600)	394 (57.2)	NONE	–	–	–	102300 (23000)	440 (63.8)	↓
L2-4-7	↓	3.28 (.129)	75.2 (2.961)	5/8 FP HOLE	15.7 (.62)		–	STATIC	↓	0	–	NONE	–	–	–	112500 (25300)	456 (66.2)	LOW AUTOCLAVE PRESSURE = 86 kN/m² (12.5 psi)
L2-4-2	↓	3.18 (.125)	75.2 (2.962)	5/8 CSK HOLE	23.4 (.92)	15.7 (.62)	–	STATIC	↓	0	–	NONE	–	–	–	89800 (20200)	376 (54.6)	↓
L2-4-3	↓	3.12 (.123)	75.2 (2.962)	↓	23.4 (.92)	15.7 (.62)	–	CYCLIC	↓	0	–	61800 (13900)	261 (37.8)	.05	10^3	95200 (21400)	405 (58.7)	↓
L2-4-4	↓	3.15 (.124)	75.3 (2.963)	↓	23.4 (.92)	15.7 (.62)	–	↓	↓	0	–	60000 (13500)	253 (36.7)	↓	1.5×10^6	121000 (27200)	510 (74.0)	↓
L2-4-5	↓	3.18 (.125)	75.2 (2.961)	↓	23.4 (.92)	15.7 (.62)	–	PRELOAD CYCLIC	↓	74300 (16700)	311 (45.1)	—	—	↓	—	—	—	FAILURE DURING PRELOAD
L2-4-6	↓	3.28 (.129)	75.2 (2.960)	↓	23.4 (.93)	16.0 (.63)	–	↓	↓	66900 (15050)	272 (39.4)	60000 (13500)	244 (35.4)	↓	1.5×10^6	111400 ([illegible])	476 (69.1)	↓

[1] LAMINATE L2 $[(0_3/\pm 80)_2]_s$

[2] GROSS SECTION STRESS

SPEC. NO.	LAYUP	THICK-NESS mm (INCH)	WIDTH mm (INCH)	FLAW TYPE	FLAW LENGTH FRONT mm (INCH)	FLAW LENGTH BACK mm (INCH)	FLAW DEPTH mm (INCH)	TEST TYPE	TEST TEMP. °K (°F)	PRELOAD LOAD N (16)	PRELOAD STRESS [2] MN/m² (KSI)	CYCLIC LOADING MAX LOAD N (16)	CYCLIC LOADING MAX STRESS [2] MN/m² (KSI)	CYCLIC LOADING R	CYCLIC LOADING CYCLES	RESIDUAL STATIC LOAD N (16)	RESIDUAL STATIC STRESS [2] MN/m² (KSI)	REMARKS
L3-1-7	L3 [1]	3.38 (.133)	75.2 (2.961)	5/8 FP HOLE	15.7 (.62)		–	STATIC	RT	0	–	NONE	–	–	–	110 800 (24900)	436 (63.2)	
L3-1-8	↓	3.23 (.127)	75.1 (2.957)	↓	15.7 (.62)		–	PRELOAD STATIC	↓	94700 (21300)	391 (56.7)	NONE	–	–	–	–	–	FAILURE DURING PRELOAD
L3-1-35	↓	3.25 (.128)	75.1 (2.958)	↓	15.7 (.62)		–	CYCLIC	↓	0	–	76900 (17300)	315 (45.7)	.05	10^3	136600 (30700)	559 (81.1)	
L3-1-36	↓	3.25 (.128)	75.1 (2.957)	↓	15.7 (.62)		–	↓	↓	0	–	76900 (17300)	315 (45.7)	↓	1.5×10^6	103600 (23300)	425 (61.6)	
L3-1-37	↓	3.33 (.131)	75.1 (2.958)	↓	15.7 (.62)		–	PRELOAD CYCLIC	↓	85400 (19200)	341 (49.5)	76900 (17300)	308 (44.6)	↓	1.5×10^6	109000 (24500)	436 (63.2)	
L3-1-38	↓	(.133)	75.1 (2.957)	↓	16.0 (.63)		–	↓	↓	85400 (19200)	336 (48.8)	76900 (17300)	303 (44.0)	↓	10^3	104100 (23400)	410 (59.5)	
L3-1-17	L3 [1]	3.30 (.130)	74.9 (2.951)	5/8 FP SLIT	16.0 (.63)		–	STATIC	↓	0	–	NONE	–	–	–	98500 (22150)	348 (57.7)	
L3-1-18	↓	3.38 (.133)	75.0 (2.951)	↓	15.7 (.62)		–	PRELOAD STATIC	↓	88700 (19950)	350 (50.8)	NONE	–	–	–	95400 (21450)	376 (54.6)	
L3-1-55	↓	3.30 (.130)	75.2 (2.959)	↓	15.7 (.62)		–	CYCLIC	↓	0	–	80100 (18000)	323 (46.8)	.05	1,394700	102700 (23100)	414 (60.0)	
L3-1-56	↓	3.43 (.135)	75.1 (2.957)	↓	15.7 (.62)		–	↓	↓	0	–	80100 (18000)	311 (45.1)	↓	10^3	95200 (21400)	370 (53.6)	
L3-1-57	↓	3.35 (.132)	75.1 (2.956)	↓	15.7 (.62)		–	PRELOAD CYCLIC	↓	88700 (19950)	352 (51.1)	80100 (18000)	318 (46.1)	↓	1500 281	97000 (21800)	385 (55.9)	
L3-1-58	↓	3.33 (.131)	75.2 (2.960)	↓	15.7 (.62)		–	↓	↓	89400 (20100)	357 (51.8)	80100 (18000)	320 (46.4)	↓	10^3	105900 (23800)	423 (61.4)	
L3-2-4	L3 [1]	2.89 (.114)	75.0 (2.951)	5/8 FP SLIT	15.7 (.62)		–	STATIC		0	–	NONE	–	–	–	68100 (15300)	314 (45.3)	
L3-2-5	↓	2.97 (.117)	75.0 (2.954)	↓	15.7 (.62)			PRELOAD STATIC		61200 (13770)	274 (39.8)	NONE	–	–	–	62000 (13950)	279 (40.4)	

[1] LAMINATE L3 $[(0/+30/0^*/-30/0)_2]_s$ * PLY OF S-GLASS IN L3-1-X, SPEC NO'S L3-2-X ALL GRAPHITE

[2] GROSS SECTION STRESS

SPEC. NO.	LAYUP	THICKNESS mm (INCH)	WIDTH mm (INCH)	FLAW TYPE	FLAW LENGTH FRONT mm (INCH)	FLAW LENGTH BACK mm (INCH)	FLAW DEPTH mm (INCH)	TEST TYPE	TEST TEMP. °K (°F)	PRELOAD LOAD N (16)	PRELOAD STRESS [2] MN/m² (KSI)	CYCLIC LOADING MAX LOAD N (16)	CYCLIC LOADING MAX STRESS [2] MN/m² (KSI)	CYCLIC LOADING R	CYCLIC LOADING CYCLES	RESIDUAL STATIC LOAD N (16)	RESIDUAL STATIC STRESS [2] MN/m² (KSI)	REMARKS
L3-1-6	L3 [1]	3.38 (.133)	75.2 (2.962)	3/8 FP HOLE	9.6 (.38)		–	STATIC	RT	0	–	NONE	–	–	–	113 400 (25 500)	446 (64.7)	
L3-1-5		3.40 (.134)	75.3 (2.964)		9.6 (.38)		–	PRELOAD STATIC		106 500 (23940)	416 (60.3)	NONE	–	–	–	119 000 (26750)	464 (67.3)	
L3-1-29		3.30 (.130)	75.1 (2.957)		9.4 (.37)			CYCLIC		0	–	91600 (20600)	370 (53.6)	.05	1.5×10^6	111200 (25000)	448 (65.0)	
L3-1-30		3.28 (.129)	75.2 (2.959)		9.4 (.37)					0	–	91600 (20600)	372 (54.0)		10^3	116 500 (26200)	473 (68.6)	
L3-1-33		3.30 (.130)	75.1 (2.957)		9.6 (.38)			PRELOAD CYCLIC		102100 (22950)	412 (59.7)	91600 (20600)	370 (53.6)		764 500	—	—	FAILURE DURING CYCLE. MACHINE OVERLOAD
L3-1-34		3.35 (.132)	75.1 (2.957)		9.4 (.37)					102 100 (22950)	405 (58.8)	91600 (20600)	364 (52.8)		10^3	124100 (27900)	493 (71.5)	
L3-1-13	L3 [1]	3.38 (.133)	75.2 (2.962)	3/8 FP SLIT	9.4 (.37)		–	STATIC		0	–	NONE	–	–	–	114 500 (25750)	451 (65.4)	
L3-1-14		3.35 (.132)	75.2 (2.960)		9.6 (.38)		–	PRELOAD STATIC		103 200 (23200)	409 (59.4)	NONE	–	–	–	114 800 (25800)	455 (66.0)	
L3-1-47		3.18 (.125)	74.4 (2.929)		9.4 (.37)			CYCLIC		0	–	93000 (20900)	394 (57.1)	.05	1.338×10^6	115600 (26000)	490 (71.0)	
L3-1-48		3.35 (.132)	74.6 (2.939)		9.1 (.36)					0	–	93000 (20900)	372 (53.9)		10^3	109400 (24600)	437 (63.4)	
L3-1-49		3.28 (.129)	75.1 (2.957)		9.4 (.37)			PRELOAD CYCLIC		103 200 (23200)	419 (60.8)	93000 (20900)	378 (54.8)		1.5×10^6	110700 (24900)	450 (65.3)	
L3-1-50		3.35 (.132)	75.1 (2.957)		9.1 (.36)					102100 (22975)	410 (59.4)	93000 (20900)	369 (53.5)		10^3	111600 (25100)	443 (64.3)	

[1] LAMINATE L3 $[(0/+30/0^{*}/-30/0)_2]_s$ * PLY OF S-GLASS IN SPEC L3-1-X

[2] GROSS SECTION STRESS

SPEC. NO.	LAYUP	THICK-NESS mm (INCH)	WIDTH mm (INCH)	FLAW TYPE	FLAW LENGTH FRONT mm (INCH)	FLAW LENGTH BACK mm (INCH)	FLAW DEPTH mm (INCH)	TEST TYPE	TEST TEMP. °K (°F)	PRELOAD LOAD N (LB)	PRELOAD STRESS [2] MN/m² (KSI)	CYCLIC LOADING MAX LOAD N (LB)	CYCLIC LOADING MAX STRESS [2] MN/m² (KSI)	CYCLIC LOADING R	CYCLIC LOADING CYCLES	RESIDUAL STATIC LOAD N (LB)	RESIDUAL STATIC STRESS [2] MN/m² (KSI)	REMARKS
L3-1-3	L3 [1]	3.35 (.132)	75.0 (2.954)	1/8 FP HOLE	3.0 (.12)		–	STATIC	RT	0	–	NONE	–	–	–	151 300 ([illegible])	599 (86.9)	
L3-1-4	↓	3.20 (.126)	75.3 (2.963)	↓	3.0 (.12)		–	PRELOAD STATIC	↓	135700 (30 500)	563 (81.7)	NONE	–	–	–	147 200 (33 100)	611 (88.6)	
L3-1-25		3.32 (.131)	75.1 (2.958)		3.0 (.12)			CYCLIC		0	–	121900 (27400)	487 (70.7)	.05	40	—	—	FATIGUE FAILURE
L3-1-26		3.32 (.131)	75.0 (2.954)		3.0 (.12)			↓		0	–	121900 (27400)	488 (70.8)	↓	10^3	145400 (32 700)	583 (84.5)	
L3-1-27		3.32 (.131)	75.1 (2.957)		3.0 (.12)			PRELOAD CYCLIC		135700 (30500)	543 (78.7)	121 900 (27400)	487 (70.7)		1232 250	147700 (33 200)	591 (85.7)	
L3-1-28		3.30 (.130)	75.1 (2.956)		3.0 (.12)			↓		135700 (30500)	547 (79.4)	121 900 (27400)	492 (71.3)		10^3	146800 (33 000)	592 (85.9)	
L3-1-9	L3 [1]	3.40 (.134)	75.1 (2.957)	1/8 FP SLIT	3.0 (.12)		–	STATIC		0	–	NONE	–	–	–	148 300 (33 350)	580 (84.2)	
L3-1-10	↓	3.35 (.132)	75.0 (2.955)	↓	3.3 (.13)		–	PRELOAD STATIC		133 400 (30 000)	530 (76.9)	NONE	–	–	–	146 300 (32 900)	581 (84.3)	
L3-1-39		3.35 (.132)	75.1 (2.957)		3.3 (.13)			CYCLIC		0	–	120 100 (27000)	477 (69.2)	.05	1543700	148 100 (33 300)	588 (85.3)	
L3-1-40		3.28 (.129)	75.0 (2.953)		3.0 (.12)			↓		0	–	120 100 (27 000)	489 (70.9)	↓	10^3	133 400 (30 000)	543 (78.7)	
L3-1-41		3.30 (.130)	75.2 (2.960)		3.3 (.13)			PRELOAD CYCLIC		133 400 (30 000)	538 (78.0)	120 100 (27000)	484 (70.2)		1.5×10^6	141 400 (31 800)	569 (82.6)	
L3-1-42		3.38 (.133)	75.2 (2.960)		3.0 (.12)			↓		133 400 (30 000)	525 (76.2)	120 100 (27000)	473 (68.6)		10^3	145400 (32 700)	573 (83.1)	
L3-2-2	L3 [1]	2.92 (.115)	75.2 (2.959)	1/8 FP SLIT	3.0 (.12)		–	STATIC		0	—	NONE	–	–	–	114300 (25700)	520 (75.5)	
L3-2-3	↓	2.97 (.117)	74.9 (2.949)	↓	3.0 (.12)		–	PRELOAD STATIC	↓	102800 (23100)	462 (67.0)	NONE	–	–	–	107 200 (24100)	481 (69.8)	

[1] LAMINATE L3 $[(0/+30/0^{*}/-30/0)_2]_S$ * PLY OF S-GLASS IN SPEC L3-1-X

[2] GROSS SECTION STRESS

SPEC. NO.	LAYUP	THICK-NESS mm (INCH)	WIDTH mm (INCH)	FLAW TYPE	FLAW LENGTH FRONT mm (INCH)	FLAW LENGTH BACK mm (INCH)	FLAW DEPTH mm (INCH)	TEST TYPE	TEST TEMP. °K (°F)	PRELOAD LOAD N (lb)	PRELOAD STRESS [2] MN/m² (KSI)	CYCLIC LOADING MAX LOAD N (lb)	CYCLIC LOADING MAX STRESS [2] MN/m² (KSI)	CYCLIC LOADING R	CYCLIC LOADING CYCLES	RESIDUAL STATIC LOAD N (lb)	RESIDUAL STATIC STRESS [2] MN/m² (KSI)	REMARKS
L3-1-19	L3 [1]	3.38 (.133)	75.1 (2.956)	5/8 HP SLIT	[illegible] (.68)	0	1.5 (.06)	STATIC	RT	—	—	NONE	-	-	-	200600 (45100)	791 (114.7)	
L3-1-20		3.28 (.129)	75.0 (2.954)		16.5 (.65)	0		PRELOAD STATIC		155200 (34900)	632 (91.6)	NONE	—	-	—	-	-	FAILURE DURING PRELOAD
L3-1-59		3.30 (.130)	75.0 (2.953)		16.5 (.65)	0		CYCLIC		0	-	125900 (28300)	508 (73.7)	.05	259986	—	—	FATIGUE FAILURE
L3-1-60		3.40 (.134)	75.1 (2.955)		15.7 (.62)	0				0	-	125900 (28300)	493 (71.5)		10^3	179300 (40300)	702 (101.8)	
L3-1-61		3.33 (.131)	75.0 (2.953)		14.7 (.58)	0		PRELOAD CYCLIC		139700 (31400)	560 (81.2)	125900 (28300)	504 (73.1)		458516	-	—	FATIGUE FAILURE
L3-1-62		3.33 (.131)	75.0 (2.955)		16.5 (.65)	0				139700 (31400)	559 (81.1)	125900 (28300)	504 (73.1)		1057	165900 (37300)	665 (96.4)	
L3-2-6	L3 [1]	2.97 (.117)	75.0 (2.952)	5/8 HP SLIT	17.0 (.67)	0	1.5 (.06)	PRELOAD		0	-	NONE	—	-	-	121000 (27200)	543 (78.8)	
L3-2-7		2.95 (.116)	75.0 (2.952)		15.7 (.62)	0		PRELOAD STATIC		109000 (24500)	493 (71.5)	NONE	-	-	—	27700 (28700)	578 (83.8)	

[1] LAMINATE L3 $[(0/+30/0/-30/0)_2]_s$ * PLY OF S-GLASS IN SPEC L3-1-X
[2] GROSS SECTION STRESS

SPEC. NO.	LAYUP	THICKNESS mm (INCH)	WIDTH mm (INCH)	FLAW TYPE	FLAW LENGTH FRONT mm (INCH)	FLAW LENGTH BACK mm (INCH)	FLAW DEPTH mm (INCH)	TEST TYPE	TEST TEMP. °K (°F)	PRELOAD LOAD N (lb)	PRELOAD STRESS (2) MN/m² (KSI)	CYCLIC LOADING MAX LOAD N (lb)	CYCLIC LOADING MAX STRESS (2) MN/m² (KSI)	CYCLIC LOADING R	CYCLIC LOADING CYCLES	RESIDUAL STATIC LOAD N (lb)	RESIDUAL STATIC STRESS (2) MN/m² (KSI)	REMARKS
L3-1-15	L3 (1)	3.38 (.133)	75.1 (2.956)	3/8 HP SLIT	9.9 (.39)	0	1.5 (.06)	STATIC	RT	0	—	NONE	—	—	—	180400 (40 550)	711 (103.1)	
L3-1-16		3.20 (.126)	75.0 (2.954)		9.9 (.39)	0	1.5 (.06)	PRELOAD STATIC		162400 (36500)	676 (98.1)	NONE	—	—	—	167000 (37550)	696 (100.9)	
L3-1-51		3.30 (.130)	75.1 (2.957)		10.4 (.41)	0		CYCLIC		0	—	135200 (30400)	545 (79.1)	.05	875 542	—	—	FATIGUE FAILURE
L3-1-52		3.40 (.134)	75.1 (2.957)		10.7 (.42)	0				0	—	135 200 (30 400)	529 (76.7)		10^3	177900 (40 000)	696 (100.9)	
L3-1-53		3.28 (.129)	75.1 (2.958)		10.2 (.40)	0		PRELOAD CYCLIC		150300 (33 800)	611 (88.6)	135 200 (30 400)	549 (79.7)		17100	—	—	FATIGUE FAILURE
L3-1-54		3.35 (.132)	75.1 (2.958)	3/8 FD SLIT	9.4 (.37)			CYCLIC		0	—	93000 (20900)	369 (53.5)		10^5	114300 (25700)	454 (65.8)	
L3-1-11	L3 (1)	3.38 (.133)	75.1 (2.955)	1/8 HP SLIT	3.0 (.12)	0	1.5 (.06)	STATIC		0	—	NONE	—	—	—	190 400 (42800)	751 (108.9)	
L3-1-12		3.22 (.127)	75.2 (2.962)		3.0 (.12)	0	1.5 (.06)	PRELOAD STATIC		171300 (38500)	705 (102.3)	NONE	—	—	—	181000 (40700)	746 (108.2)	
L3-1-43		3.22 (.127)	75.2 (2.960)		3.0 (.12)	0		CYCLIC		0	—	153900 (34600)	634 (92.0)	.05	7,177	—	—	FATIGUE FAILURE
L3-1-44		3.30 (.130)	75.1 (2.958)		3.0 (.12)	0				0	—	153900 (34600)	621 (90.0)		10^3	183700 (41 300)	741 (107.4)	
L3-1-45		3.30 (.130)	74.6 (2.937)		3.0 (.12)	0		PRELOAD CYCLIC		171200 (38500)	695 (100.8)	153900 (34600)	625 (90.6)		280 400	—	—	FATIGUE FAILURE
L3-1-46		3.38 (.133)	74.6 (2.939)		2.0 (.12)	0				171200 (38500)	679 (98.5)	153900 (34 600)	610 (88.5)		10^3	191700 (43 100)	761 (110.3)	

(1) LAMINATE L3 $[(0/+30/0/-30/0)_2]_S$ * PLY OF S-GLASS IN SPEC L3-1-X

(2) GROSS SECTION STRESS

SPEC. NO.	LAYUP	THICK-NESS mm (INCH)	WIDTH mm (INCH)	FLAW TYPE	FLAW LENGTH FRONT mm (INCH)	FLAW LENGTH BACK mm (INCH)	FLAW DEPTH mm (INCH)	TEST TYPE	TEST TEMP. °K (°F)	PRELOAD LOAD N (lb)	PRELOAD STRESS [2] MN/m² (KSI)	CYCLIC LOADING MAX LOAD N (lb)	CYCLIC LOADING MAX STRESS [2] MN/m² (KSI)	CYCLIC LOADING R	CYCLIC LOADING CYCLES	RESIDUAL STATIC LOAD N (lb)	RESIDUAL STATIC STRESS [2] MN/m² (KSI)	REMARKS
L3-1-1	L3 [1]	3.45 (.136)	75.2 (2.960)	NONE	0	0	0	STATIC	RT	0	–	NONE	–	–	–	240200 (54000)	924 (134.1)	
L3-1-2	↓	3.32 (.131)	75.1 (2.957)	↓	0	0	0	PRELOAD STATIC	↓	216200 (48600)	865 (125.5)	NONE	–	–	–	227700 (51200)	912 (132.2)	
L3-1-21	↓	3.30 (.130)	75.1 (2.958	↓	0	0	0	CYCLIC	↓	0	–	153900 (34600)	621 (90.0)	.05	122 284	–	–	FATIGUE FAILURE
L3-1-22	↓	3.35 (.132)	75.0 (2.954)	↓	0	0	0	↓	↓	0	–	153900 (34600)	612 (88.7)	↓	10^3	234900 (52800)	934 (135.4)	
L3-1-23	↓	3.35 (.132)	75.1 (2.956)	↓	0	0	0	PRELOAD CYCLIC	↓	219300 (49300)	871 (126.3)	–	–	–	–	–	–	FAILURE DURING PRELOAD
L3-1-24	↓	3.25 (.128)	75.1 (2.958)	↓	0	0	0	↓	↓	212200 (47700)	869 (126.0)	–	–	–	–	–	–	"

[1] LAMINATE L3 $[(0/+30/0/-30/0)_2]_s$ * PLY OF S-GLASS IN SPEC L3-1-X

[2] GROSS SECTION STRESS

APPENDIX B

ULTRASONIC INSPECTION DATA

This appendix contains copies of the ultrasonic C-scan records that were developed for the test specimens. The records are identified by the test specimen number, the defect code and a brief description of the point in the test sequence the inspection was made. For many of the test specimens, ultrasonic inspection was performed several times during the test showing the progressive development of the damage.

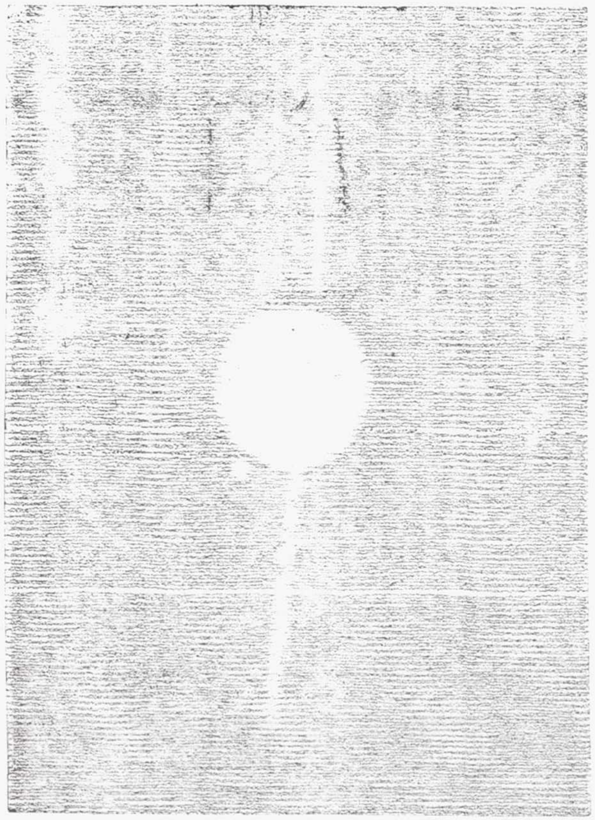

BEFORE TEST

SPECIMEN NUMBER LI-5-6
5/8 FP HOLE

NO PRELOAD

AFTER PRELOAD

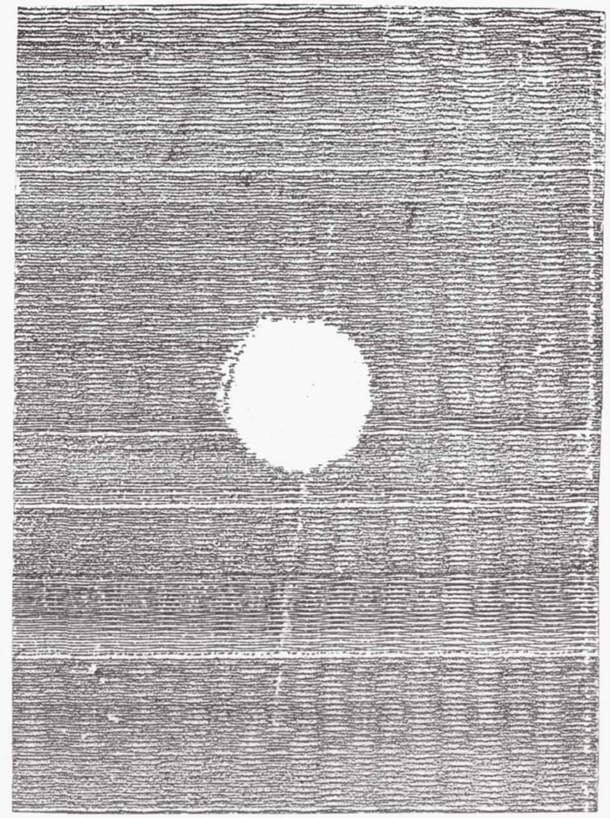

AFTER CYCLIC TEST

10^3 CYCLES

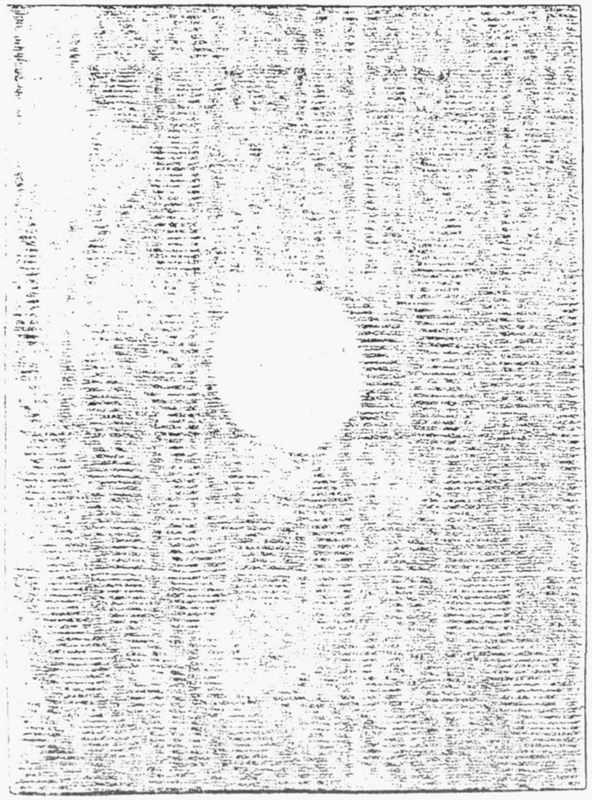

BEFORE TEST

SPECIMEN NUMBER LI-5-9
5/8 FP HOLE

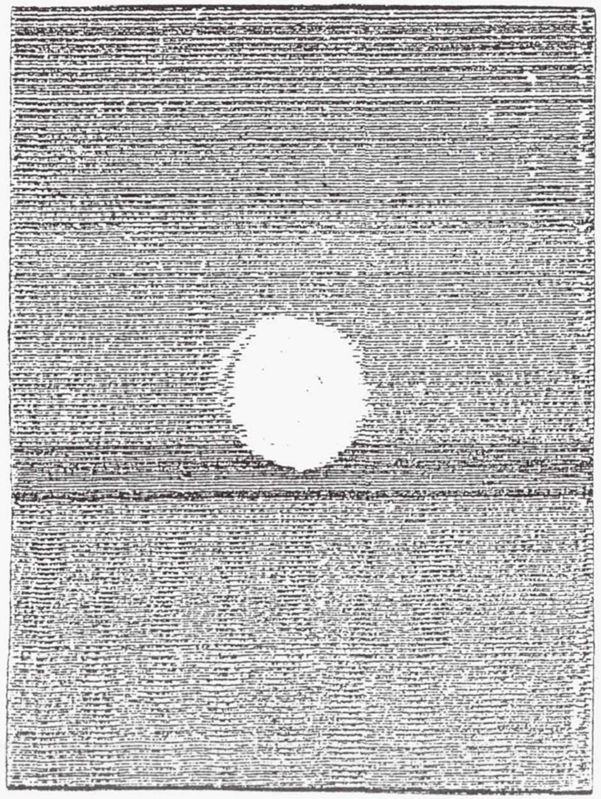

AFTER PRELOAD

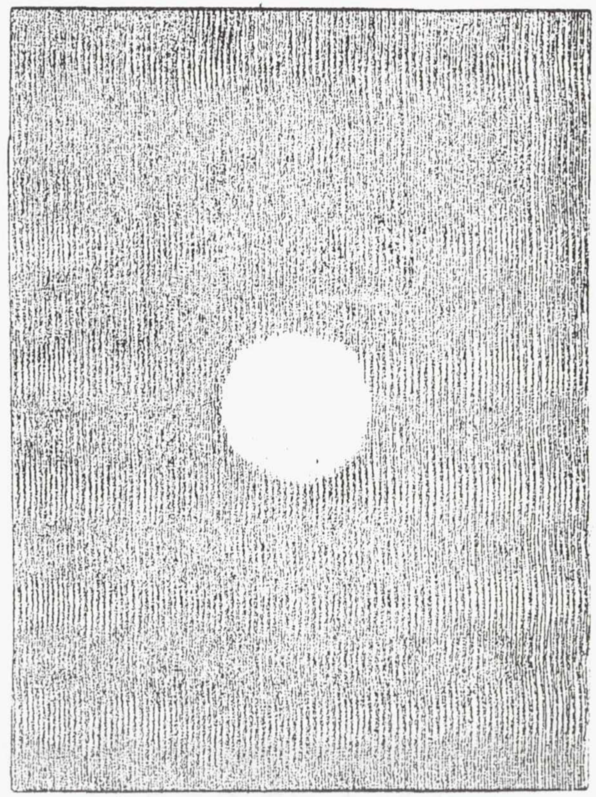

AFTER CYCLIC TEST

10^5 CYCLES

NOT INSPECTED

NO PRELOAD

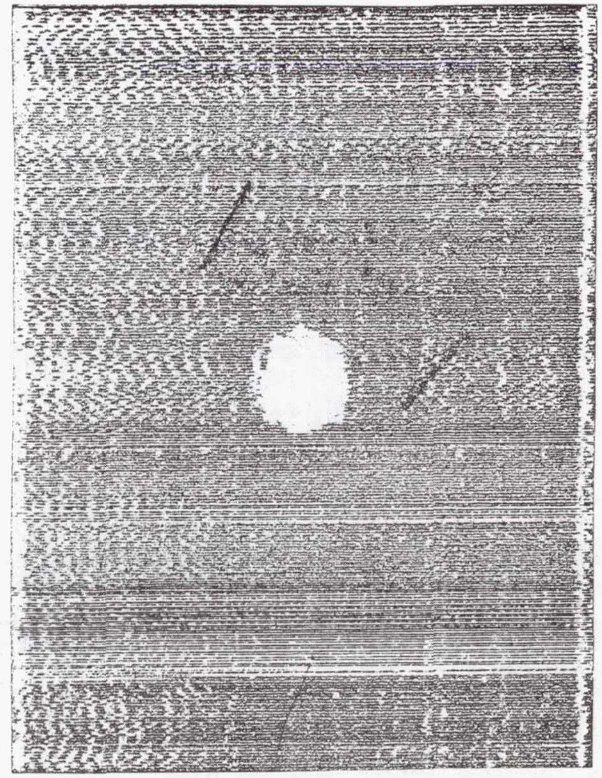

BEFORE TEST

SPECIMEN NUMBER LI-4-12
3/8 FP HOLE

AFTER CYCLIC TEST
10^5 CYCLES

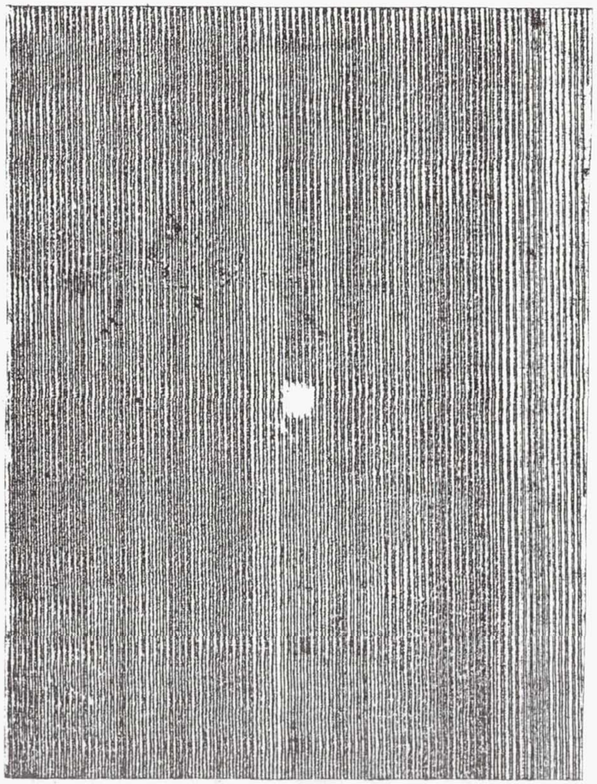

NO PRELOAD

AFTER 10^3 CYCLES
SPECIMEN NUMBER LI-4-1
1/8 FULL PENETRATION HOLE

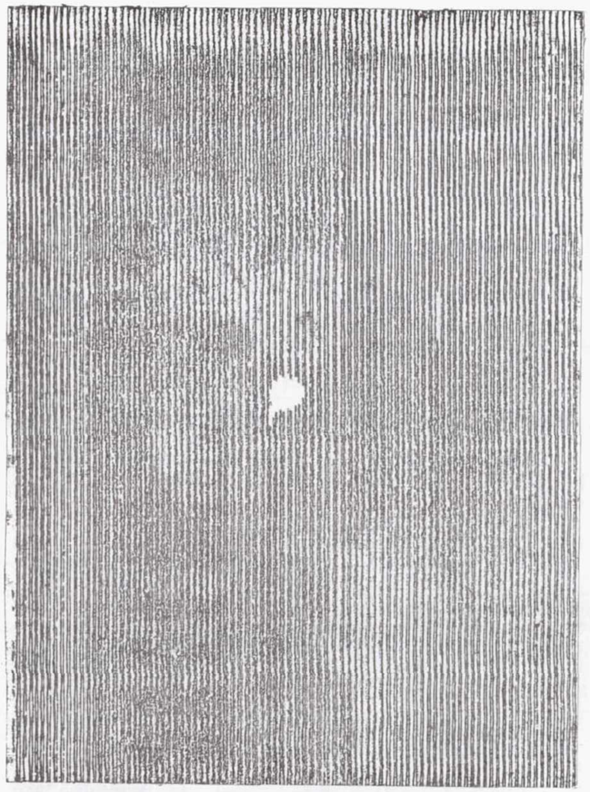

PRELOADED

AFTER 10^3 CYCLES

SPECIMEN NUMBER LI-4-3
1/8 FULL PENETRATION HOLE

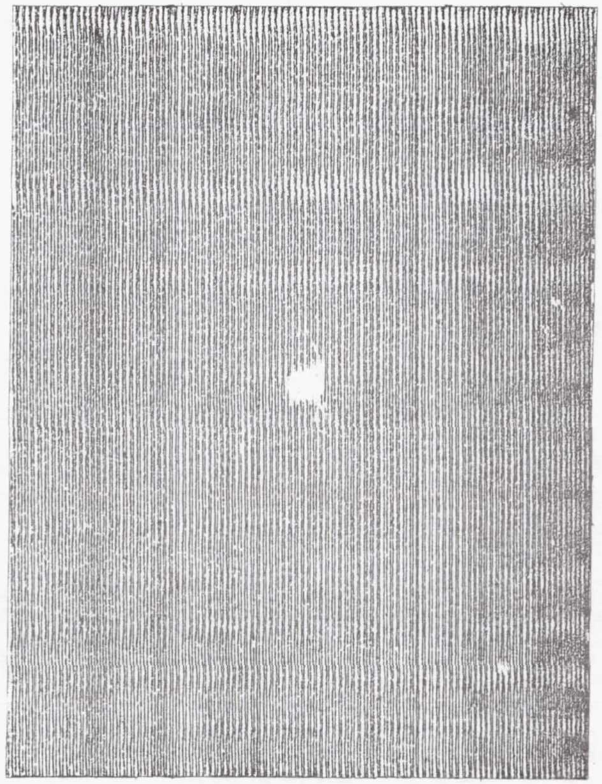

PRELOADED

AFTER 10^5 CYCLES

SPECIMEN NUMBER LI-4-4
1/8 FULL PENETRATION HOLE

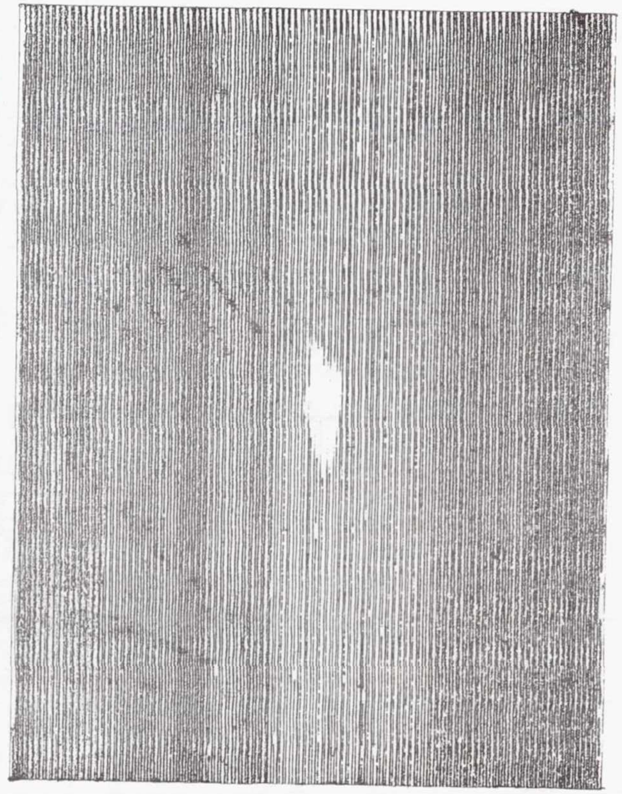

PRELOADED

AFTER 1.5×10^6 CYCLES

SPECIMEN NUMBER LI-4-2
1/8 FULL PENETRATION HOLE

NO PRELOAD

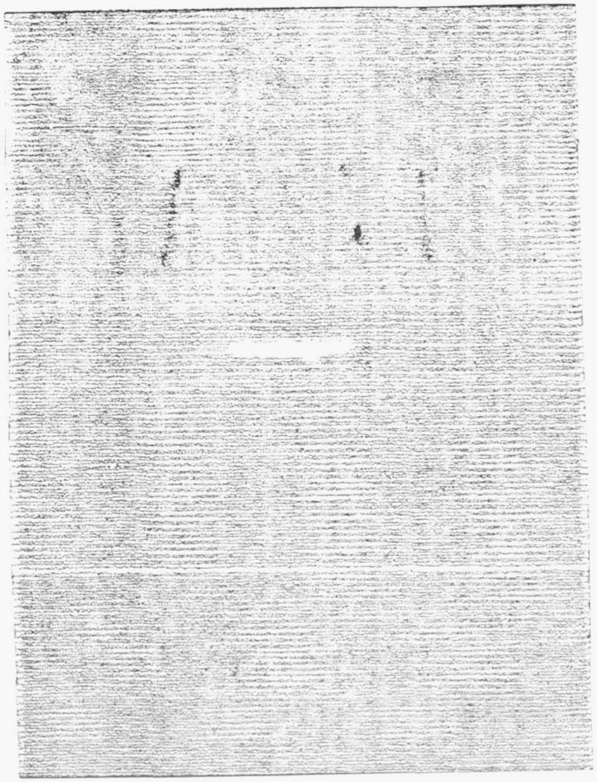

BEFORE TEST

SPECIMEN NUMBER LI-7-11

5/8 FP SLIT

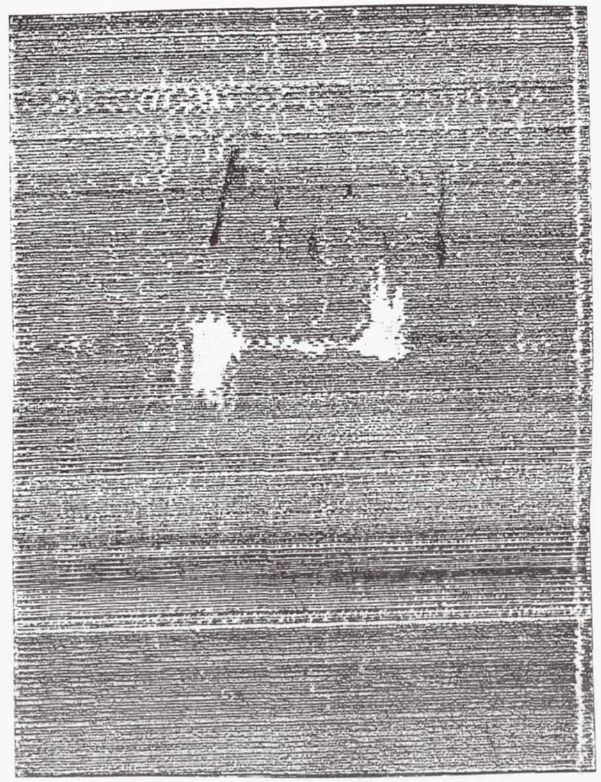

AFTER CYCLIC TEST

10^3 CYCLES

NOT INSPECTED

NO PRELOAD

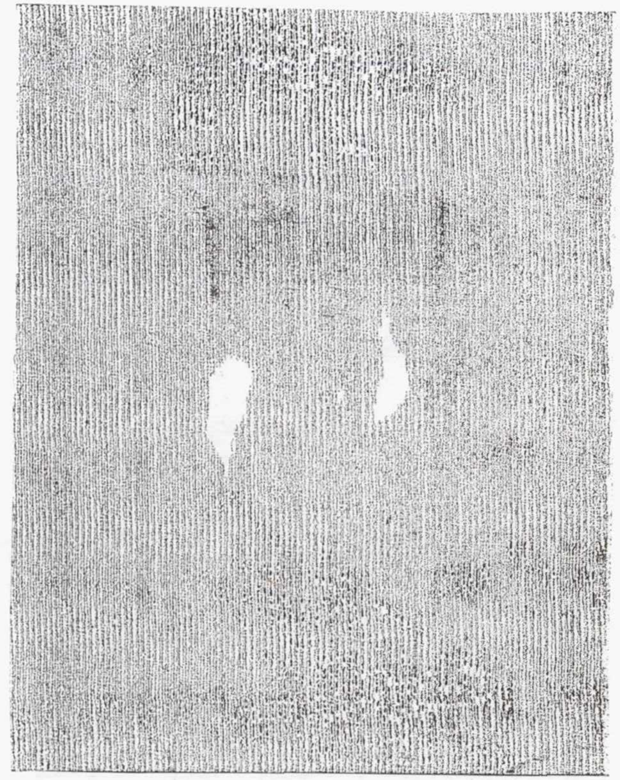

BEFORE TEST

SPECIMEN NUMBER LI-7-10

5/8 FP SLIT

AFTER CYCLIC TEST

10^5 CYCLES

NOT INSPECTED

NO PRELOAD

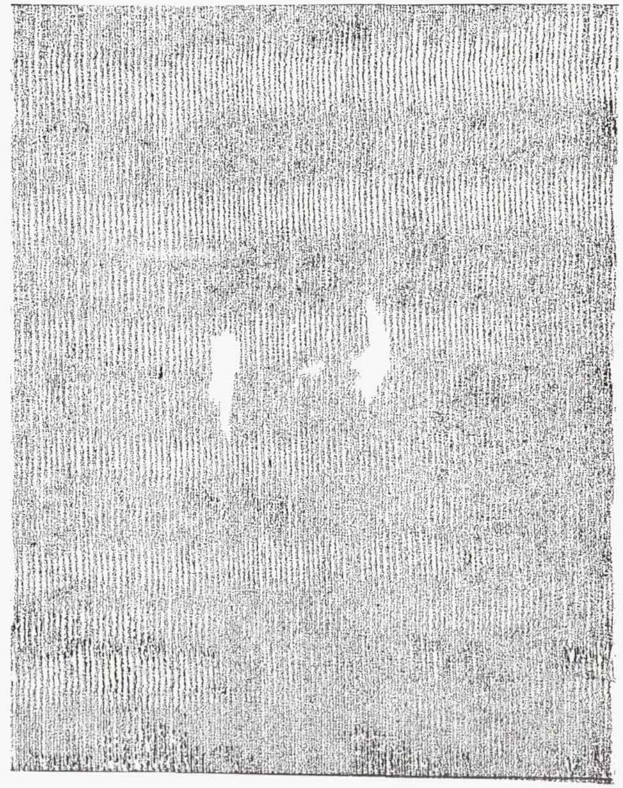

BEFORE TEST

SPECIMEN NUMBER LI-7-9

5/8 FP SLIT

AFTER CYCLIC TEST

1.5 x 10^6 CYCLES

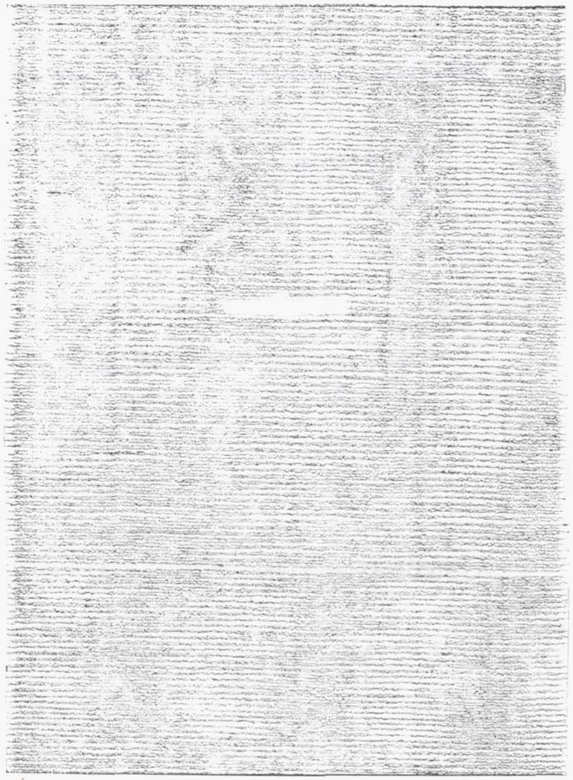

BEFORE TEST

SPECIMEN NUMBER LI-7-14
5/8 FP SLIT

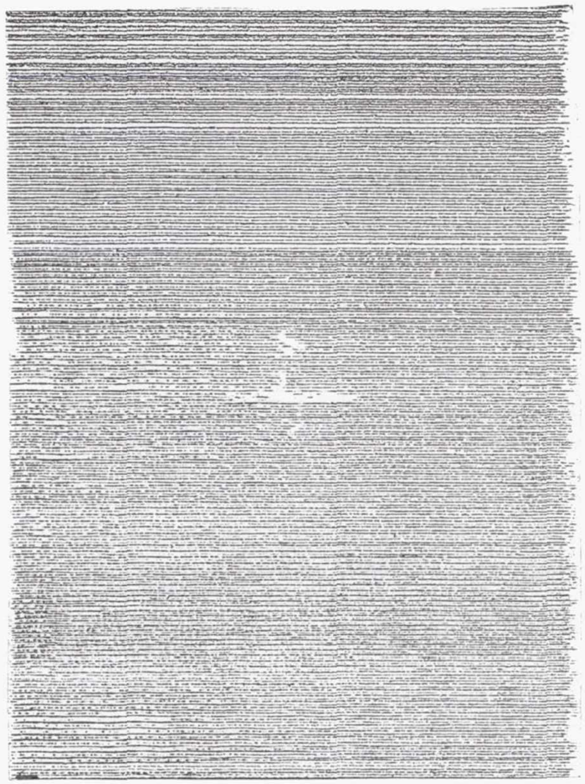

AFTER PRELOAD

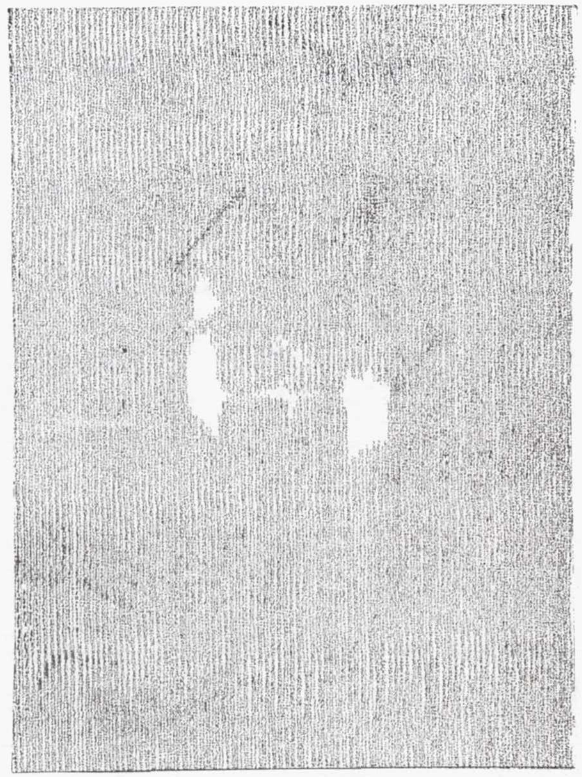

AFTER CYCLIC TEST

1.5 x 10^6 CYCLES

NOT INSPECTED	NOT INSPECTED	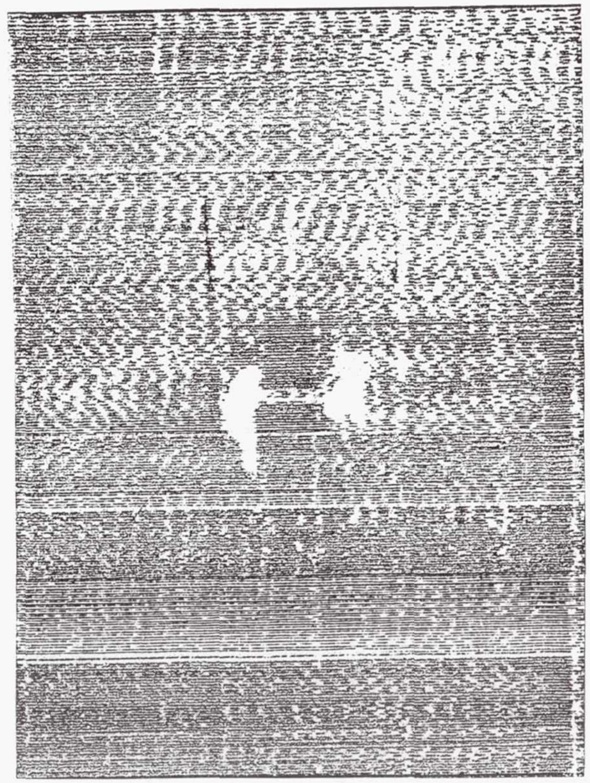
BEFORE TEST	AFTER PRELOAD	AFTER CYCLIC TEST
SPECIMEN NUMBER LI-7-7		10^5 CYCLES
3/8 FP SLIT		

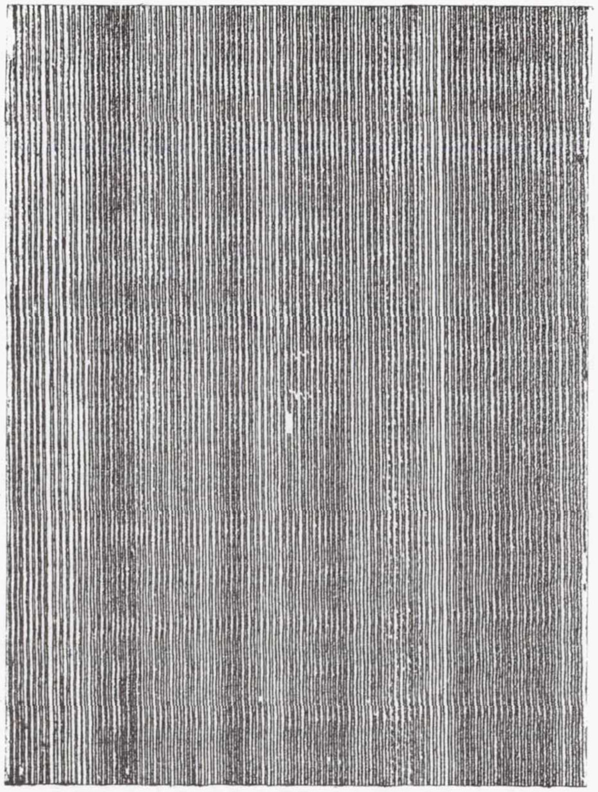

NO PRELOAD

AFTER 10^3 CYCLES

SPECIMEN NUMBER LI-6-4

1/8 FULL PENETRATION SLIT

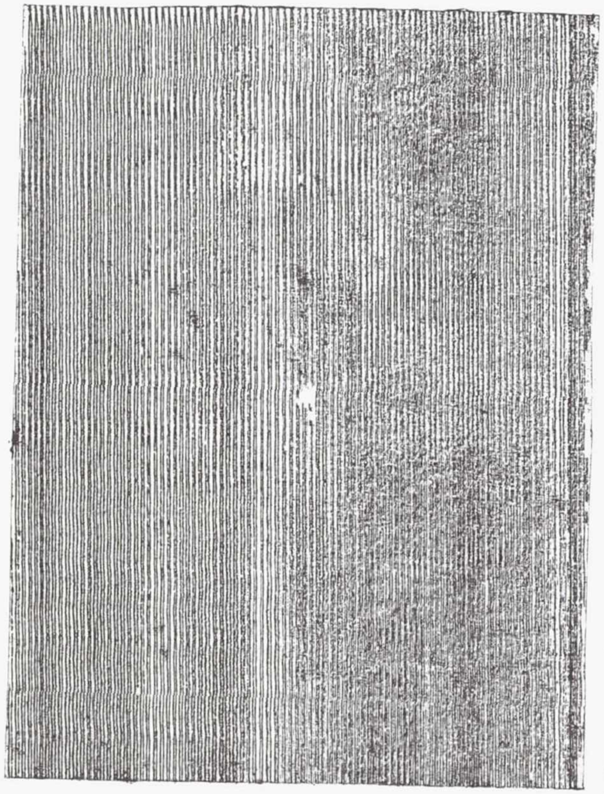

PRELOADED

AFTER 10^3 CYCLES

SPECIMEN NUMBER LI-6-7

1/8 FULL PENETRATION SLIT

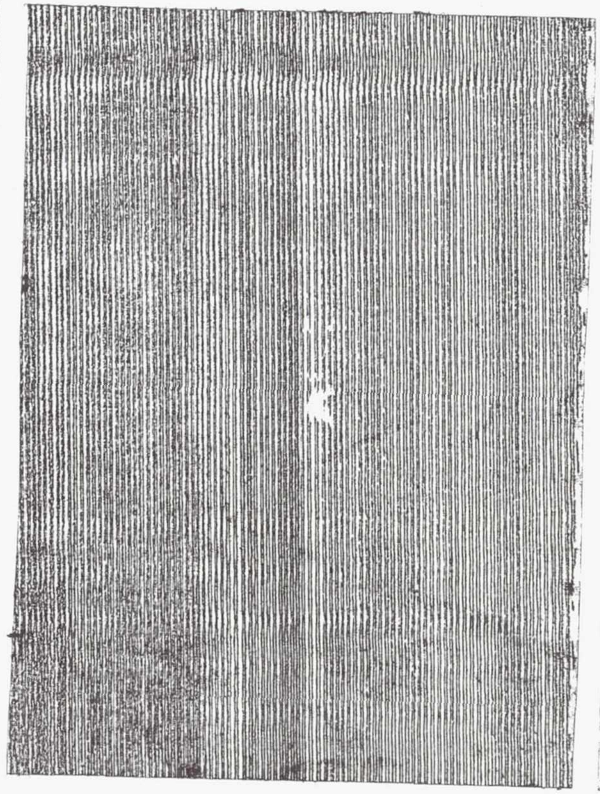

PRELOADED

AFTER 10^5 CYCLES

SPECIMEN NUMBER LI-6-8

1/8 FULL PENETRATION SLIT

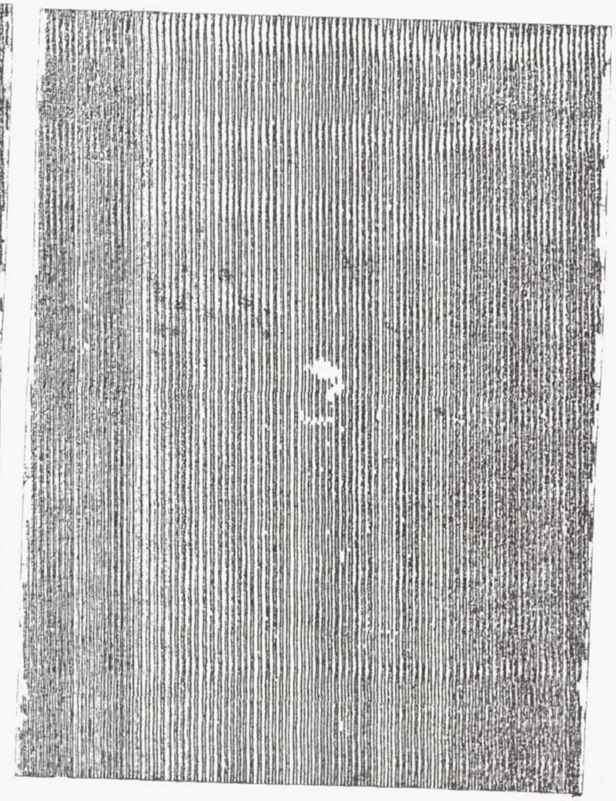

PRELOADED

AFTER 1.5×10^6 CYCLES

SPECIMEN NUMBER LI-6-9

1/8 FULL PENETRATION SLIT

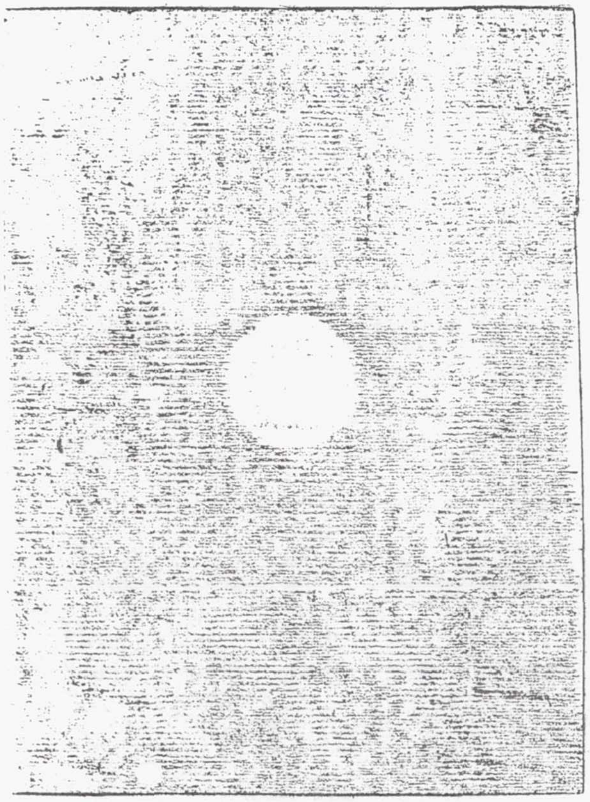
BEFORE TEST

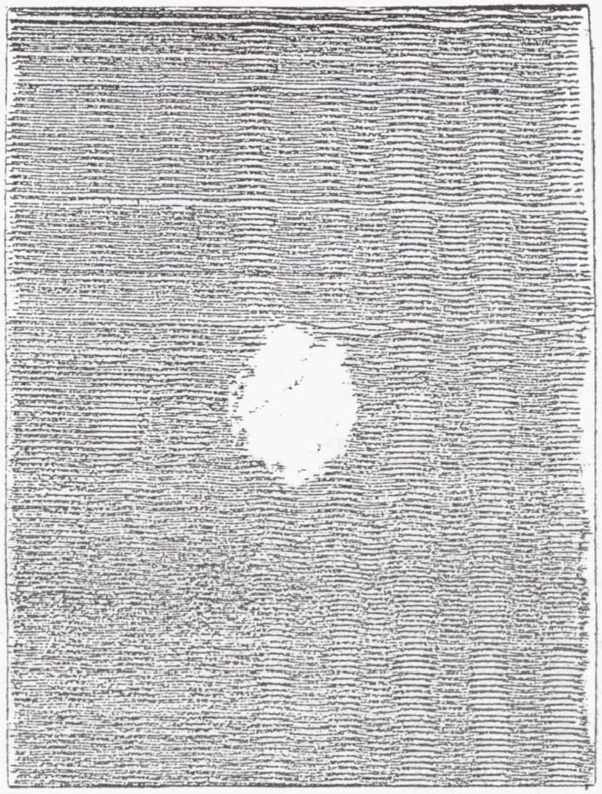
AFTER PRELOAD

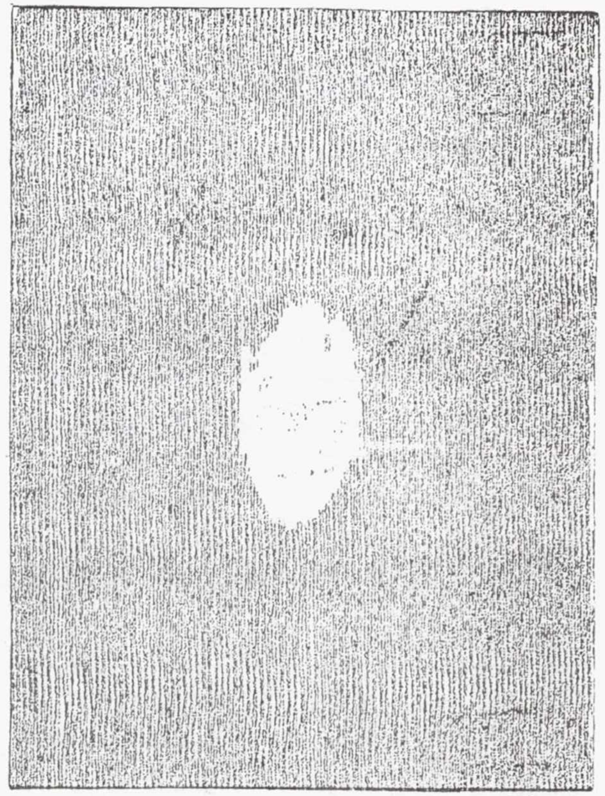
AFTER 10^3 CYCLES

SPECIMEN NUMBER LI-6-3

5/8 HP HOLE

NO PRELOAD

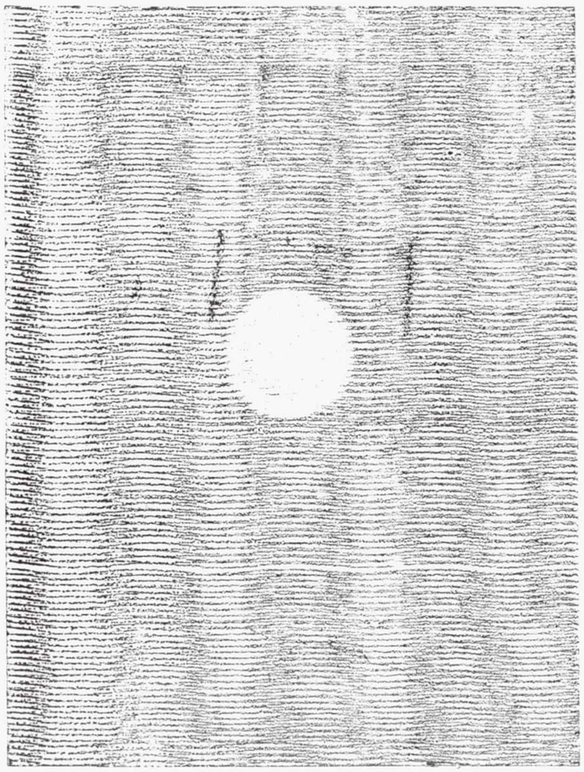

BEFORE TEST

SPECIMEN NUMBER LI-5-12

5/8 HP HOLE

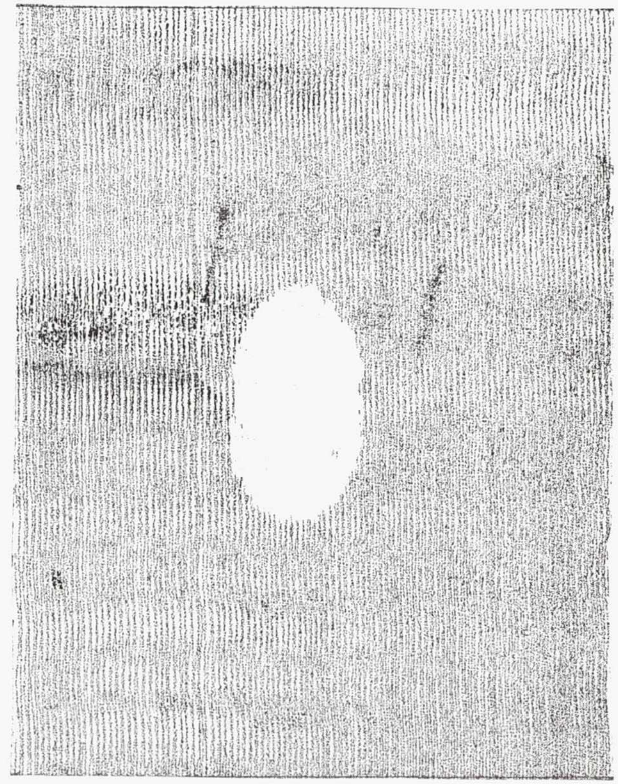

AFTER CYCLIC TEST

10^3 CYCLES

NO PRELOAD

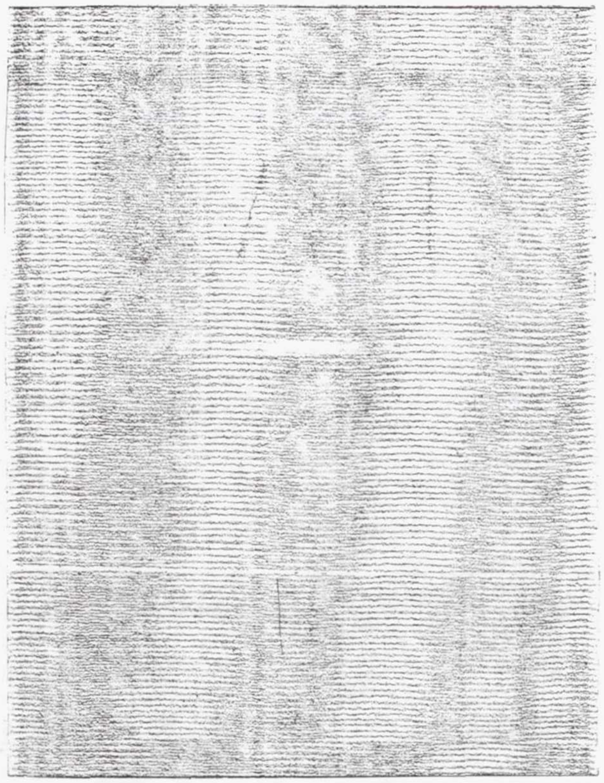

BEFORE TEST

SPECIMEN NUMBER LI-8-3

5/8 HP SLIT

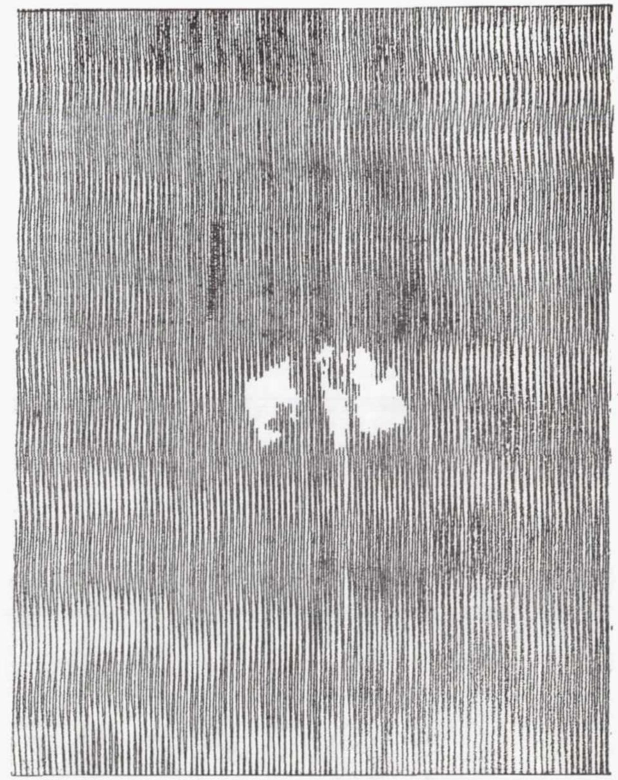

AFTER CYCLIC TEST

10^3 CYCLES

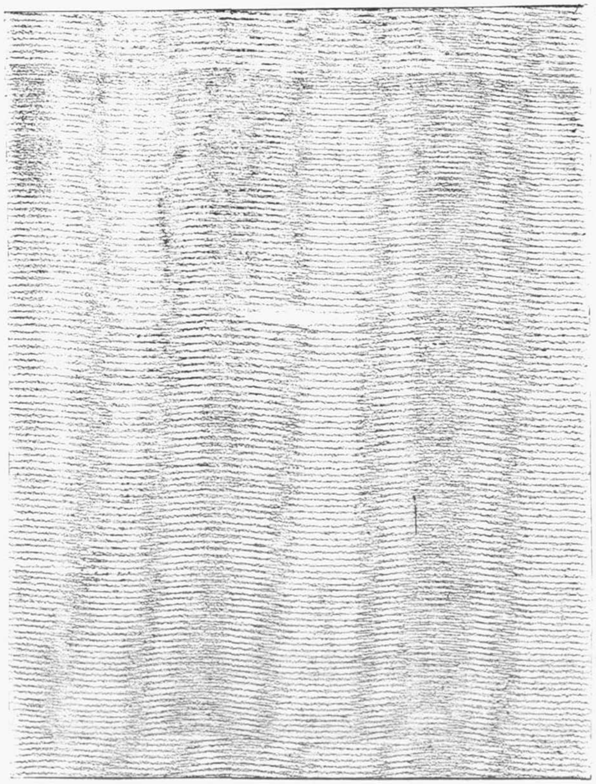

BEFORE TEST

SPECIMEN NUMBER LI-8-6

5/8 HP SLIT

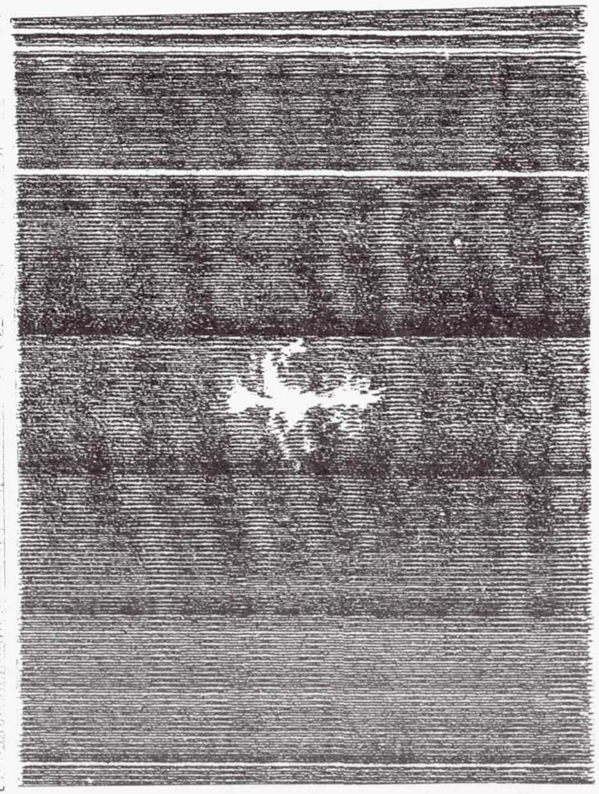

AFTER PRELOAD

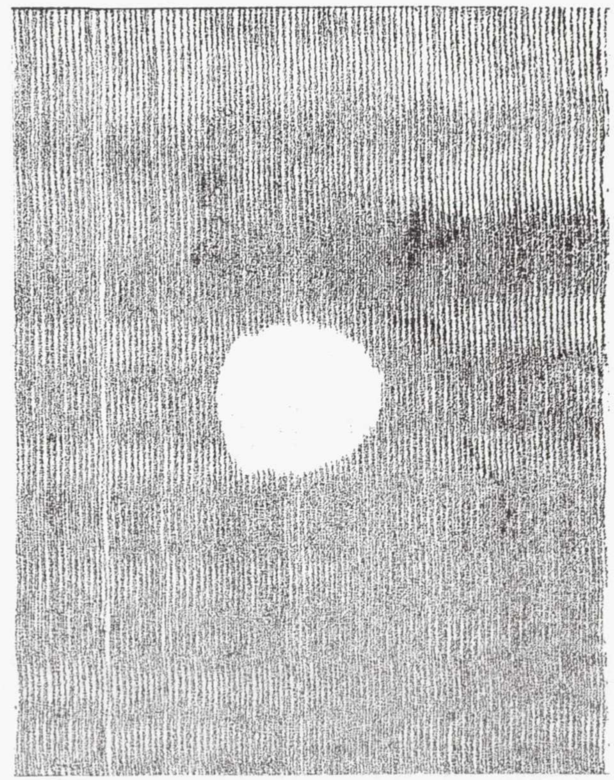

AFTER CYCLIC TEST

10^3 CYCLES

BEFORE TEST	AFTER PRELOAD	AFTER CYCLIC TEST
NOT INSPECTED	NOT INSPECTED	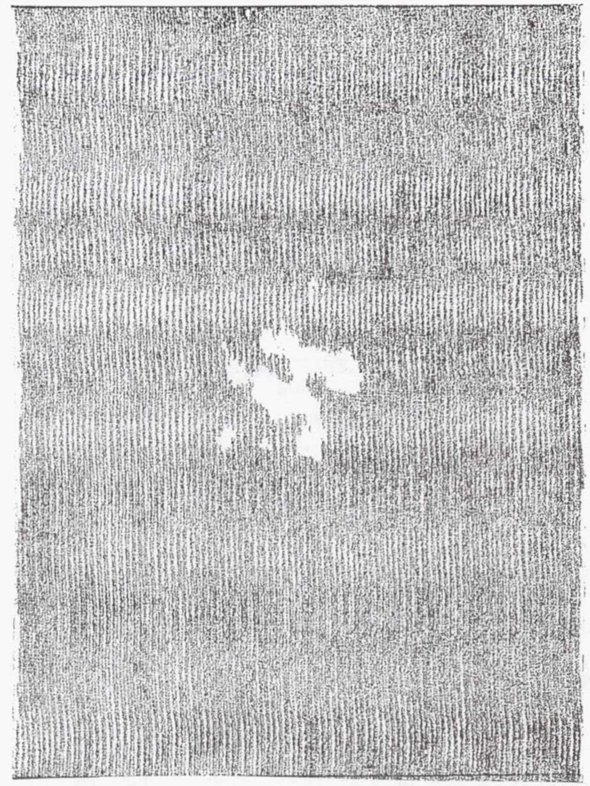
BEFORE TEST SPECIMEN NUMBER LI-8-5 5/8 HP SLIT	AFTER PRELOAD	AFTER CYCLIC TEST 10^5 CYCLES

NOT INPSECTED

BEFORE TEST

SPECIMEN NUMBER LI-8-4

5/8 HP SLIT

NOT INSPECTED

AFTER PRELOAD

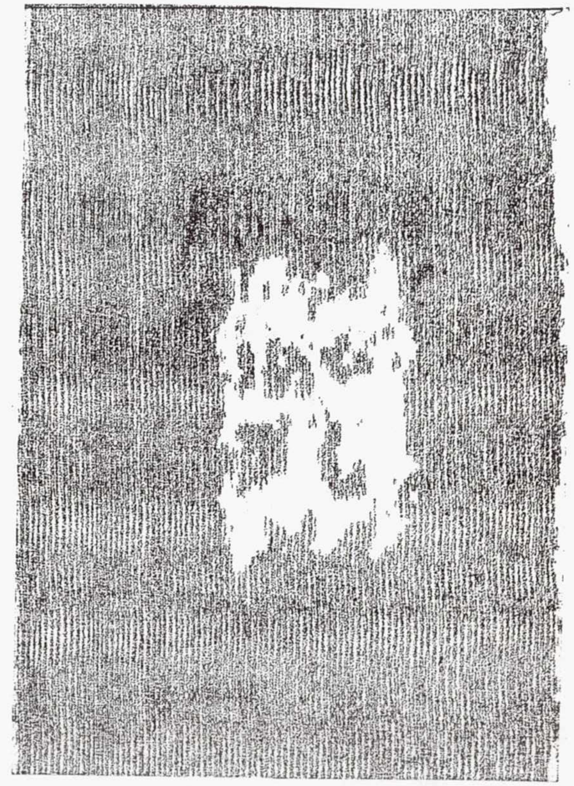

AFTER CYCLIC TESTS

1.5×10^6 CYCLES

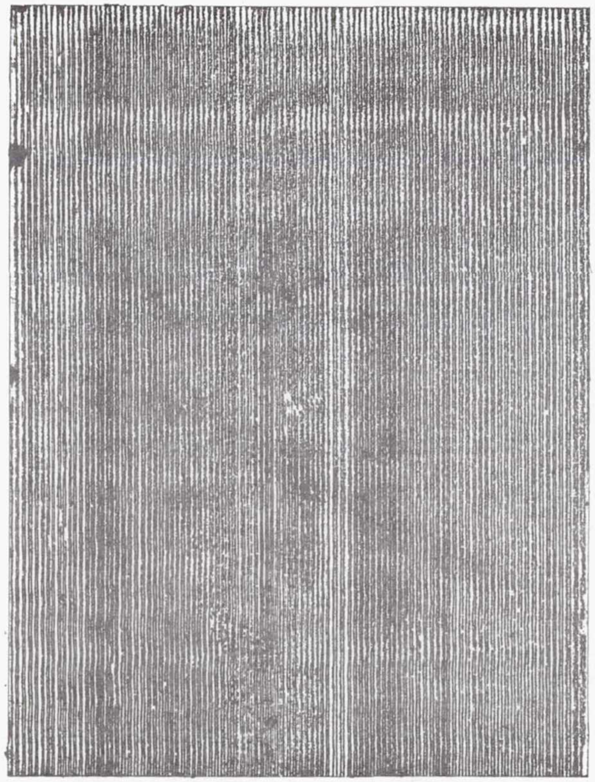

NO PRELOAD
AFTER 10^3 CYCLES
SPECIMEN NUMBER LI-6-12
1/8 HALF PENETRATION SLIT

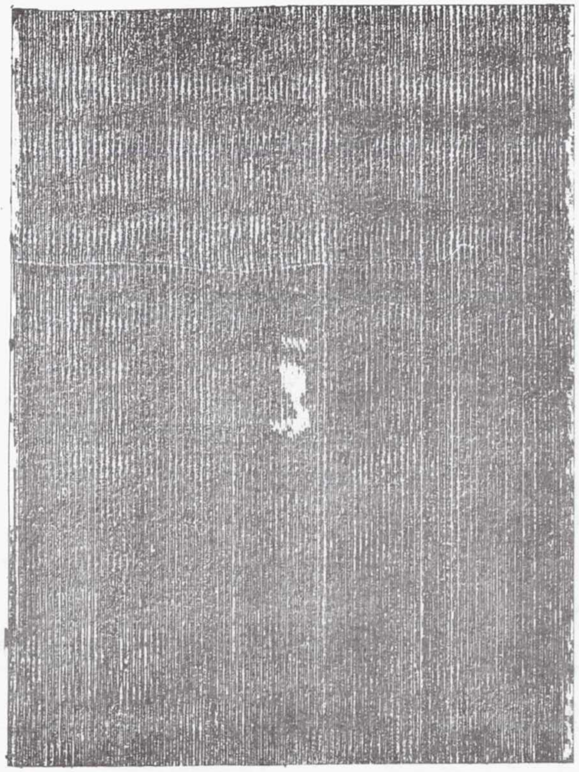

NO PRELOAD
AFTER 1.5×10^6 CYCLES
SPECIMEN LI-7-1
1/8 HALF PENETRATION SLIT

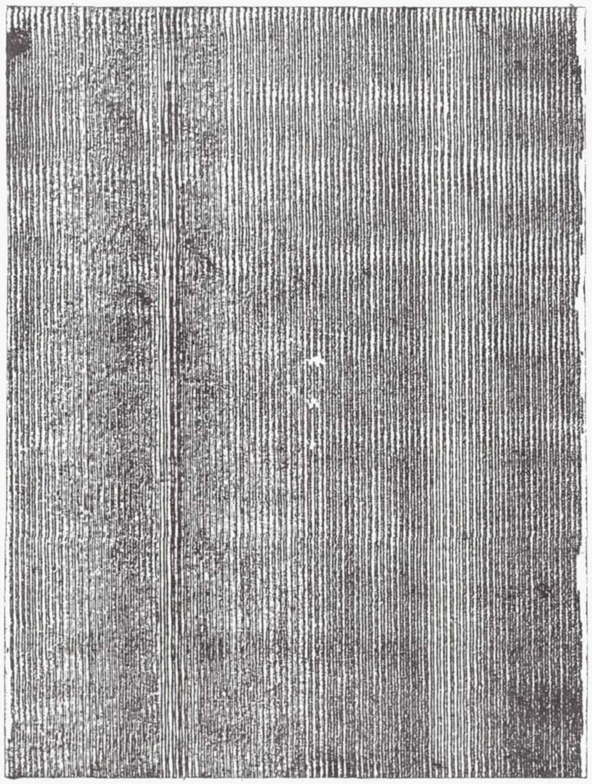

PRELOADED

10^3 CYCLES

SPECIMEN NUMBER LI-7-3

1/8 HALF PENETRATION SLIT

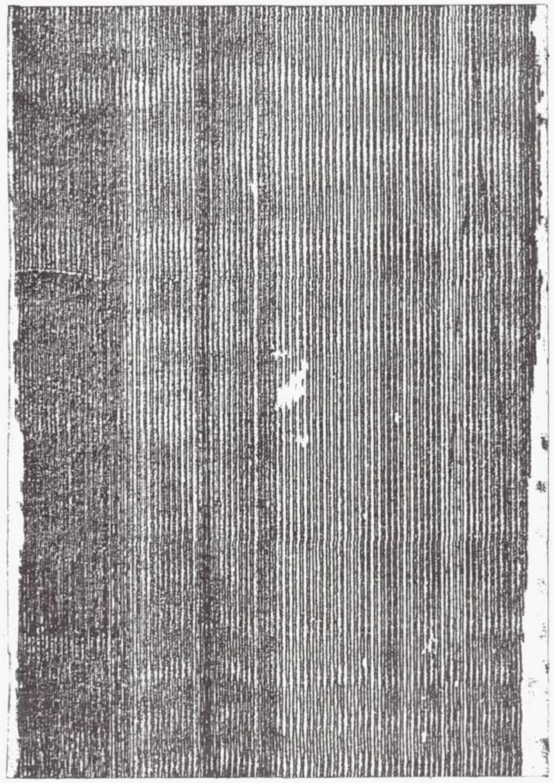

PRELOADED

10^5 CYCLES

SPECIMEN NUMBER LI-7-2

1/8 HALF PENETRATION SLIT

NO PRELOAD

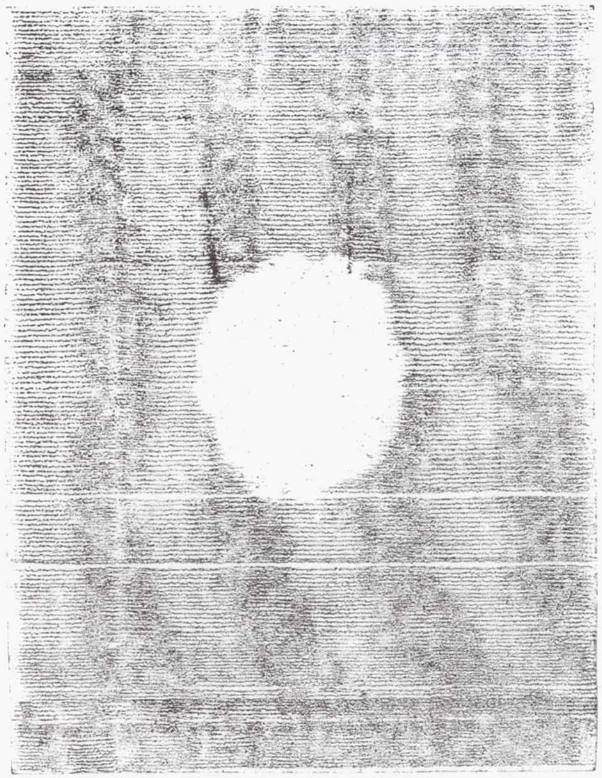

BEFORE TEST

SPECIMEN NUMBER LI-8-11

5/8 CSK HOLE

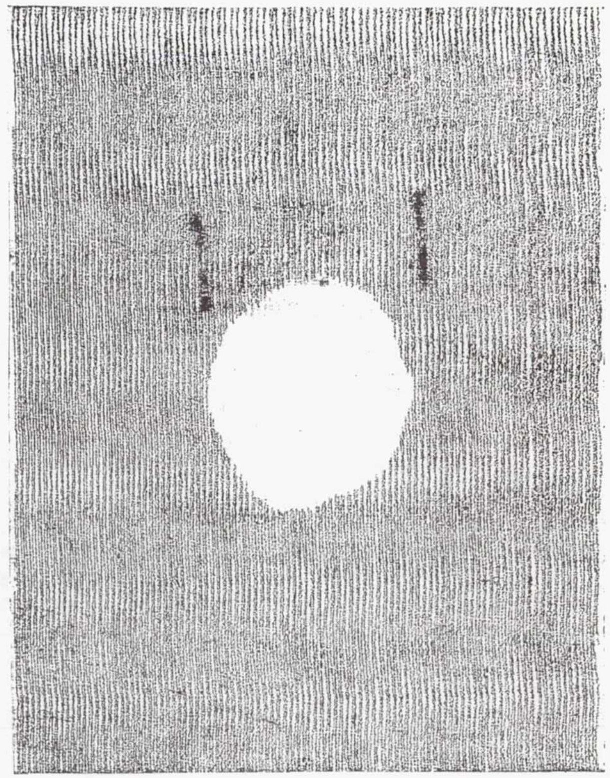

AFTER CYCLIC TEST

10^3 CYCLES

NO PRELOAD

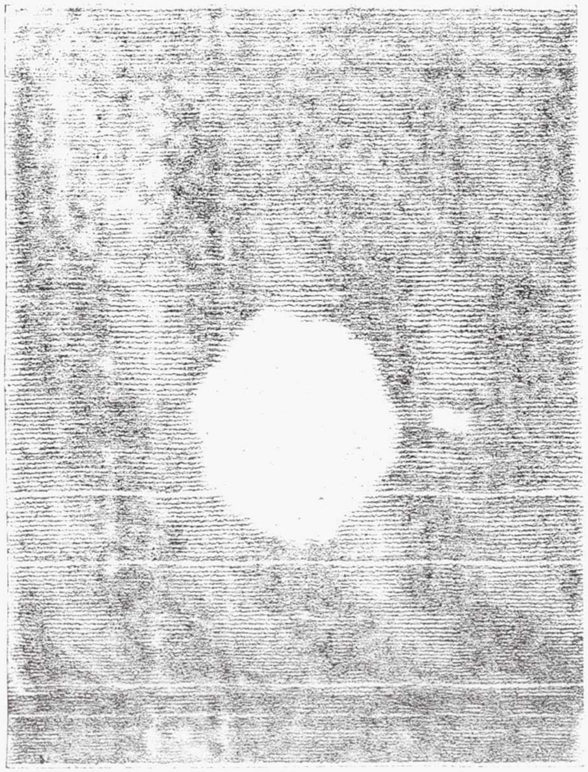

BEFORE TEST

SPECIMEN NUMBER LI-8-12

5/8 CSK HOLE

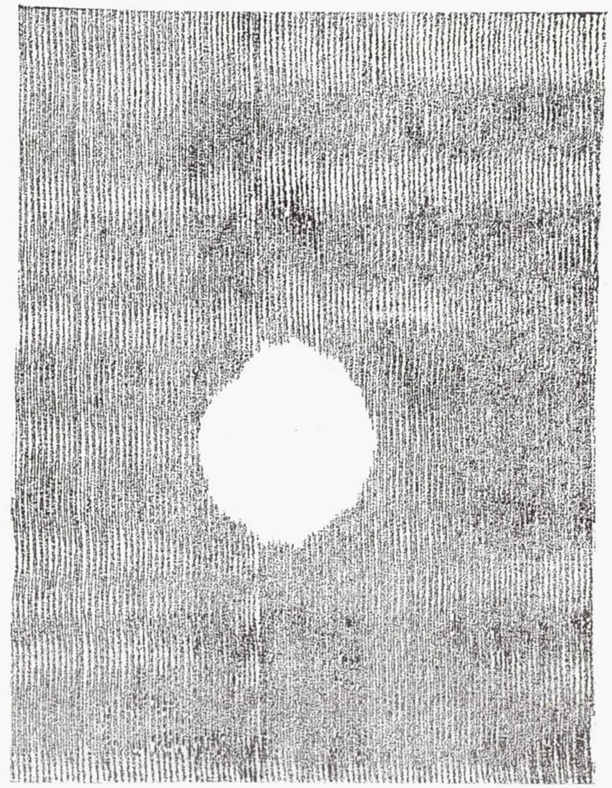

AFTER CYCLIC TEST

1.5 x 10^6 CYCLES

NOT INSPECTED

BEFORE TEST

SPECIMEN NUMBER LI-8-14

5/8 CSK HOLE

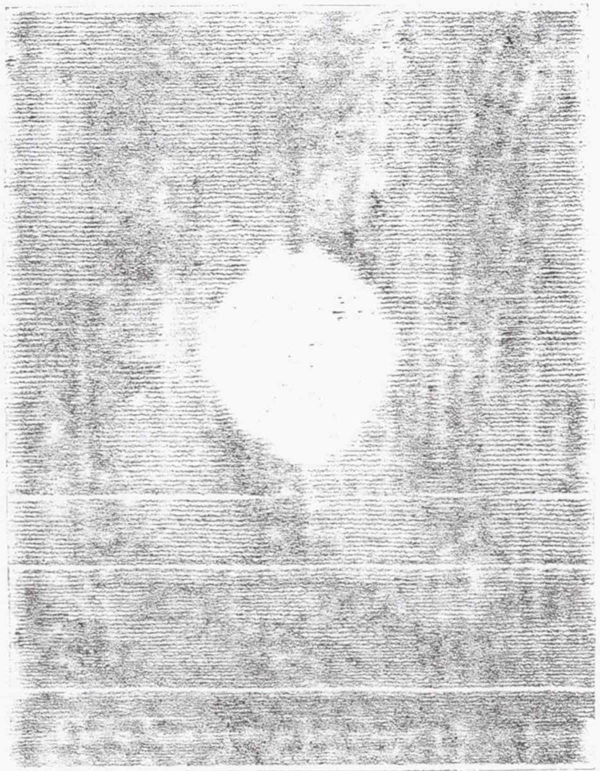

AFTER PRELOAD

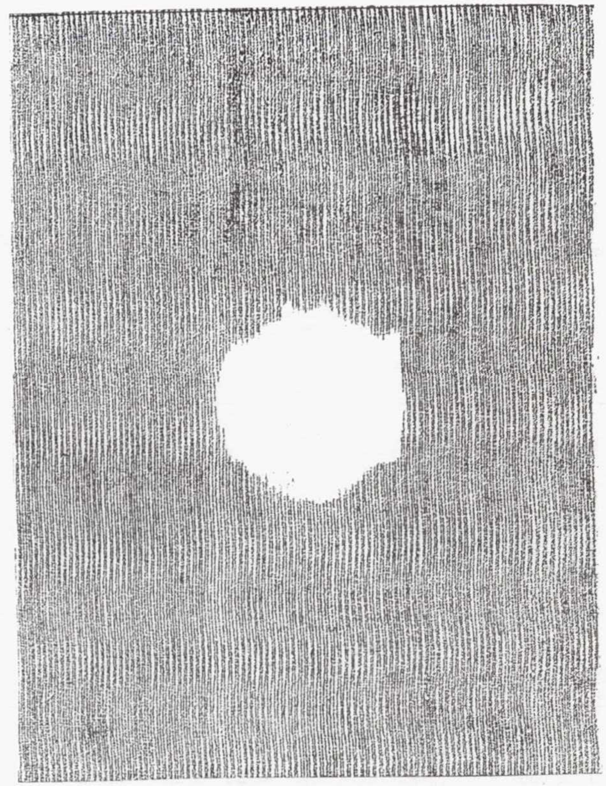

AFTER CYCLIC TEST

1.5×10^6 CYCLES

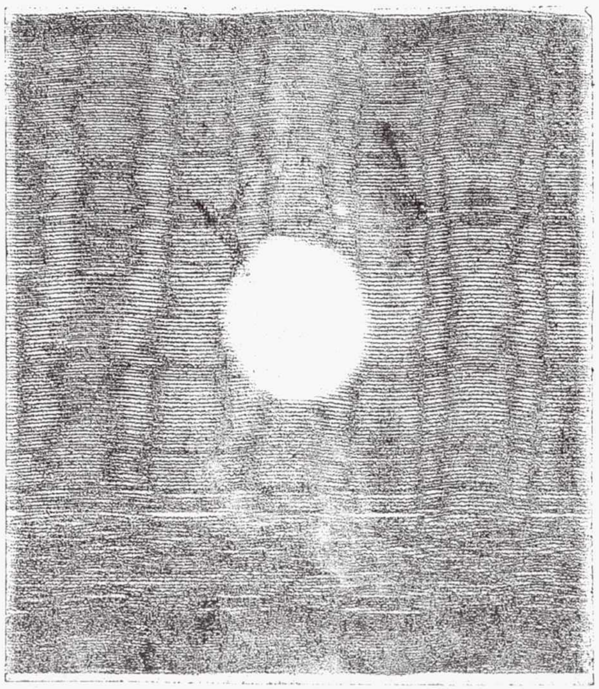

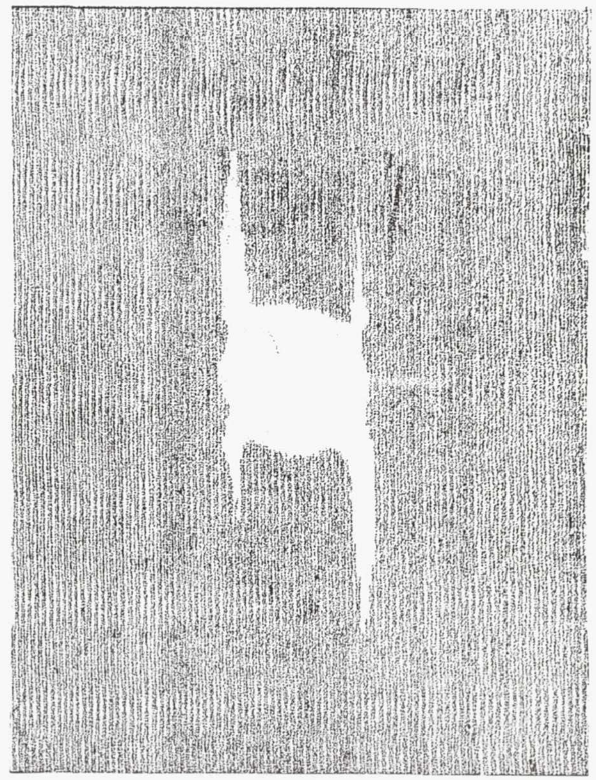

NO PRELOAD

BEFORE TEST

SPECIMEN NUMBER L2-1-30

5/8 FP HOLE

AFTER CYCLIC TEST

10^3 CYCLES

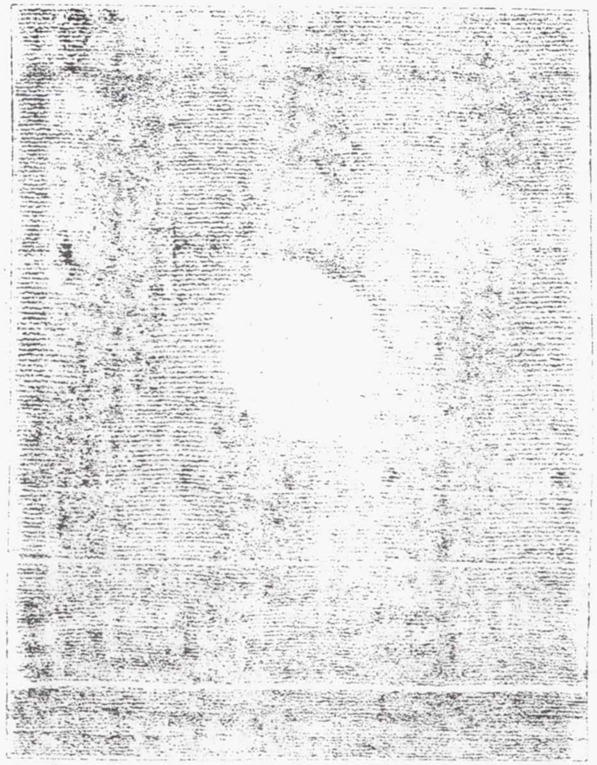

BEFORE TEST

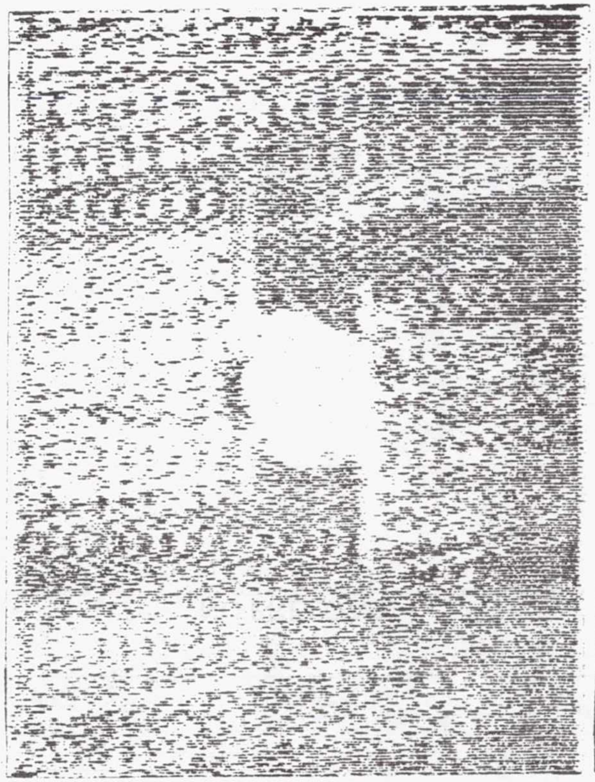

AFTER PRELOAD

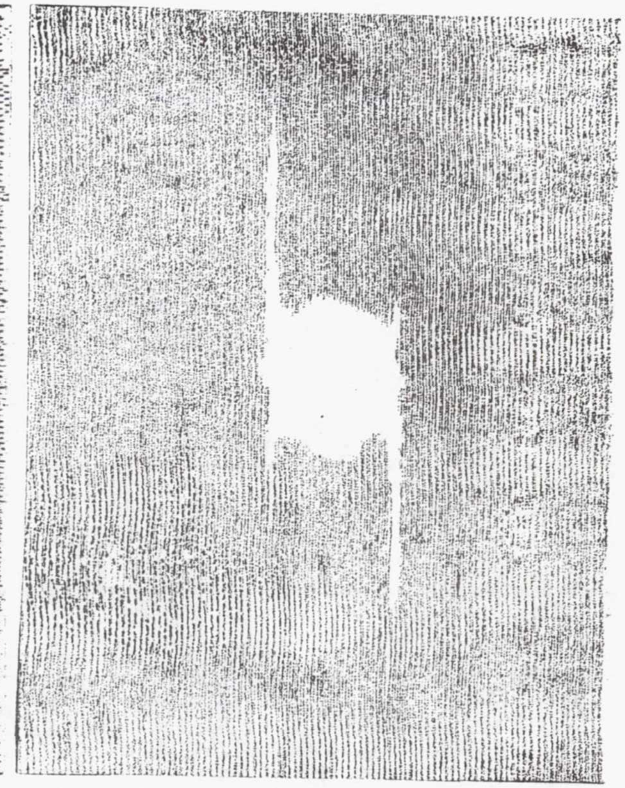

AFTER 10^3 CYCLES

SPECIMEN NUMBER L2-1-32

5/8 FP HOLE

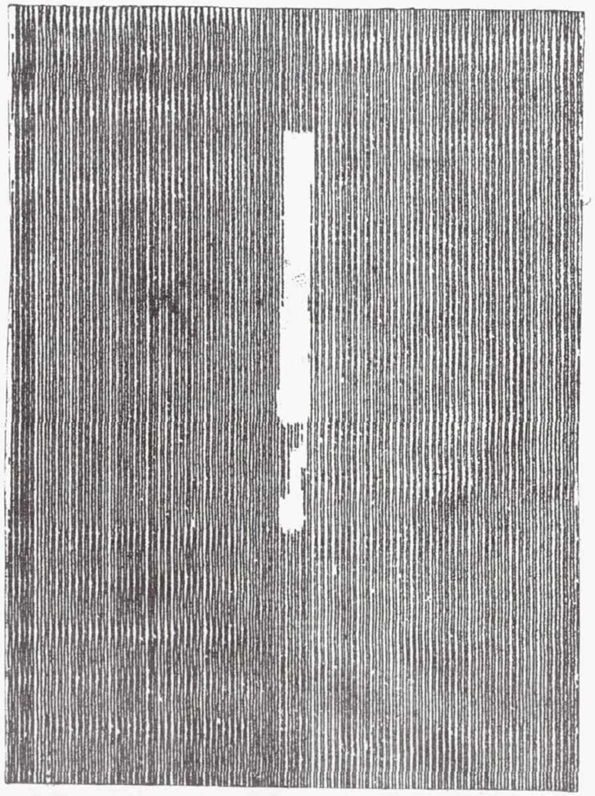

NO PRELOAD

10^3 CYCLES

1/8 FULL PENETRATION HOLE

SPECIMEN L2-1-26

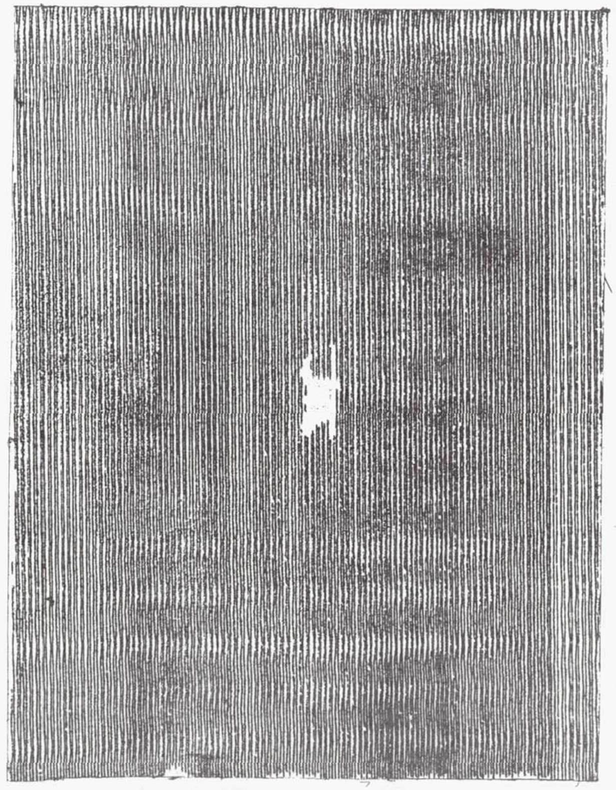

PRELOADED

10^3 CYCLES

1/8 FULL PENETRATION HOLE

SPECIMEN L2-1-28

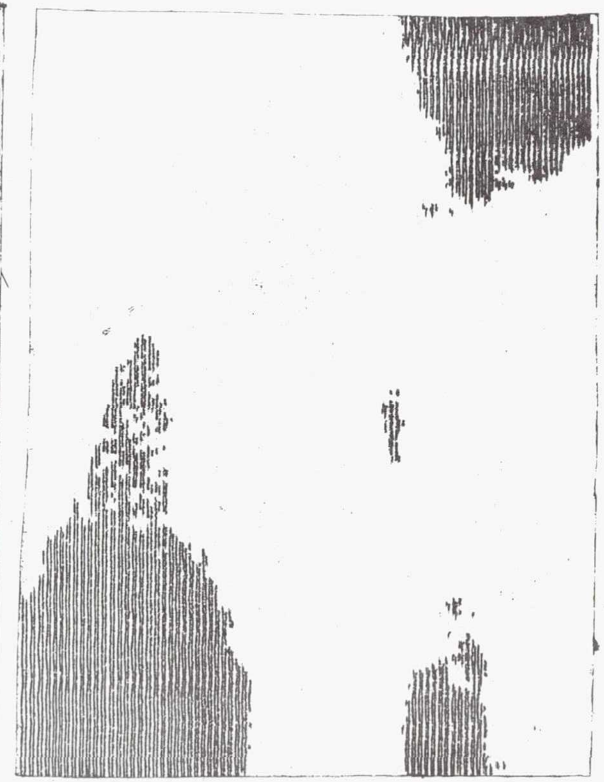

NO PRELOAD

1.5×10^6 CYCLES

1/8 FULL PENETRATION HOLE

SPECIMEN L2-1-29

NO PRELOAD

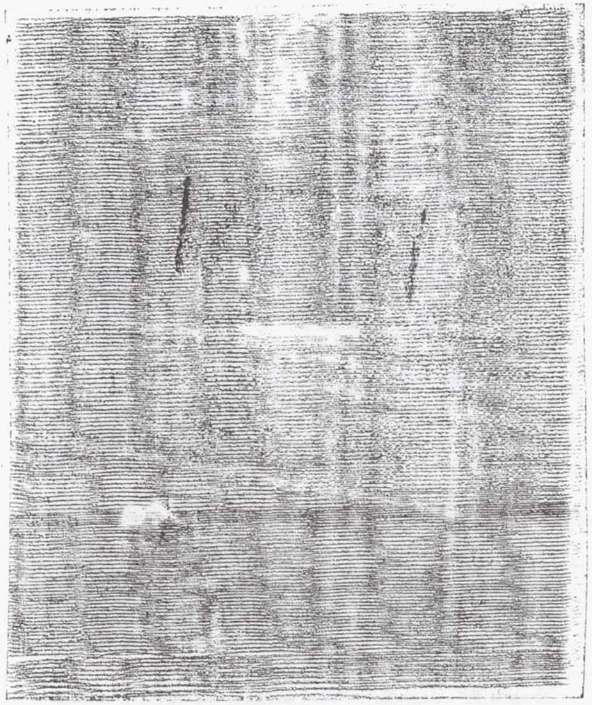

BEFORE TEST

SPECIMEN NUMBER L2-1-42

5/8 FP SLIT

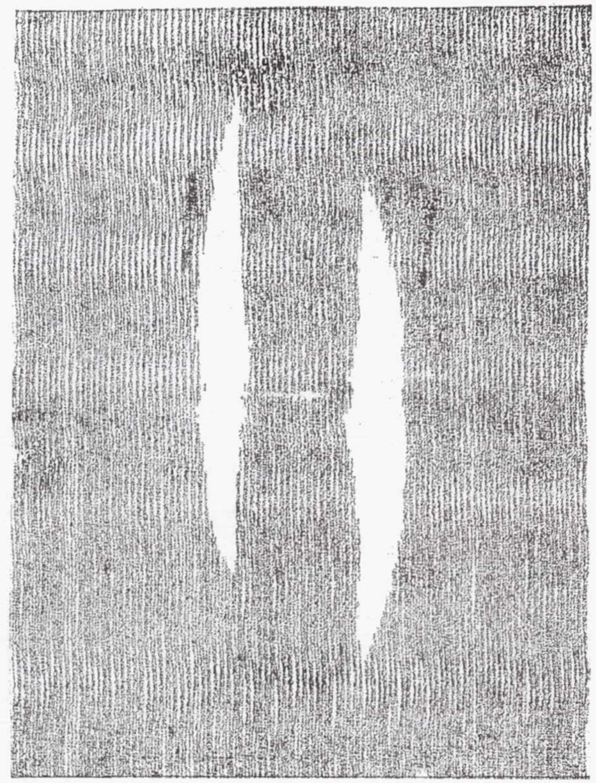

AFTER CYCLIC TEST

10^3 CYCLES

BEFORE TEST	AFTER PRELOAD	AFTER CYCLIC TEST
NOT INSPECTED	NOT INSPECTED	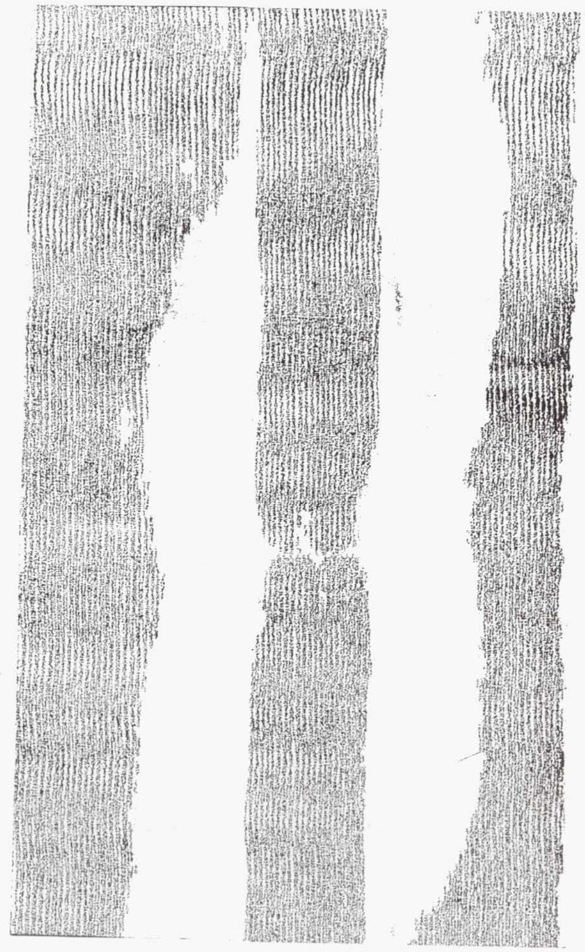
BEFORE TEST SPECIMEN NUMBER L2-1-43 5/8 FP SLIT	AFTER PRELOAD	AFTER CYCLIC TEST 1.5 x 10^6 CYCLES

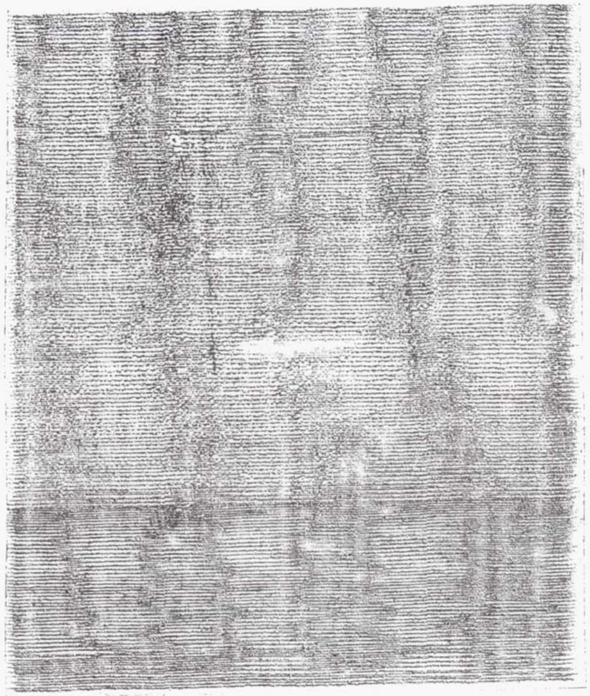

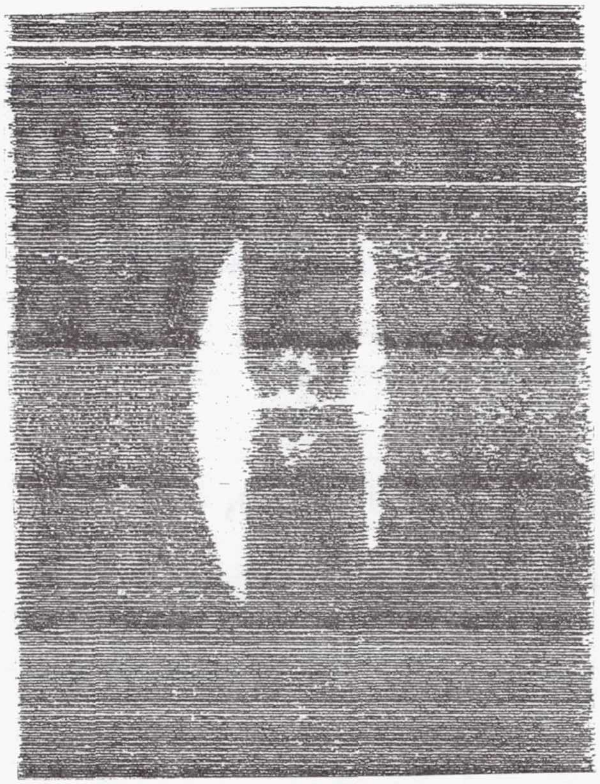

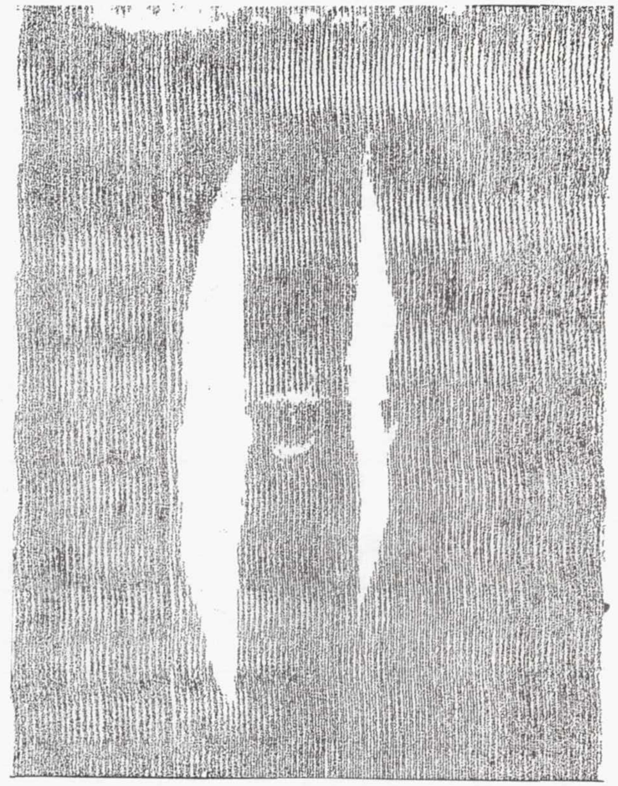

BEFORE TEST

SPECIMEN NUMBER L2-1-44

5/8 FP SLIT

AFTER PRELOAD

AFTER CYCLIC TEST

10^3 CYCLES

NO PRELOAD

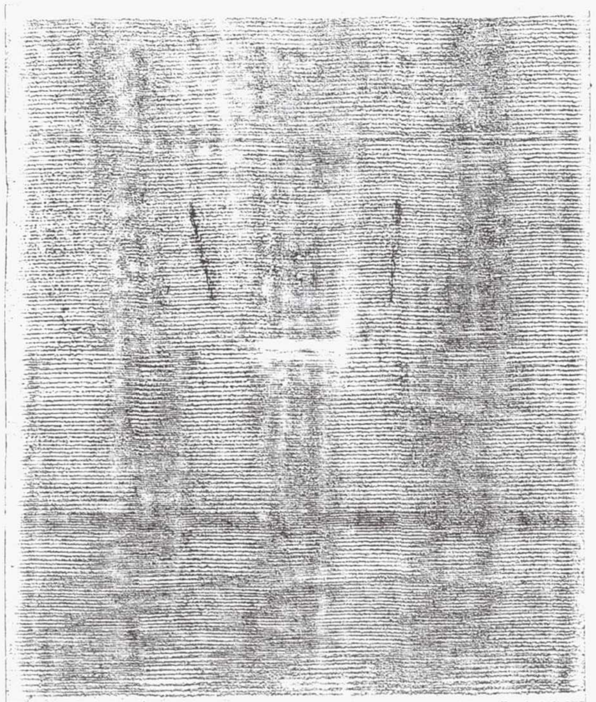

BEFORE TEST

SPECIMEN NUMBER L2-1-46

5/8 HP SLIT

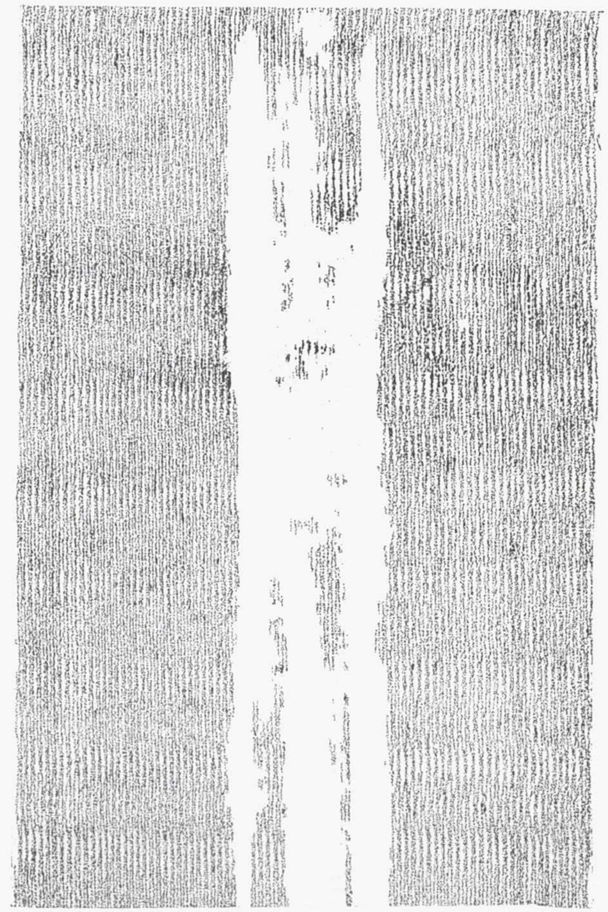

AFTER CYCLIC TEST

10^3 CYCLES

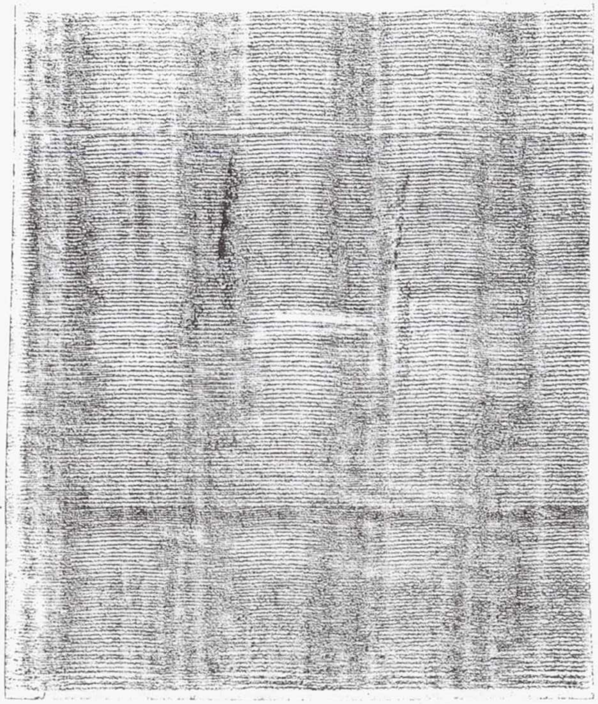

BEFORE TEST

SPECIMEN NUMBER L2-1-48

5/8 HP SLIT

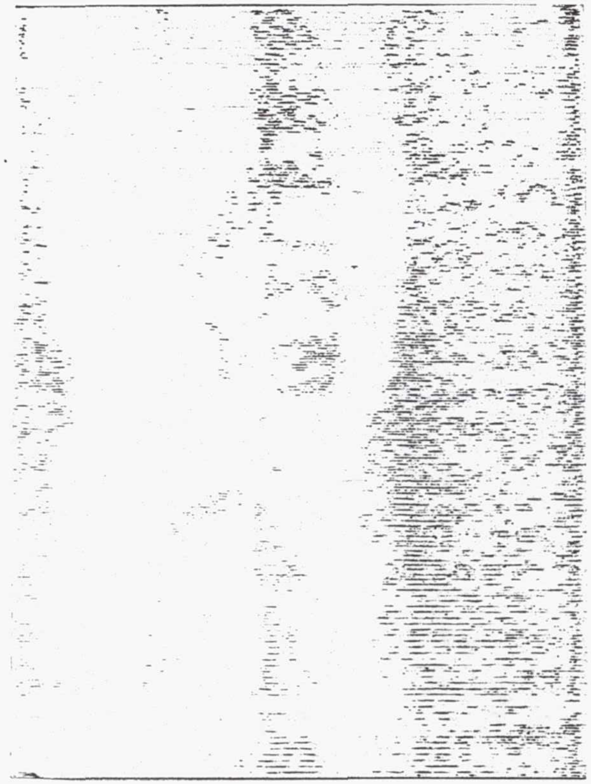

AFTER PRELOAD

FAILURE DURING

CYCLIC TEST

NO PRELOAD

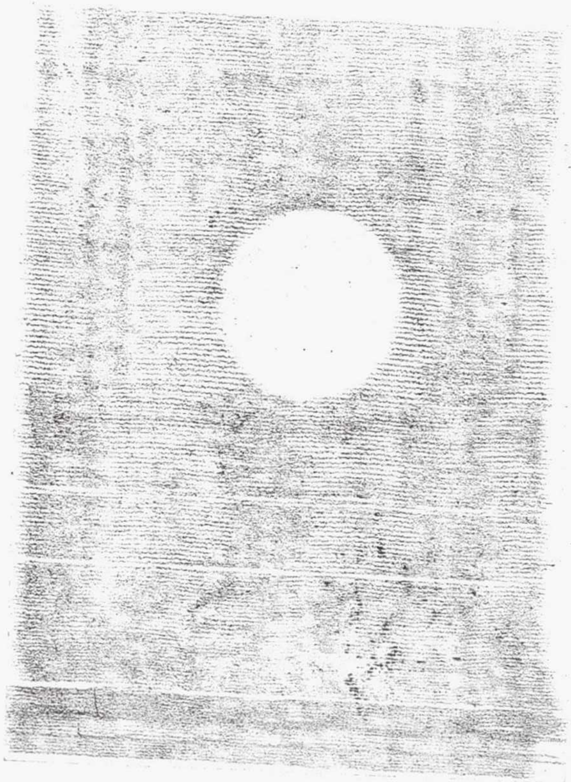

BEFORE TEST

SPECIMEN NUMBER L2-4-4

5/8 CSK HOLE

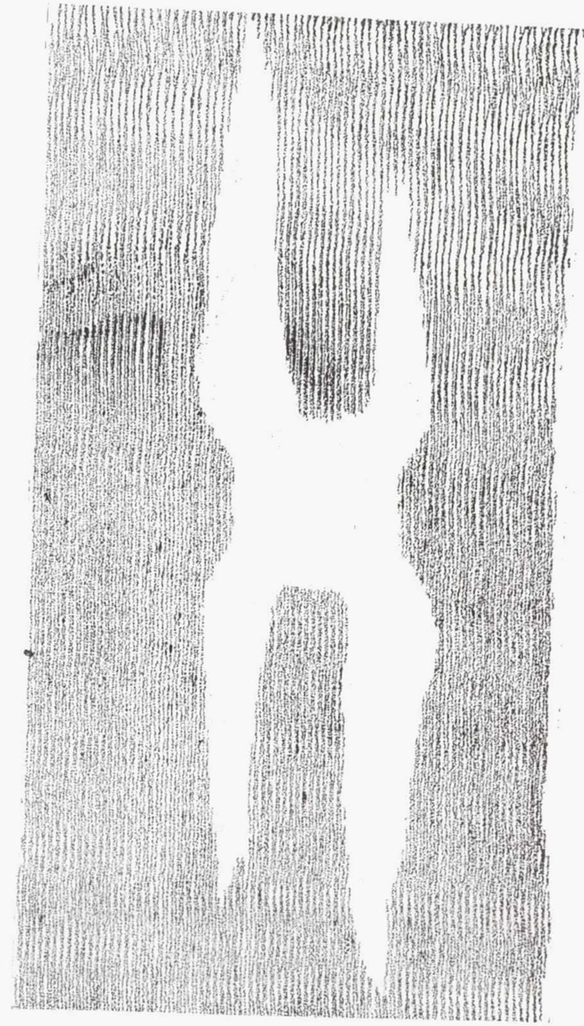

AFTER CYCLIC TEST

1.5×10^6 CYCLES

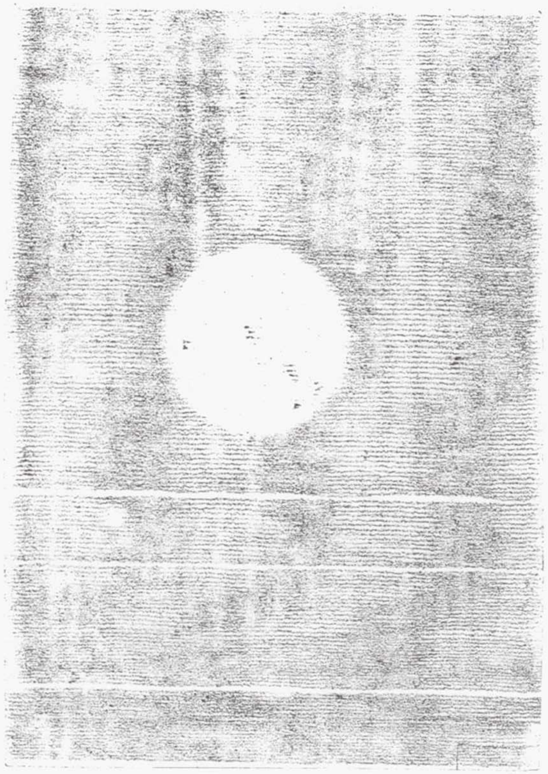

BEFORE TEST

SPECIMEN NUMBER L2-4-6

5/8 CSK HOLE

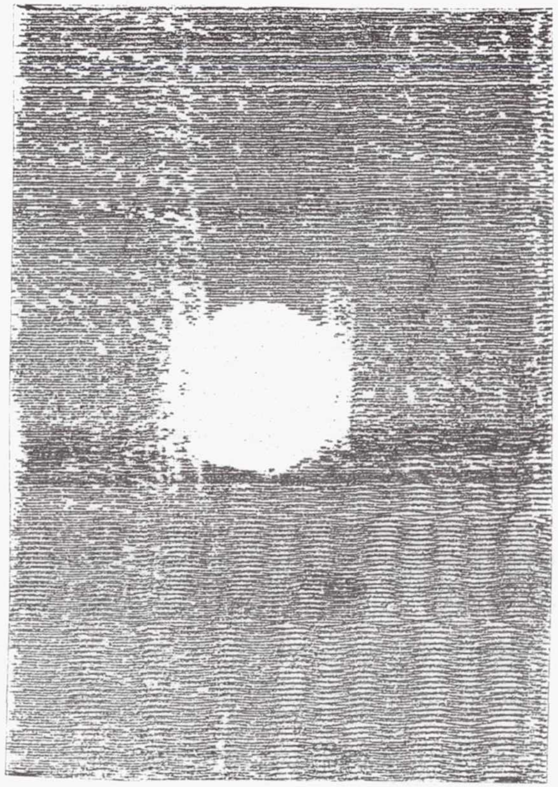

AFTER PRELOAD

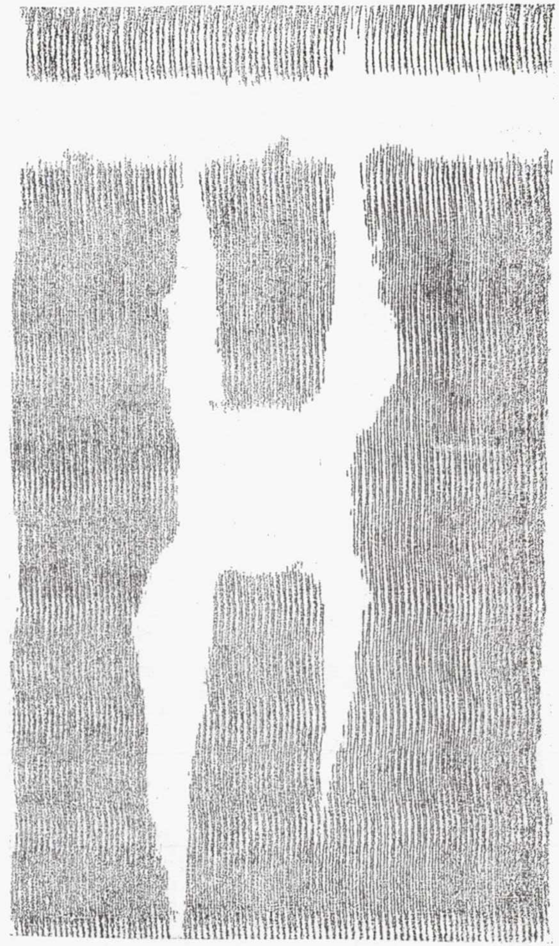

AFTER CYCLIC TEST

1.5×10^6 CYCLES

NO PRELOAD

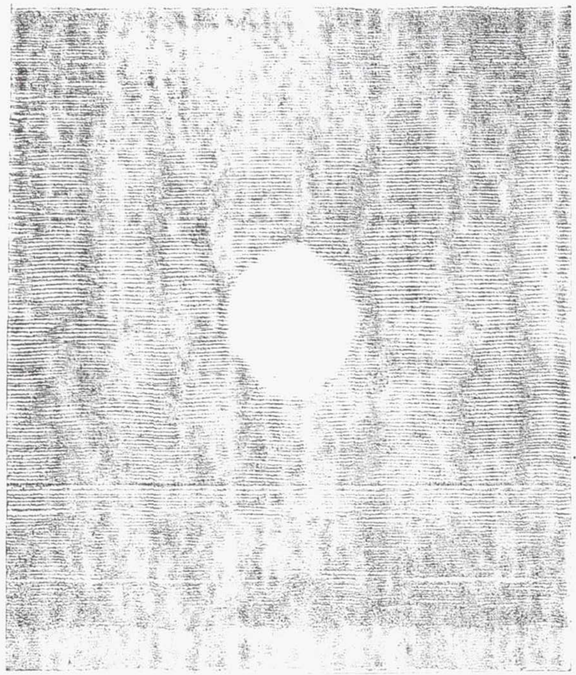

BEFORE TEST

SPECIMEN NUMBER L3-1-3C

5/8 FP HOLE

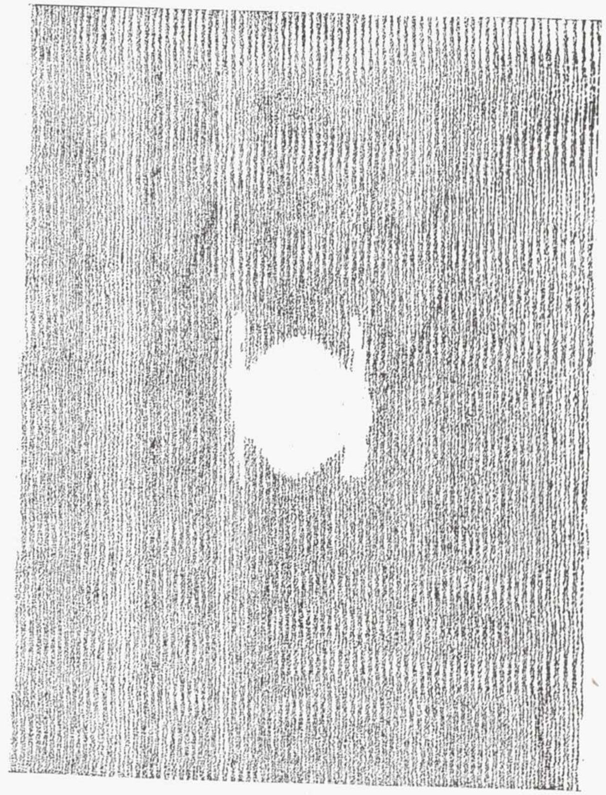

AFTER CYCLIC TEST

1.5 x 10^6 CYCLES

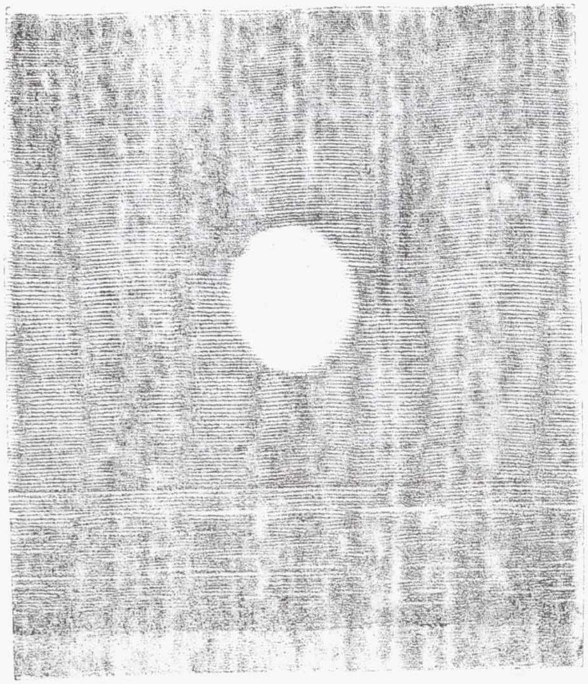

BEFORE TEST

SPECIMEN NUMBER L3-1-38

5/8 FP HOLE

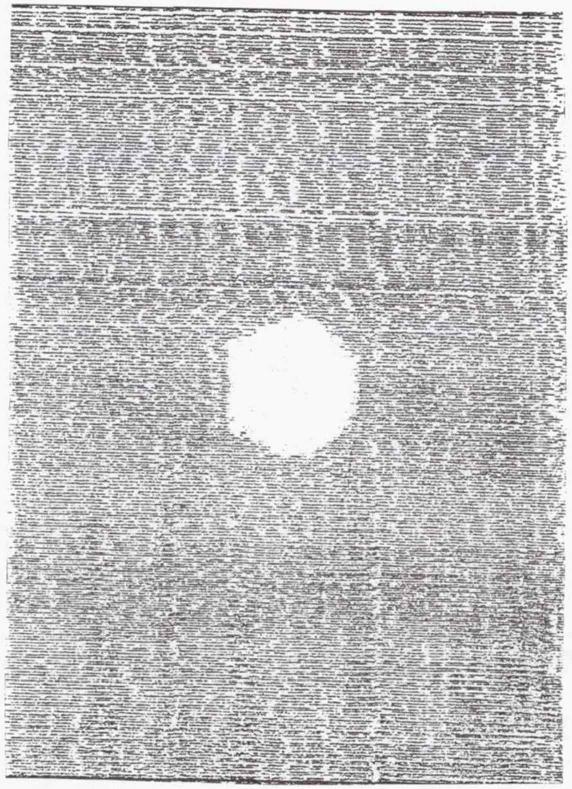

AFTER PRELOAD

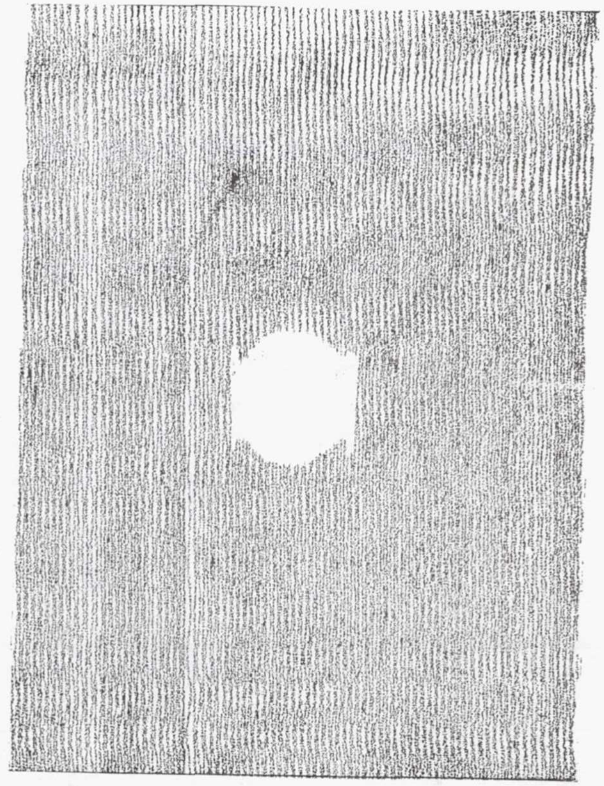

AFTER CYCLIC TEST

10^3 CYCLES

NO PRELOAD

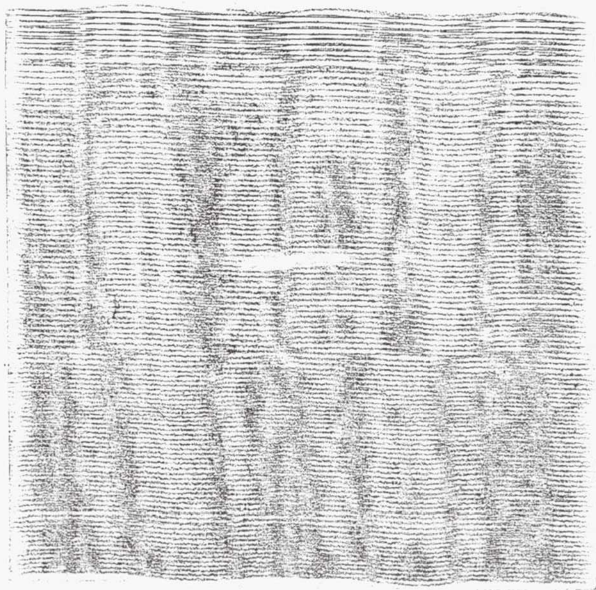

BEFORE TEST

SPECIMEN NUMBER L3-1-56

5/8 FP SLIT

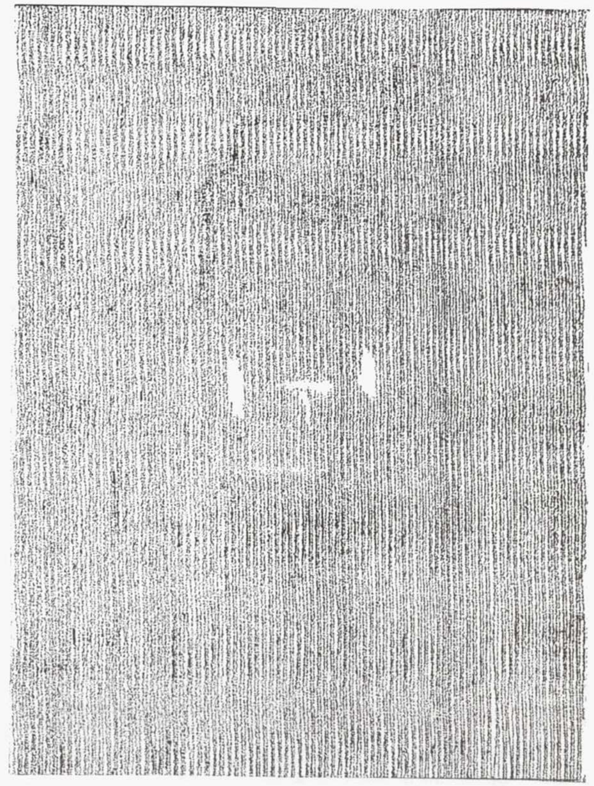

AFTER CYCLIC TEST

10^3 CYCLES

NOT INSPECTED

BEFORE TEST

SPECIMEN NUMBER L3-1-55

5/8 FP SLIT

NO PRELOAD

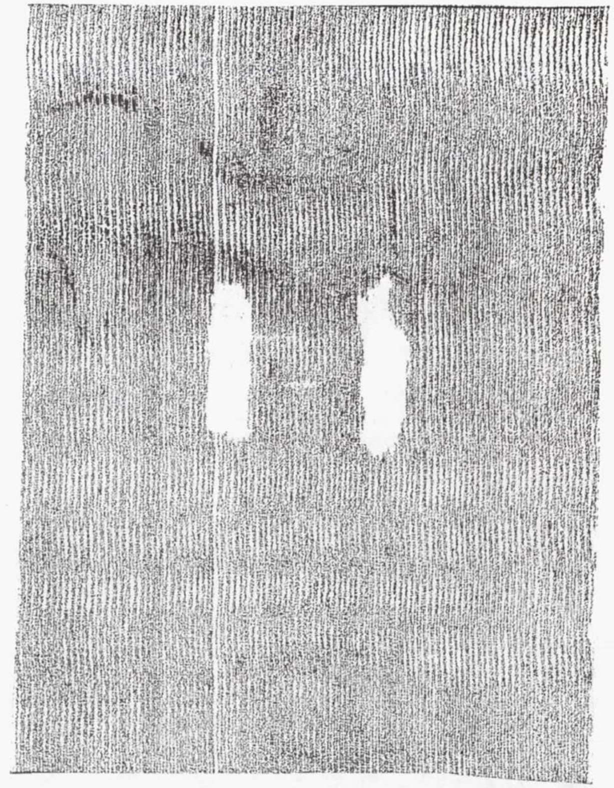

AFTER CYCLIC TEST

1.5×10^6 CYCLES

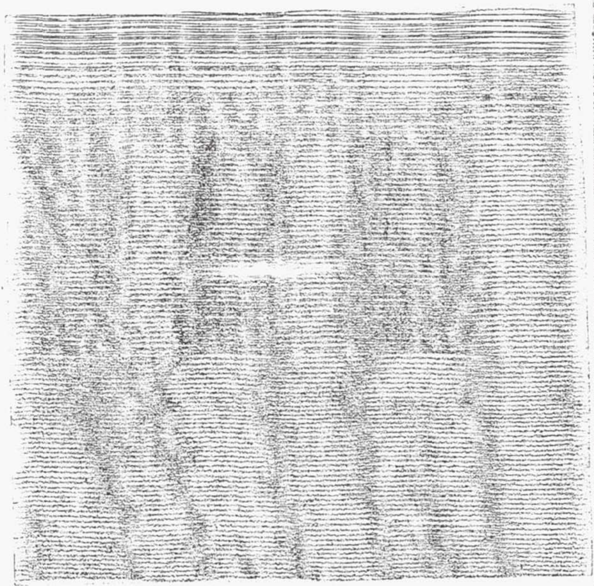

BEFORE TEST

SPECIMEN NUMBER L3-1-58

5/8 FP SLIT

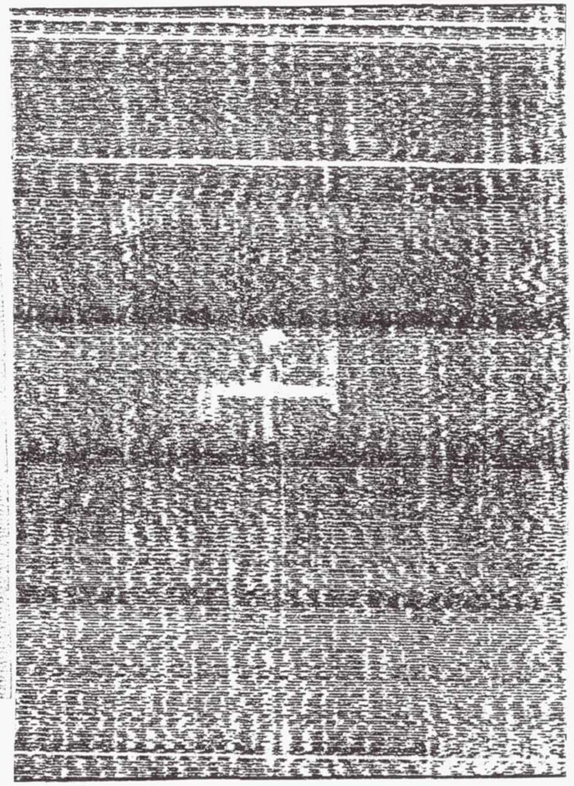

AFTER PRELOAD

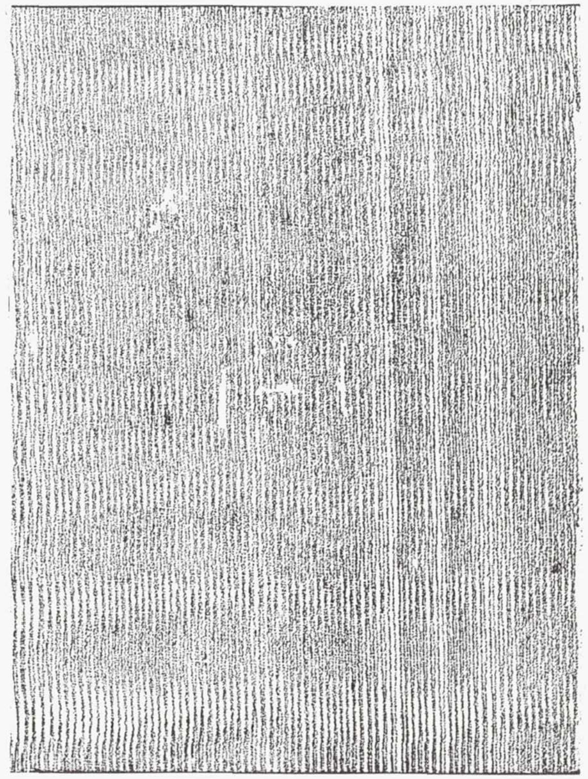

AFTER CYCLIC TEST

10^3 CYCLES

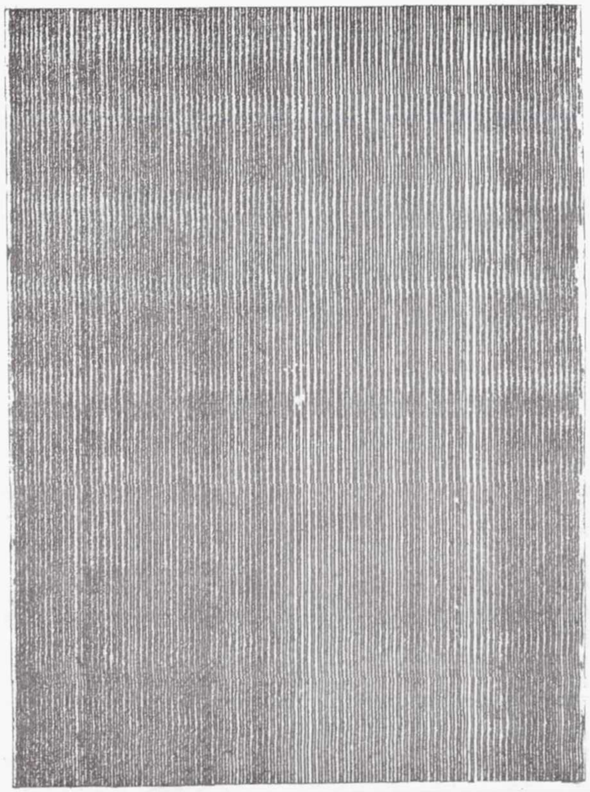

NO PRELOAD
10^3 CYCLES
SPECIMEN NUMBER L3-1-40
1/8 FULL PENETRATION SLIT

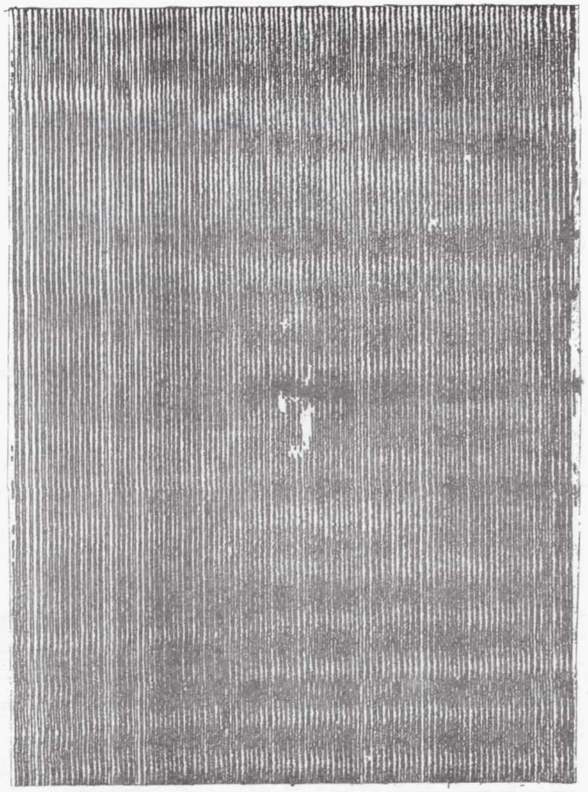

PRELOADED
10^3 CYCLES
SPECIMEN NUMBER L3-1-42
1/8 FULL PENETRATION SLIT

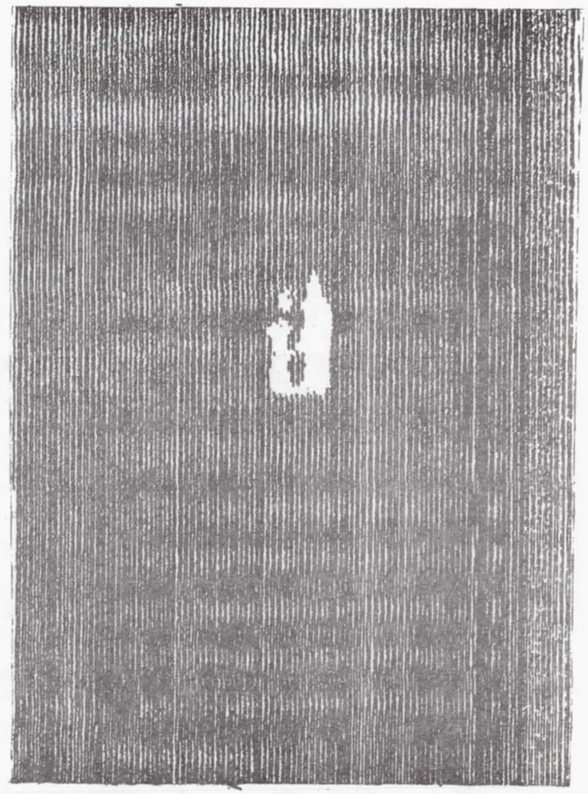

PRELOADED
1.5×10^6 CYCLES
SPECIMEN NUMBER L3-1-41
1/8 FULL PENETRATION SLIT

NO PRELOAD

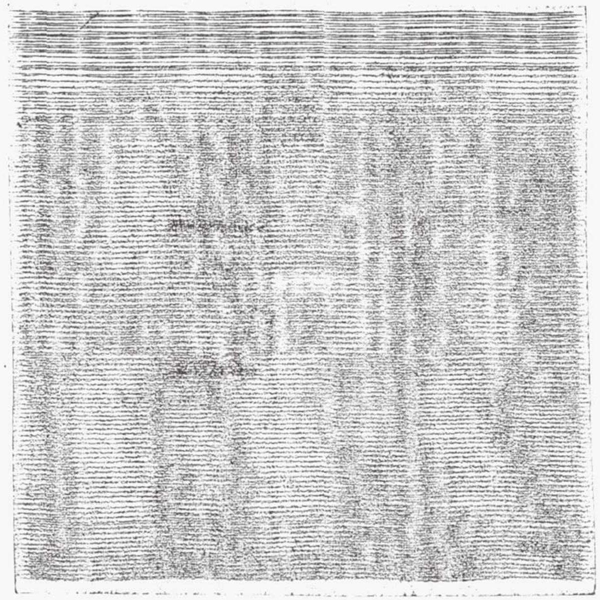

BEFORE TEST

SPECIMEN NUMBER L3-1-60

5/8 HP SLIT

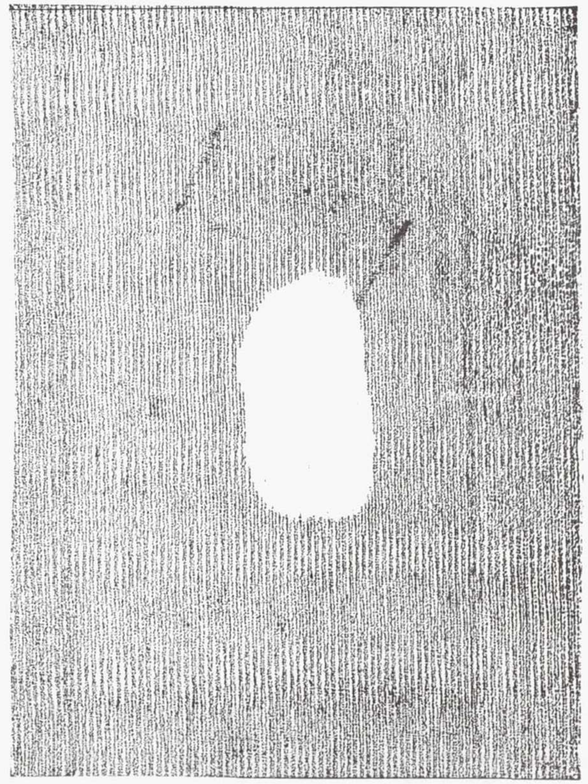

AFTER CYCLIC TEST

10^3 CYCLES

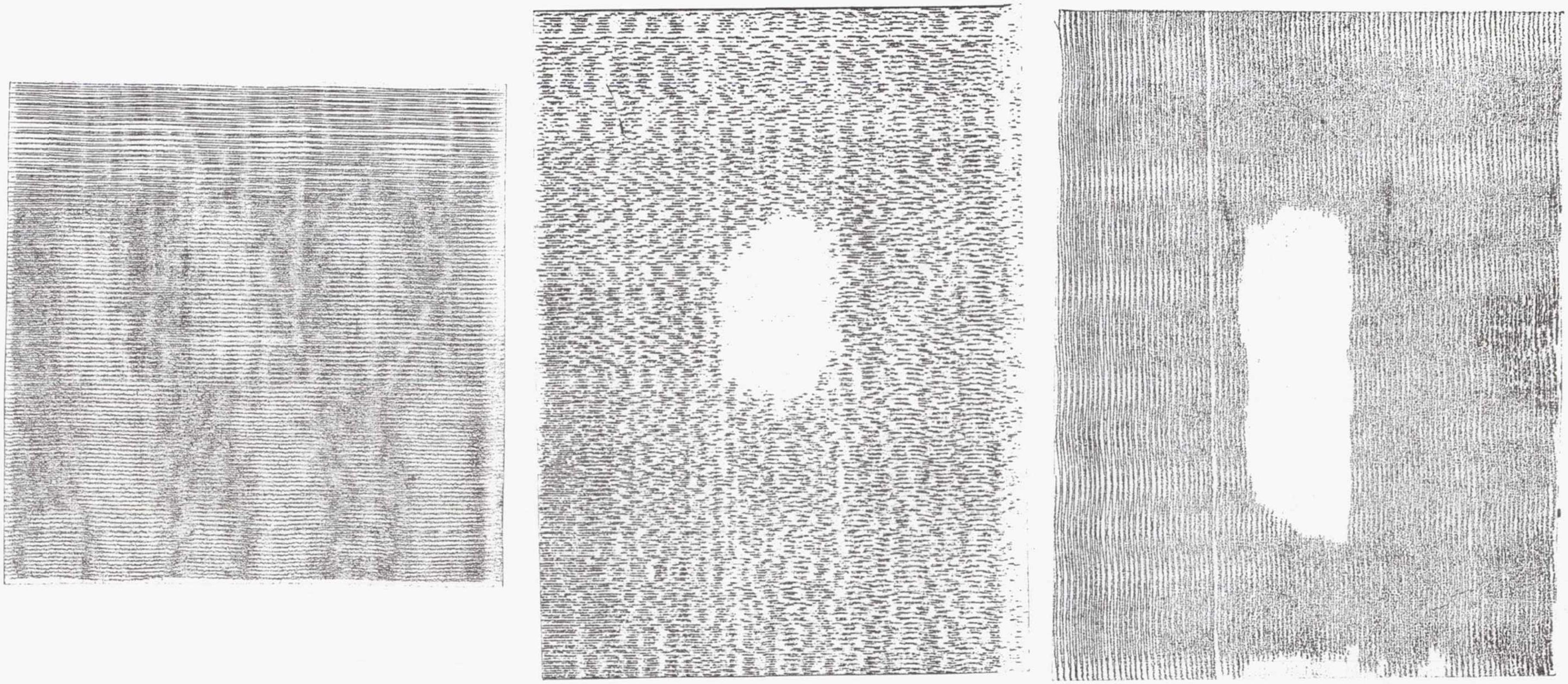

BEFORE TEST

SPECIMEN NUMBER L3-1-62

5/8 HP SLIT

AFTER PRELOAD

AFTER CYCLIC TEST

10^3 CYCLES

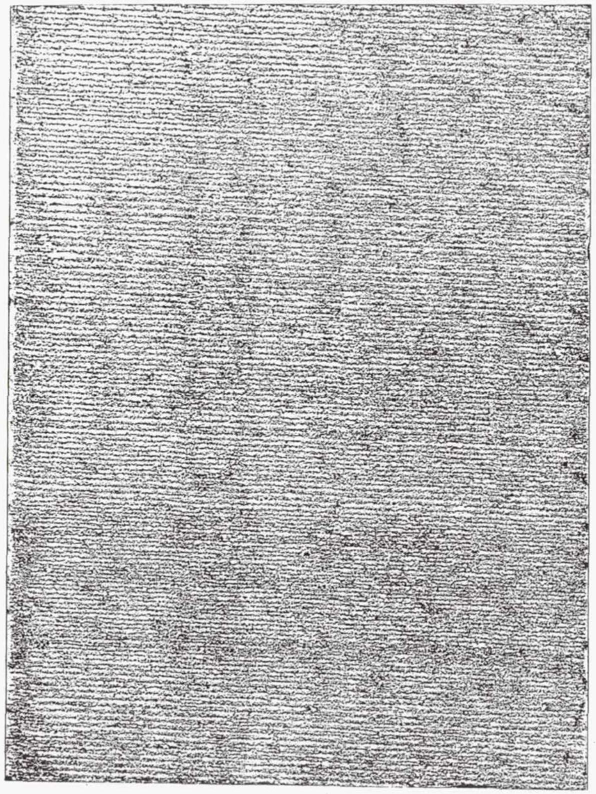

BEFORE TEST

SPECIMEN NUMBER L1-10-1

NO DEFECT

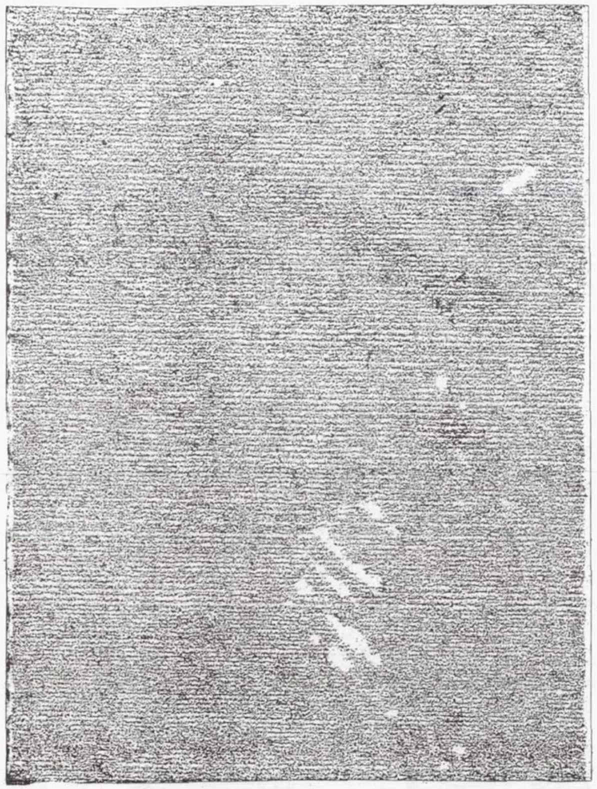

BEFORE TEST

SPECIMEN NUMBER L1-10-2

NO DEFECT

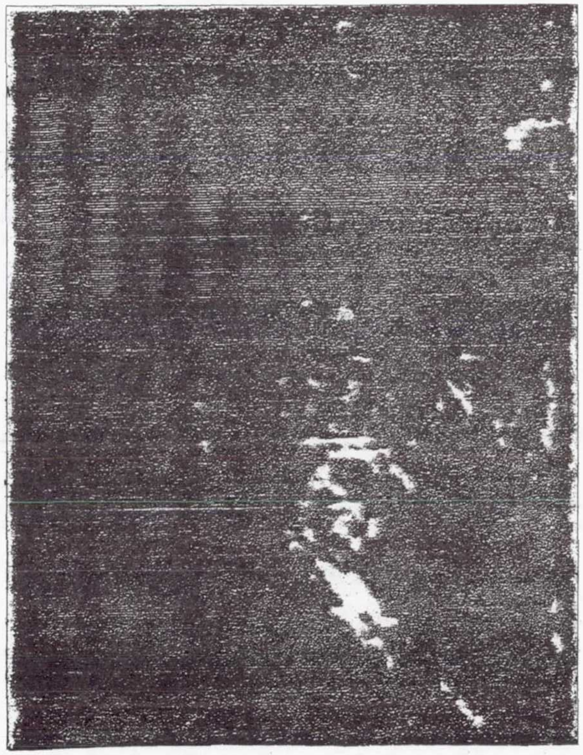

AFTER CYCLIC TEST

10^3 CYCLES

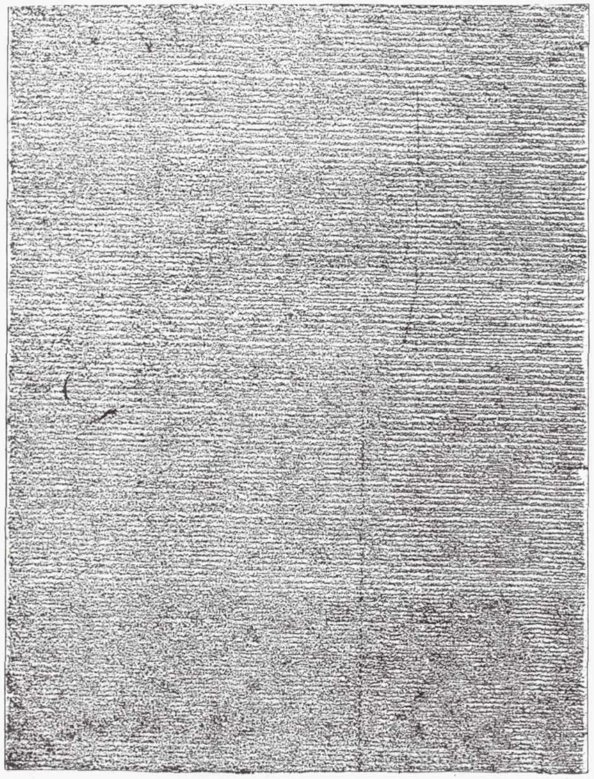

BEFORE TEST

SPECIMEN NUMBER L1-10-3

NO DEFECT

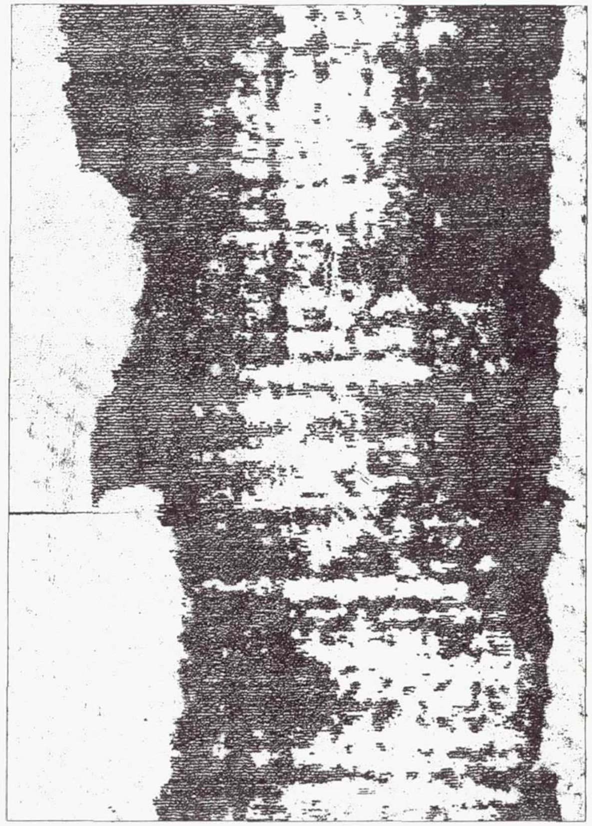

AFTER CYCLIC TEST

337 700 CYCLES

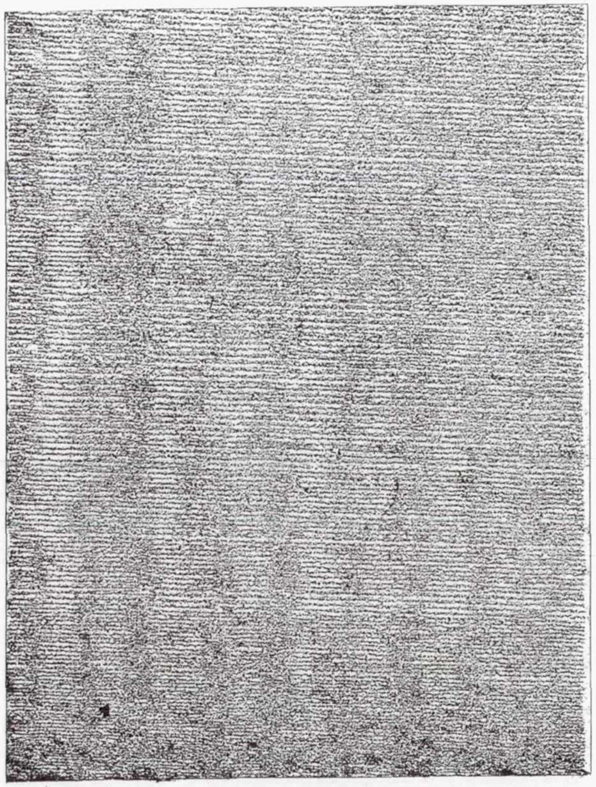

BEFORE TEST

SPECIMEN NUMBER L1-10-4

NO DEFECT

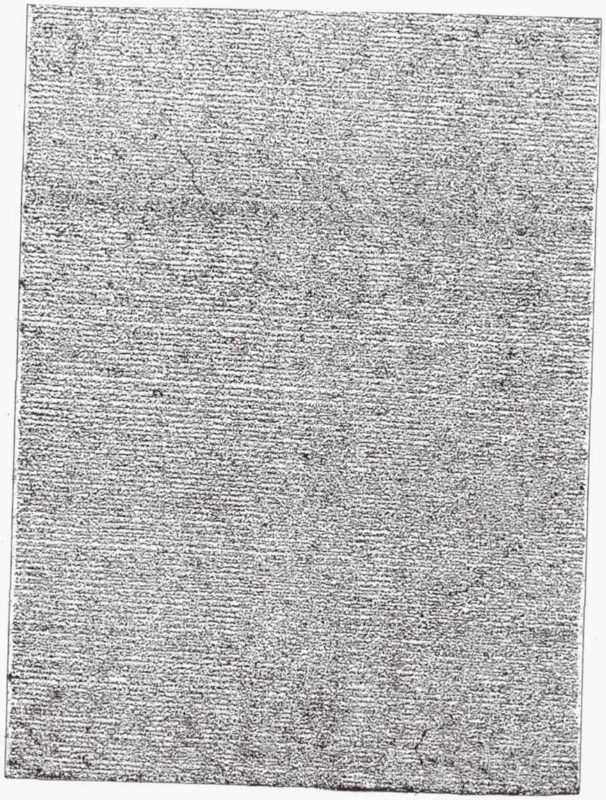

BEFORE TEST

SPECIMEN NUMBER L1-10-5

NO DEFECT

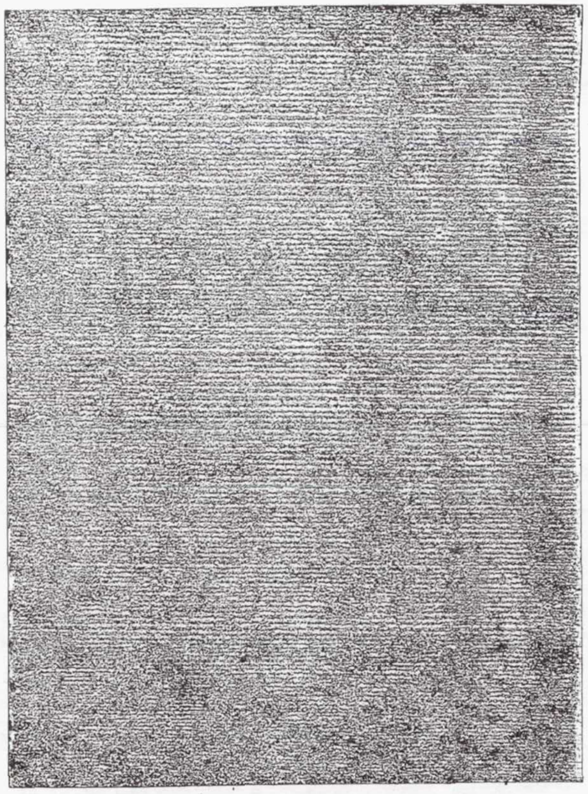

BEFORE TEST

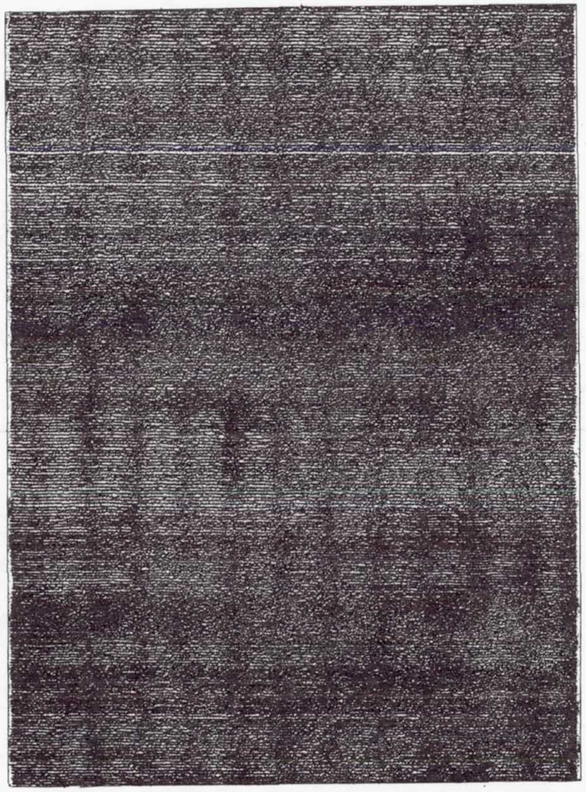

AFTER PRELOAD

SPECIMEN L1-10-6

NO DEFECT

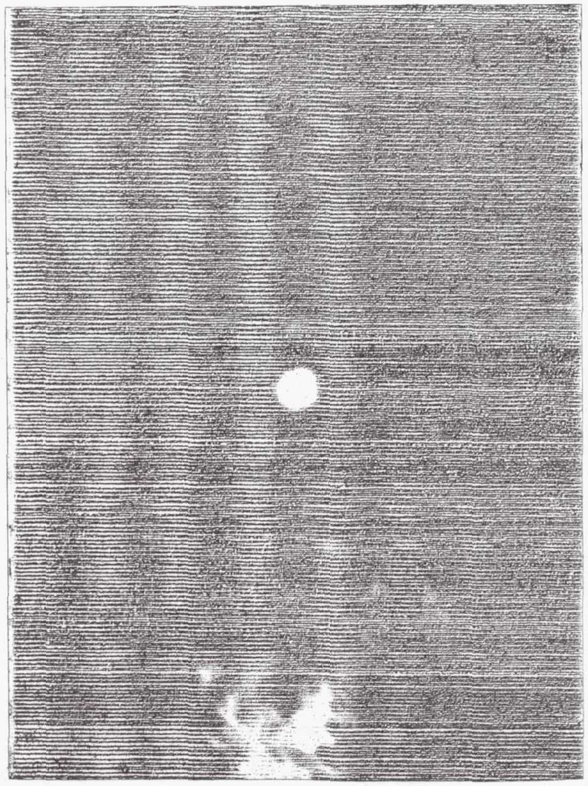

BEFORE TEST
SPECIMEN NUMBER L1-10-7
1/8 FULL PENETRATION HOLE

AFTER CYCLIC TEST
83,900 CYCLES

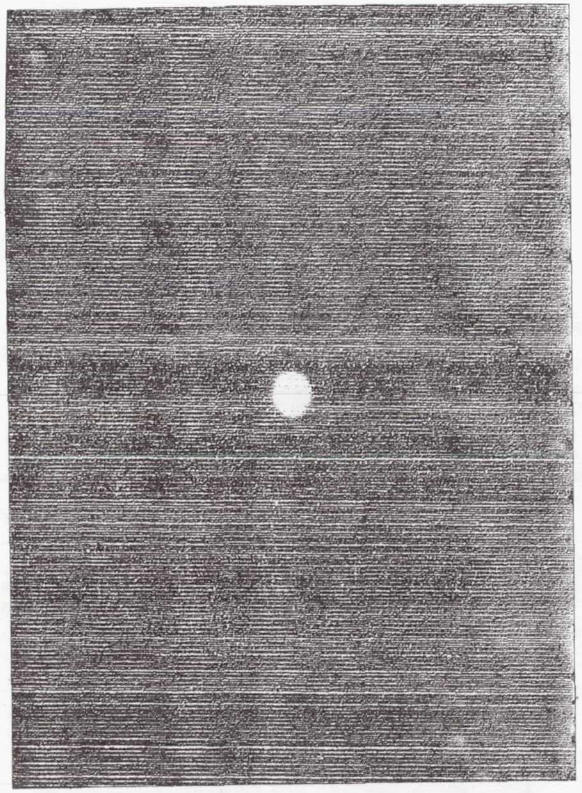

BEFORE TEST

SPECIMEN NUMBER L1-10-8

1/8 FULL PENETRATION HOLE

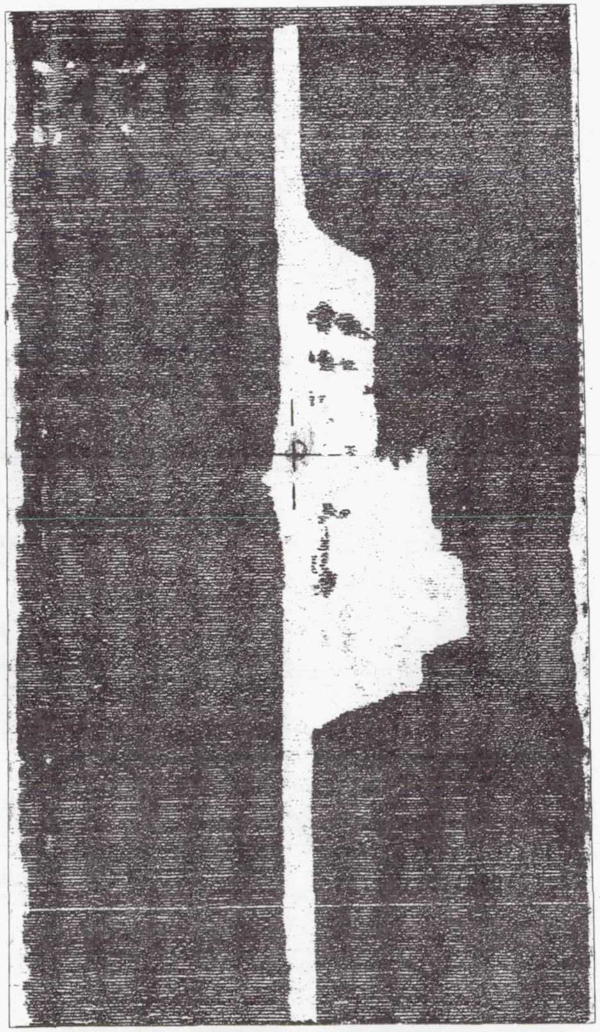

AFTER CYCLIC TEST

566 600 CYCLES

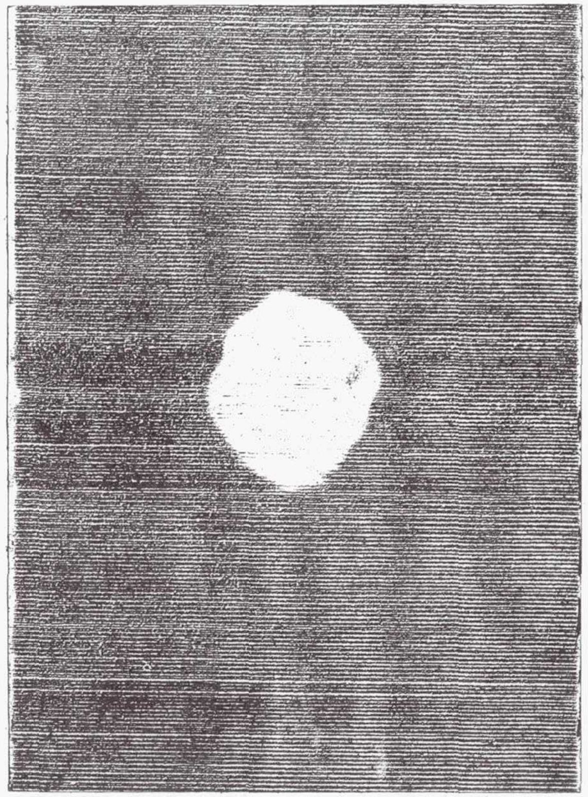

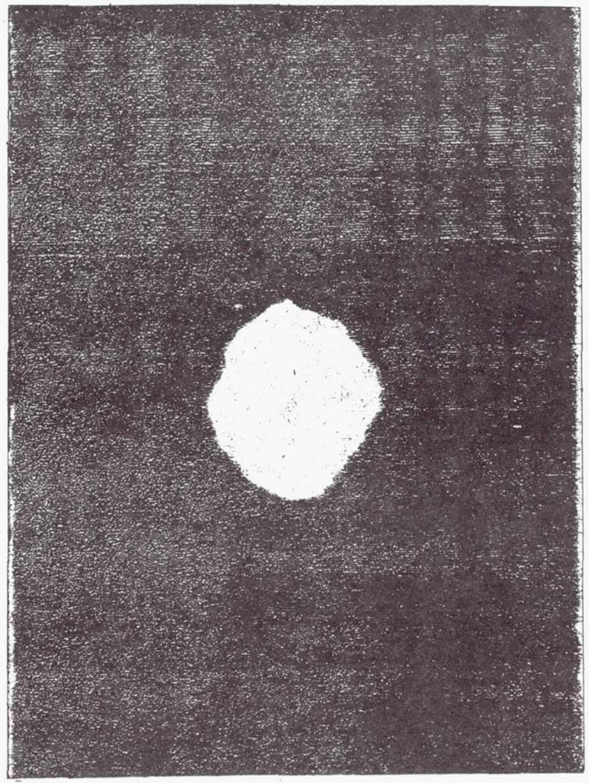

BEFORE TEST

SPECIMEN NUMBER L1-10-9

5/8 FULL PENETRATION HOLE

AFTER CYCLIC TEST

10^3 CYCLES

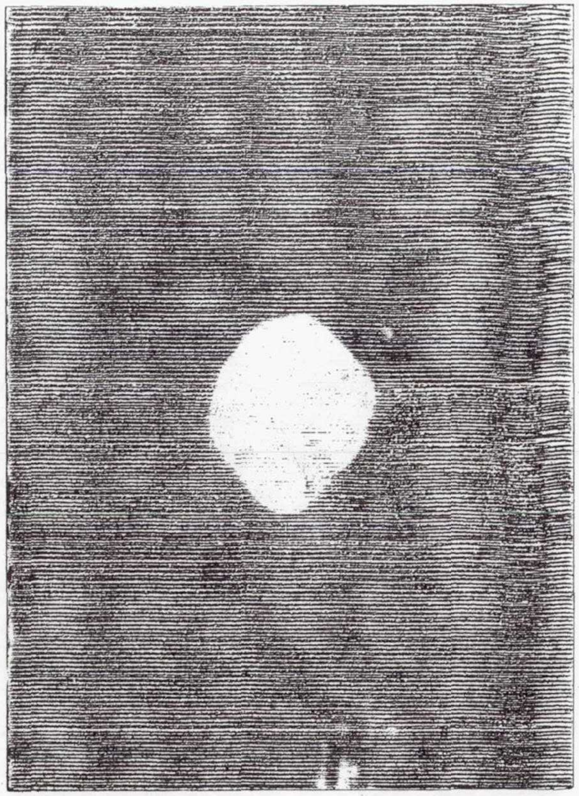

BEFORE TEST

SPECIMEN NUMBER L1-10-10

5/8 FULL PENETRATION HOLE

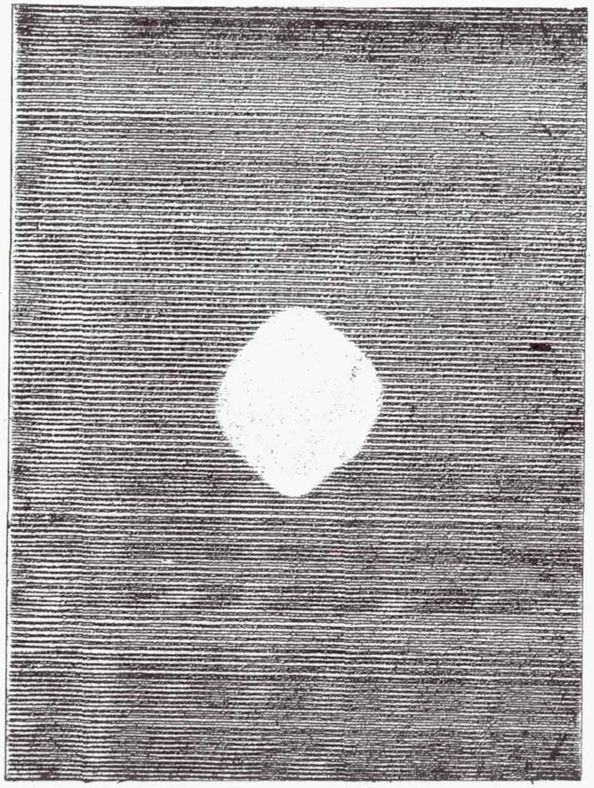

BEFORE TEST

SPECIMEN NUMBER L1-10-11

5/8 FULL PENETRATION HOLE

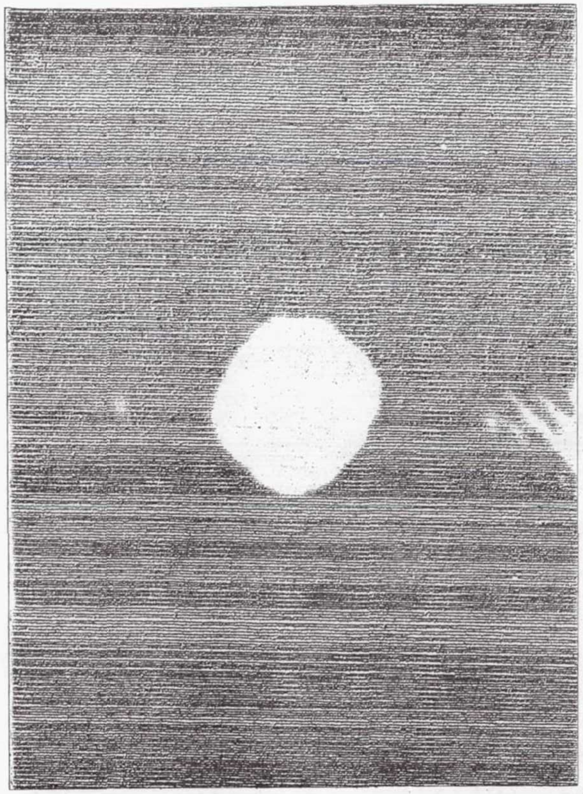

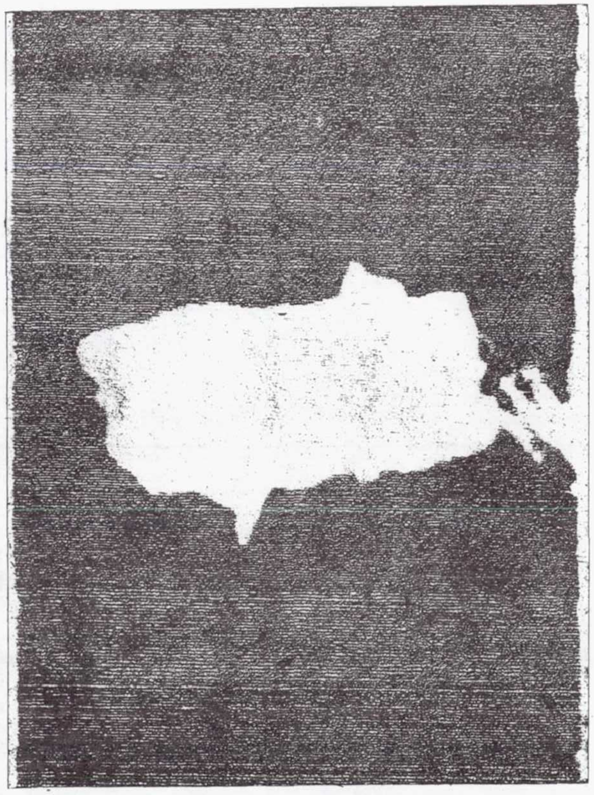

BEFORE TEST

SPECIMEN NUMBER L1-10-12

5/8 FULL PENETRATION HOLE

AFTER CYCLIC TEST

1.5×10^6 CYCLES

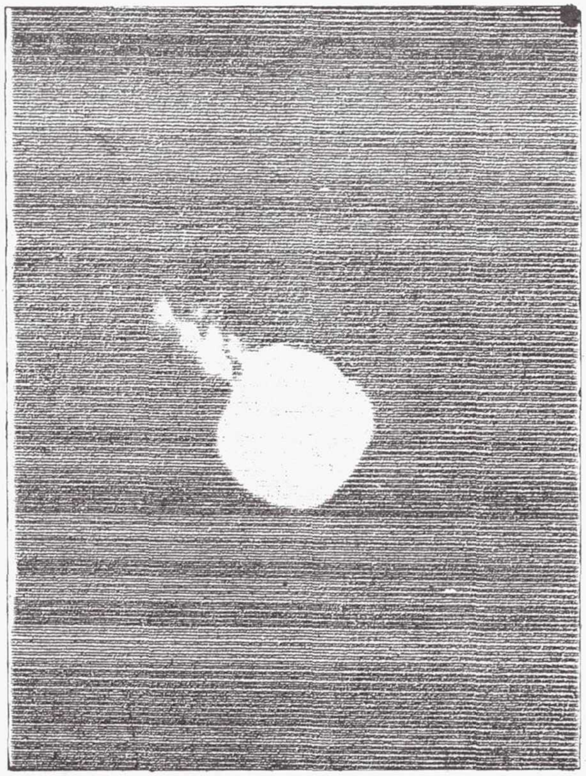

BEFORE TEST

SPECIMEN NUMBER L1-10-13

5/8 FULL PENETRATION HOLE

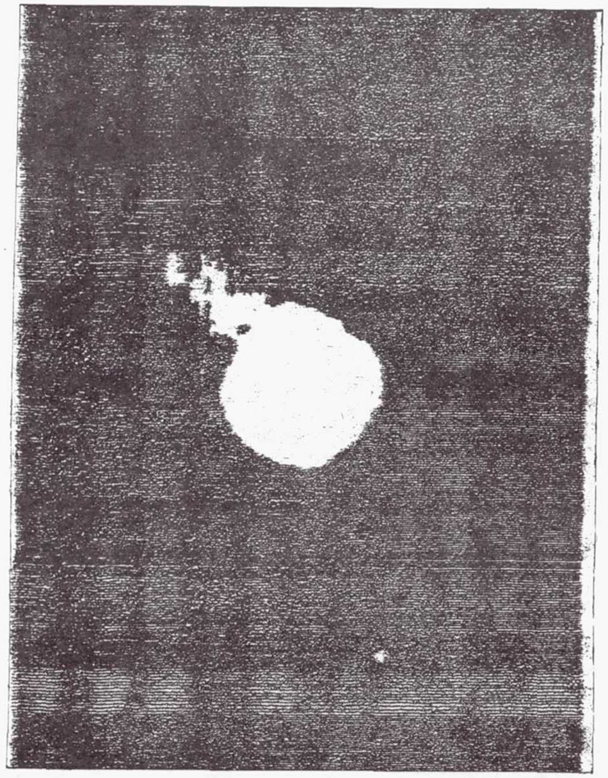

AFTER PRELOAD

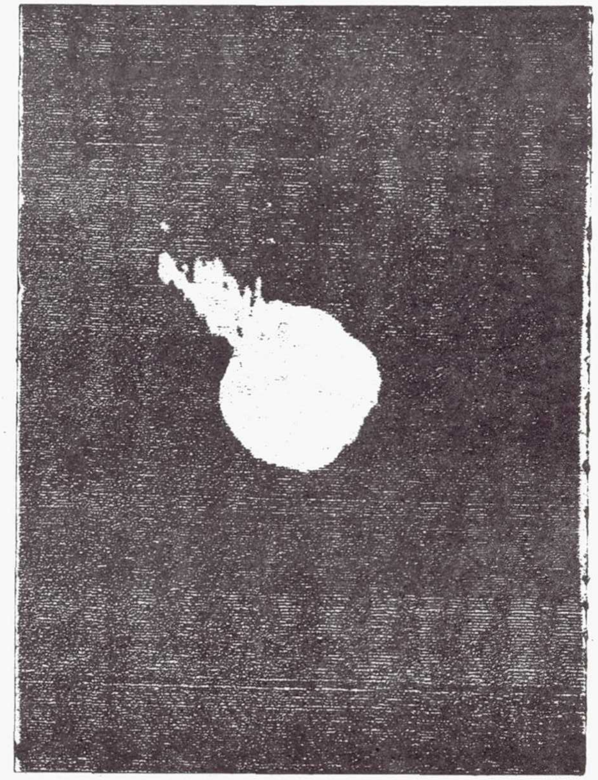

AFTER CYCLIC TEST

10^3 CYCLES

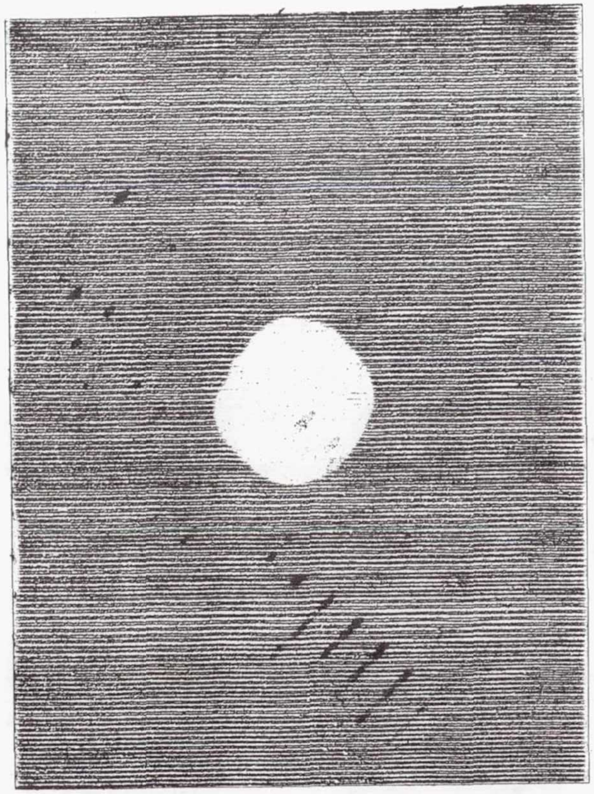

BEFORE TEST

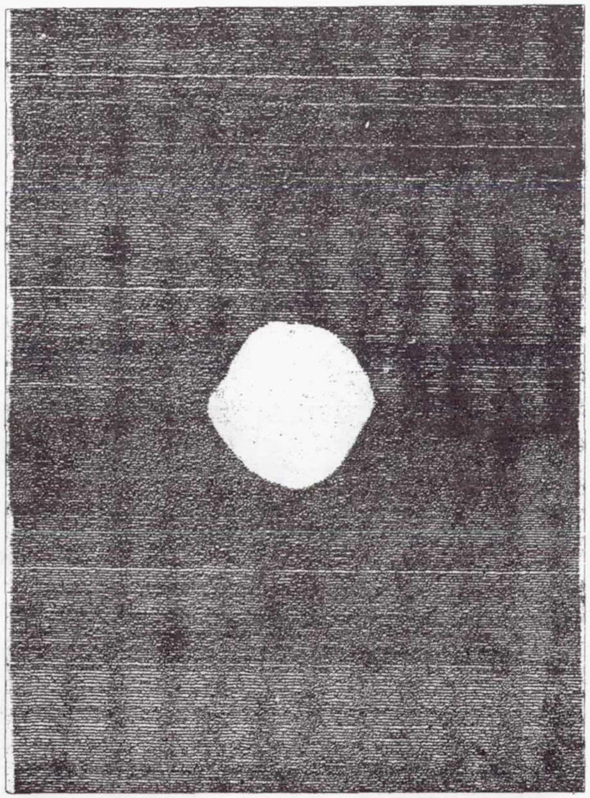

AFTER PRELOAD

SPECIMEN NUMBER L1-10-14

5/8 FULL PENETRATION HOLE

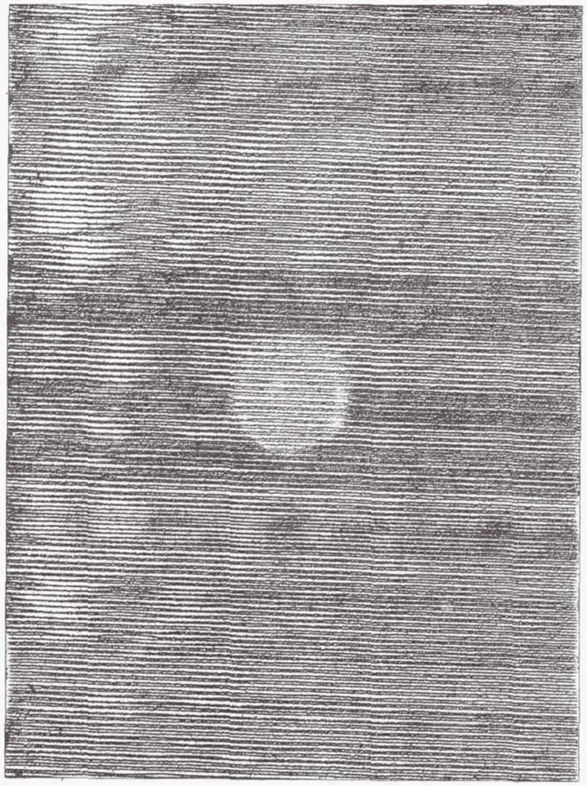

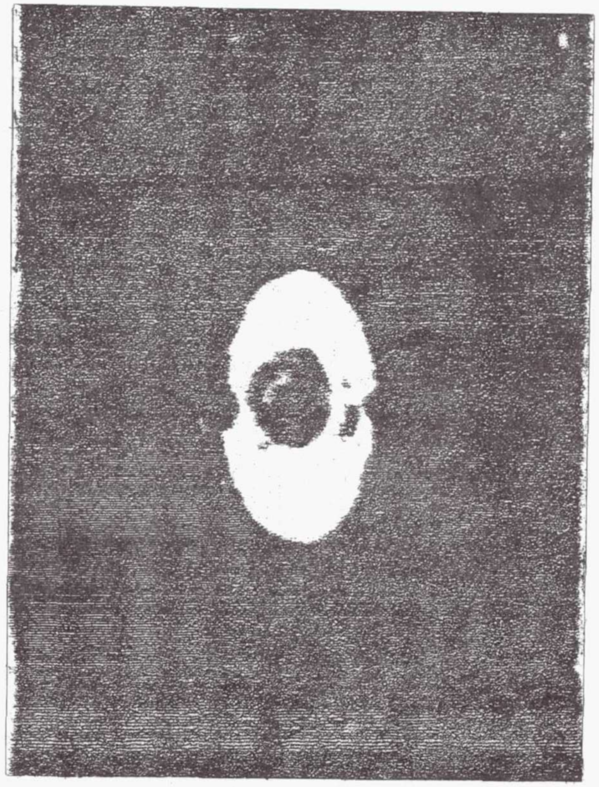

BEFORE TEST

SPECIMEN NUMBER L1-10-15

5/8 HALF PENETRATION HOLE

AFTER CYCLIC TEST

10^3 CYCLES

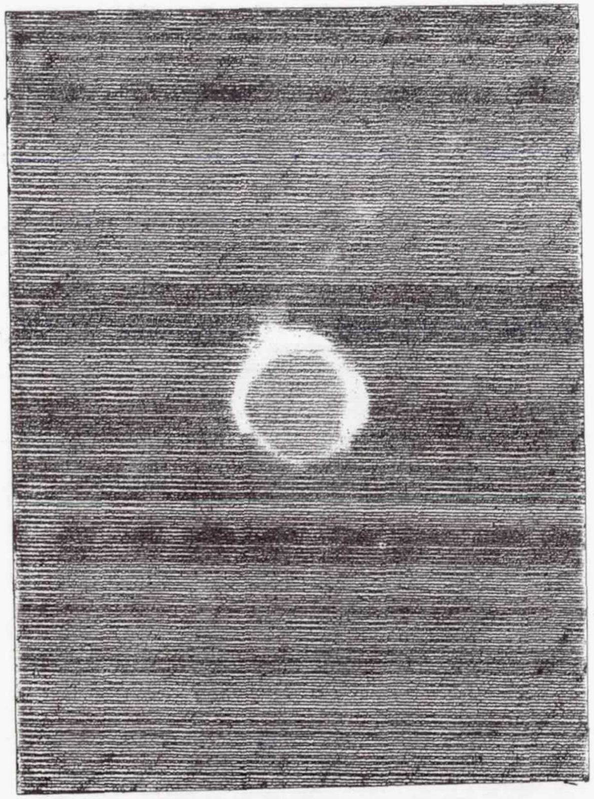

BEFORE TEST

SPECIMEN NUMBER L1-10-16

5/8 HALF PENETRATION HOLE

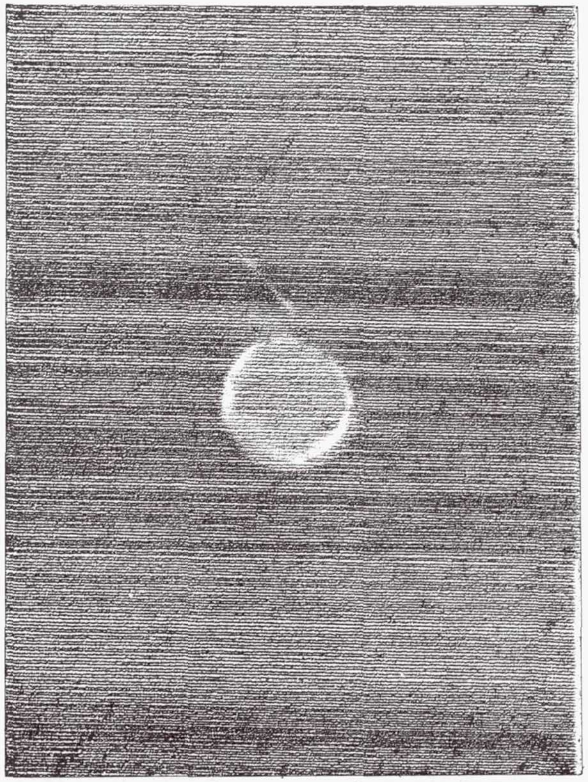

BEFORE TEST

SPECIMEN NUMBER L1-10-17

5/8 HALF PENETRATION HOLE

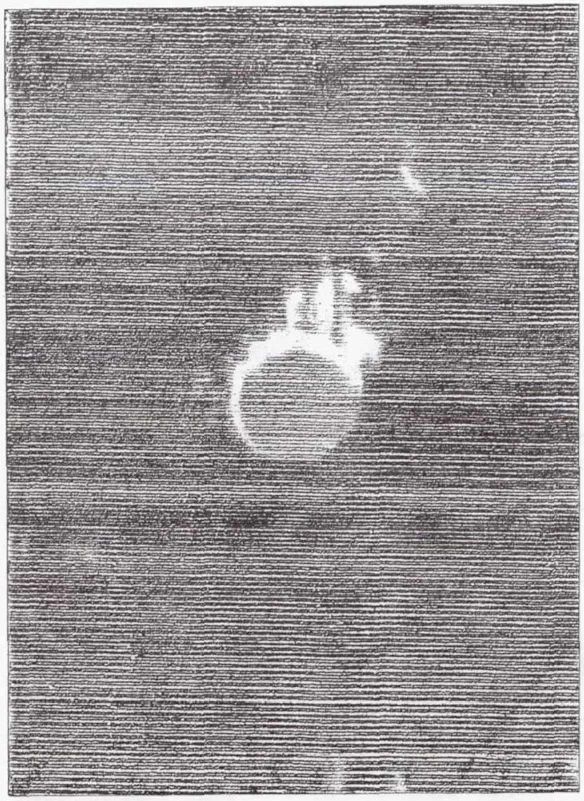

BEFORE TEST

SPECIMEN NUMBER L1-10-18

5/8 HALF PENETRATION HOLE

AFTER CYCLIC TEST

1.5 x 10^6 CYCLES

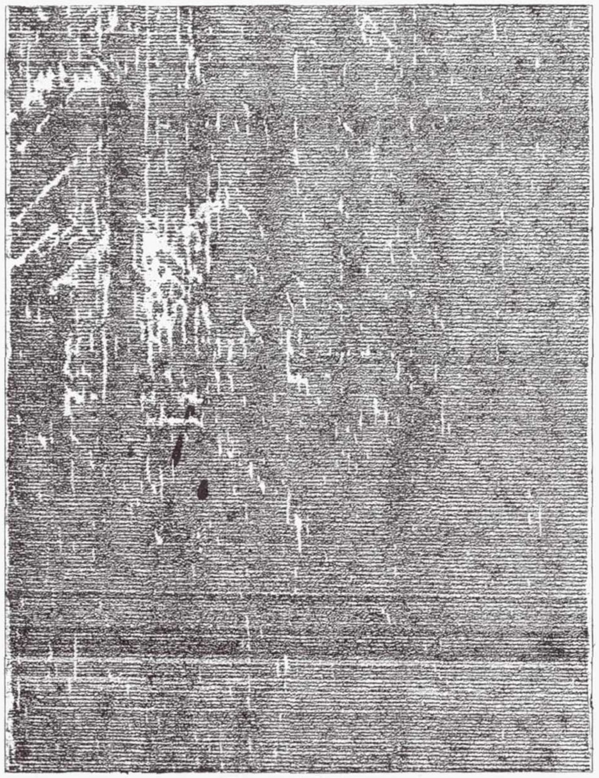

BEFORE TEST

SPECIMEN NUMBER L1-10-19

1/8 FULL PENETRATION SLIT

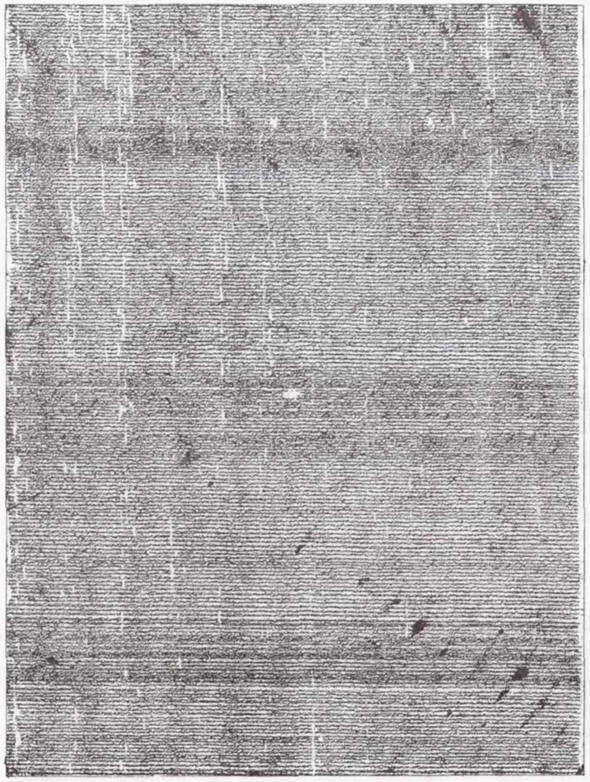

BEFORE TEST

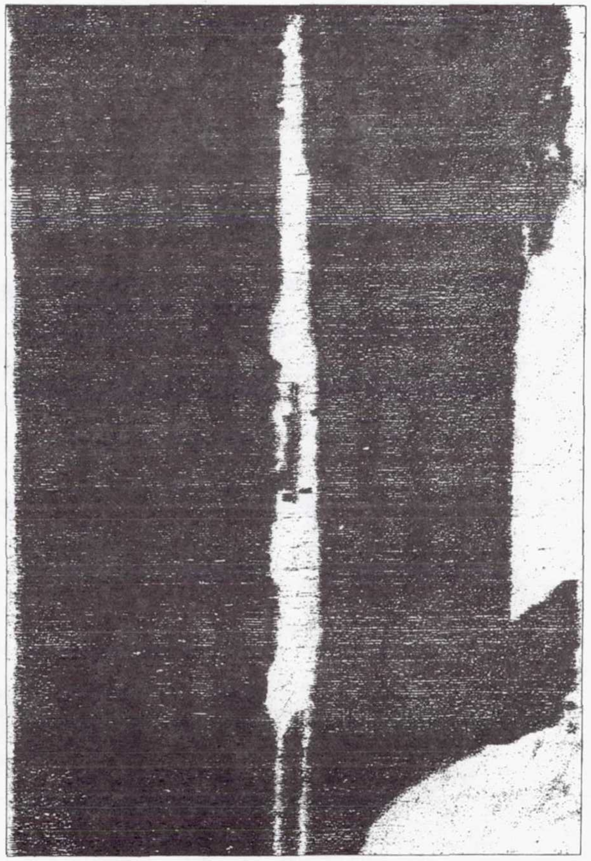

AFTER CYCLIC TEST

SPECIMEN NUMBER L1-10-20

1/8 FULL PENETRATION SLIT

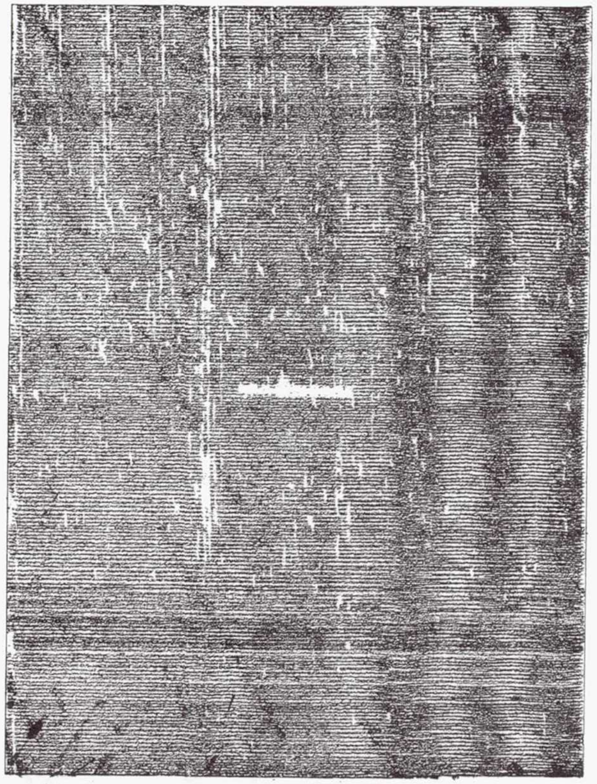

BEFORE TEST

SPECIMEN NUMBER L1-10-21

5/8 FULL PENETRATION SLIT

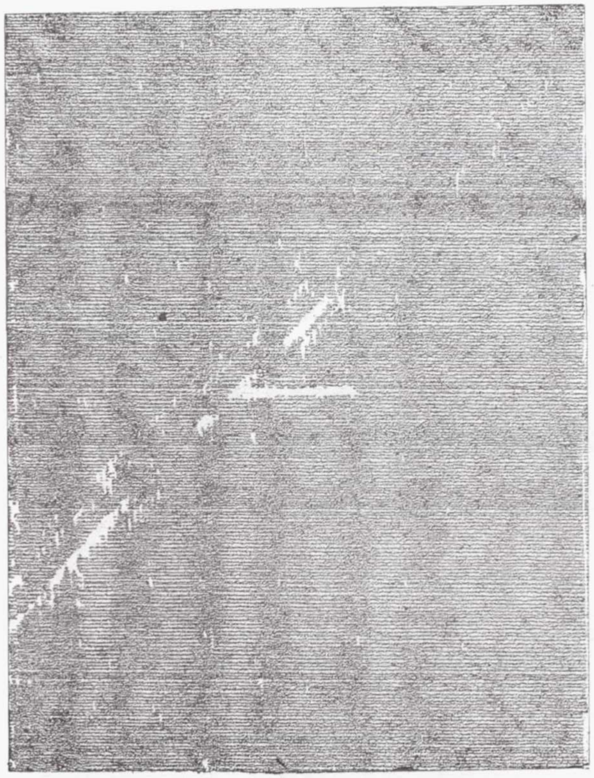

BEFORE TEST

SPECIMEN NUMBER L1-10-22

5/8 FULL PENETRATION SLIT

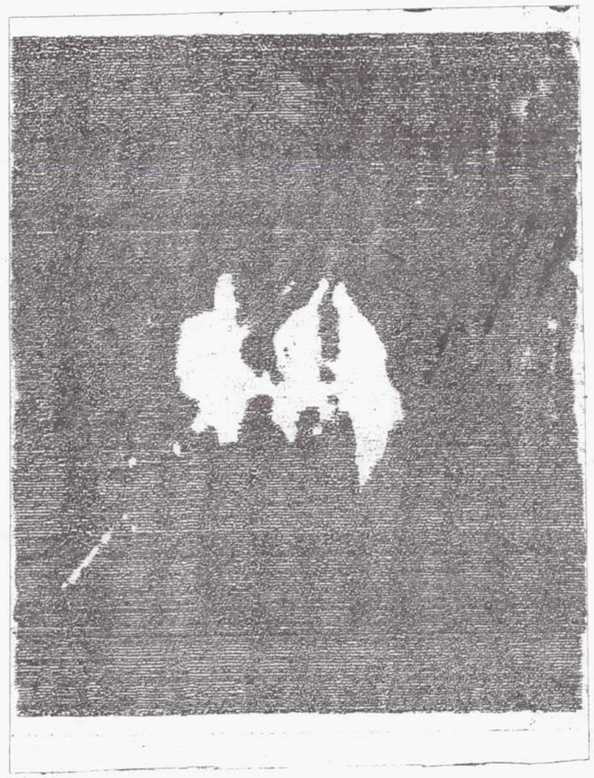

AFTER CYCLIC TEST

1.5 x 10^6 CYCLES

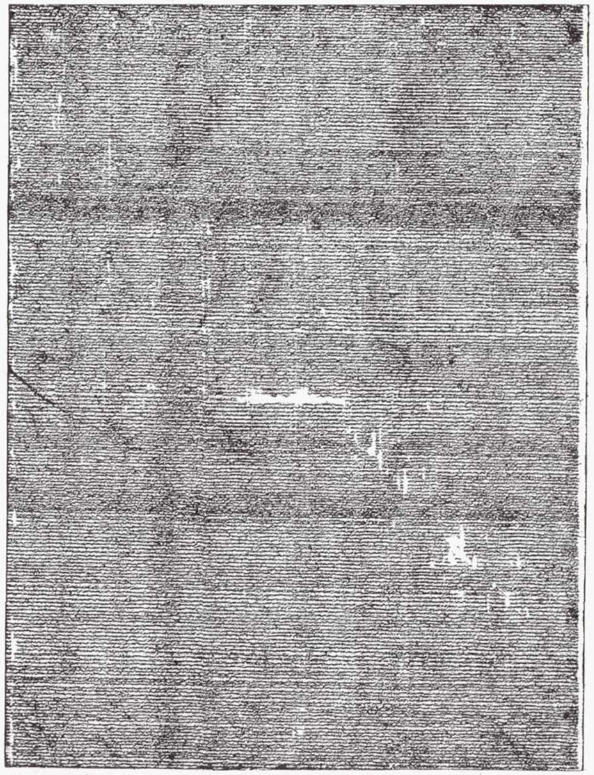

BEFORE TEST

SPECIMEN NUMBER L1-10-23

5/8 FULL PENETRATION SLIT

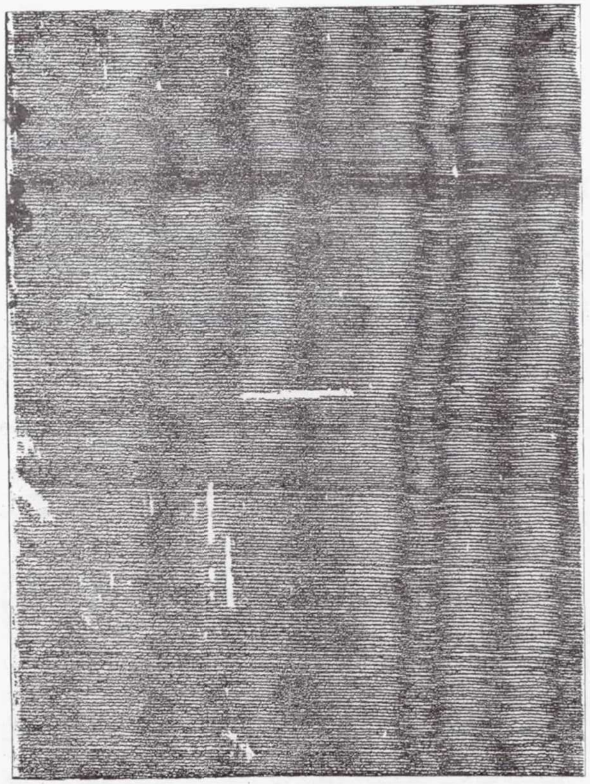

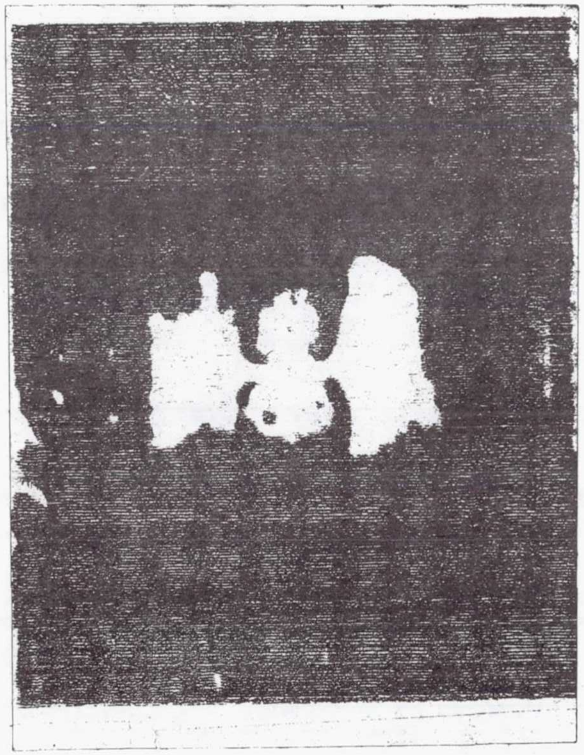

BEFORE TEST

SPECIMEN NUMBER L1-10-24

5/8 FULL PENETRATION SLIT

AFTER CYCLIC TEST

1.5×10^6 CYCLES

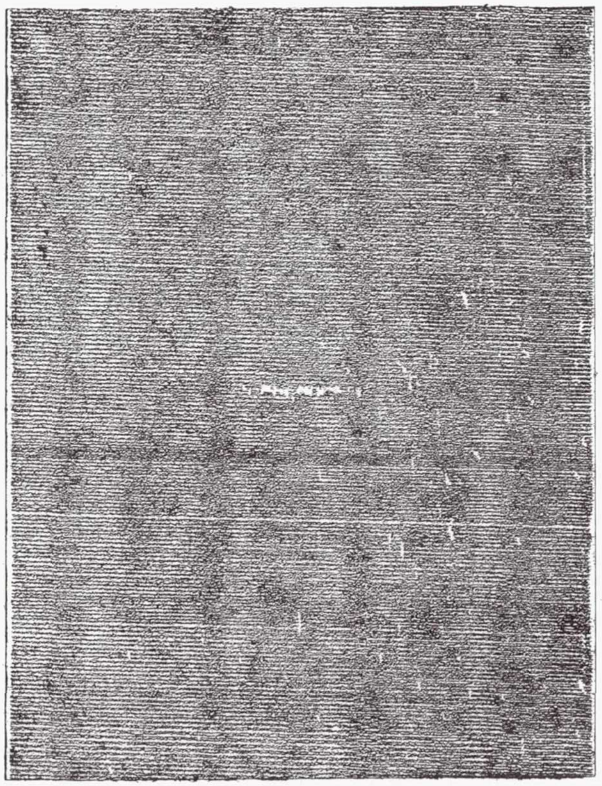

BEFORE TEST

SPECIMEN NUMBER L1-10-25

5/8 FULL PENETRATION SLIT

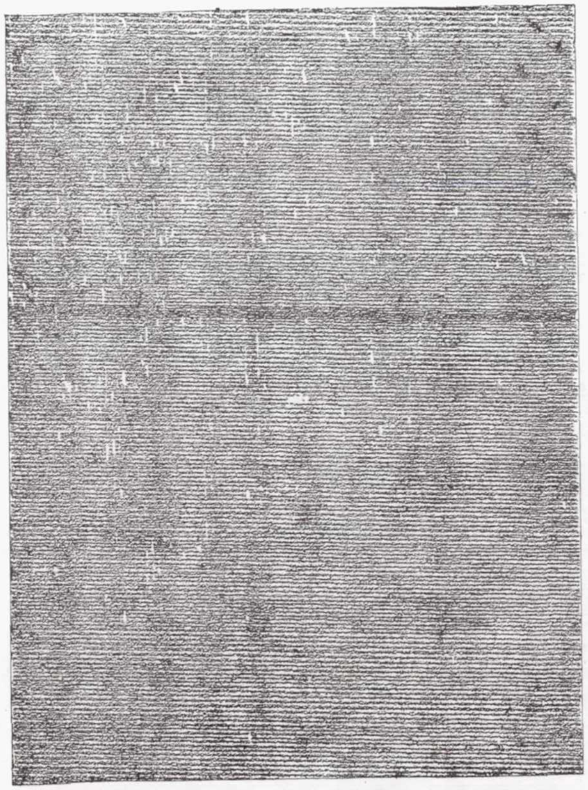

BEFORE TEST

SPECIMEN NUMBER L1-10-26

1/8 HALF PENETRATION SLIT

AFTER CYCLIC TEST

23 800 CYCLES

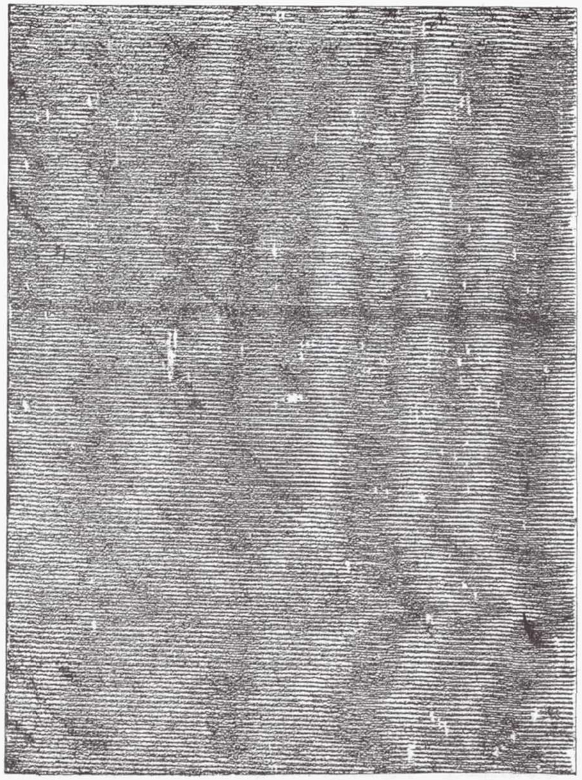

BEFORE TEST

SPECIMEN NUMBER L1-10-27

1/8 HALF PENETRATION SLIT

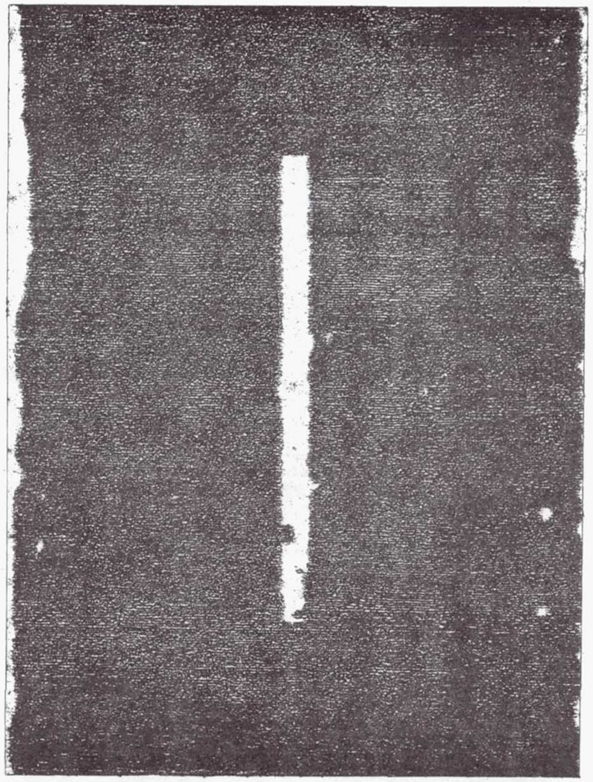

AFTER CYCLIC TEST

114 600 CYCLES

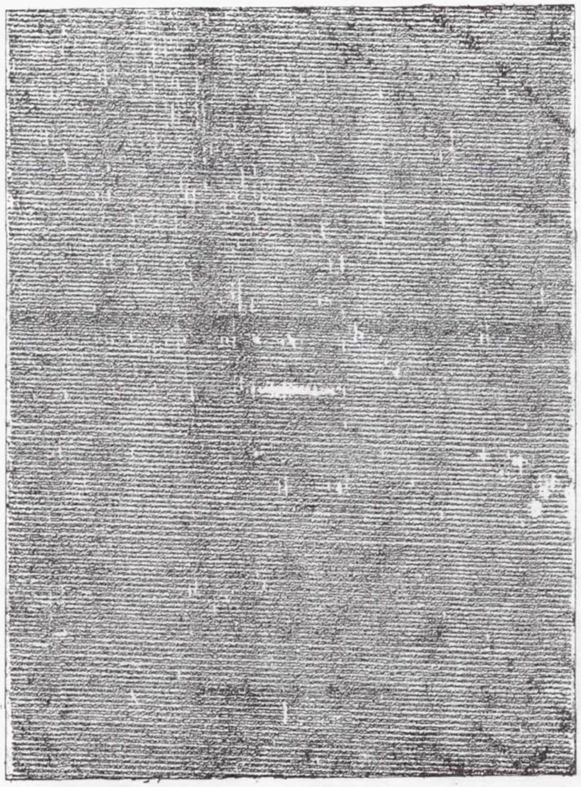

BEFORE TEST

SPECIMEN NUMBER L1-10-28

5/8 HALF PENETRATION SLIT

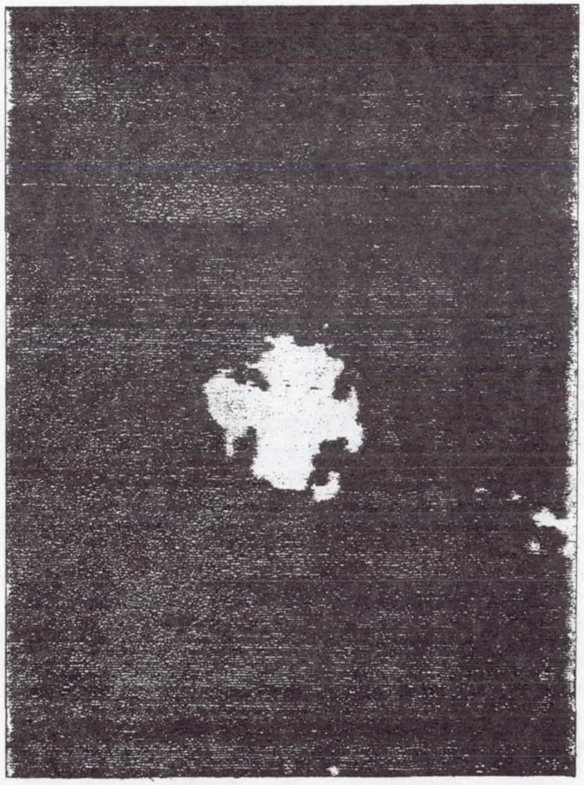

AFTER CYCLIC TEST

10^3 CYCLES

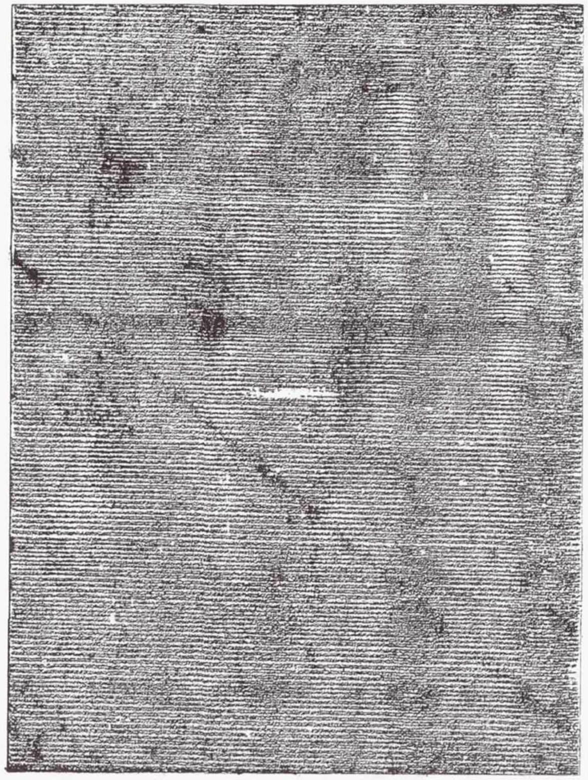

BEFORE TEST

SPECIMEN NUMBER L1-10-29

5/8 HALF PENETRATION SLIT

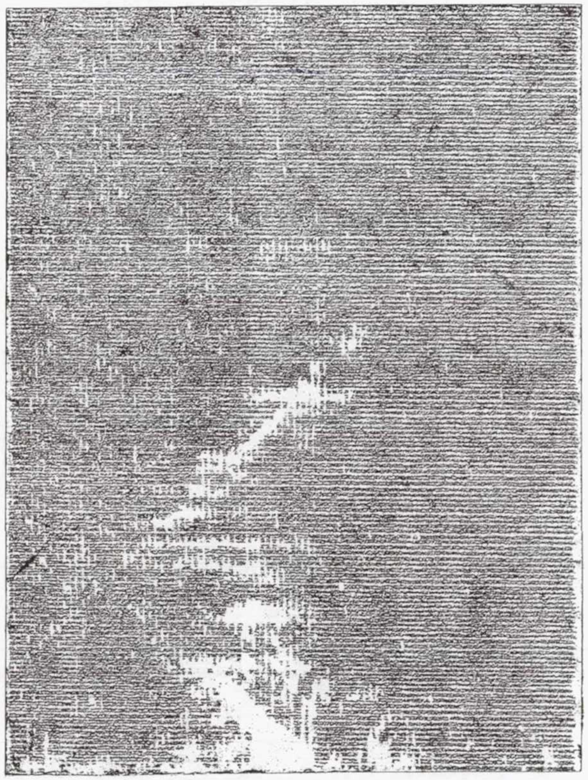

BEFORE TEST

SPECIMEN L1-10-30

5/8 HALF PENETRATION SLIT

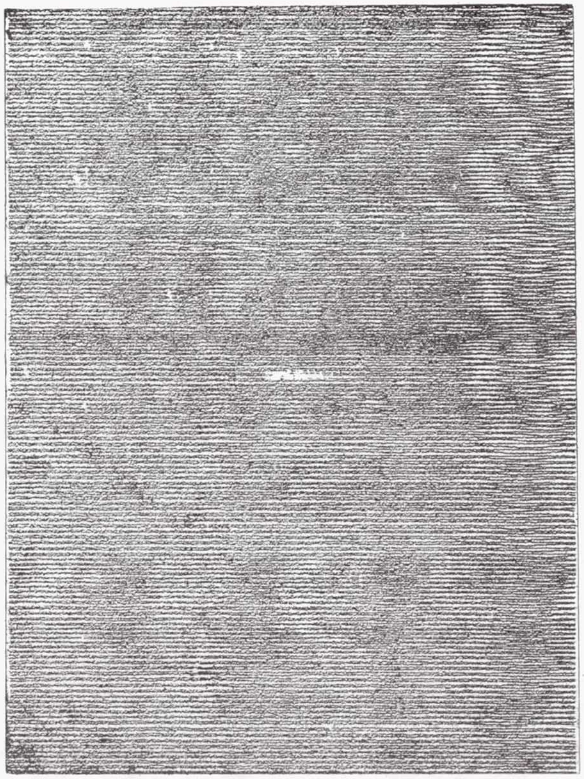

BEFORE TEST

SPECIMEN NUMBER L1-10-31

5/8 HALF PENETRATION SLIT

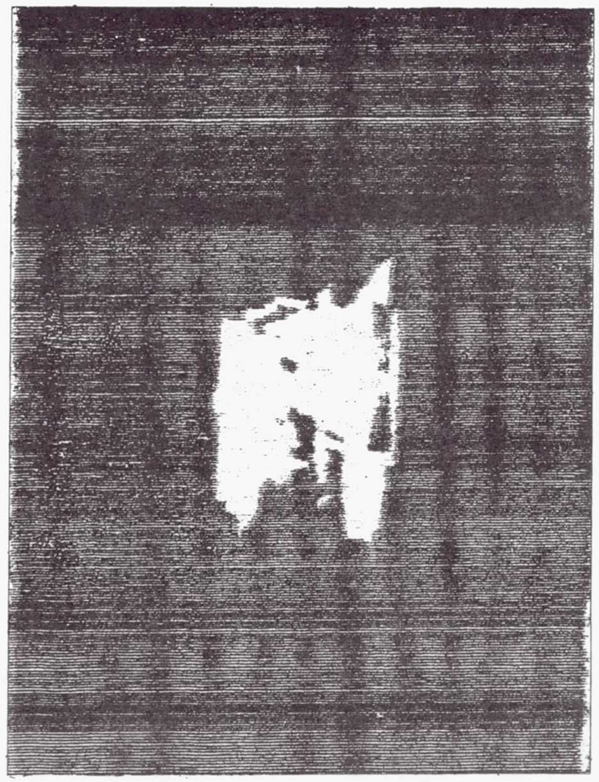

AFTER CYCLIC TEST

10^5 CYCLES

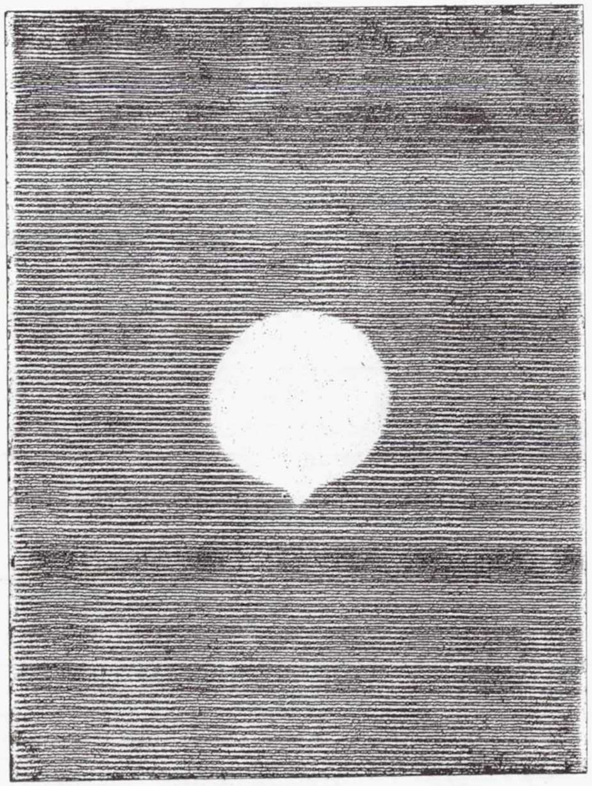

BEFORE TEST

SPECIMEN NUMBER L1-10-32

5/8 COUNTERSINK HOLE

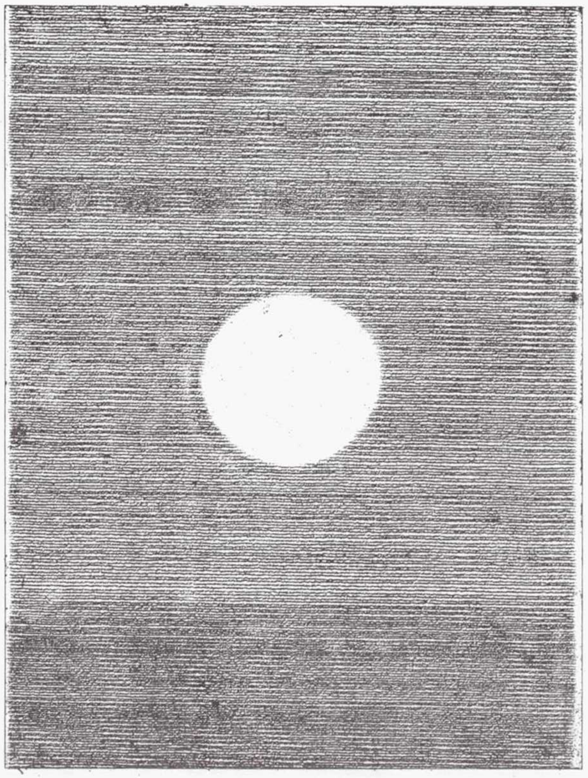

BEFORE TEST

SPECIMEN NUMBER L1-10-33

5/8 COUNTERSINK HOLE

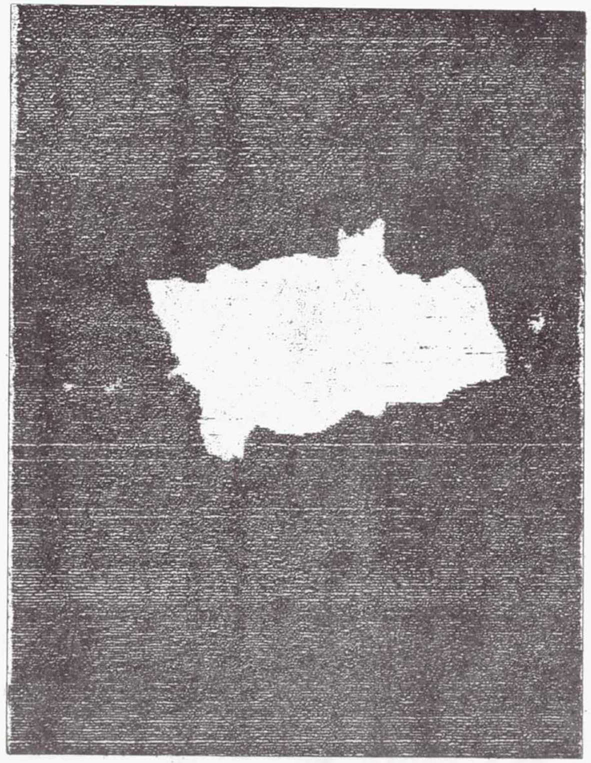

AFTER CYCLIC TEST

1.5 x 10^6 CYCLES

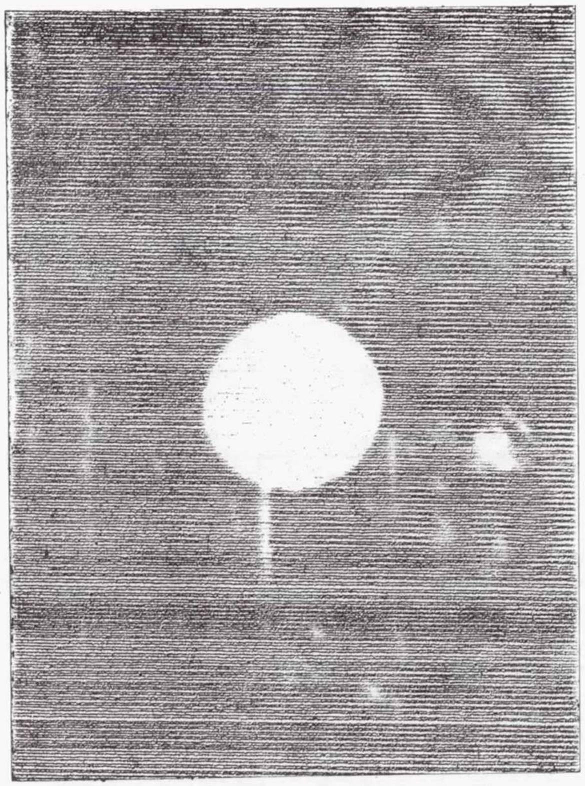

BEFORE TEST

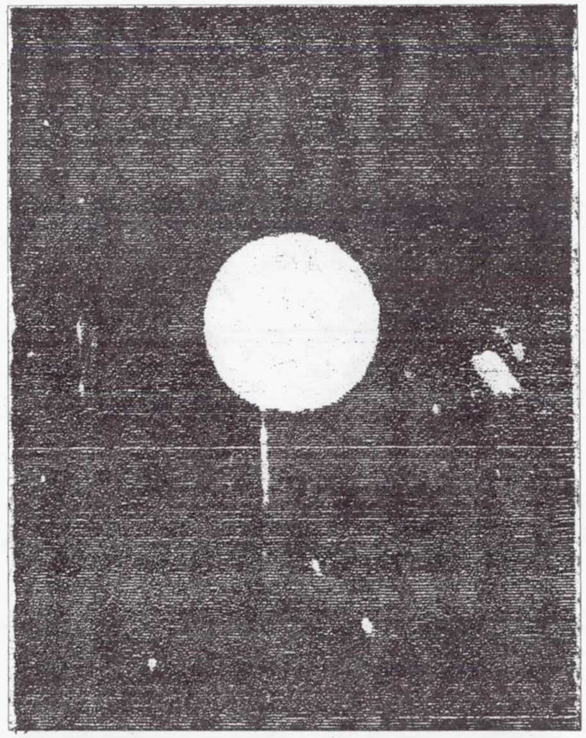

AFTER PRELOAD

SPECIMEN NUMBER L1-10-34

5/8 COUNTERSINK HOLE

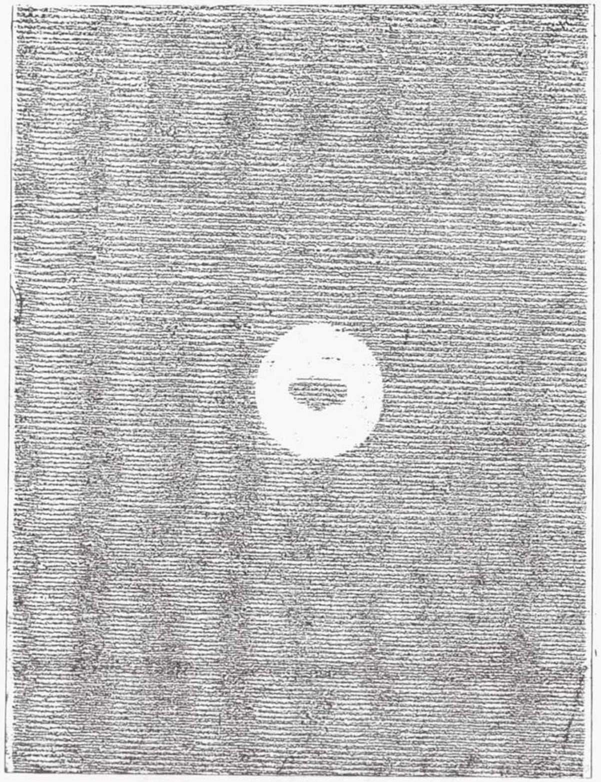

BEFORE TEST

SPECIMEN NUMBER L1-11-1

5/8 DISBOND DEFECT

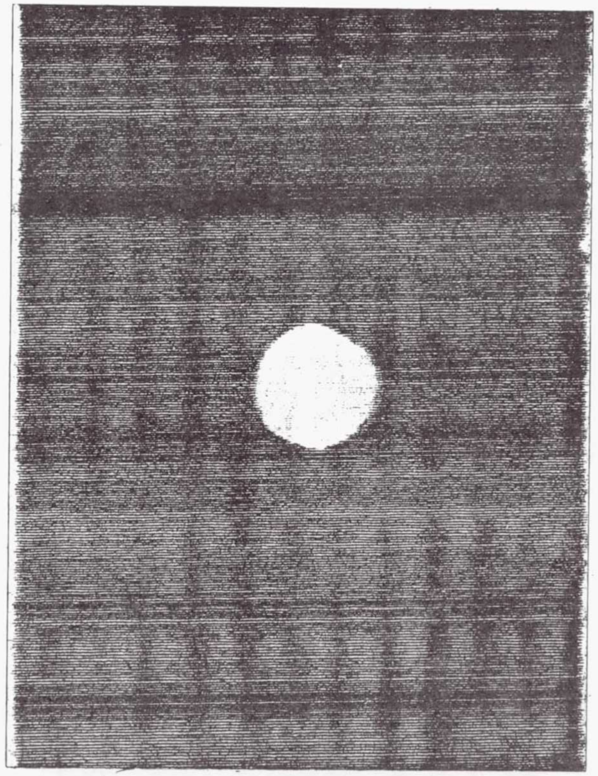

AFTER CYCLIC TEST

10^2 CYCLES

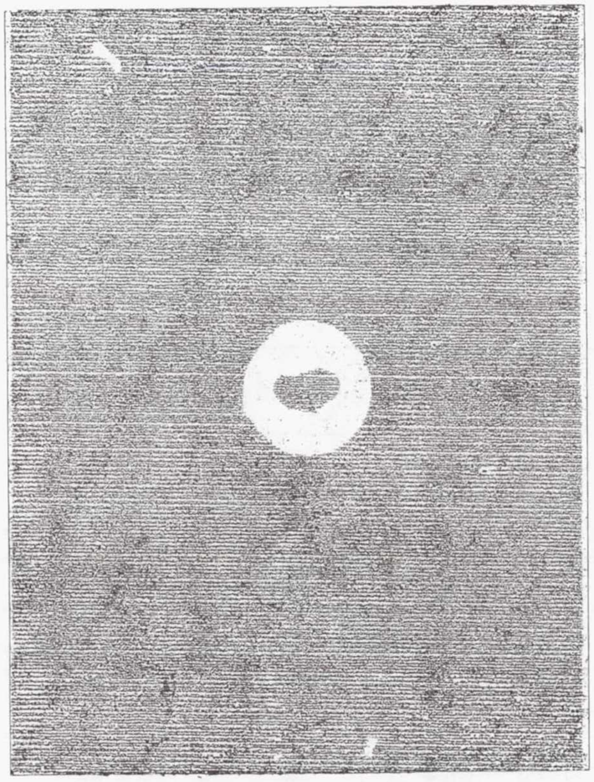

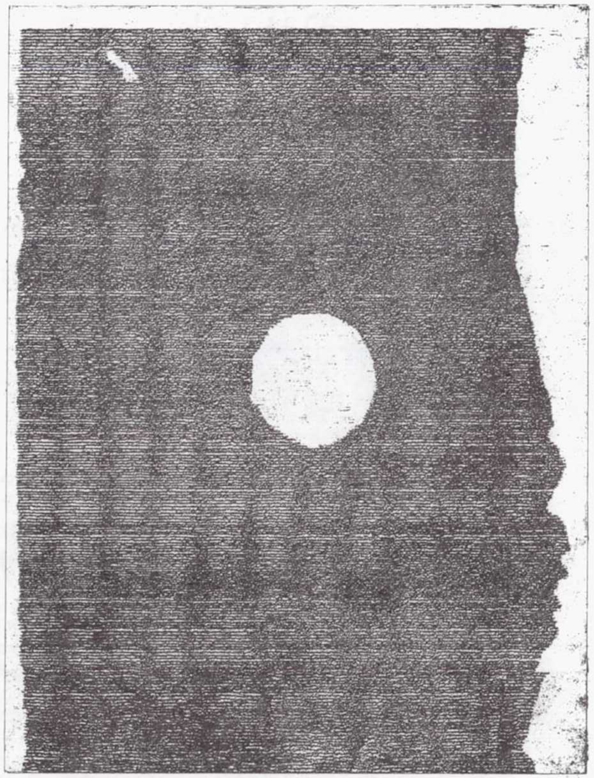

BEFORE TEST

SPECIMEN NUMBER L1-11-2

5/8 DISBOND DEFECT

AFTER CYCLIC TEST

15 780 CYCLES

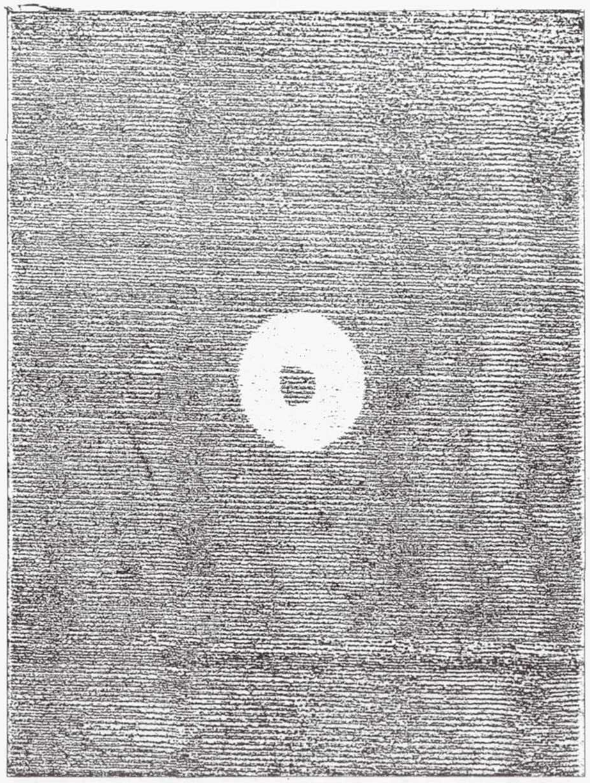

BEFORE TEST

SPECIMEN NUMBER L1-11-3

5/8 DISBOND DEFECT

AFTER CYCLIC TEST

77 CYCLES

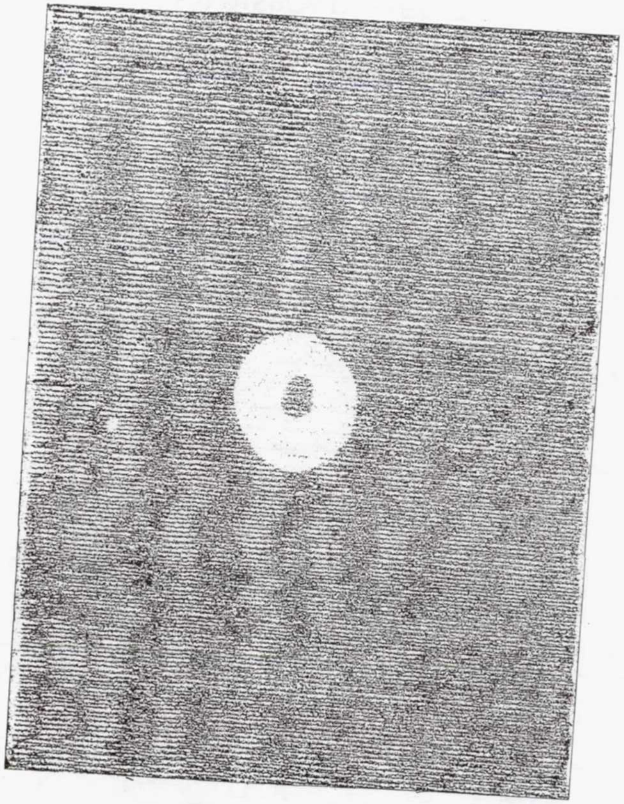

BEFORE TEST

SPECIMEN L1-11-4

5/8 DISBOND DEFECT

BEFORE TEST

SPECIMEN NUMBER L1-11-5

5/8 DISBOND DEFECT

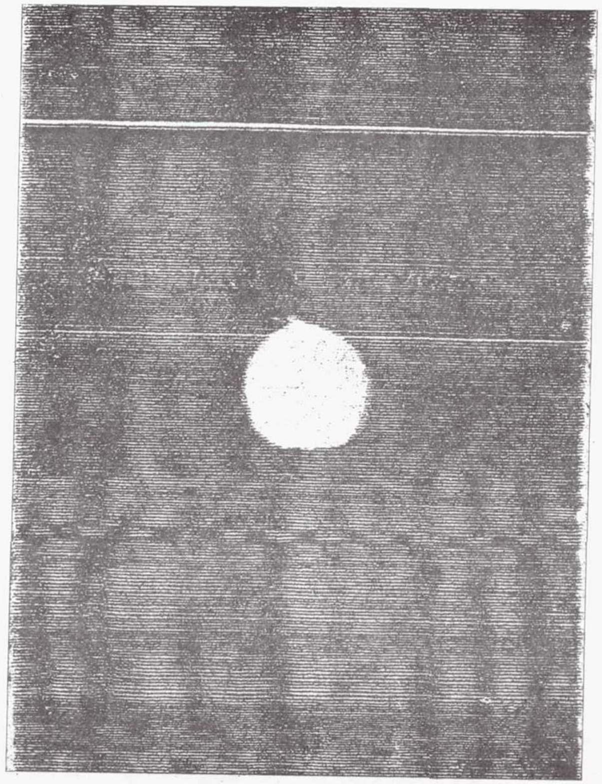

AFTER CYCLIC TEST

10^2 CYCLES

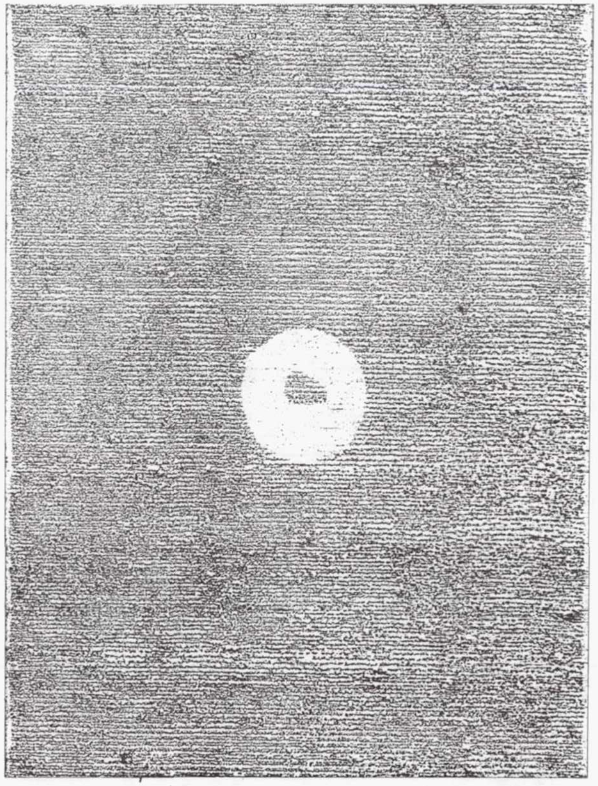

BEFORE TEST

SPECIMEN NUMBER L1-11-6

5/8 DISBOND DEFECT

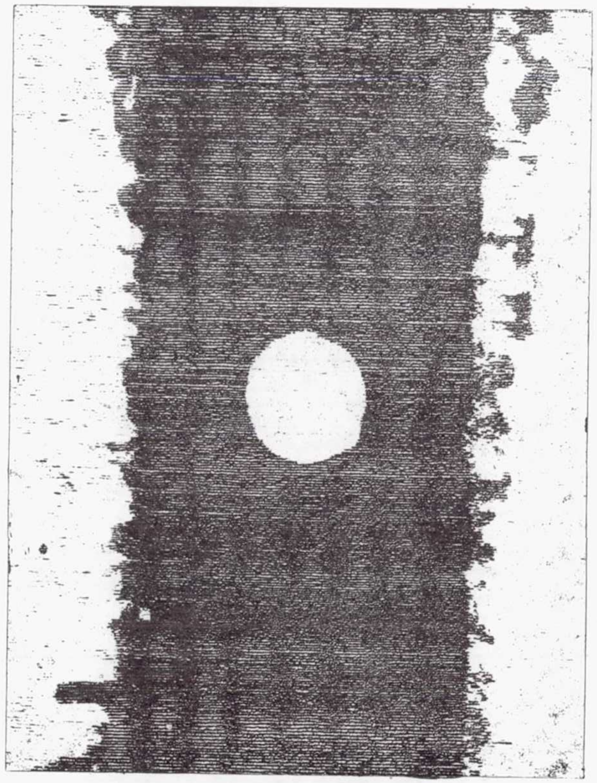

AFTER CYCLIC TEST

1.5 x 10^6 CYCLES

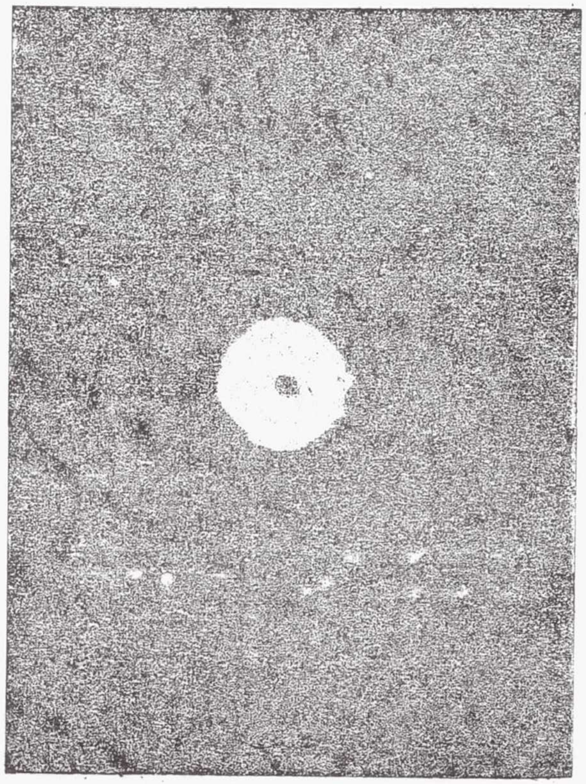

BEFORE TEST

SPECIMEN NUMBER L1-11-7

5/8 DISBOND DEFECT

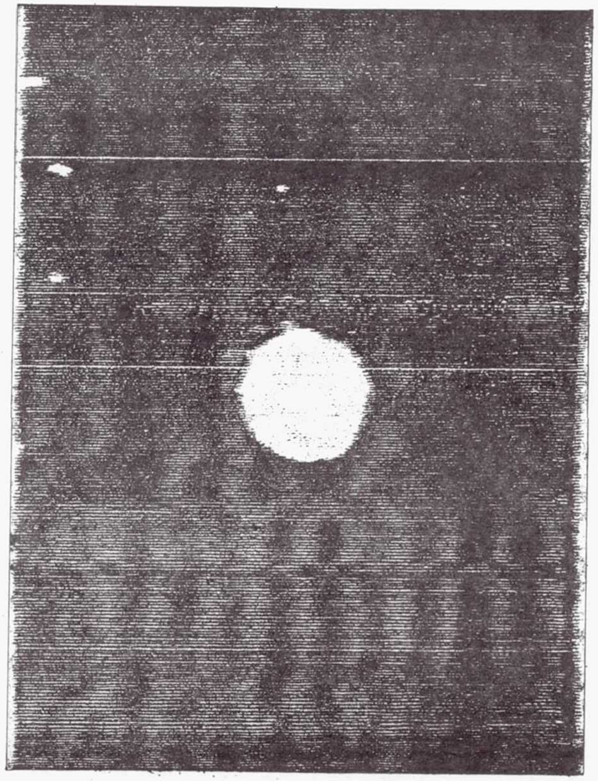

AFTER PRELOAD

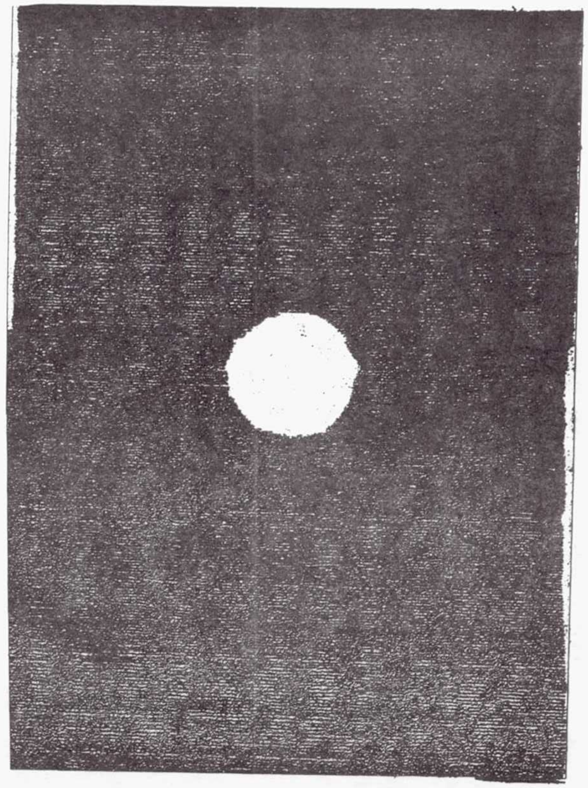

AFTER CYCLIC TEST

10^2 CYCLES

APPENDIX C

STATIC TEST CRACK OPENING DISPLACEMENT RECORDS

This appendix contains copies the machine records giving the crack opening displacement gage reading versus the static test machine load. Each page generally contains the records for all the static, preload and residual static tests for each defect configuration and laminate type. The curves are identified by specimen number and defect code. The value of the maximum test machine load as read from test machine dial is also recorded on the record. The letters ULT designate an ultimate or specimen failure load.

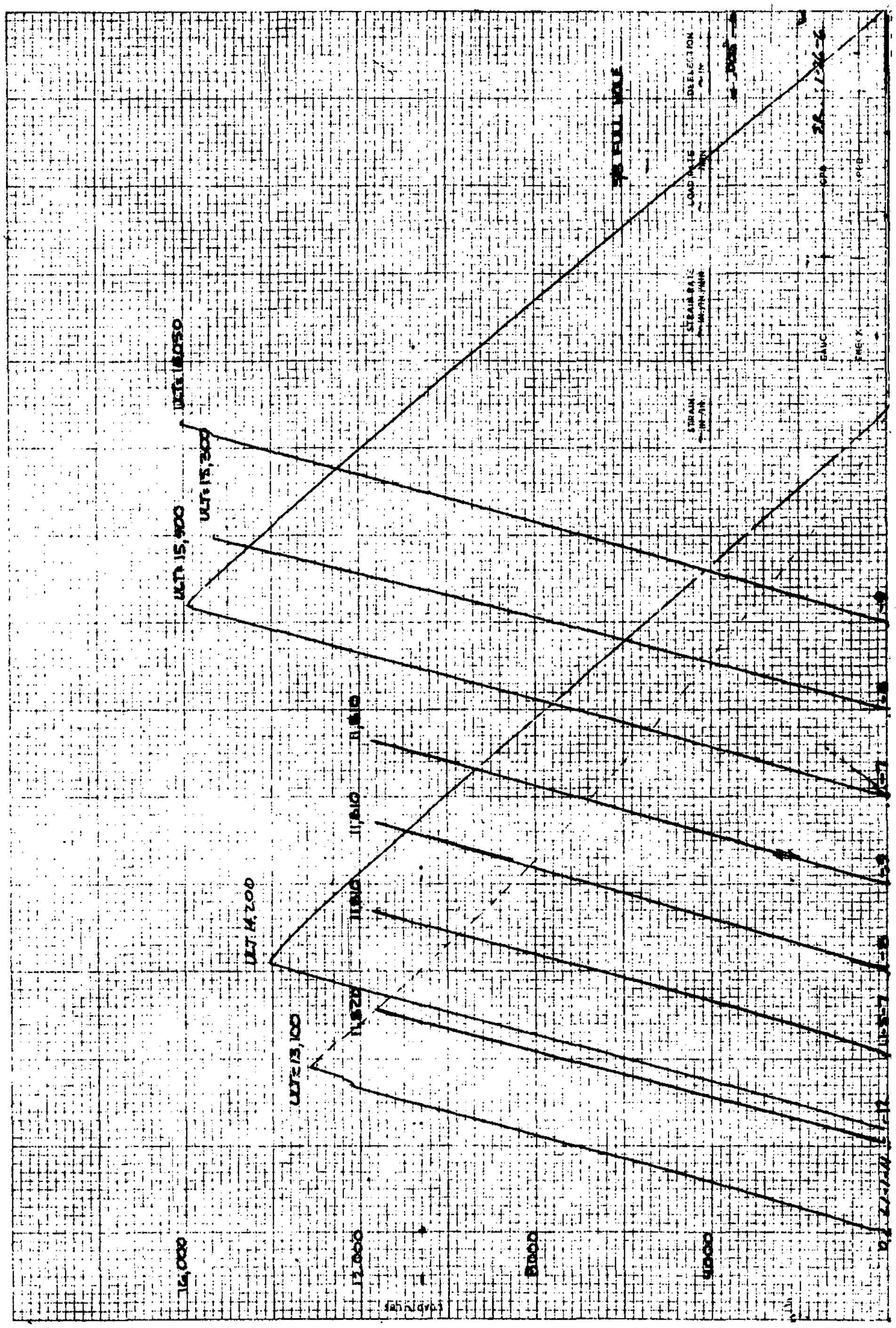

ULT: 16,050
ULT: 15,300
ULT: 15,900
ULT: 14,200
ULT: 13,100
16,000
12,000
8000
4000

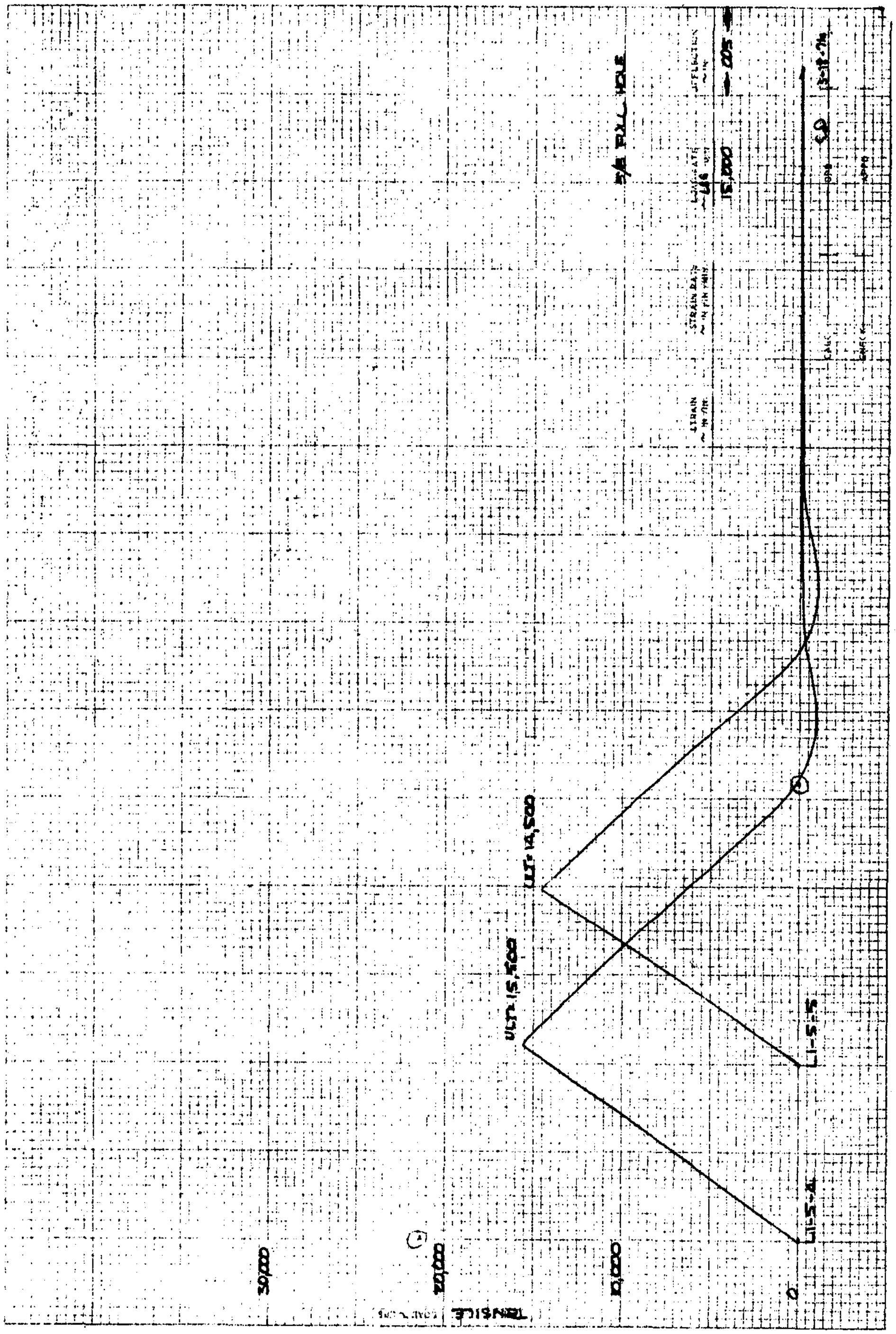

30,000
20,000
10,000
0
TENSILE
ULT=15,500
ULT=14,500

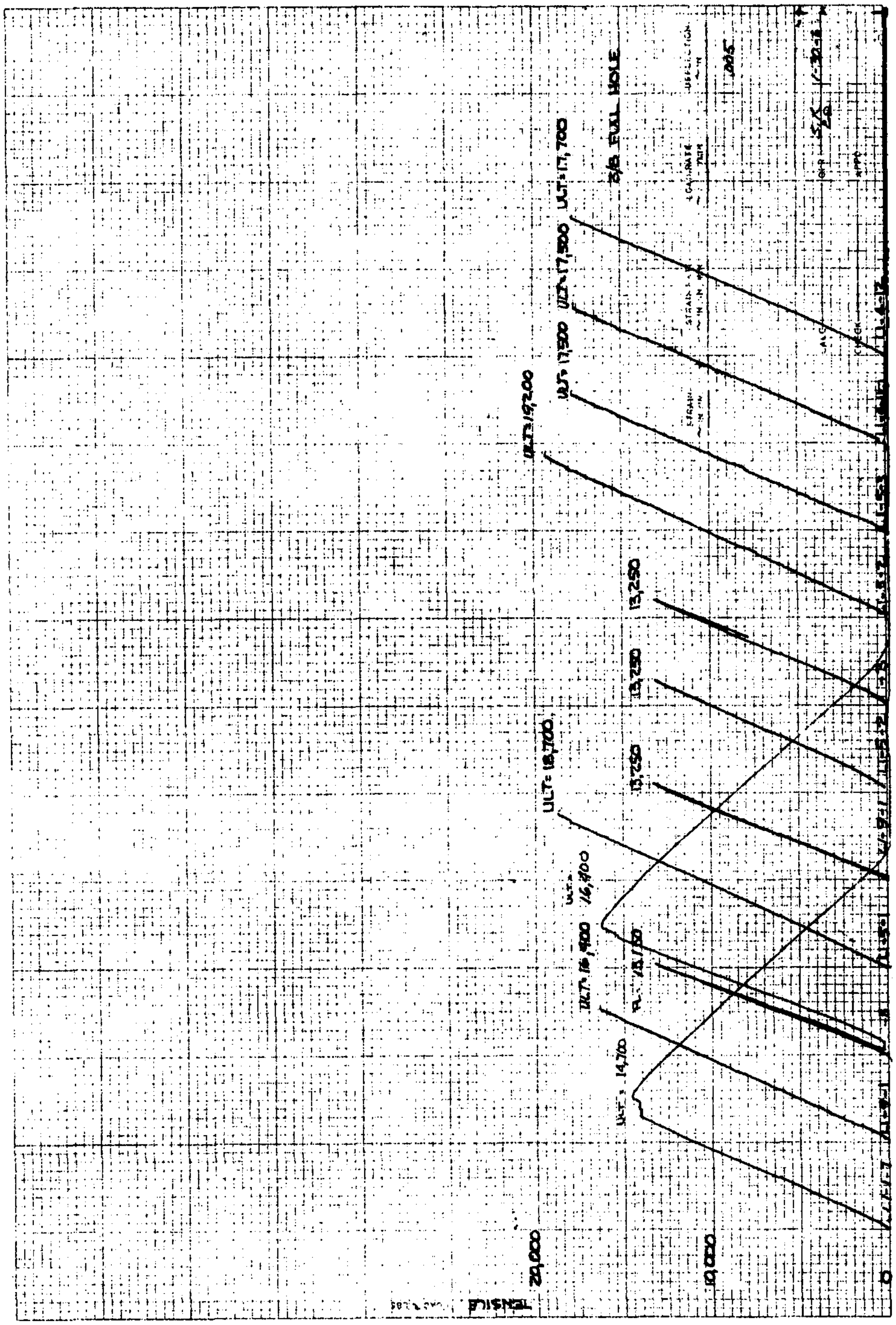
TENSILE
20,000
10,000
0
ULT=14,700
ULT=16,400
ULT=18,700
13,250
ULT=19,200
ULT=17,700
3/8 FULL HOLE

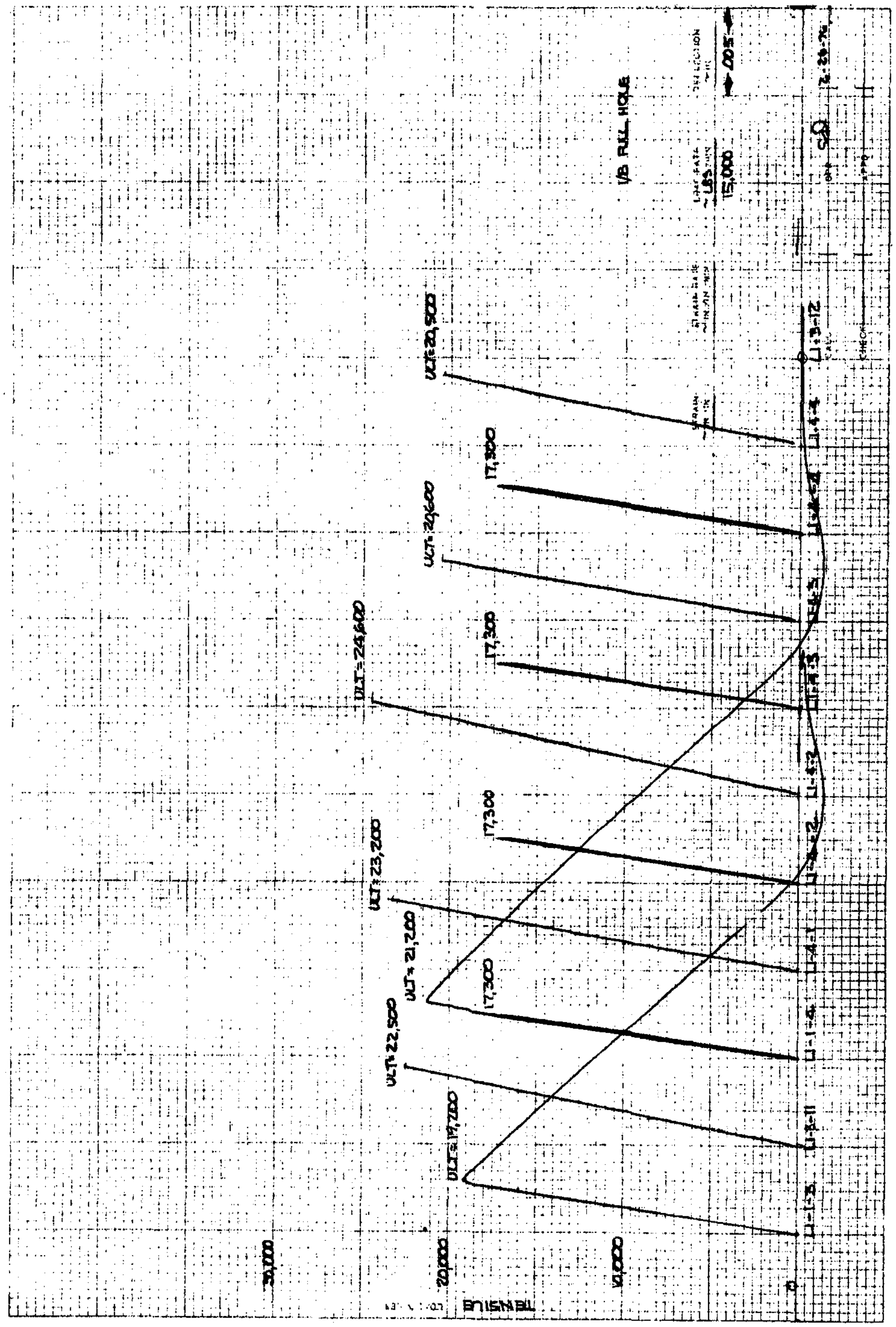
1/8 FULL HOLE
TENSILE
30,000
20,000
10,000
0
ULT=20,500
17,300
ULT=20,600
17,300
ULT=24,600
17,300
ULT=23,200
ULT=21,200
17,300
ULT=22,500
ULT=19,200
15,000
.005

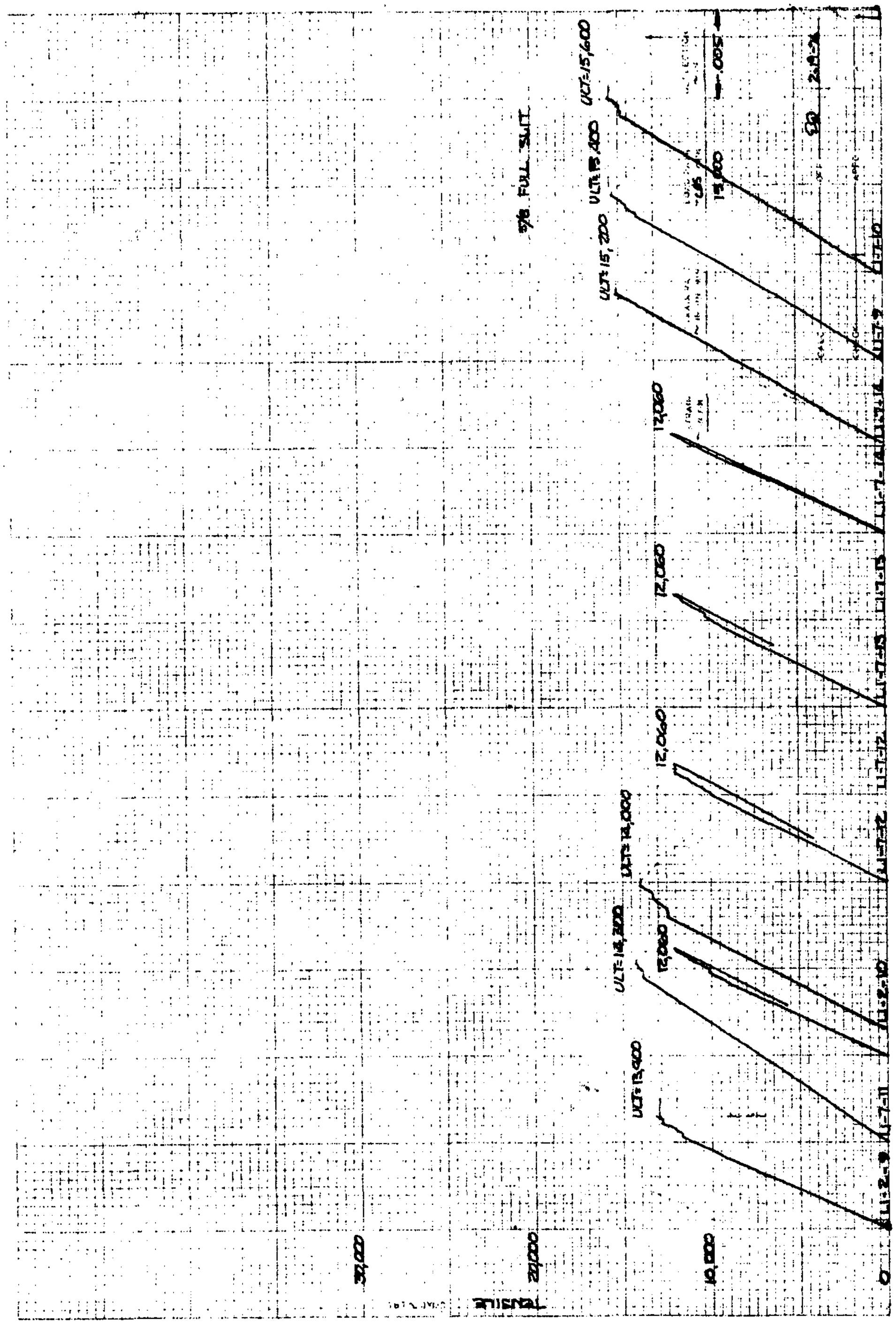

5/8 FULL SLIT
ULT=15,600
ULT 15,200
12,000
ULT=14,000
ULT=13,400
30,000
20,000
10,000
0
TENSILE

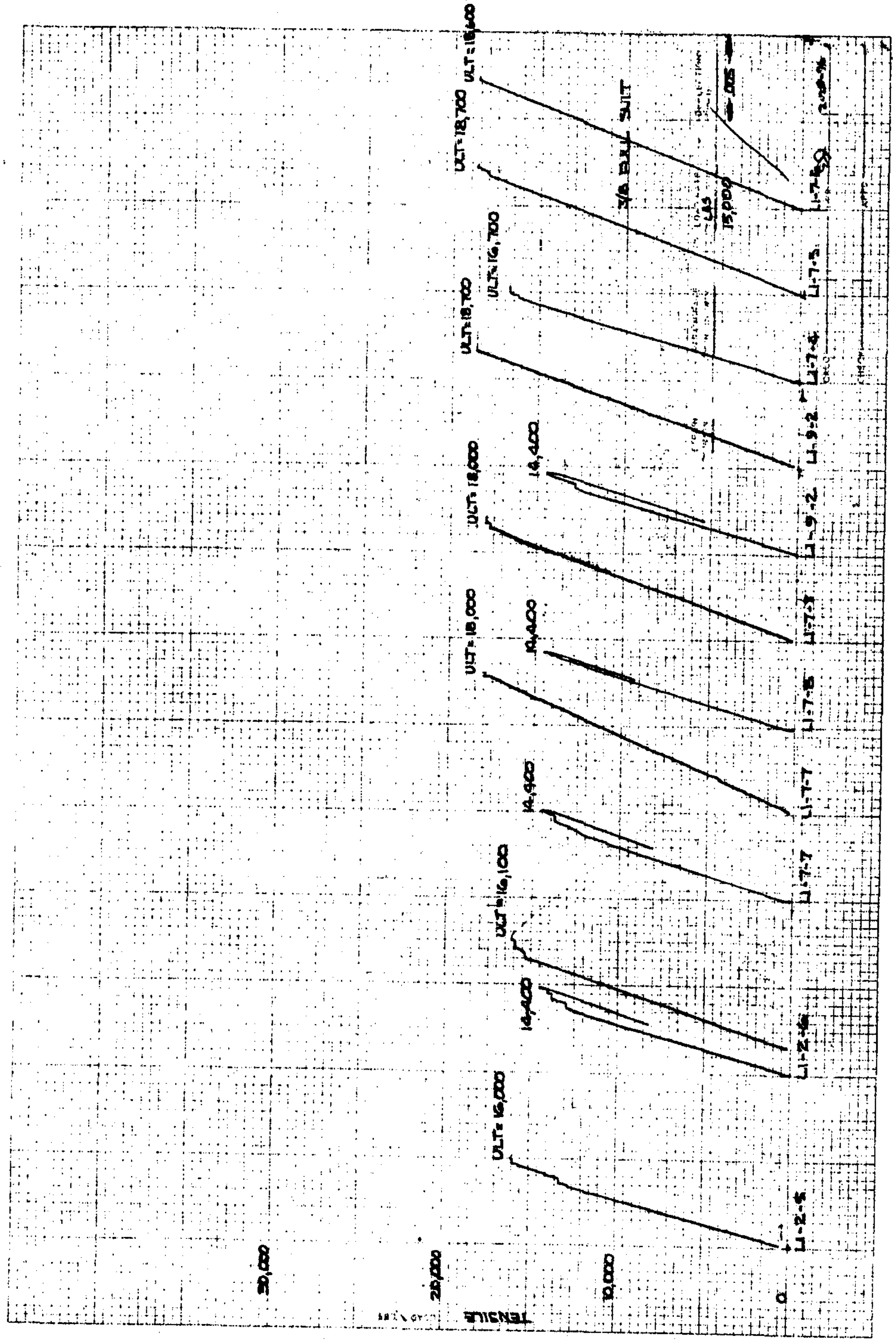

30,000
20,000
10,000
0
TENSILE

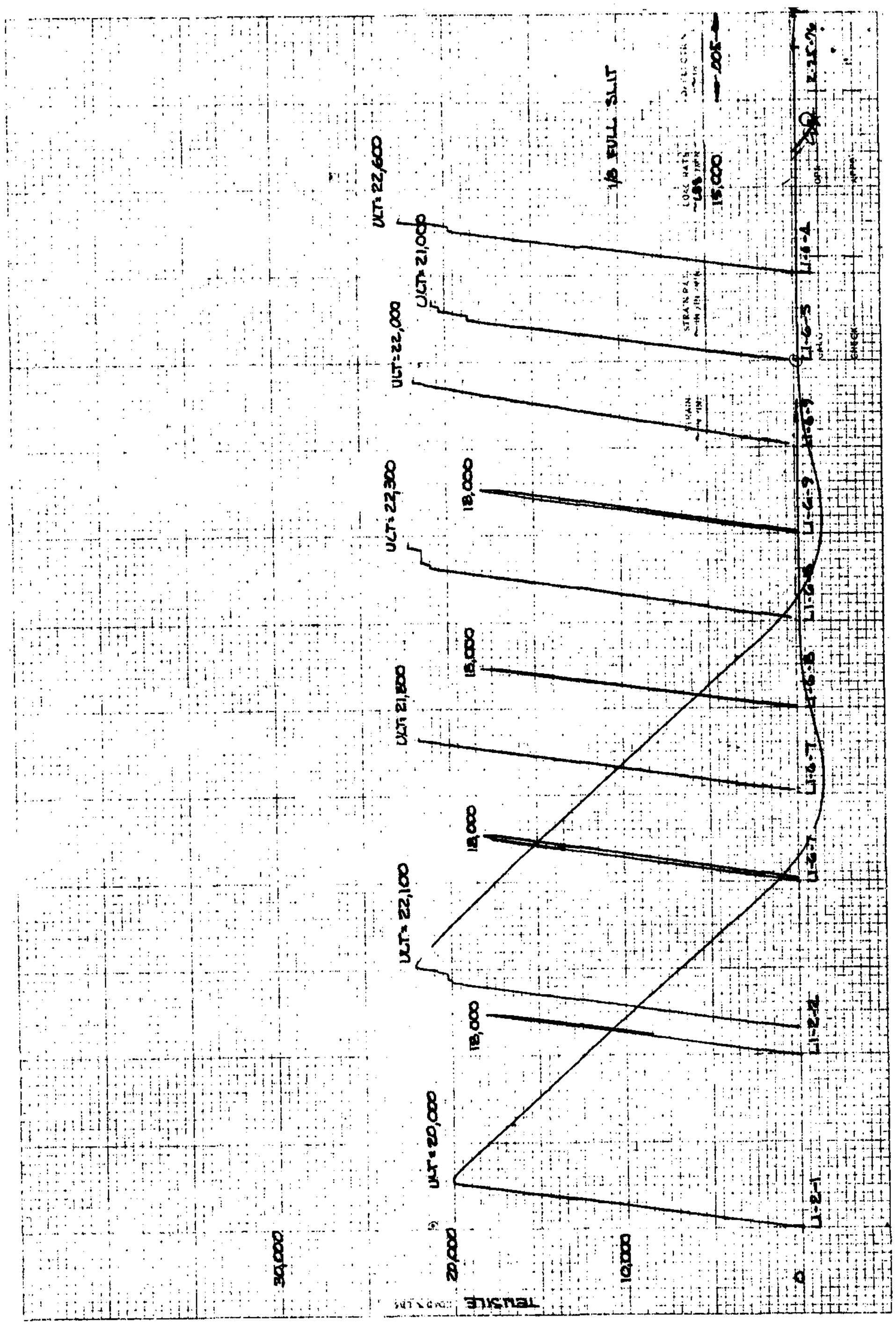

TENSILE
30,000
20,000
10,000
0
ULT=20,000
18,000
ULT=22,100
18,000
ULT=21,800
18,000
ULT=22,300
18,000
ULT=22,000
ULT=21,000
ULT=22,600
1/8 FULL SLIT
15,000

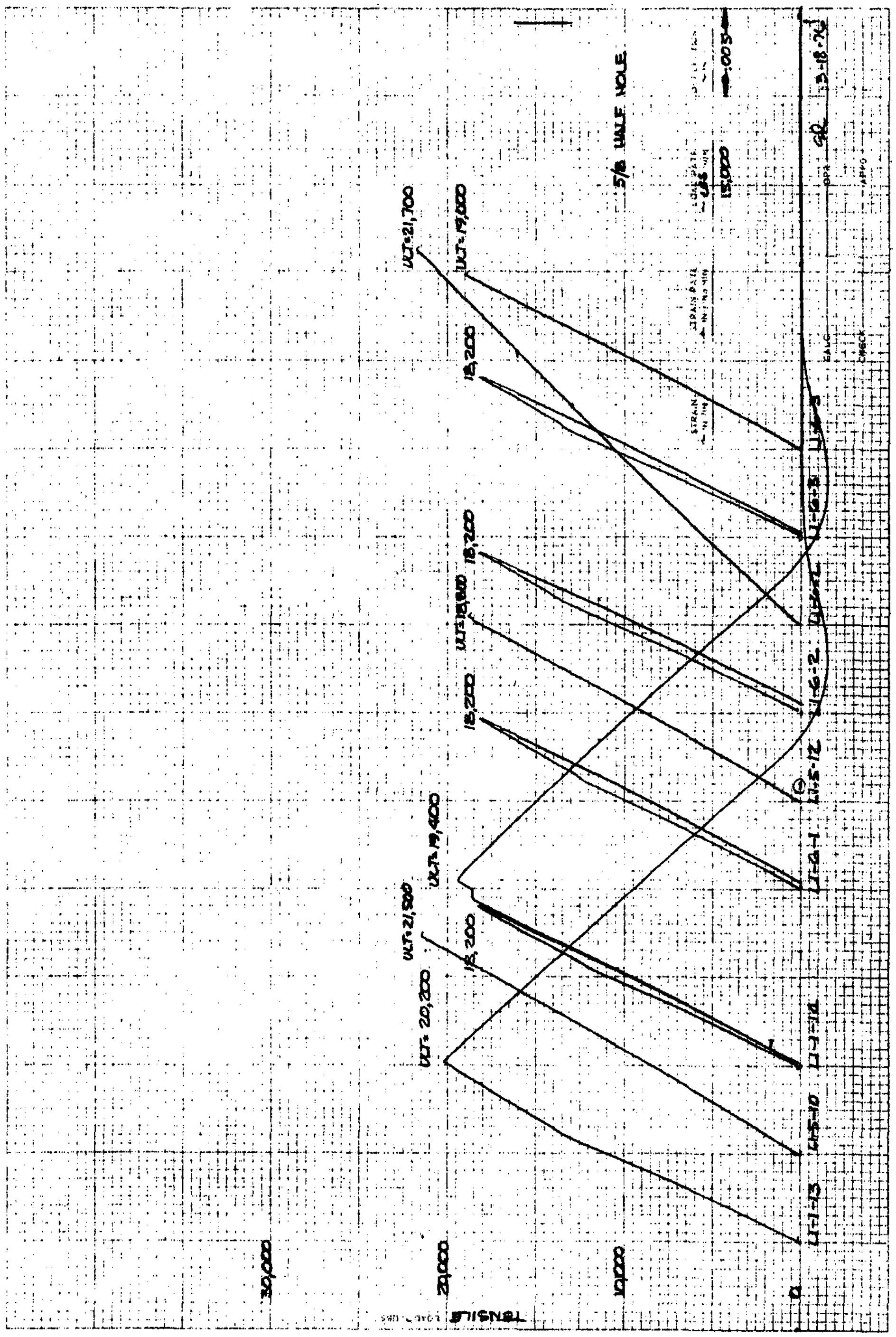
5/8 HALF HOLE
ULT=21,700
ULT=19,000
18,200
18,200
ULT=19,800
18,200
ULT=19,400
ULT=21,500
18,200
ULT=20,200
30,000
20,000
10,000
0
TENSILE
15,000
.005

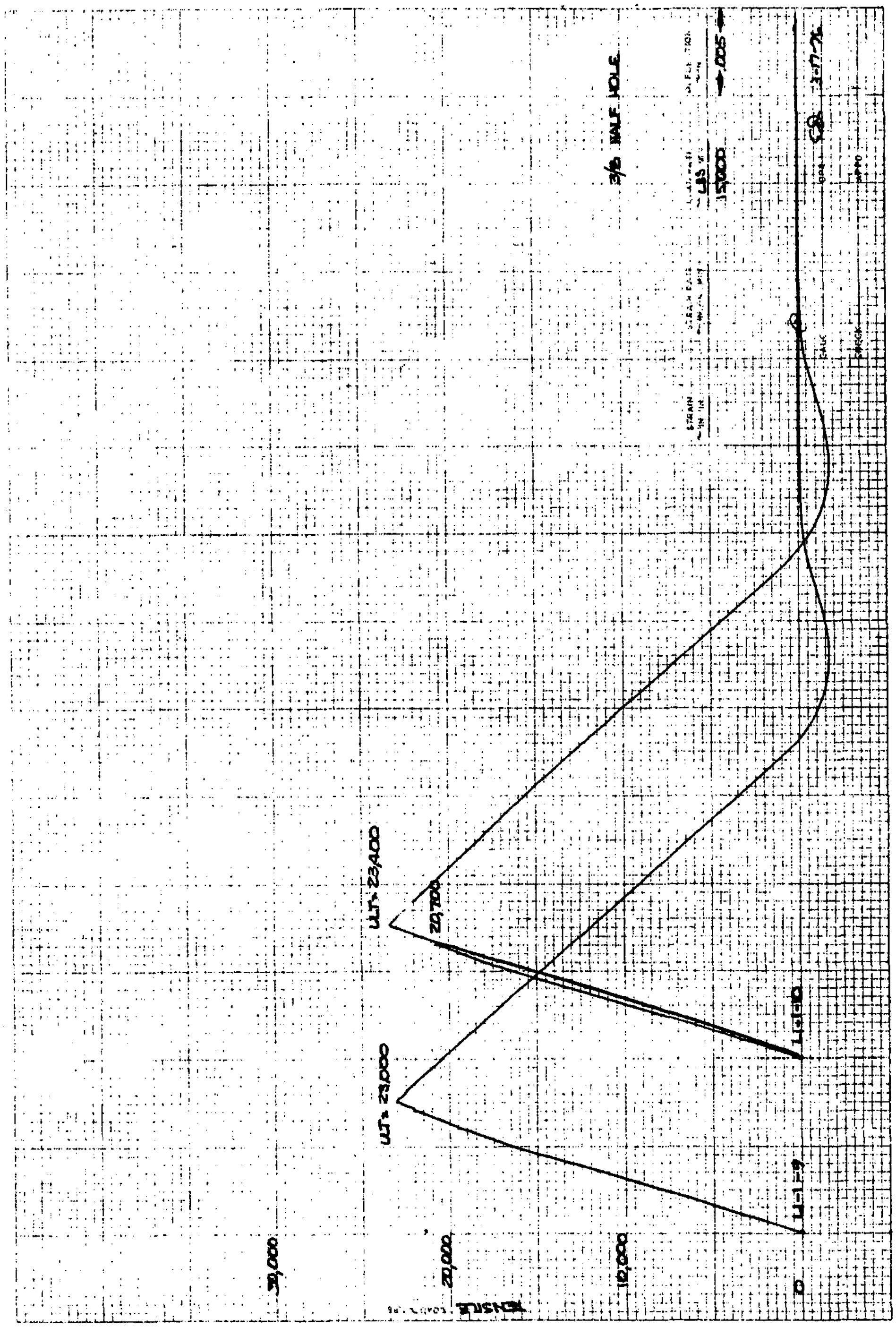
3/16 HALF HOLE
ULT. 23,400
20,700
ULT. 23,000
30,000
20,000
10,000
0
TENSILE
15000
.005

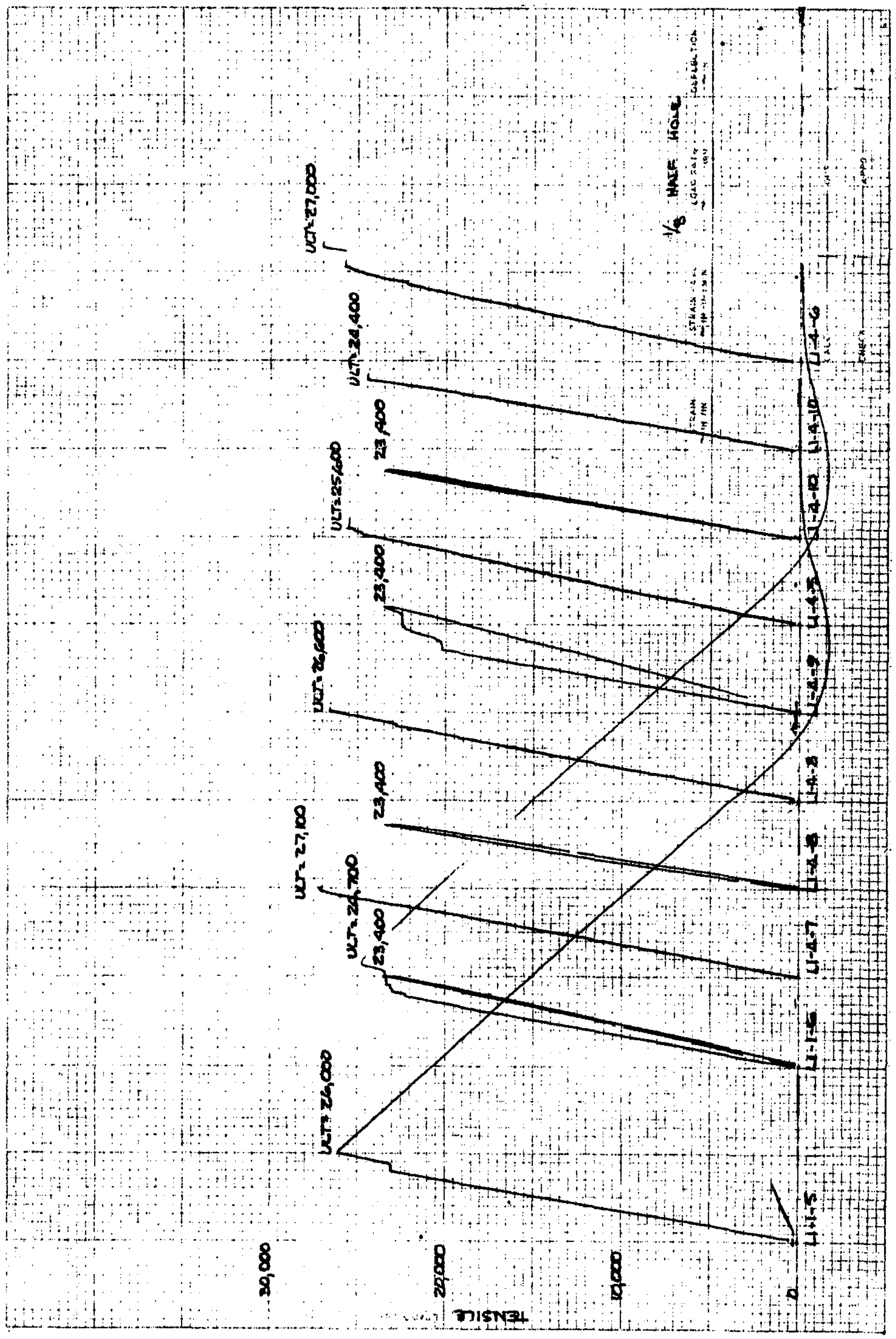

ULT=27,000
ULT=28,400
23,900
ULT=25,600
23,200
ULT=26,800
23,400
ULT=27,100
ULT=26,700
23,400
ULT=26,000
30,000
20,000
10,000
0
TENSILE
1/8 HALF HOLE

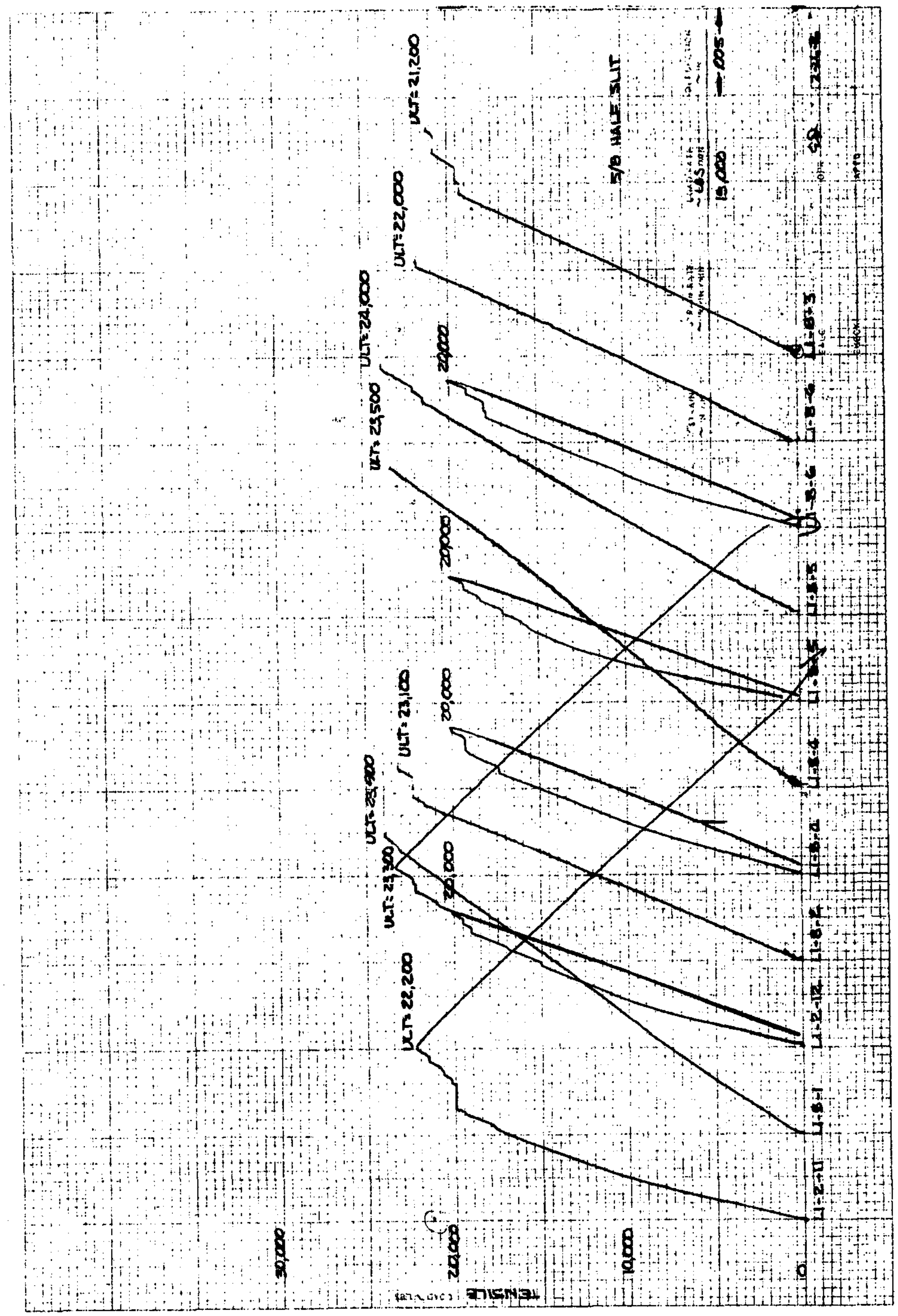
ULT=21,200
ULT=22,000
ULT=24,000
ULT=23,500
ULT=23,100
ULT=23,900
ULT=23,300
ULT=22,200
20,000
5/8 HALF SLIT
15,000
30,000
10,000
0
TENSILE

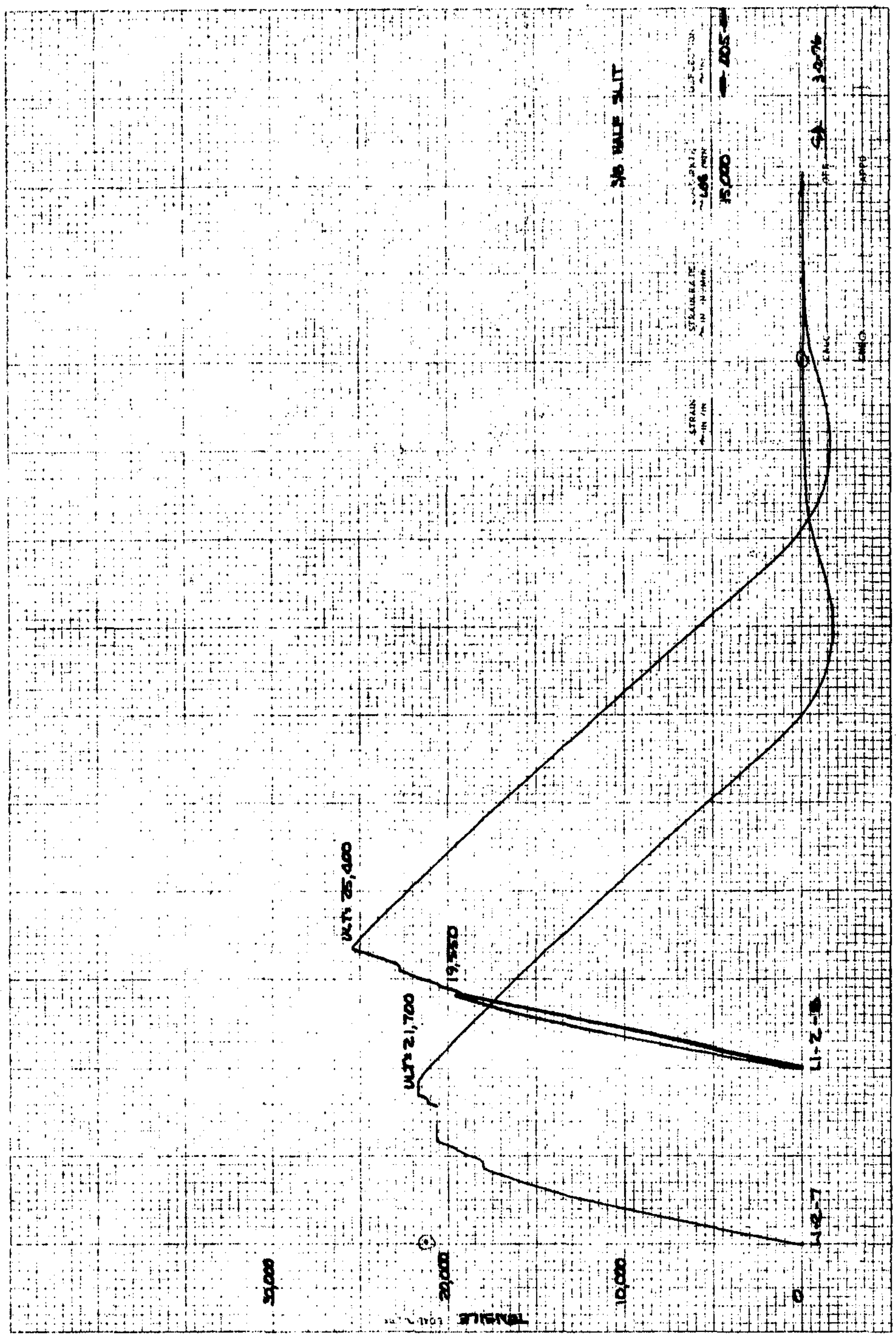

3/8 HALF SLIT
ULT= 21,700
20,000
10,000
0
TENSILE

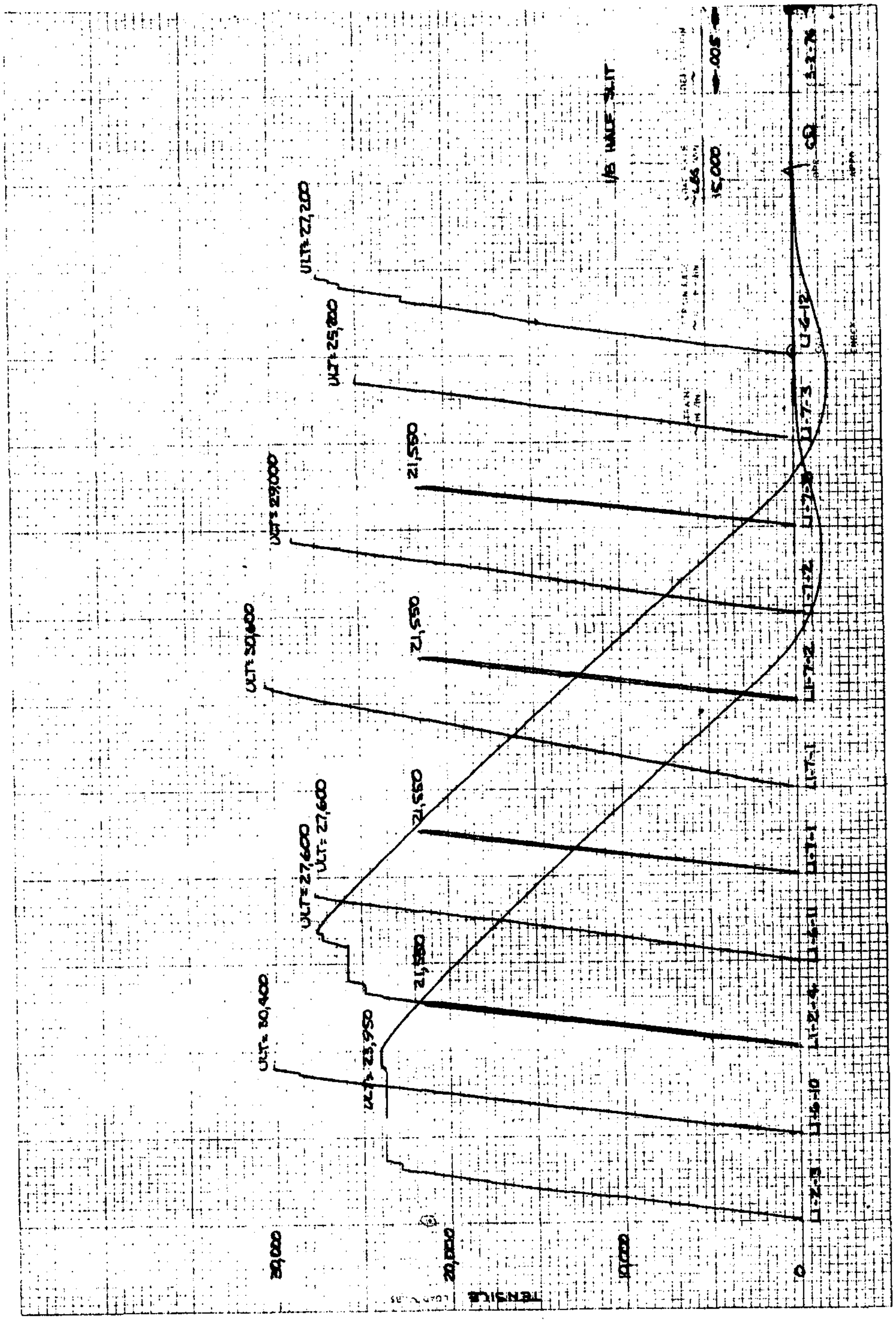

ULT= 30,400
ULT= 23,950
21,580
ULT= 27,600
ULT= 27,600
21,550
ULT= 30,600
21,550
ULT= 29,000
21,550
ULT= 25,800
ULT= 27,200
1/8 HALF SLIT
15,000
.005
30,000
20,000
10,000
0
TENSILE

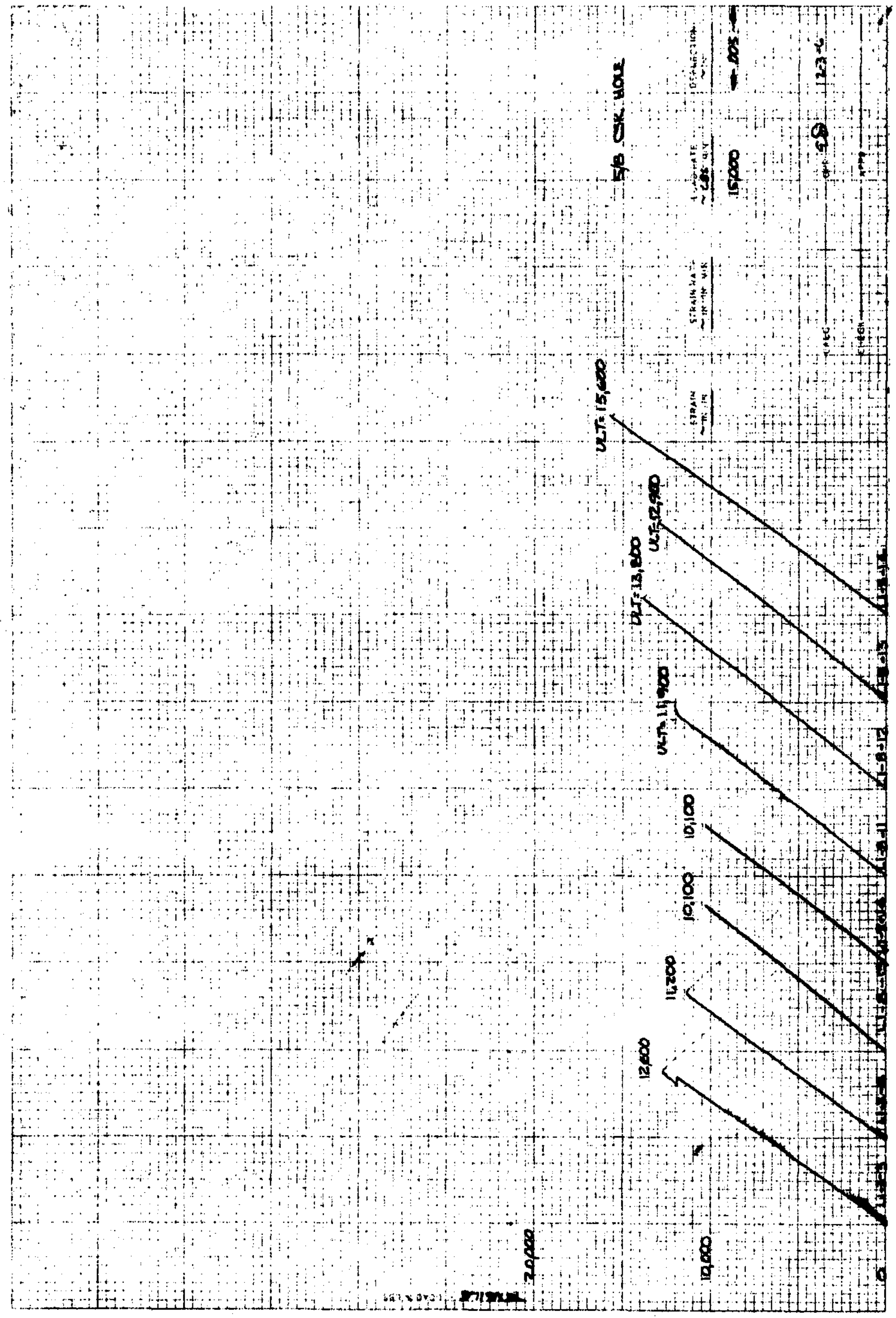
5/8 CSK. HOLE
15,000
.005
ULT= 15,620
ULT= 12,910
ULT= 13,800
ULT= 11,900
10,100
10,100
11,200
12,800
20,000
10,000

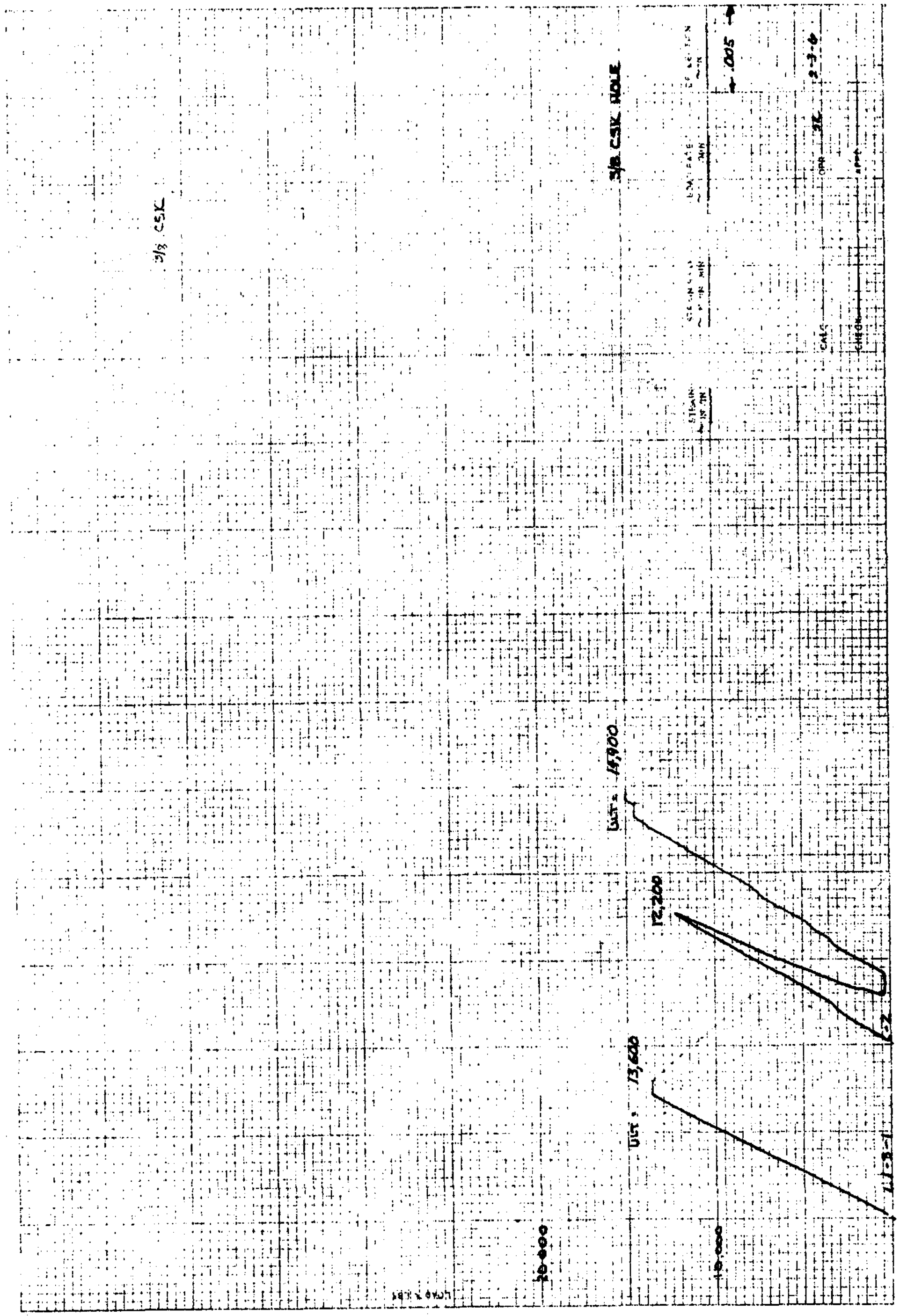
3/8 CSK HOLE
.005
CALC
CHECK
ULT = 13,600
12,200
20,000
10,000

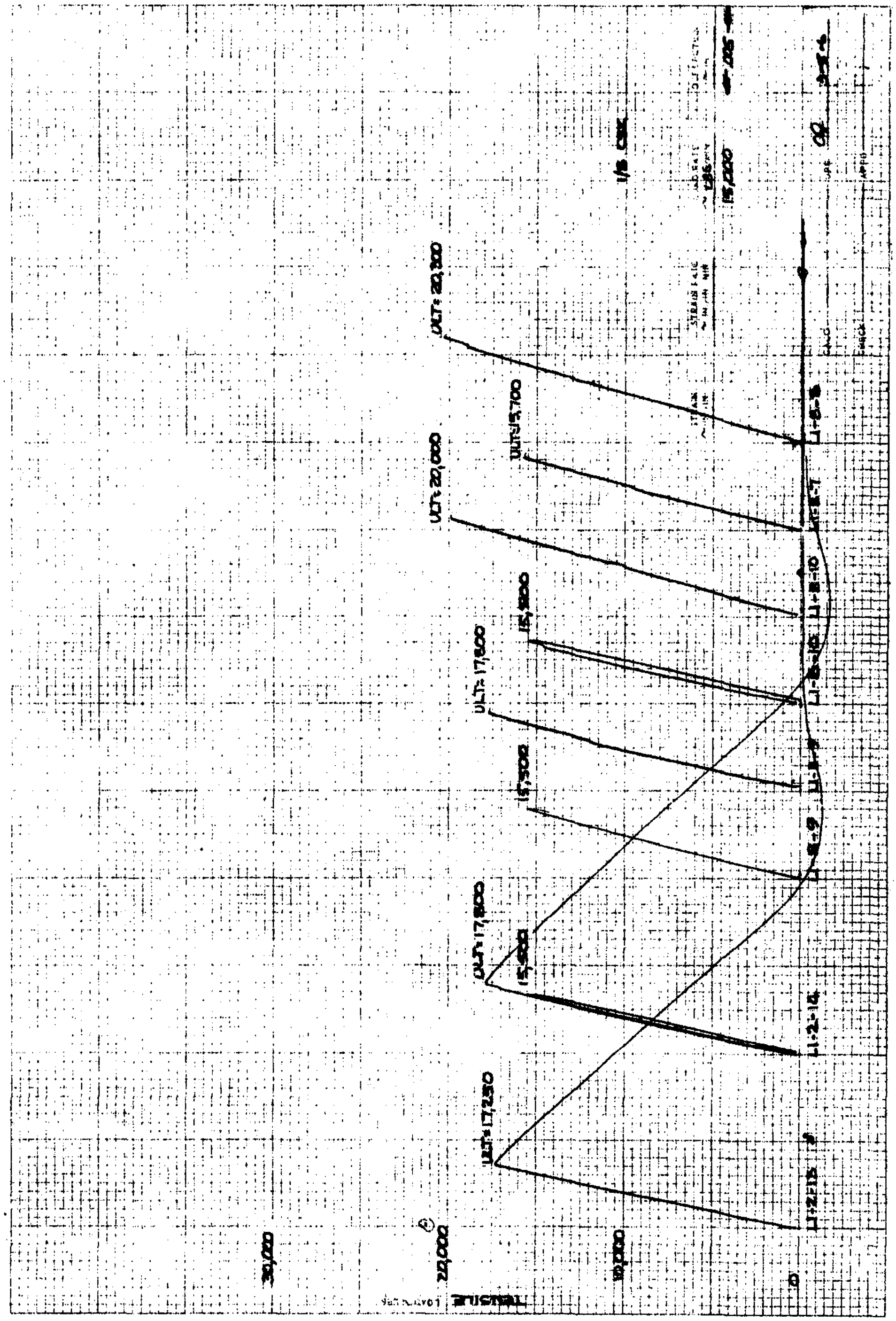
ULT: 22,300
ULT: 20,000
ULT: 17,500
ULT: 17,800
ULT: 17,250
30,000
20,000
10,000
0
1/8 CBC

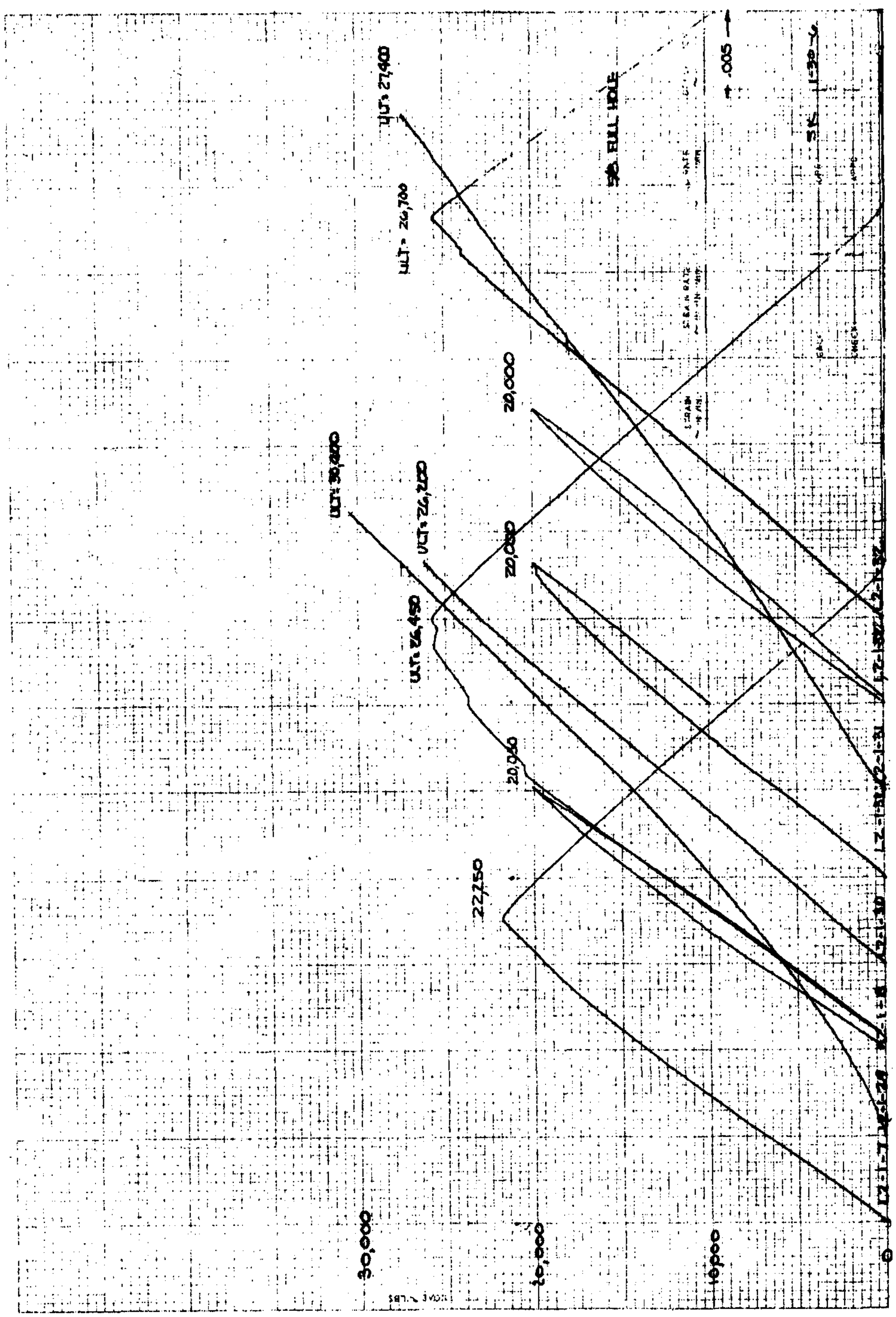

ULT = 27,400
ULT = 26,700
5/8 FULL HOLE
.005
20,000
ULT = 30,800
ULT = 26,200
20,000
ULT = 26,450
20,950
22,250
30,000
20,000
10000
0

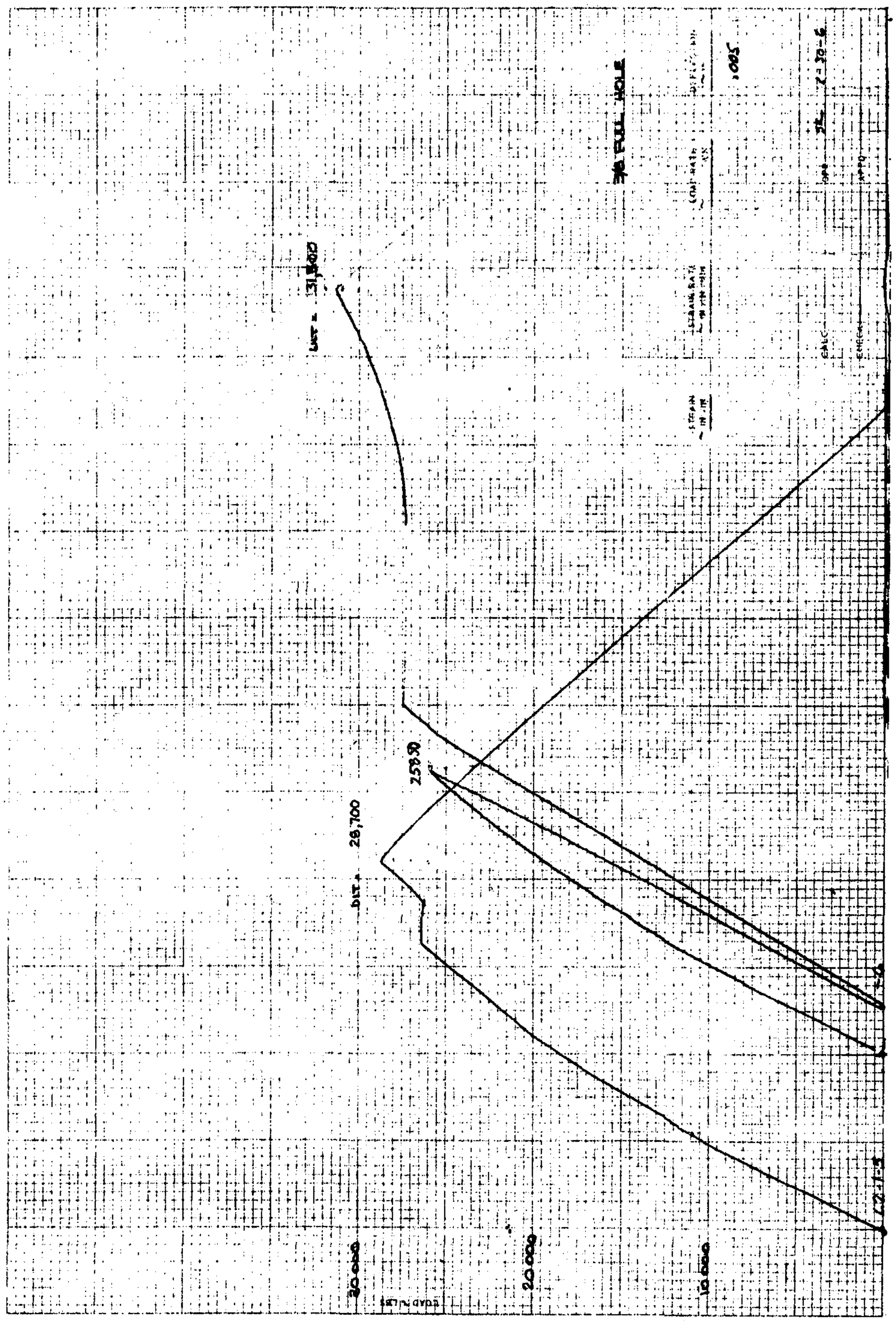

ULT = 31,800
28,700
25,850
30,000
20,000
10,000

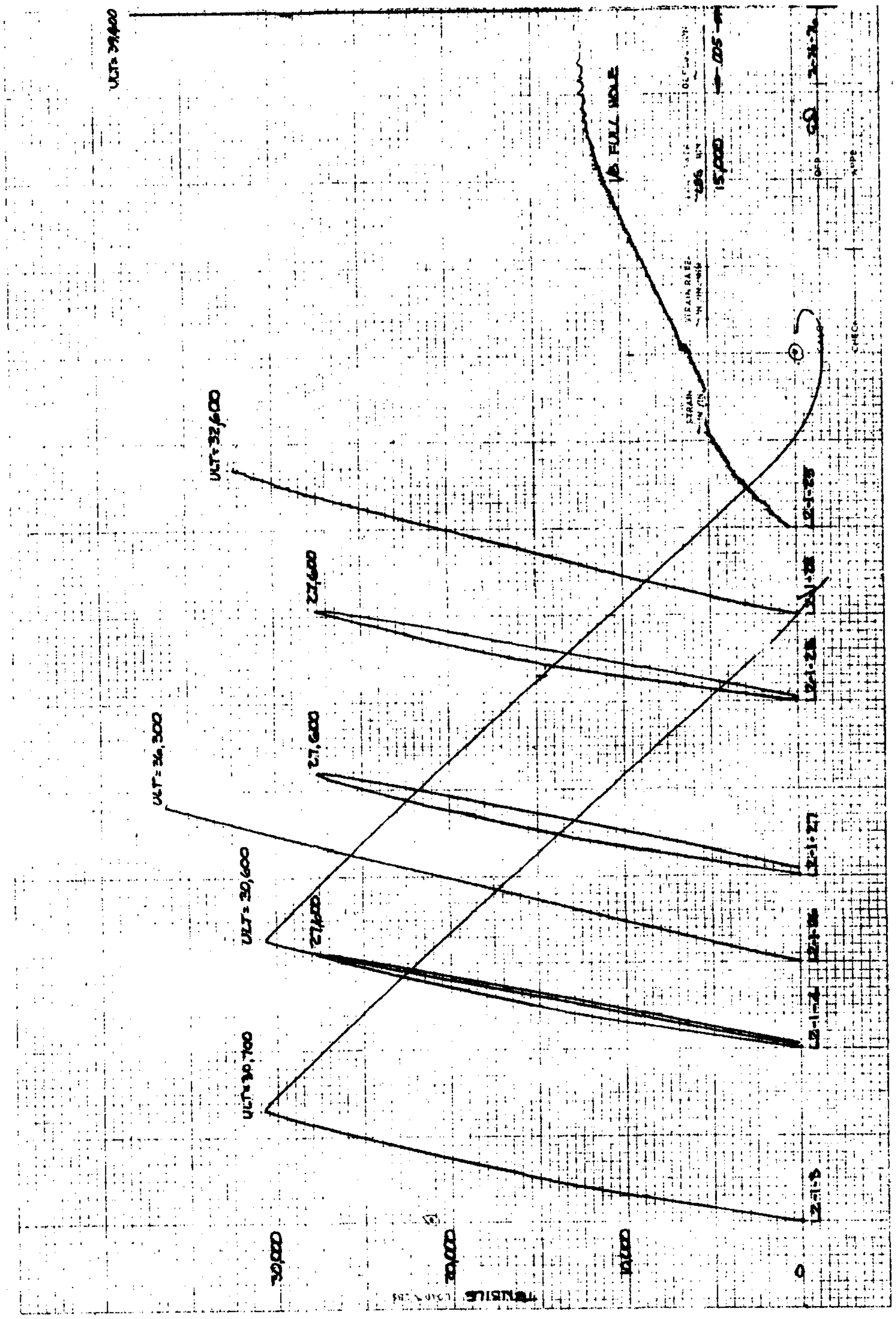
1/8 FULL HOLE
TENSILE
30,000
20,000
10,000
0

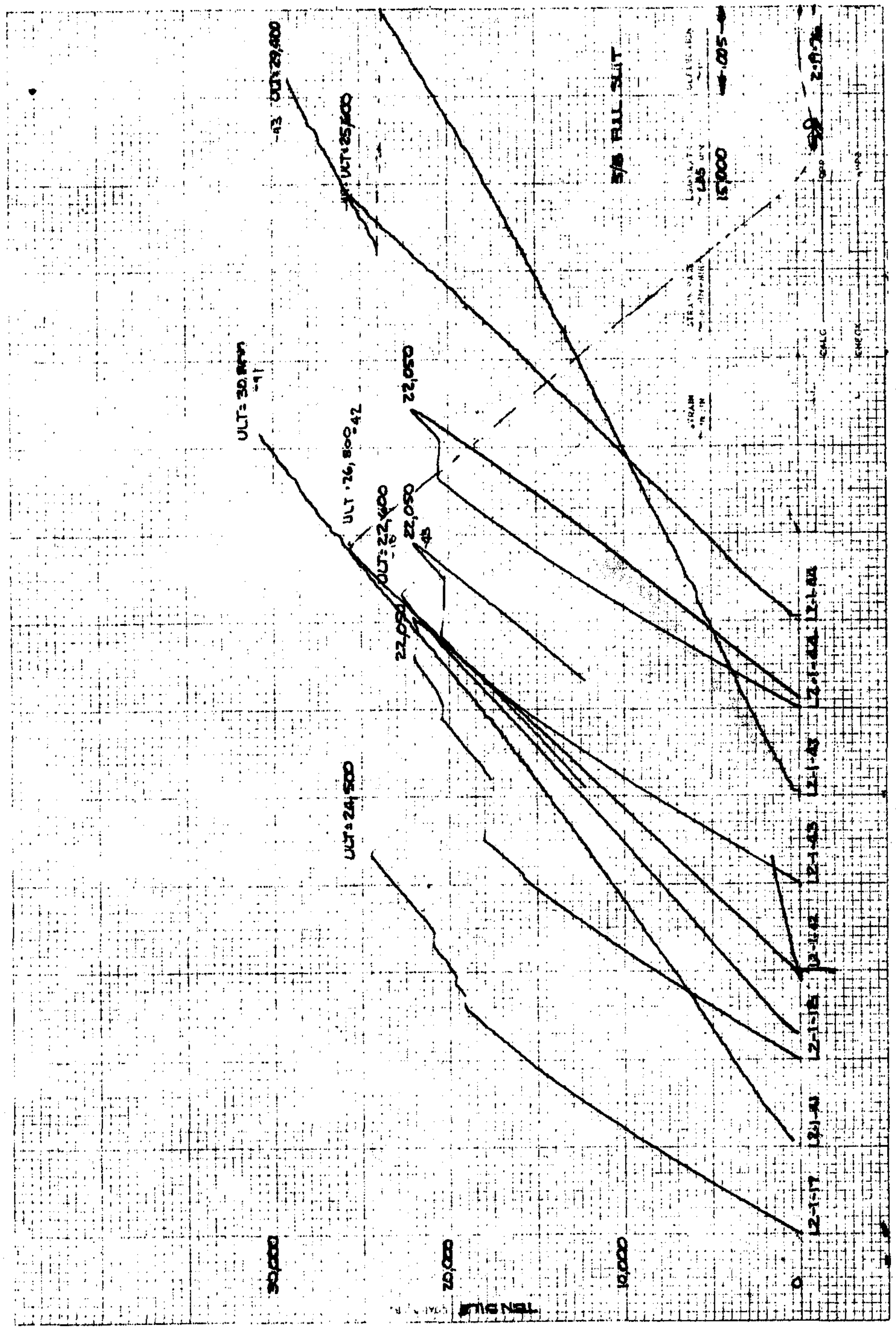

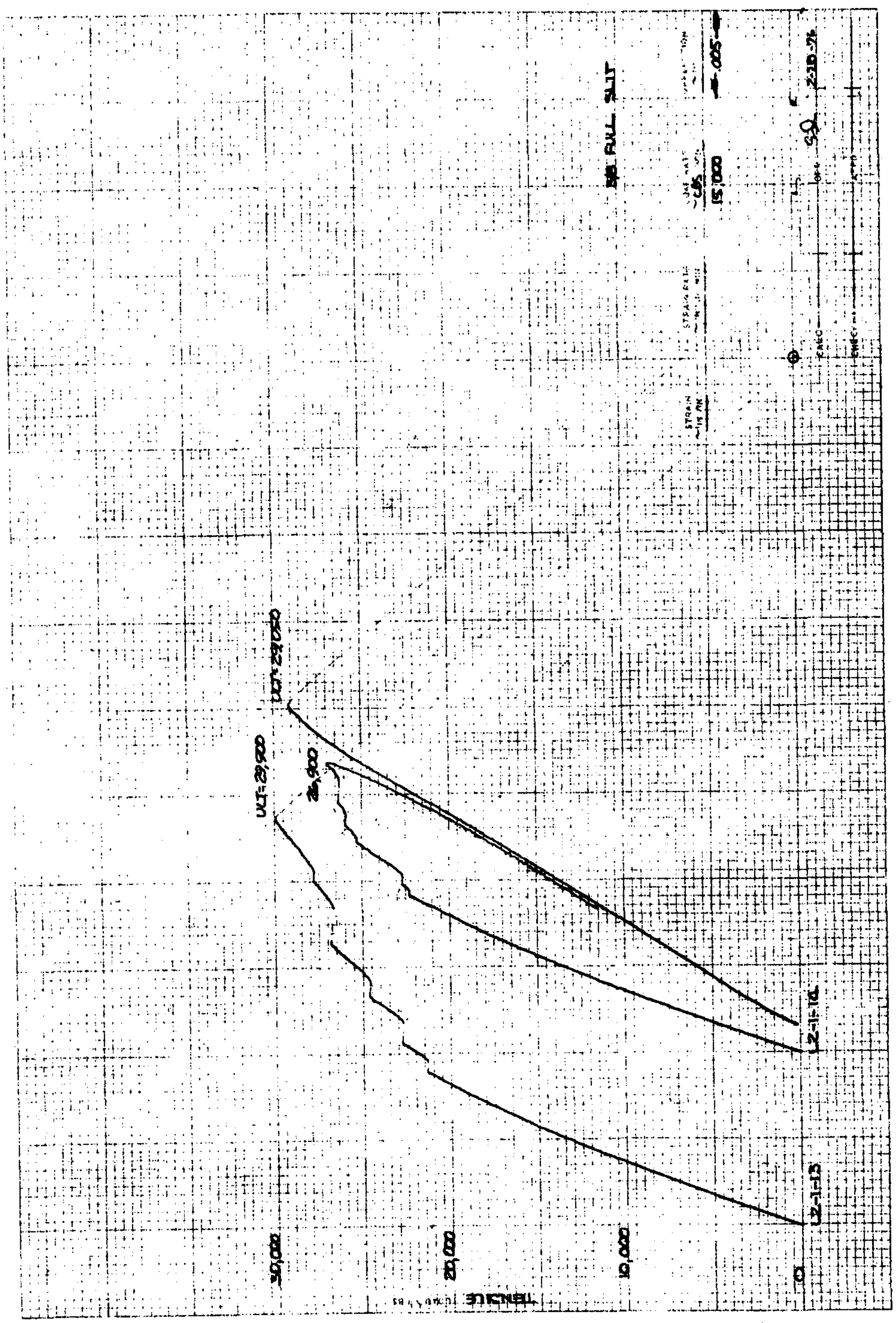

FULL SLIT
15,000
.005
UCT=29,900
UCT=29,050
28,900
30,000
20,000
10,000
0
TENSILE

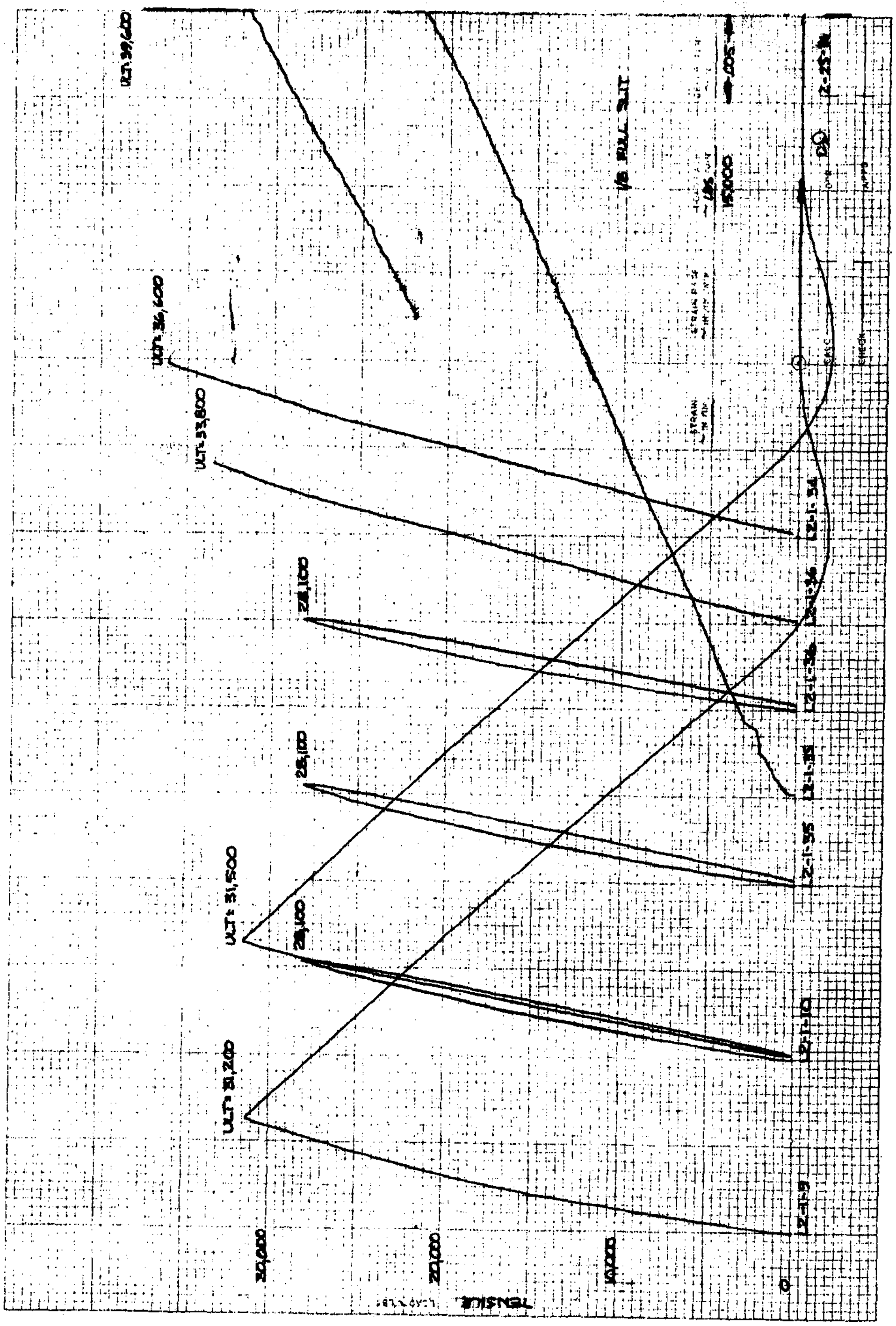
ULT. 31,200
ULT. 31,500
28,100
28,100
28,100
ULT. 33,800
ULT. 36,600
ULT. 39,600
30,000
20,000
10,000
0
TENSILE

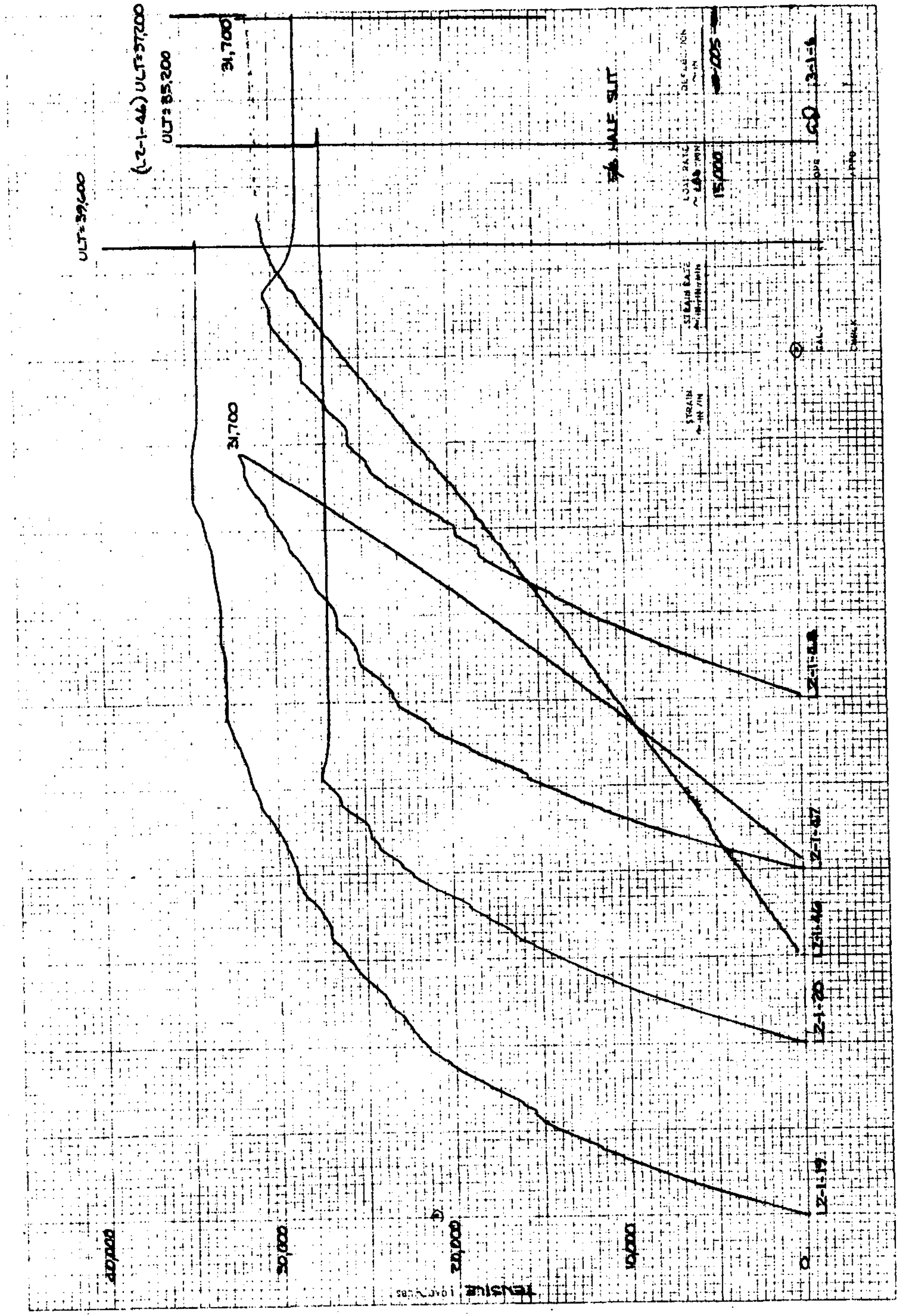
ULT=39,600
(12-1-46) ULT=37,200
ULT=35,200
31,700
34,700
HALF SLIT
15,000
12-1-19
12-1-20
12-1-46
12-1-47
40,000
30,000
20,000
10,000
0
TENSILE

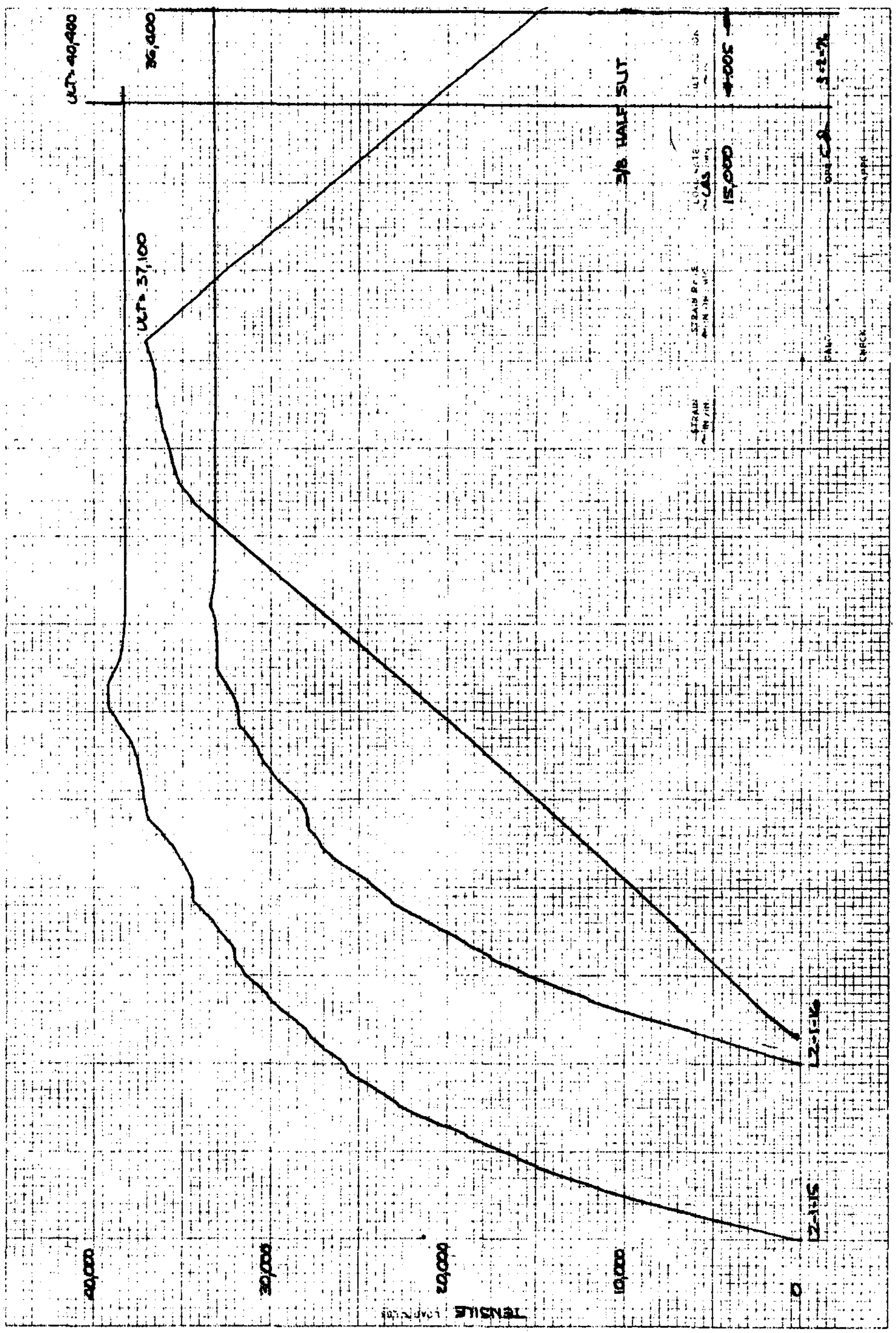

ULT= 37,100
3/8 HALF SLIT
15,000
12-1-16
12-1-15
10,000
0
TENSILE

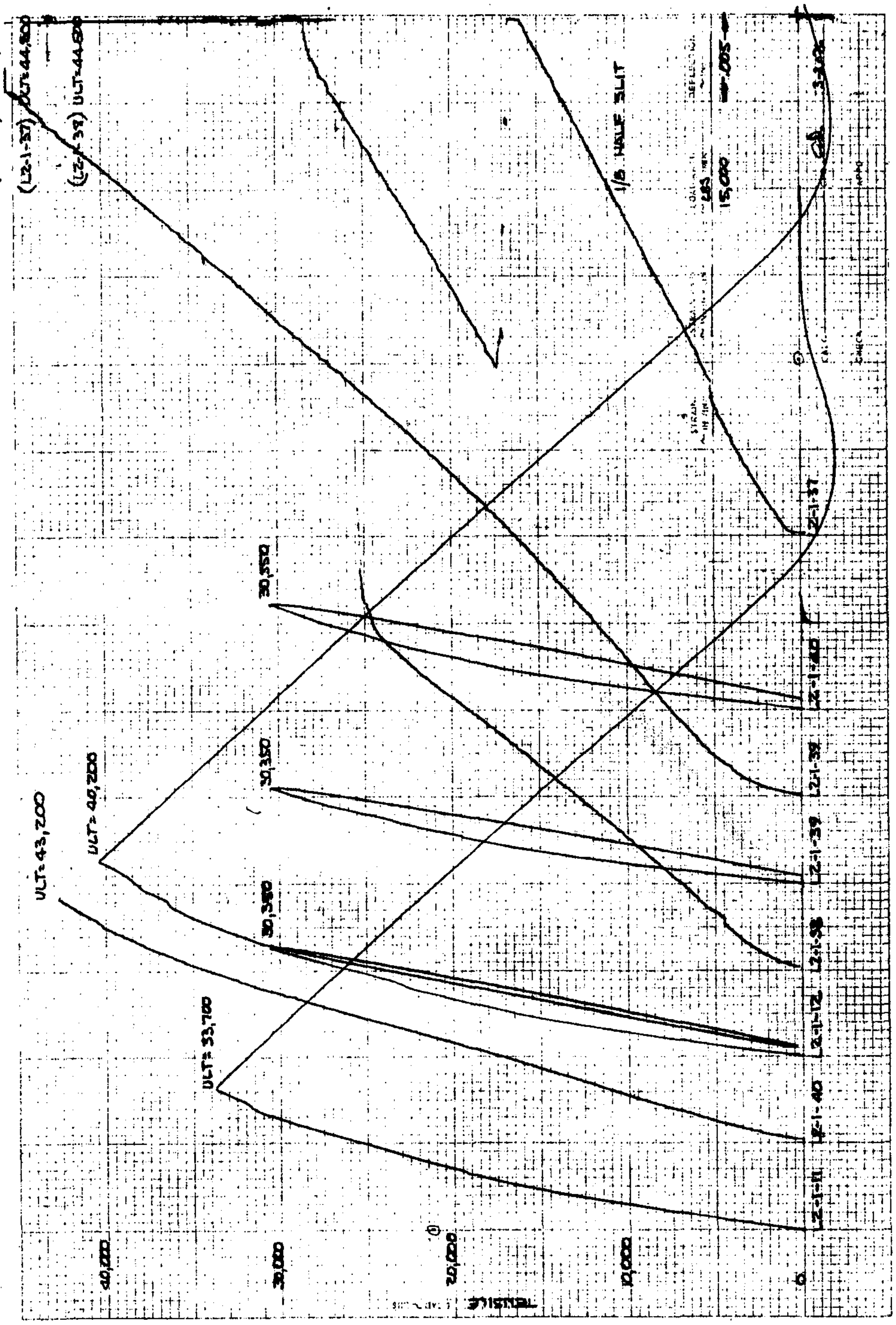

(L2-1-39) ULT=47,100
(L2-1-37) ULT=44,800
(L2-1-38) ULT=44,600
ULT= 43,200
ULT= 40,200
ULT= 33,700
30,380
30,350
1/8 HALF SLIT
15,000
40,000
30,000
20,000
10,000
0
TENSILE

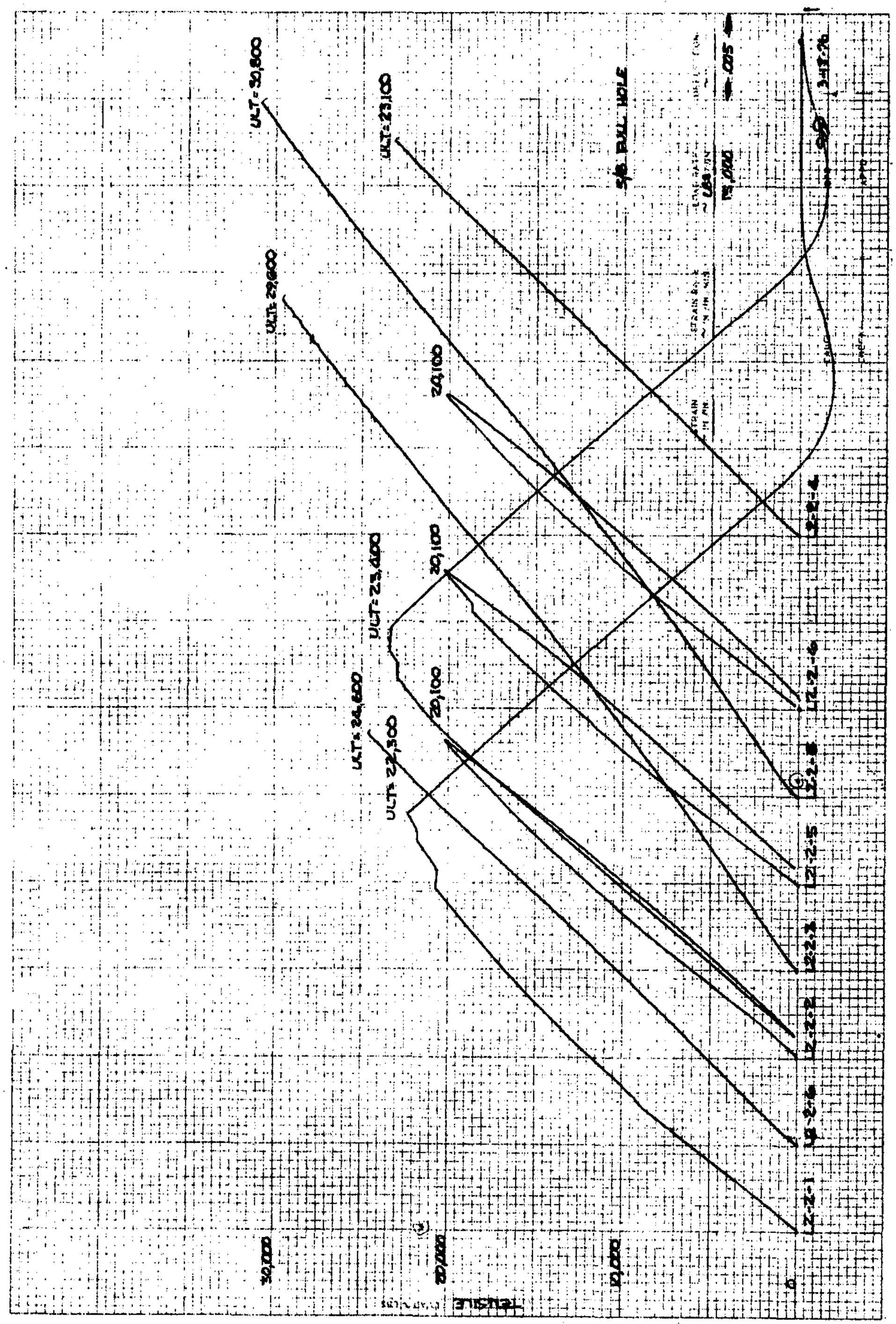

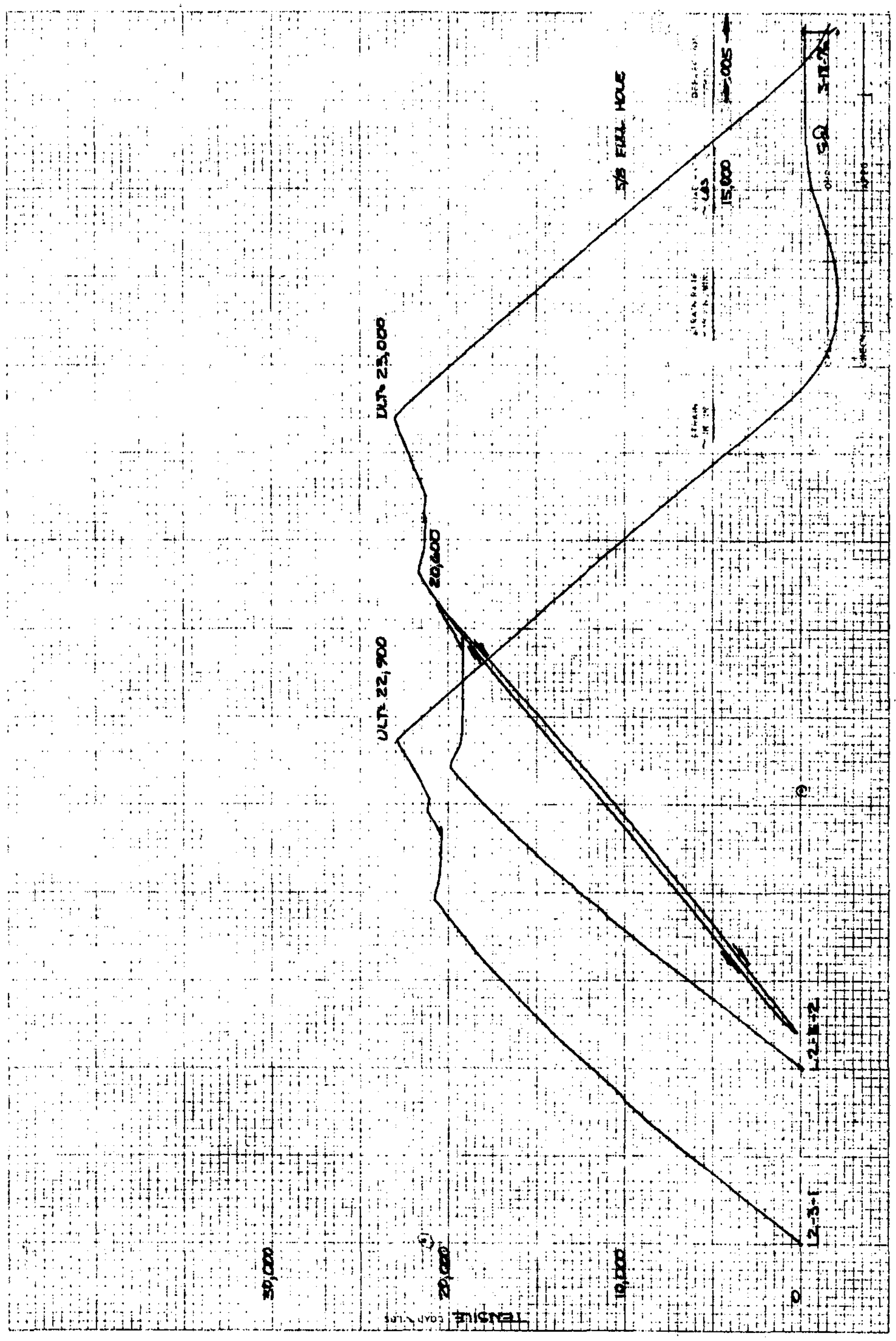
ULT. 23,000
20,600
ULT. 22,900
5/8 FULL HOLE
15,000
30,000
20,000
10,000
0
TENSILE

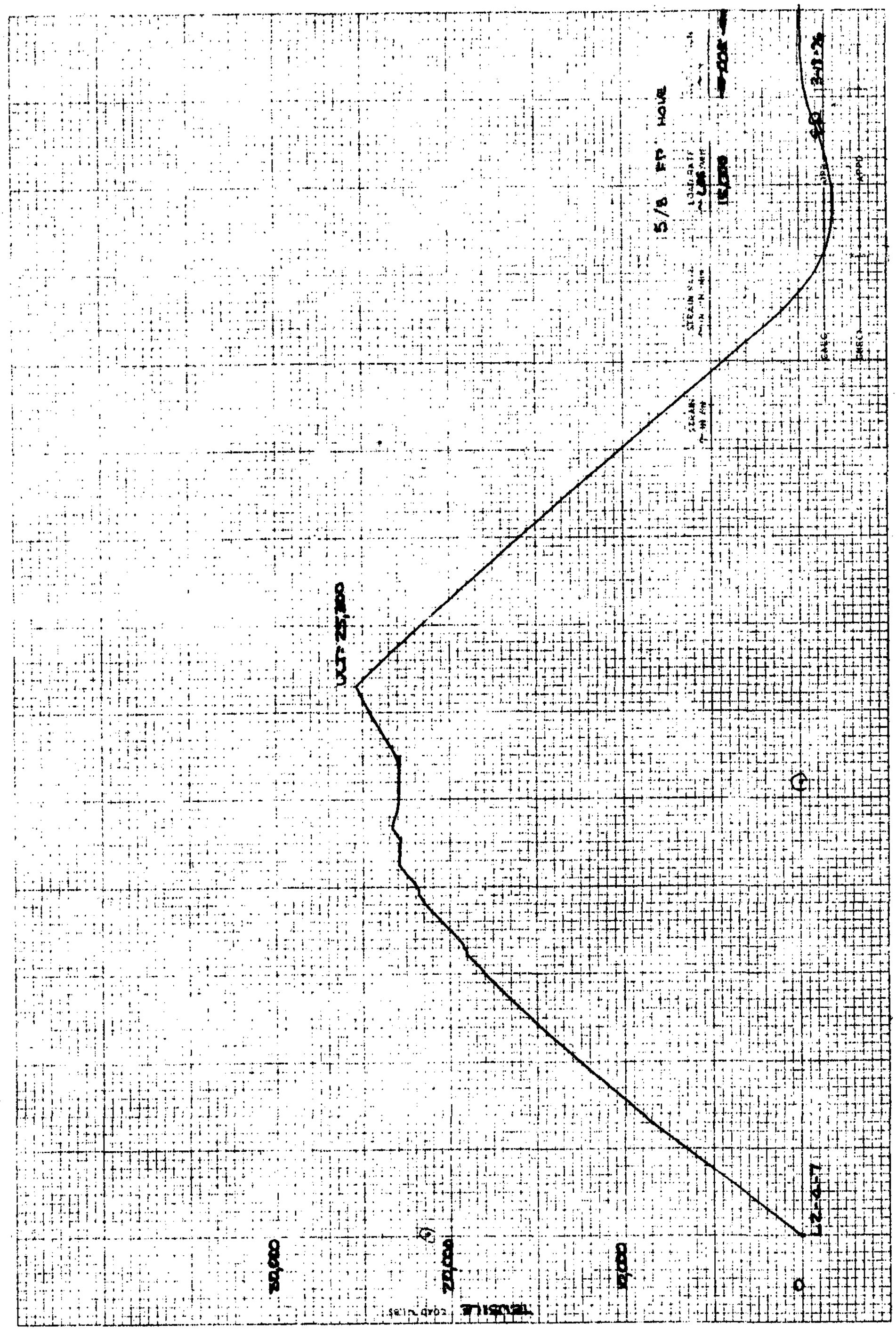
30,000
20,000
10,000
0

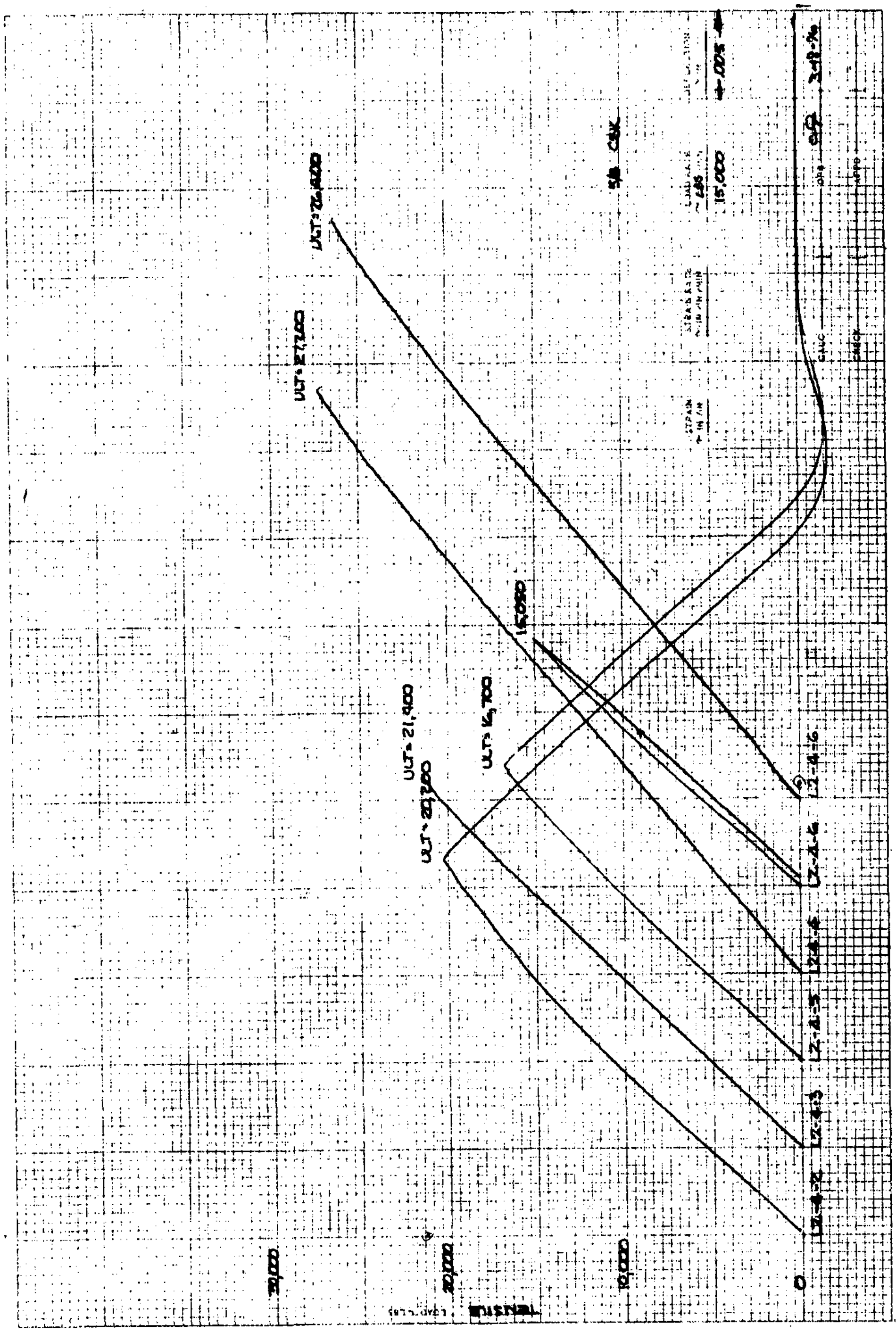
ULT = 21,900
ULT = 16,700
15,000
10,000
20,000
0

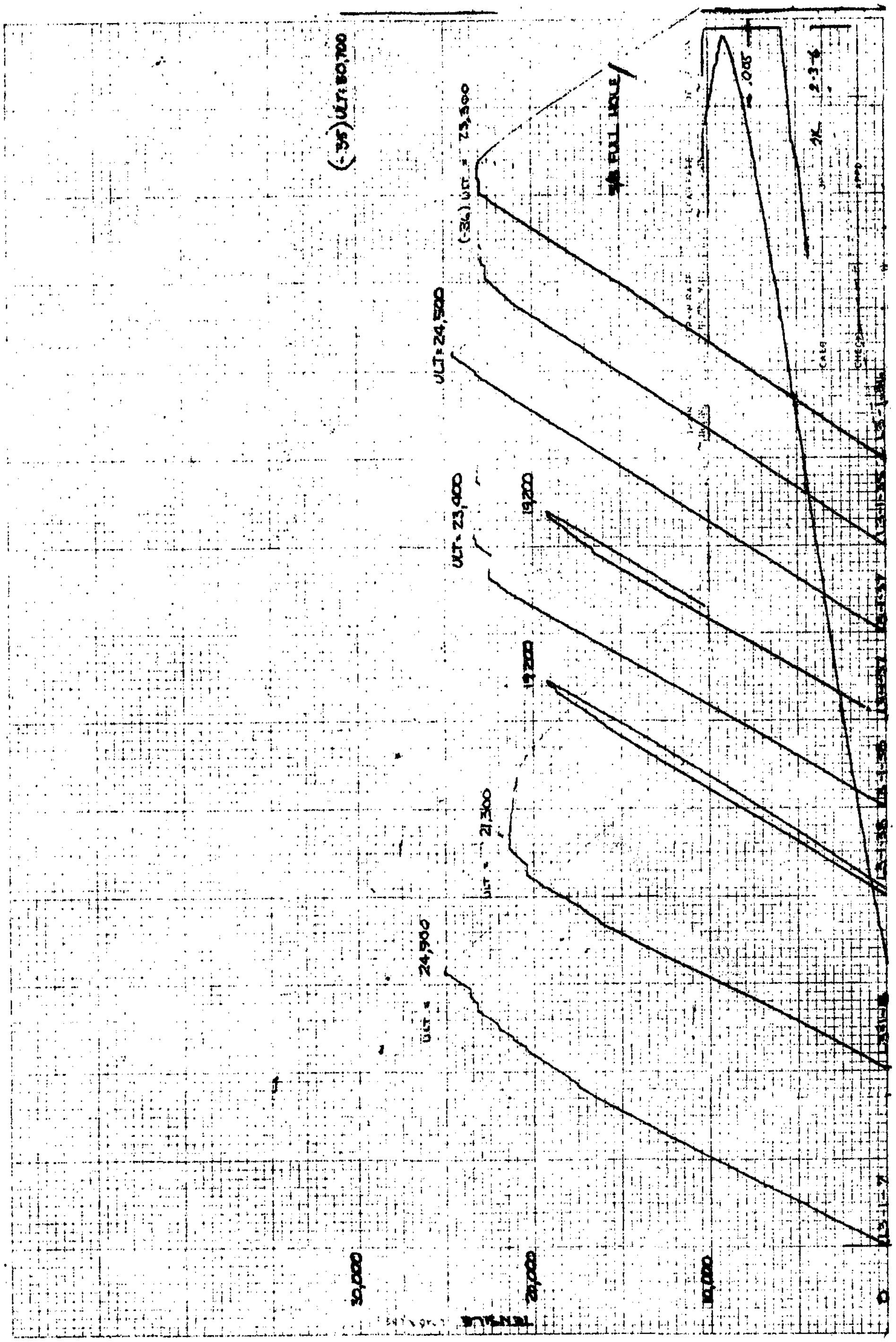
(-35) ULT = 30,700
(-36) ULT = 23,500
FULL HOLE
ULT = 24,500
ULT = 23,400
19,200
19,200
ULT = 21,300
ULT = 24,500
30,000
20,000
10,000
0
TENSILE

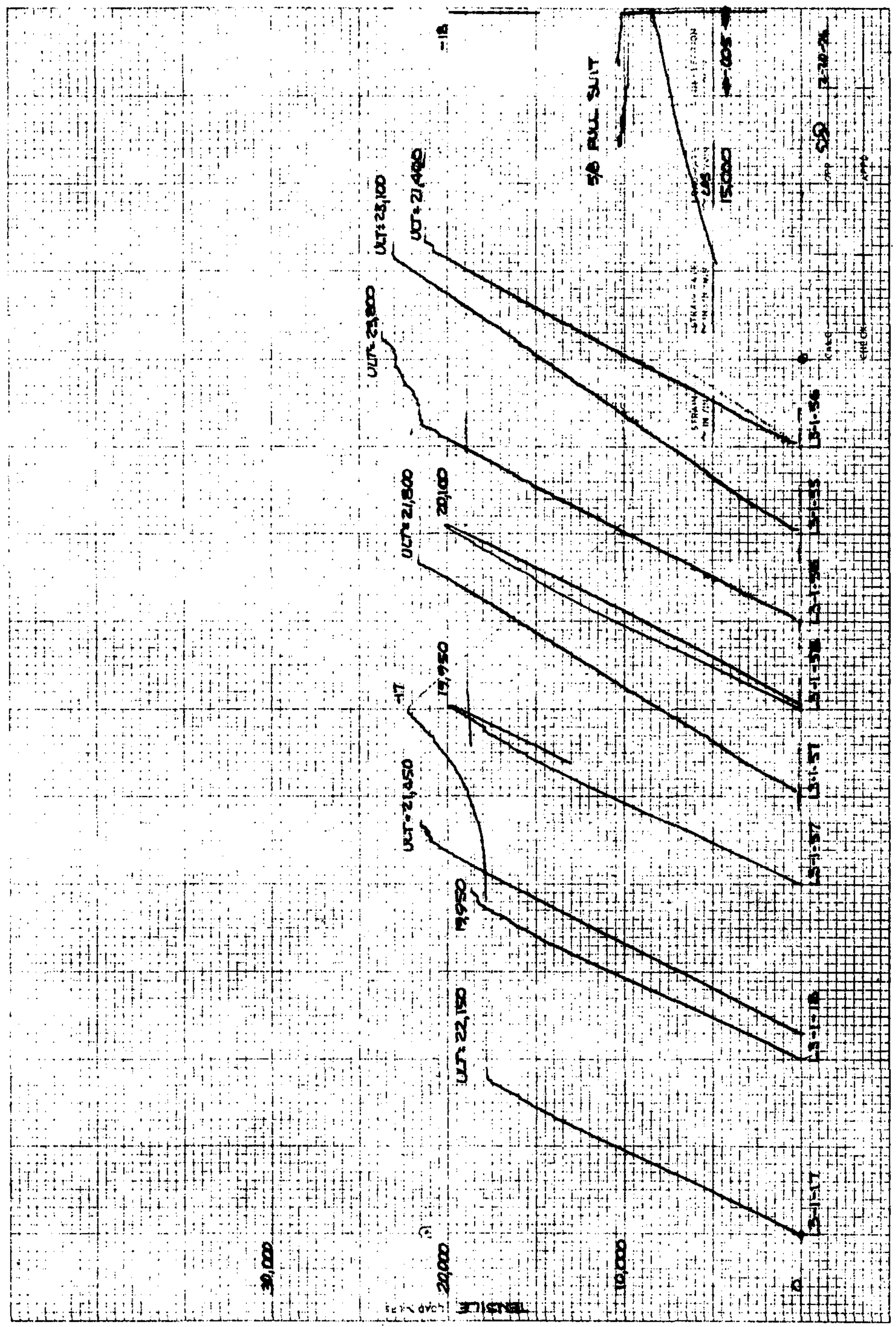
ULT = 23,100
ULT = 21,400
ULT = 23,800
ULT = 21,800
20,100
19,950
ULT = 21,850
19,950
ULT = 22,150
5/8 FULL SLIT
TENSILE
30,000
20,000
10,000
0

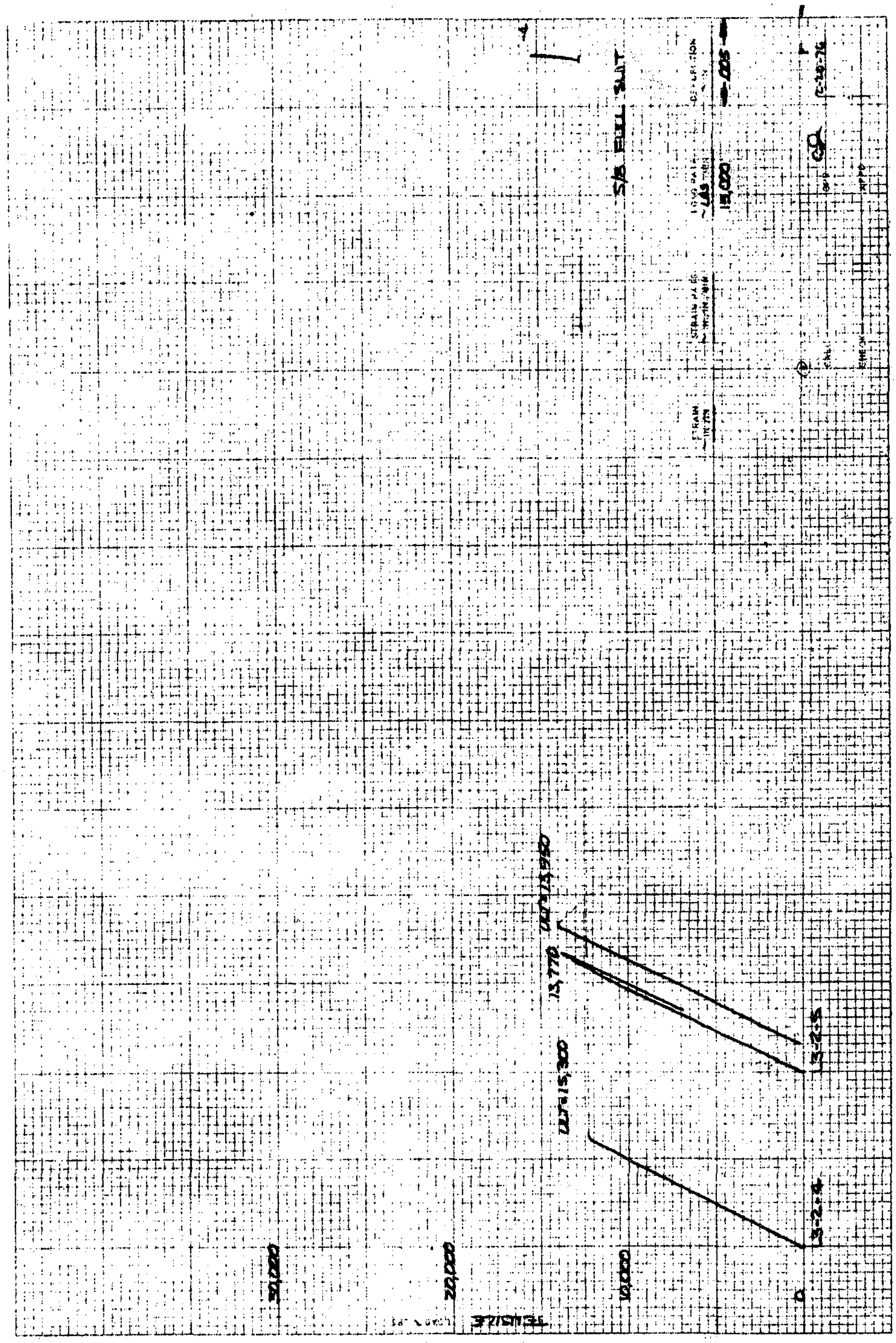

30,000
20,000
10,000
0
ULT=15,300
13,770
ULT=13,950
3-2-4
3-2-5

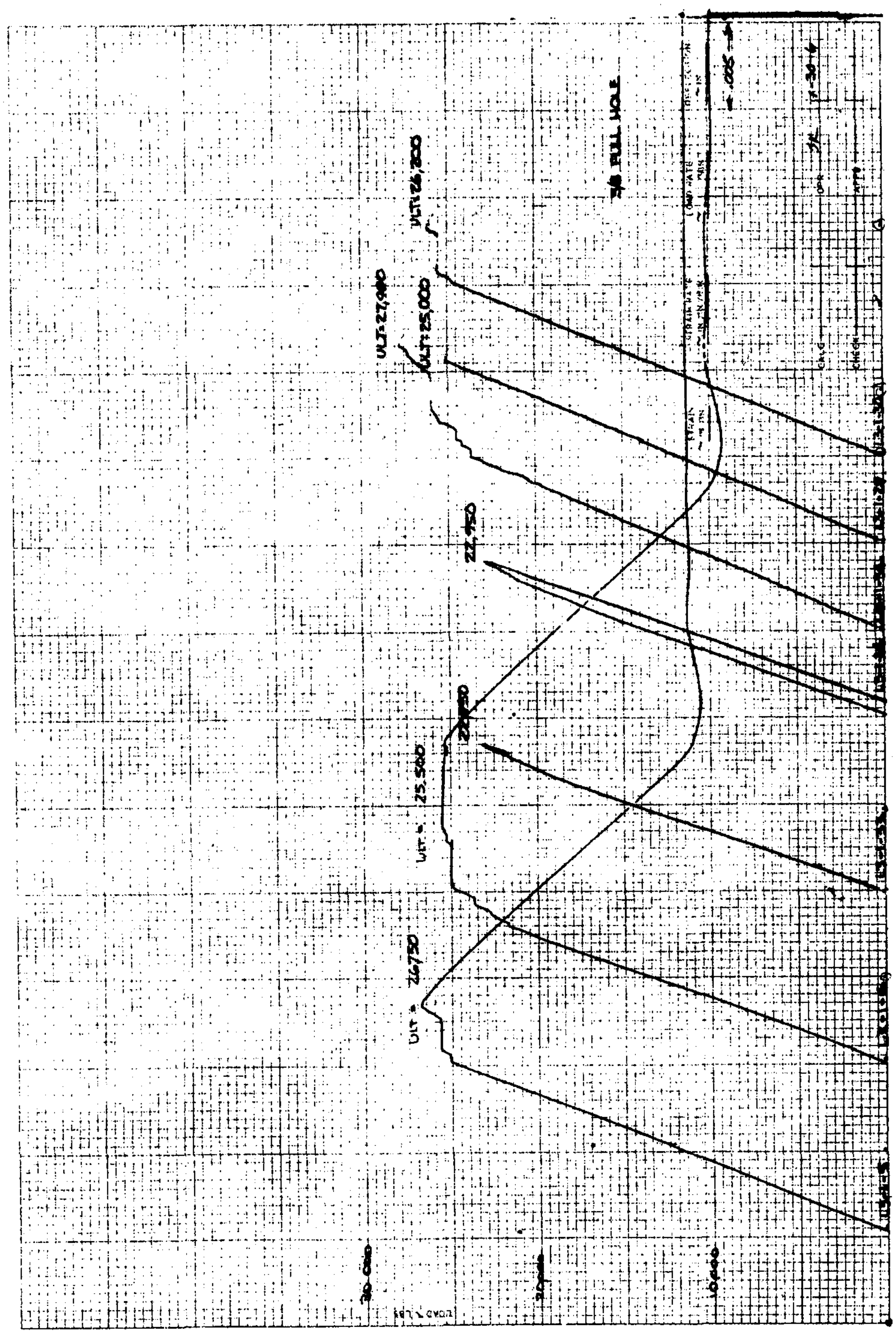

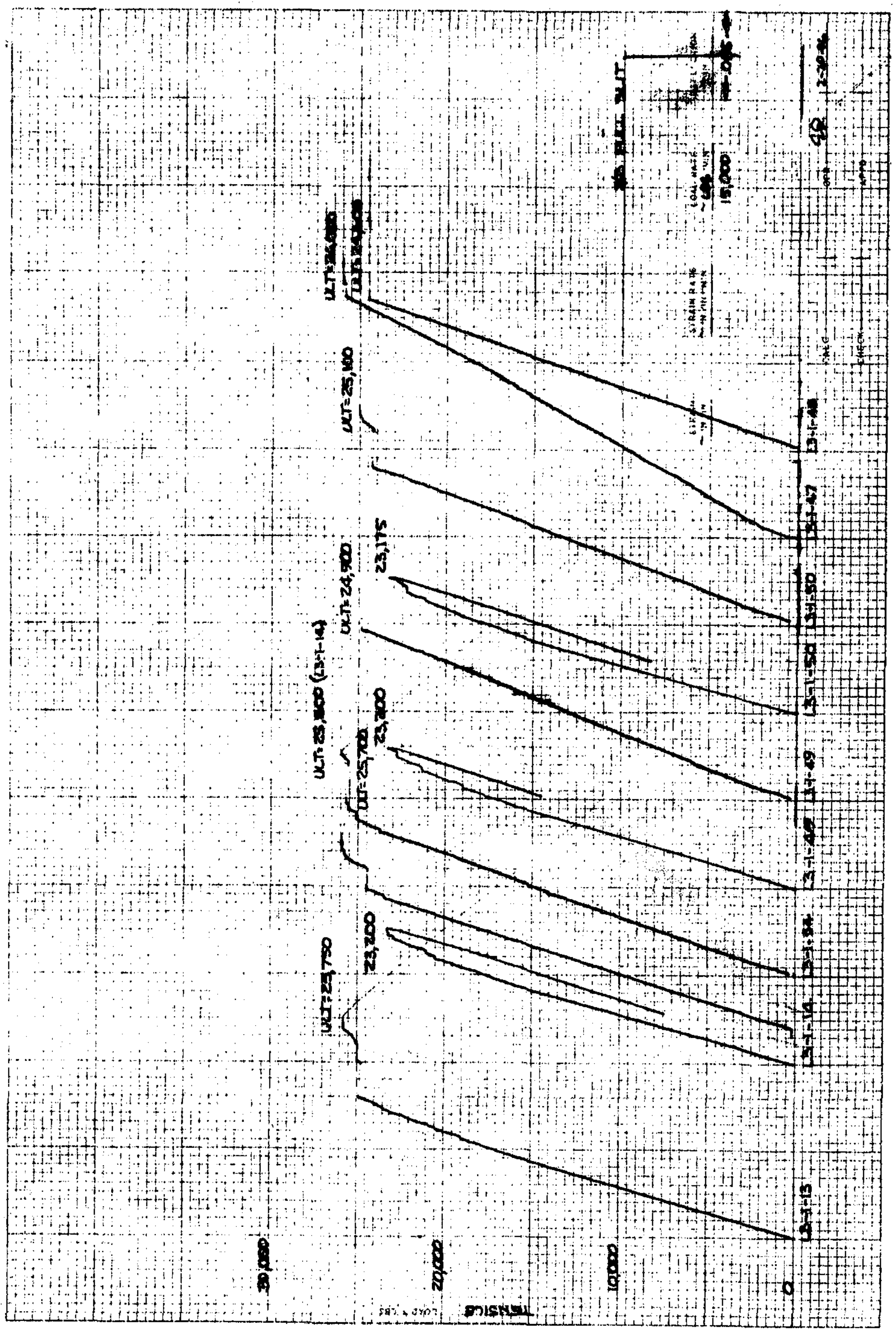
ULT=25,750
23,200
ULT=25,800 (L3-1-14)
ULT=25,700
23,700
ULT=24,900
23,175
ULT=25,100
30,000
20,000
10,000
0
TENSILE
L3-1-15
L3-1-14
L3-1-54
L3-1-49
L3-1-50
L3-1-47
L3-1-48
15,000

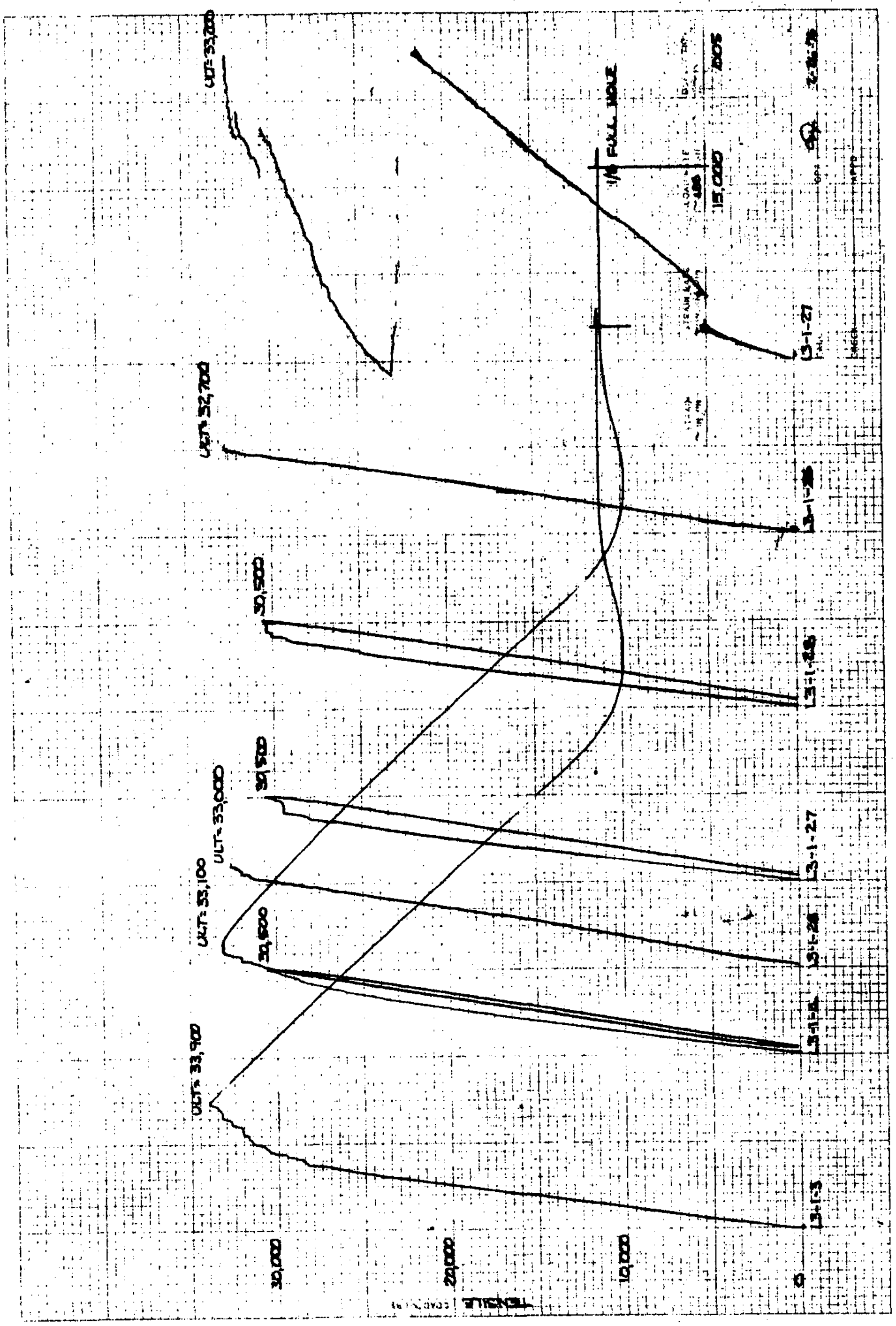

ULT= 33,900
ULT= 33,100
ULT= 33,000
30,800
30,500
30,500
ULT= 32,700
ULT= 33,200
L3-1-27
L3-1-27
L3-1-3
1/4 FULL WAVE
15,000
30,000
20,000
10,000
0
TENSILE

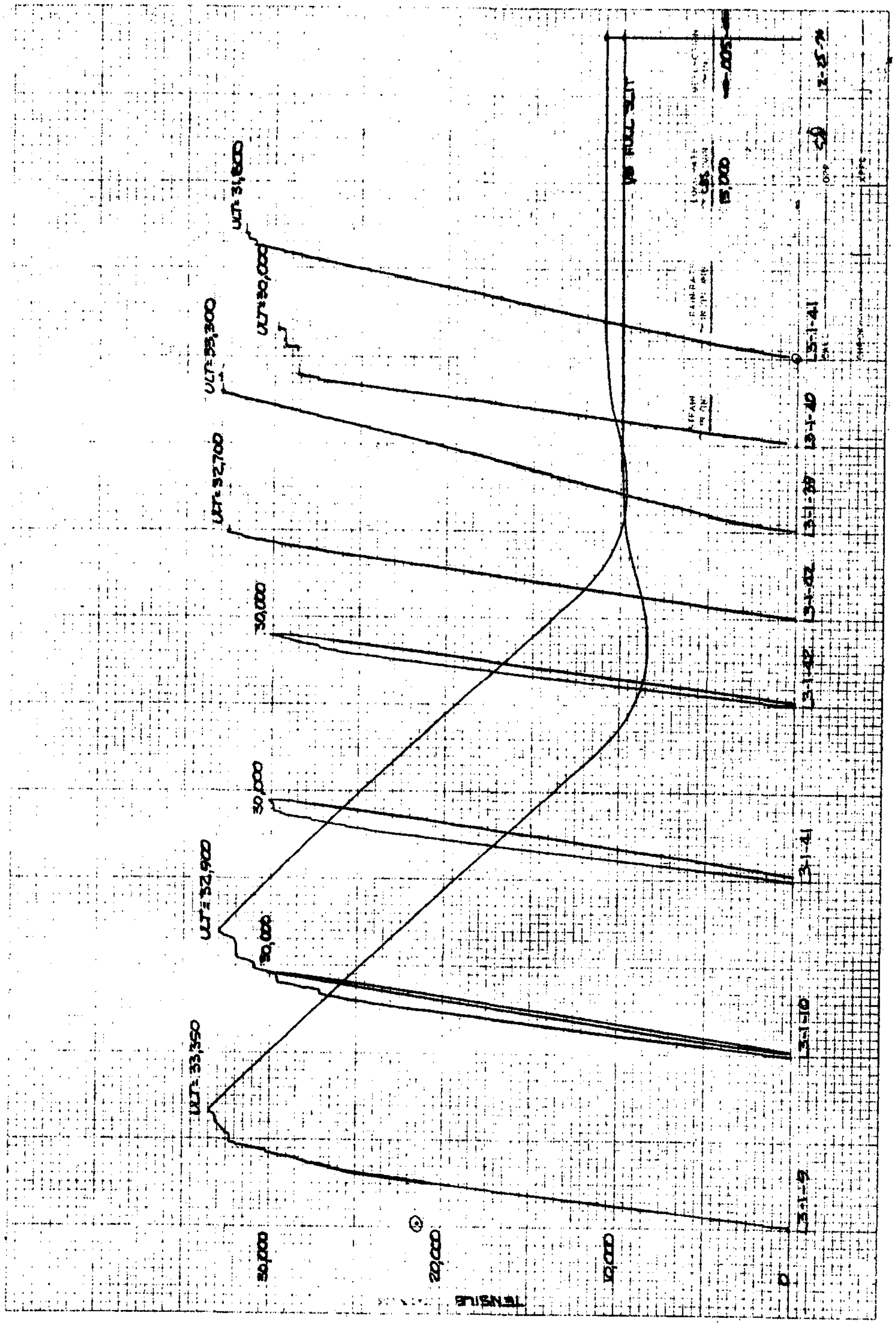
ULT=33,350
ULT=32,900
30,000
30,000
30,000
ULT=32,700
ULT=33,300
ULT=30,000
ULT=31,800
30,000
20,000
10,000
0
TENSILE

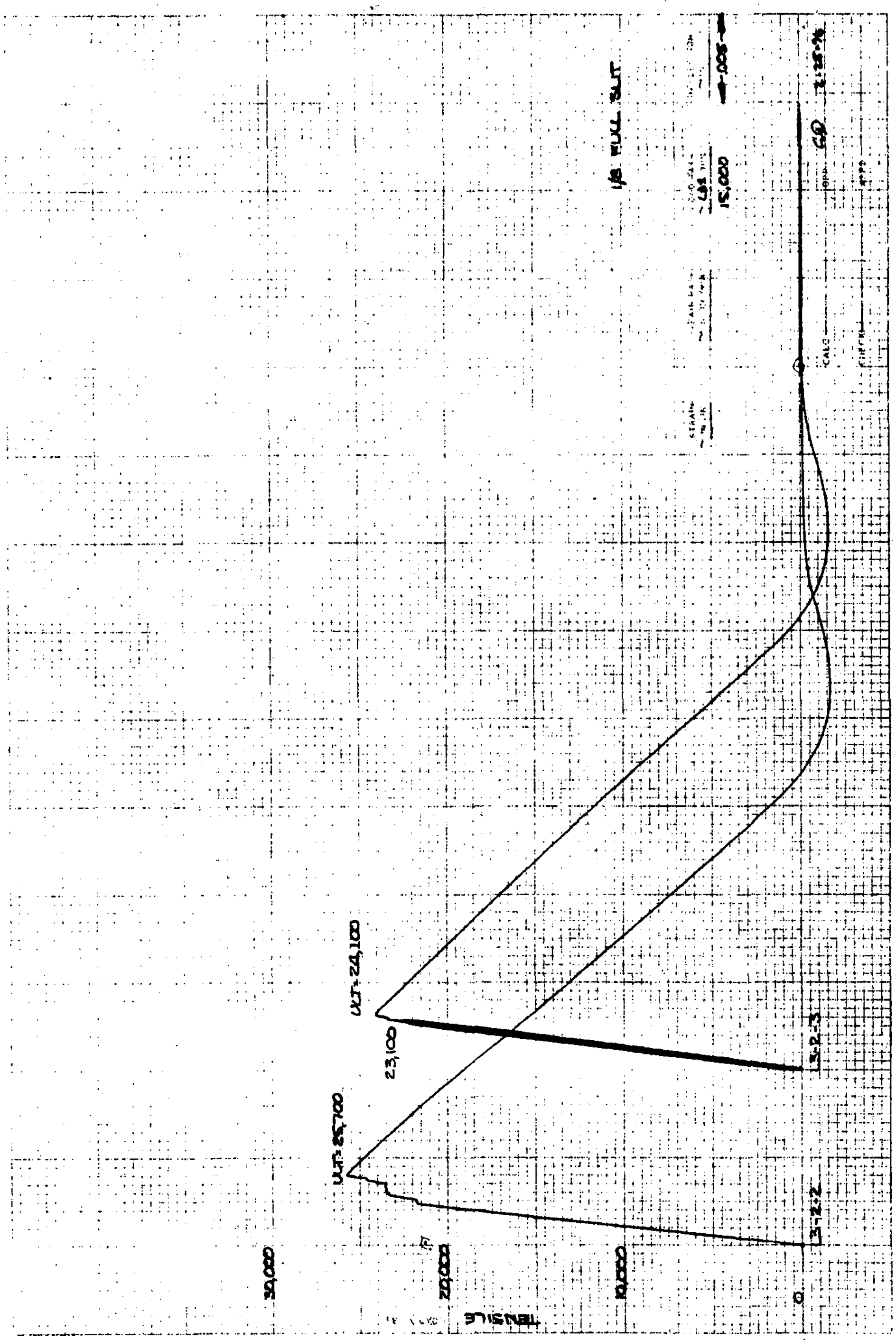
ULT=24,100
23,100
3-2-2
3-2-3
1/8 FULL SLIT
15,000
30,000
20,000
10,000
0
TENSILE

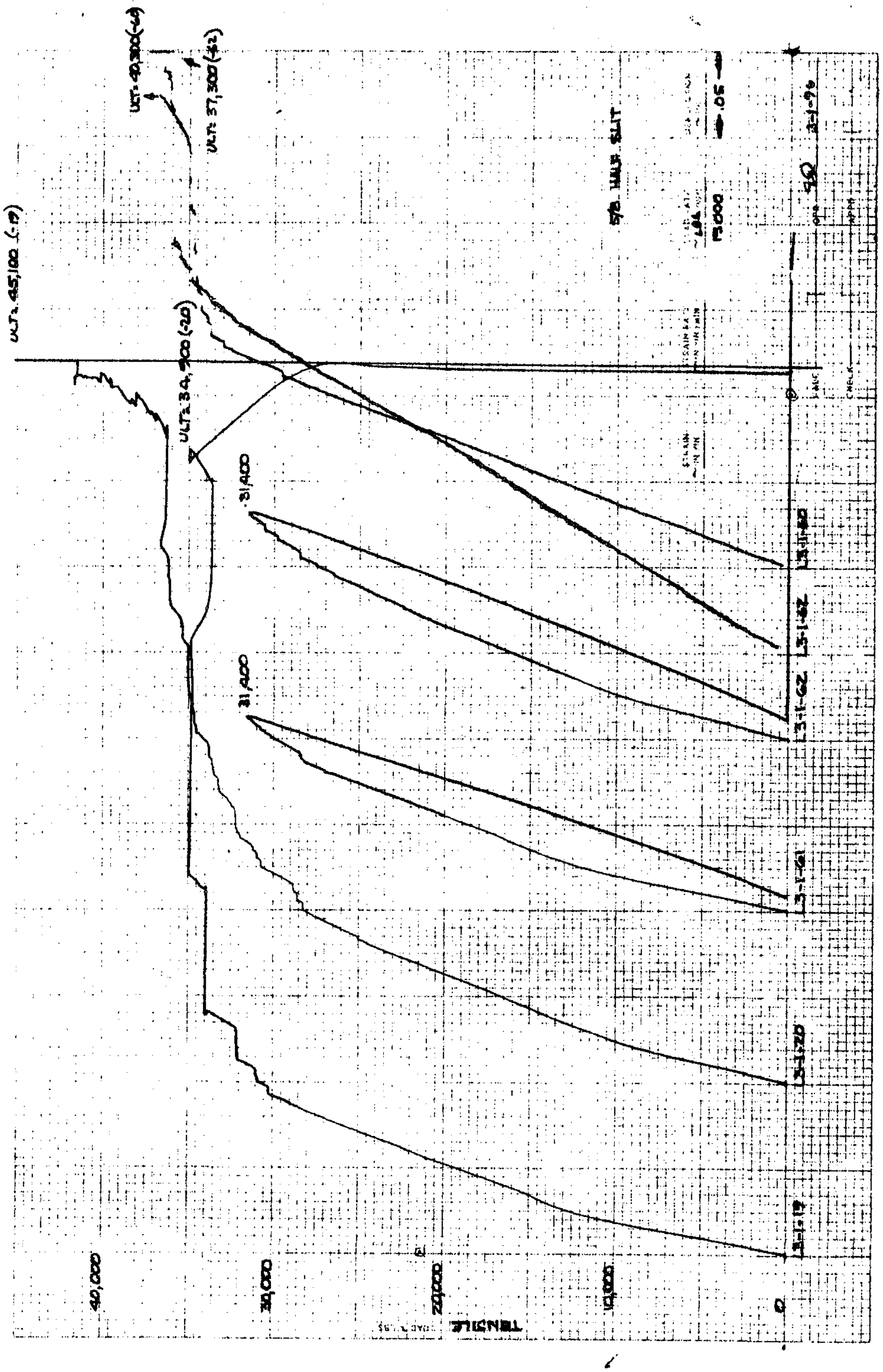
ULT: 45,100 (-19)
ULT: 34,900 (-20)
ULT: 40,300 (-64)
ULT: 37,300 (-62)
31,400
31,400
5/8 HALF SLIT
13000
.05
L3-1-19
L3-1-20
L3-1-21
L3-1-62
L3-1-62
L3-1-60
40,000
30,000
20,000
10,000
0
TENSILE

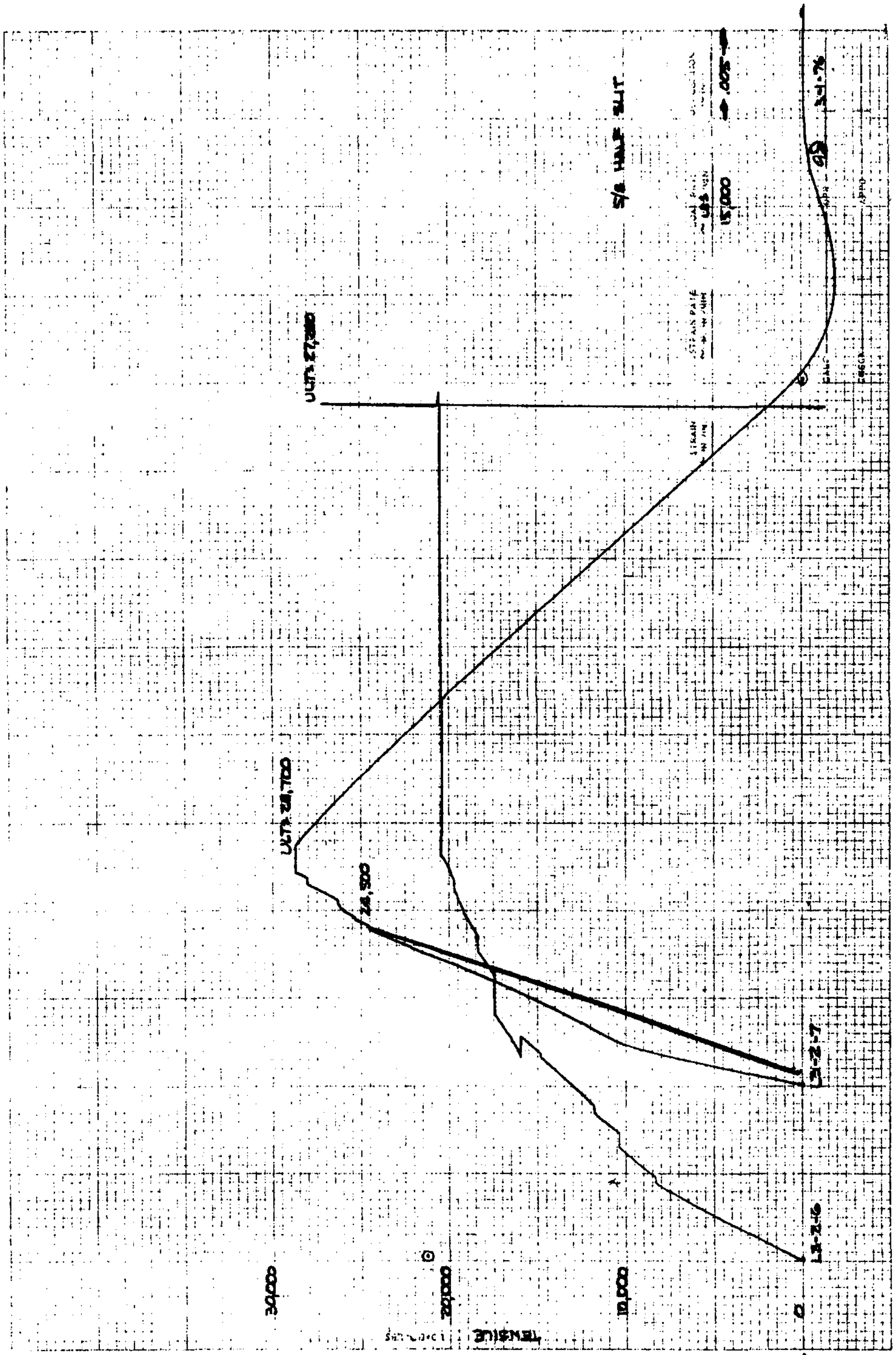
5/8 HALF SLIT
ULT. 28,700
24,500
30,000
20,000
10,000
0
TENSILE

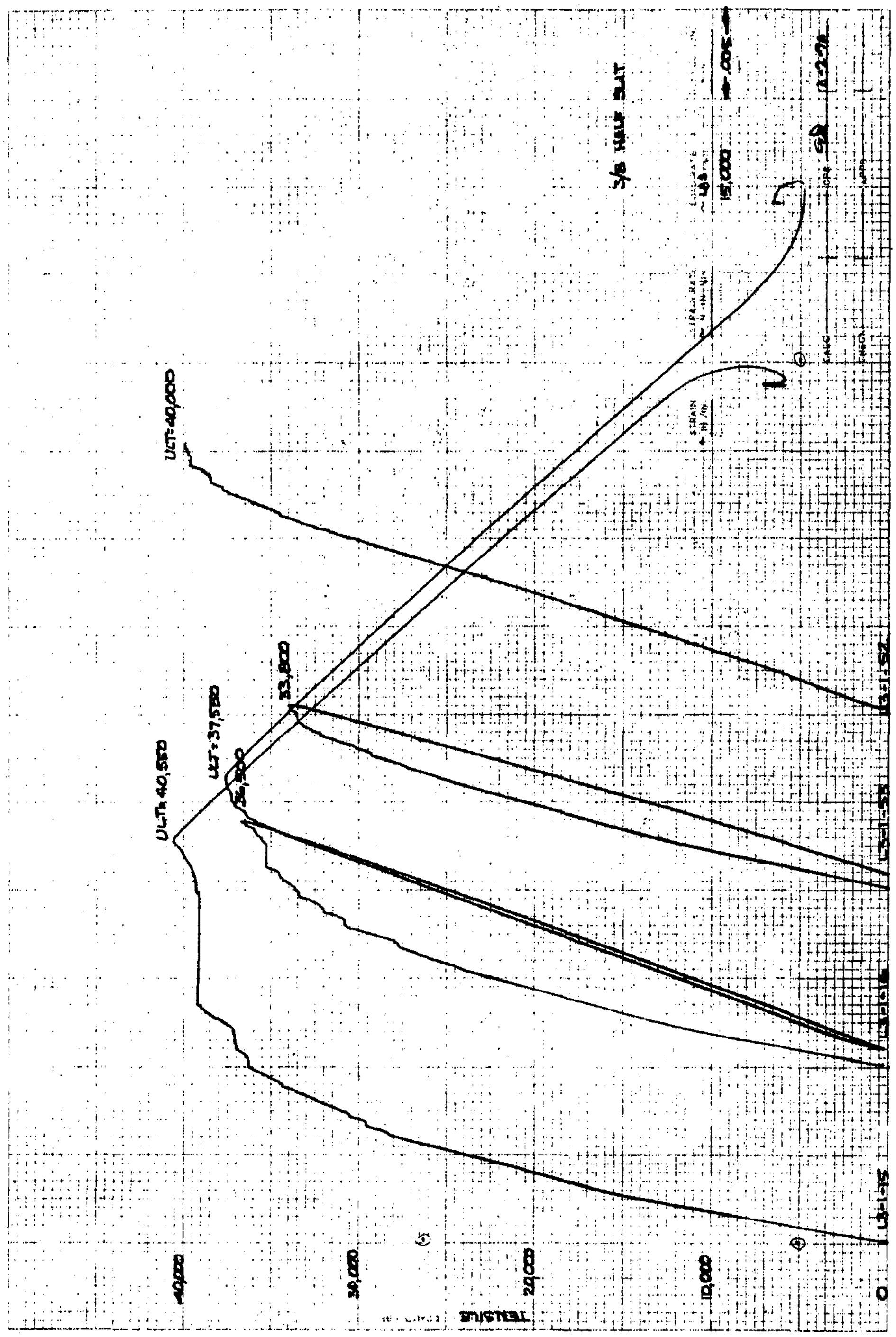
ULT=40,000
ULT=40,550
ULT=37,550
33,800
3/8 HALF SLIT
15,000
40,000
30,000
20,000
10,000
0
TENSILE

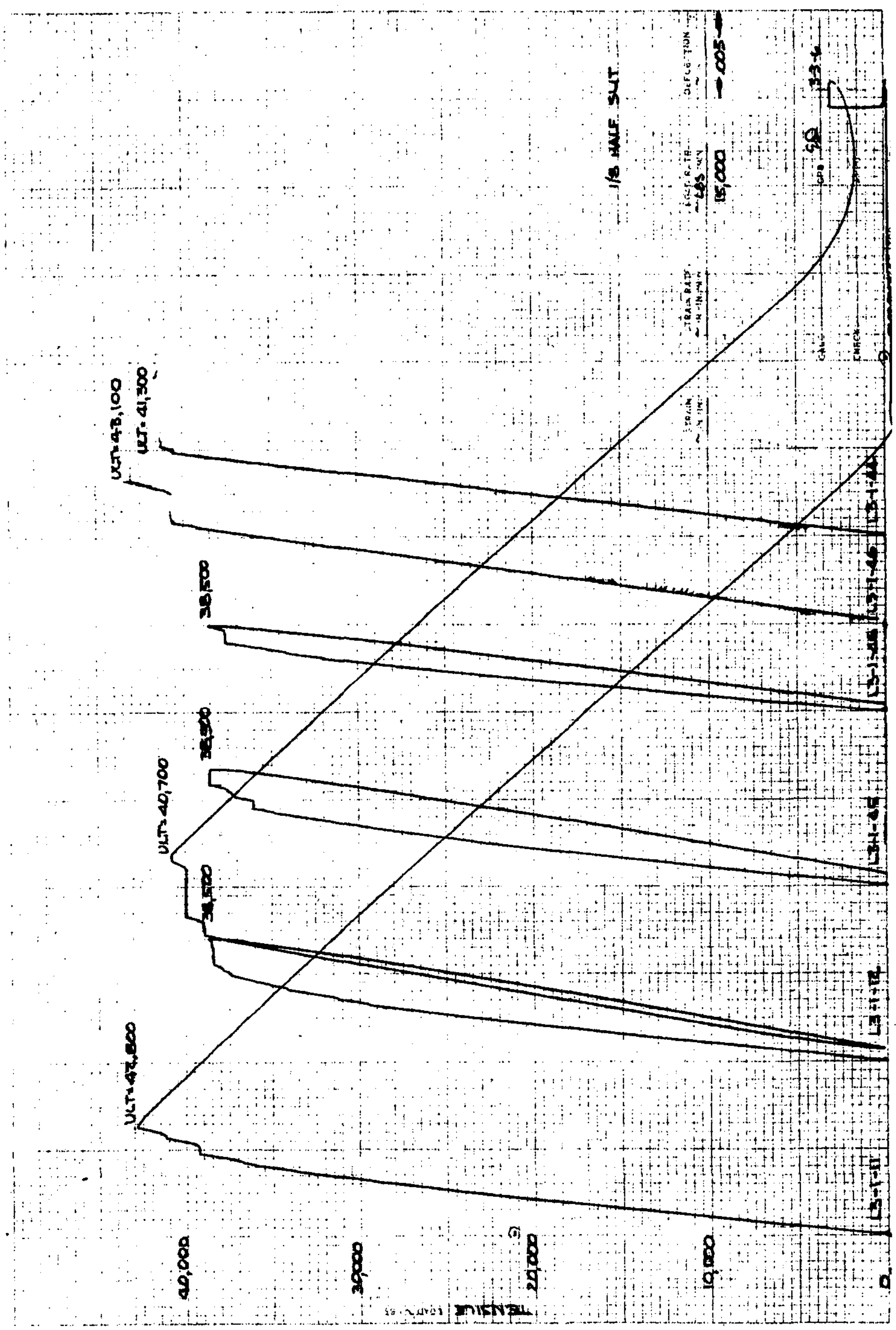

ULT=47,800
ULT=40,700
ULT=43,100
ULT=41,300
1/8 HALF SLIT
40,000
30,000
20,000
10,000
0
TENSILE

APPENDIX D

CYCLIC TEST CRACK OPENING DISPLACEMENT DATA

This appendix contains the results of crack opening displacement measurements made during cyclic loading. The total displacement measured during a cycle was divided by the stress excursion giving a "compliance" value. This data was recorded periodically during the cyclic test. All the results found for a particular defect type are given in each figure. Each figure is identified with the defect code and laminate type.

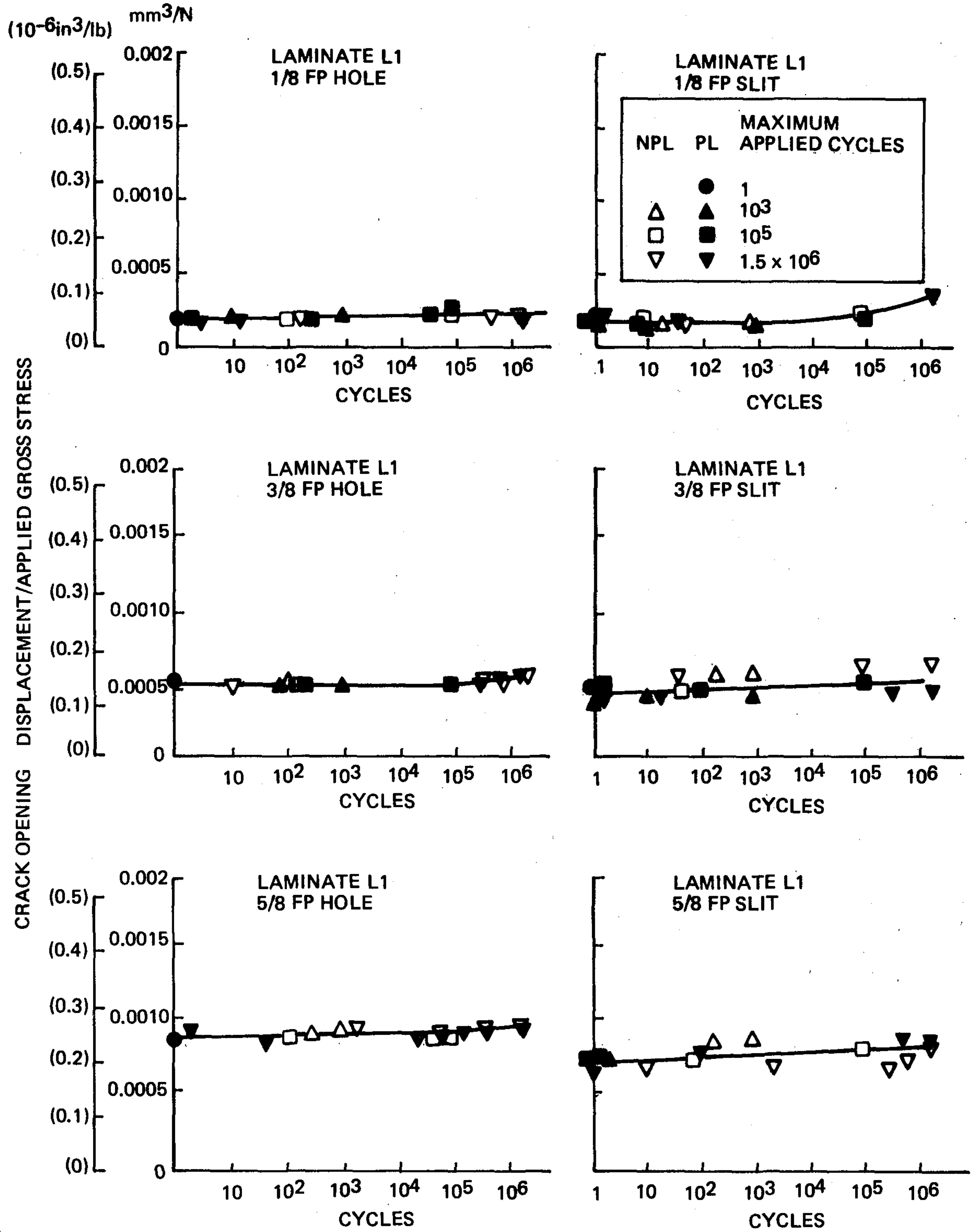

Figure D-1. Cyclic Load Crack Opening Displacement Result (Sheet 1 of 6)

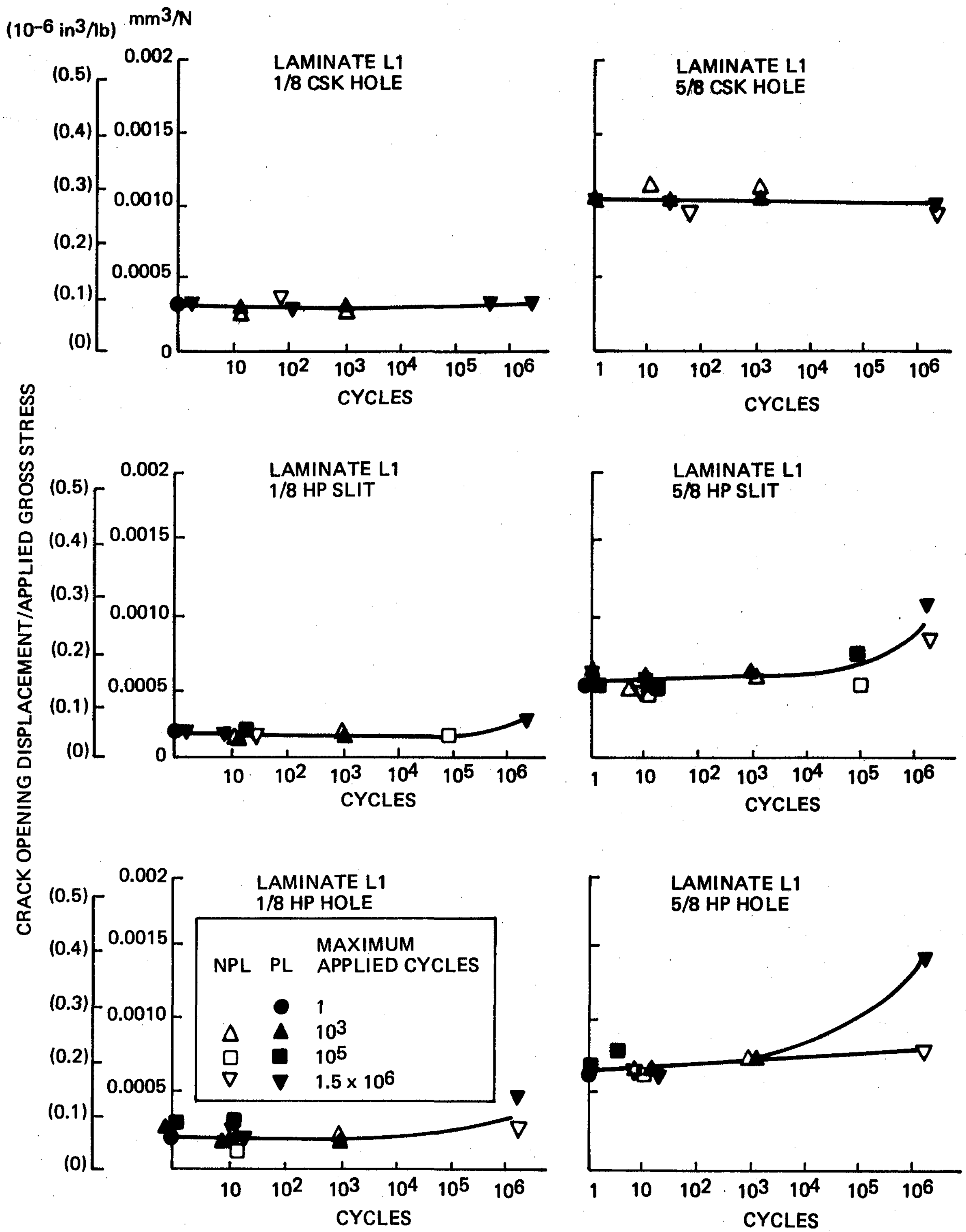

Figure D-1. Cyclic Load Crack Opening Displacement Result (Sheet 2 of 6)

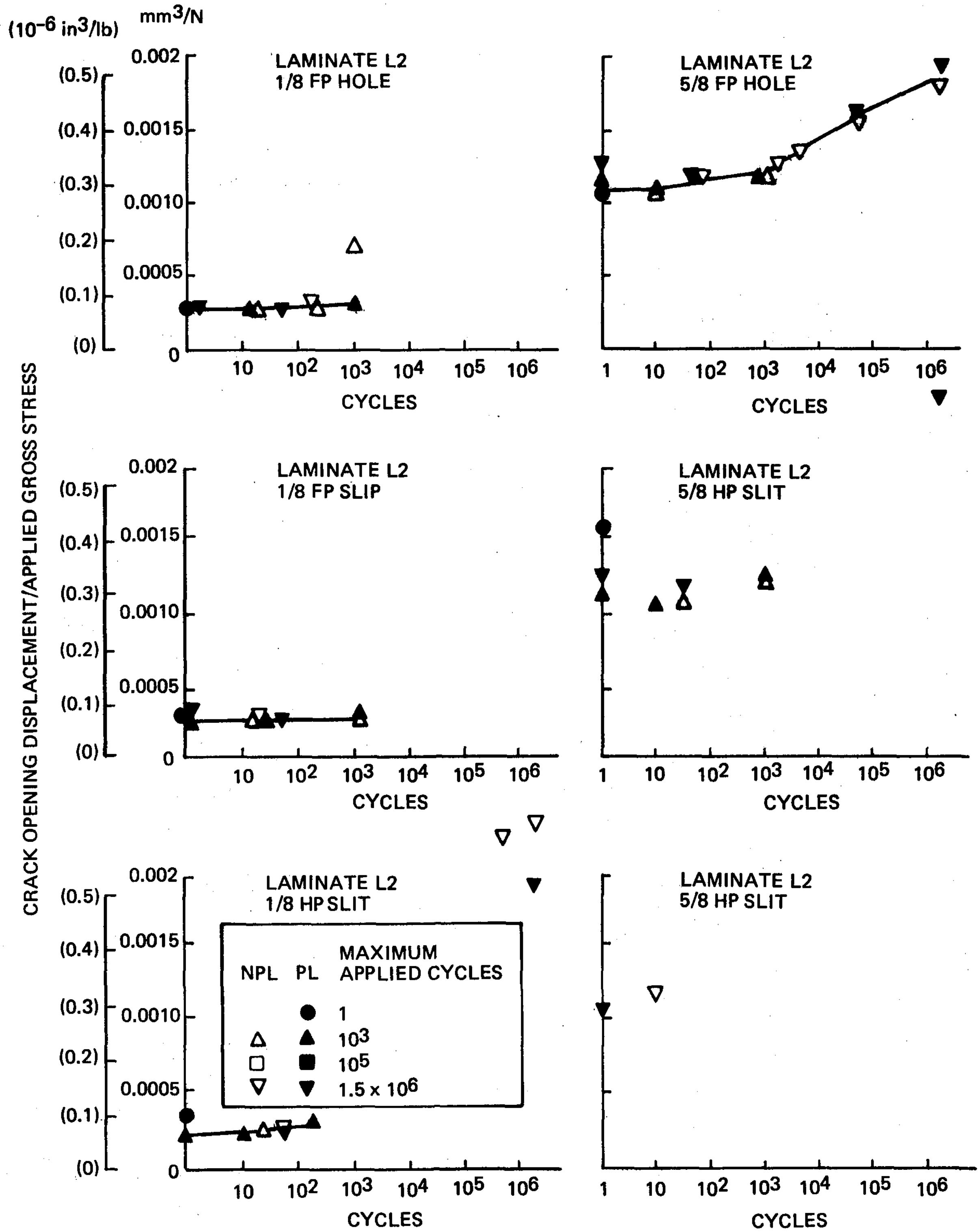

Figure D-1. Cyclic Load Crack Opening Displacement Result (Sheet 3 of 6)

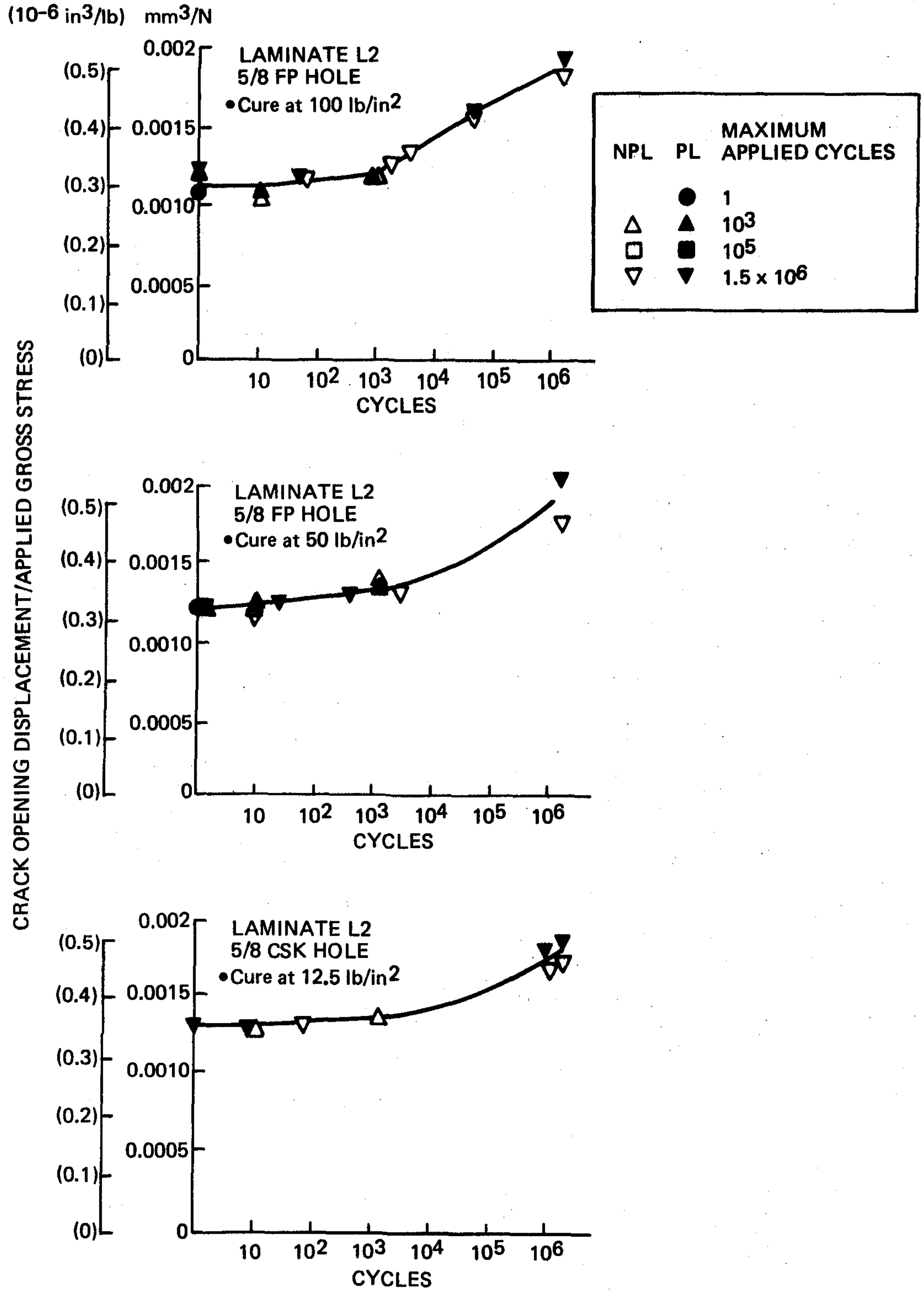

Figure D-1. Cyclic Load Crack Opening Displacement Result (Sheet 4 of 6)

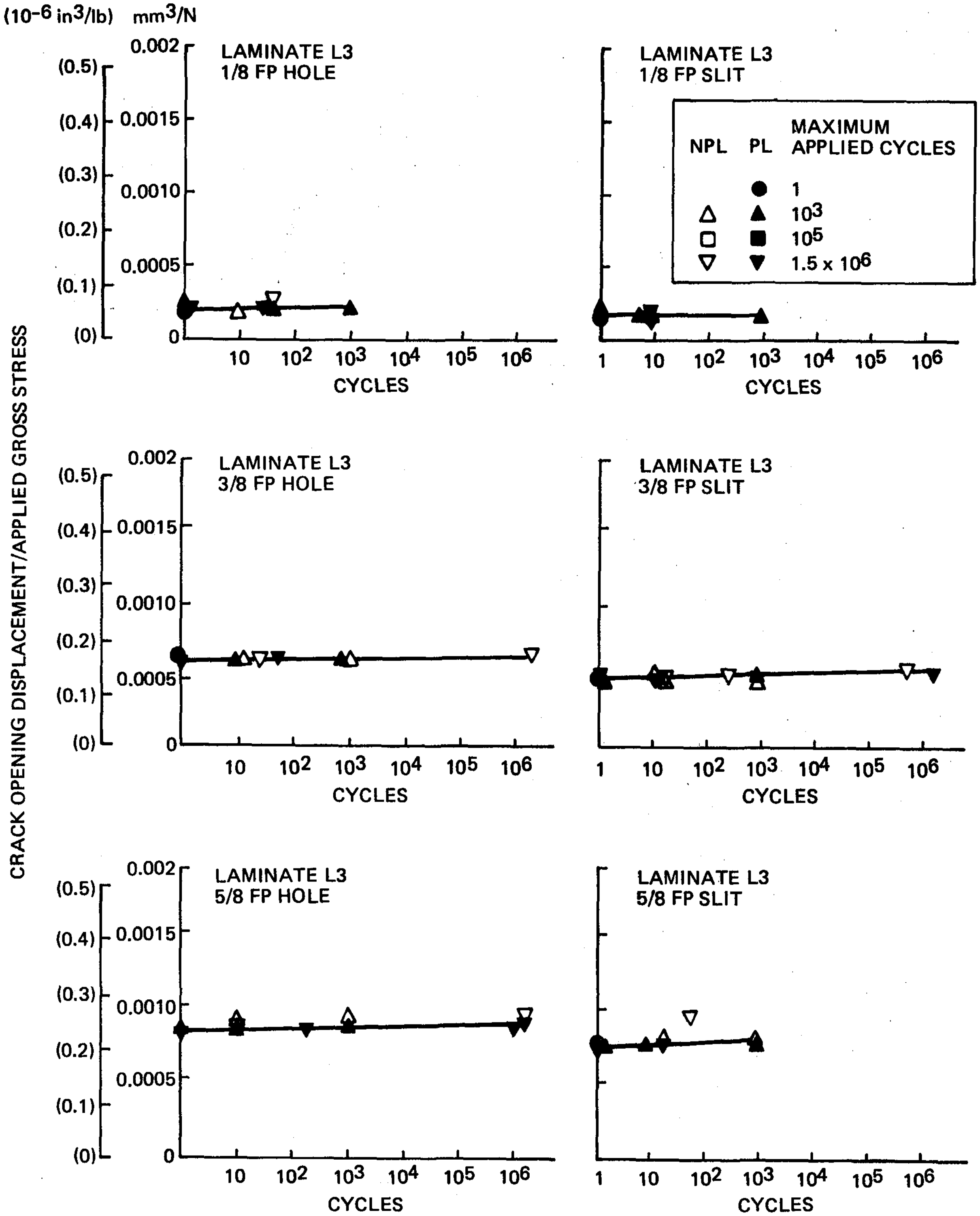

Figure D-1. Cyclic Load Crack Opening Displacement Result (Sheet 5 of 6)

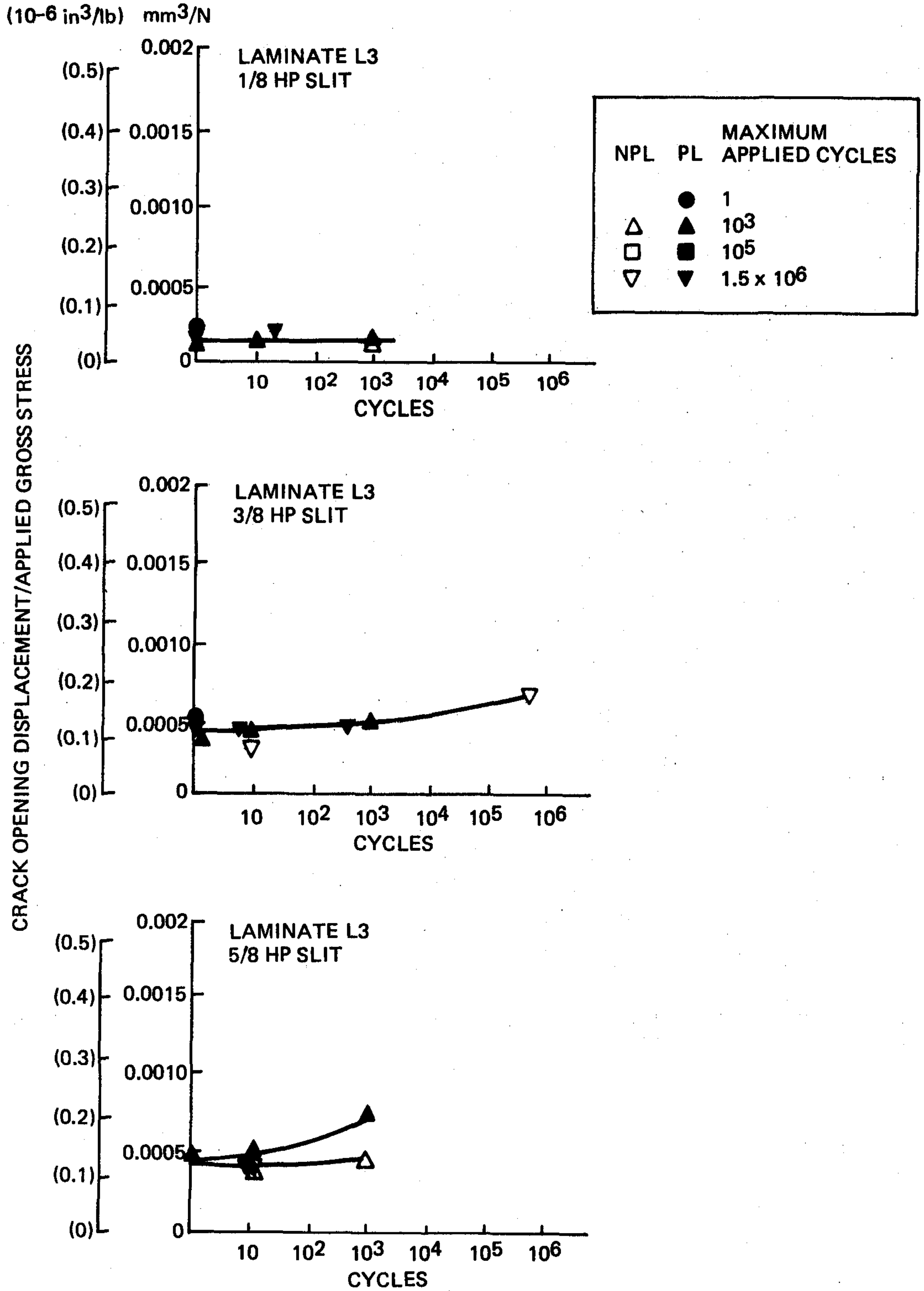

Figure D-1. Cyclic Load Crack Opening Displacement Result (Sheet 6 of 6)

Page intentionally left blank

APPENDIX E

PHOTOGRAPHS OF FAILED TEST SPECIMENS

This appendix contains photographs of typical test specimens after completion of the testing. One test specimen is included for each laminate configuration, defect type, and defect size. The specimens are identified by specimen number, defect code, and testing history.

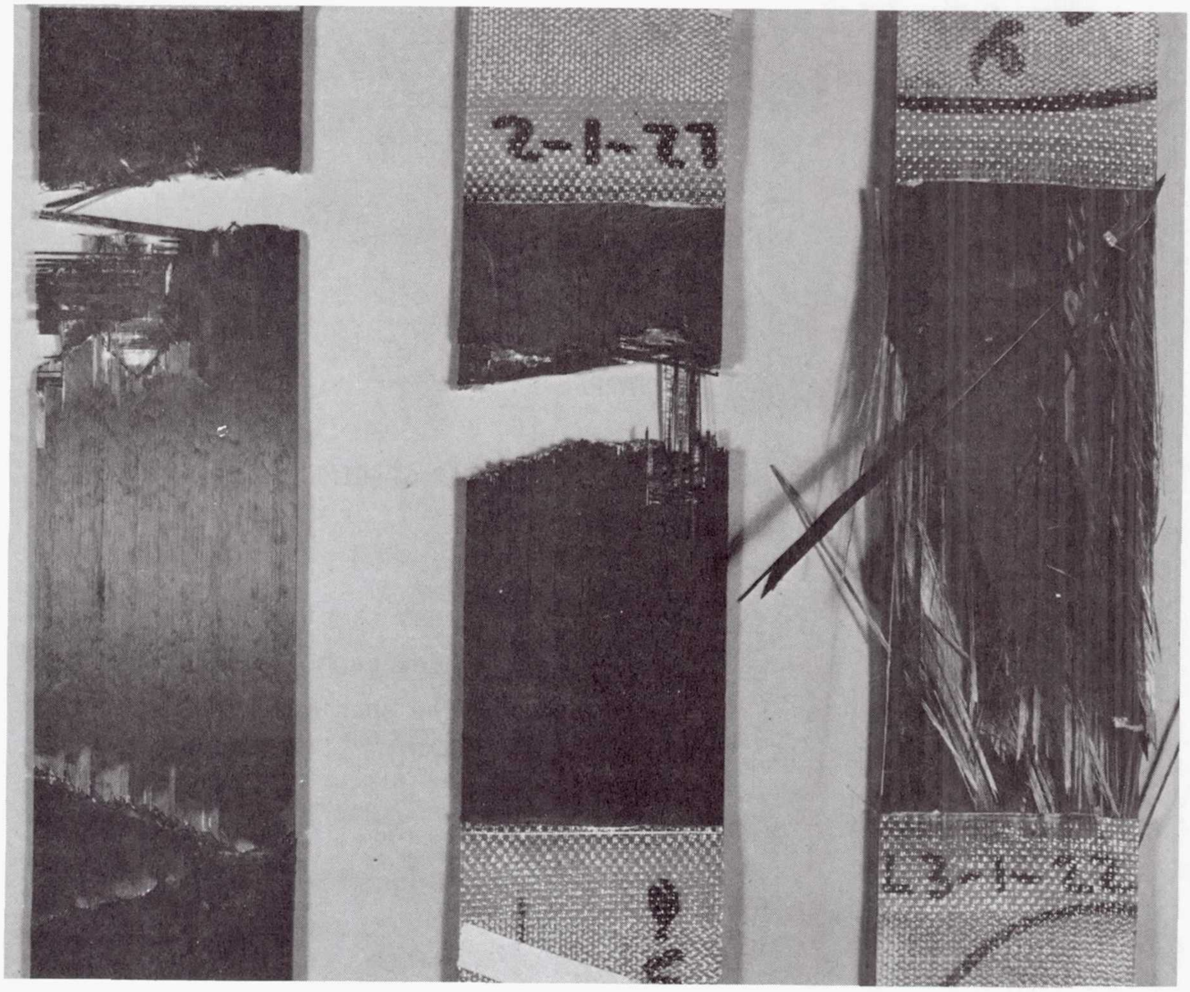

- Specimen L1-10-2
- Laminate L-1
- 10^3 cycles
- Residual static

- Specimen L2-1-2
- Laminate L2
- Preload
- Residual static

- Specimen L3-1-22
- Laminate L3
- 10^3 cycles
- Residual static

Figure E-1. Test Specimens With No Initial Defect

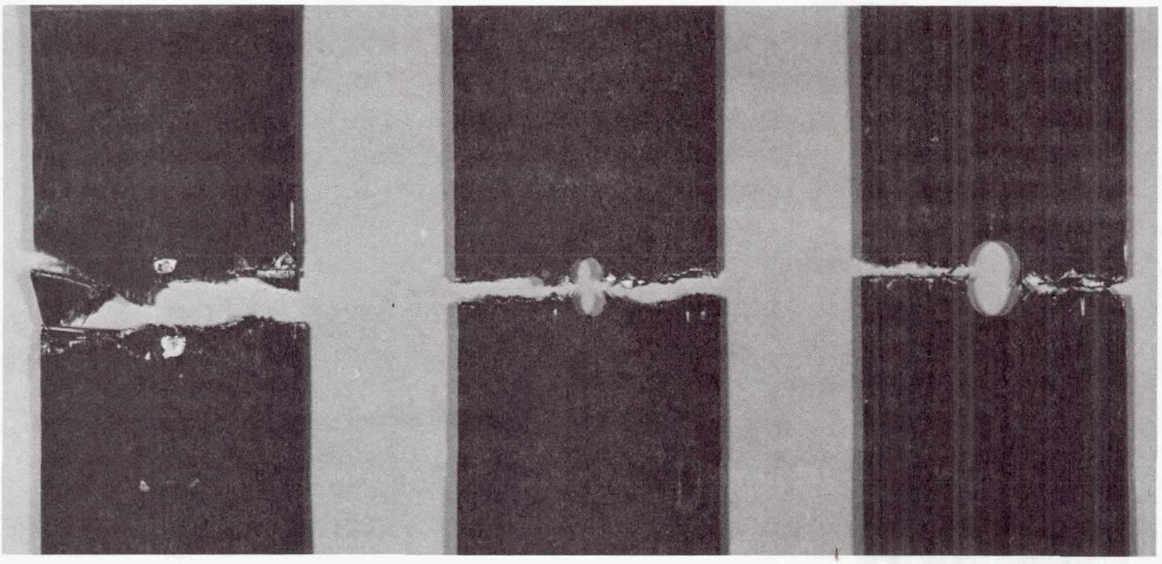

- Specimen L1-3-11
- 1/8 FP hole
- 1.5×10^6 cycles
- Residual static

- Specimen L1-1-7
- 3/8 FP hole
- Static

- Specimen L1-5-5
- 5/8 FP hole
- 10^5 cycles
- Residual static

Figure E-2. Laminate L1 Test Specimens Containing a Full-Penetration Hole

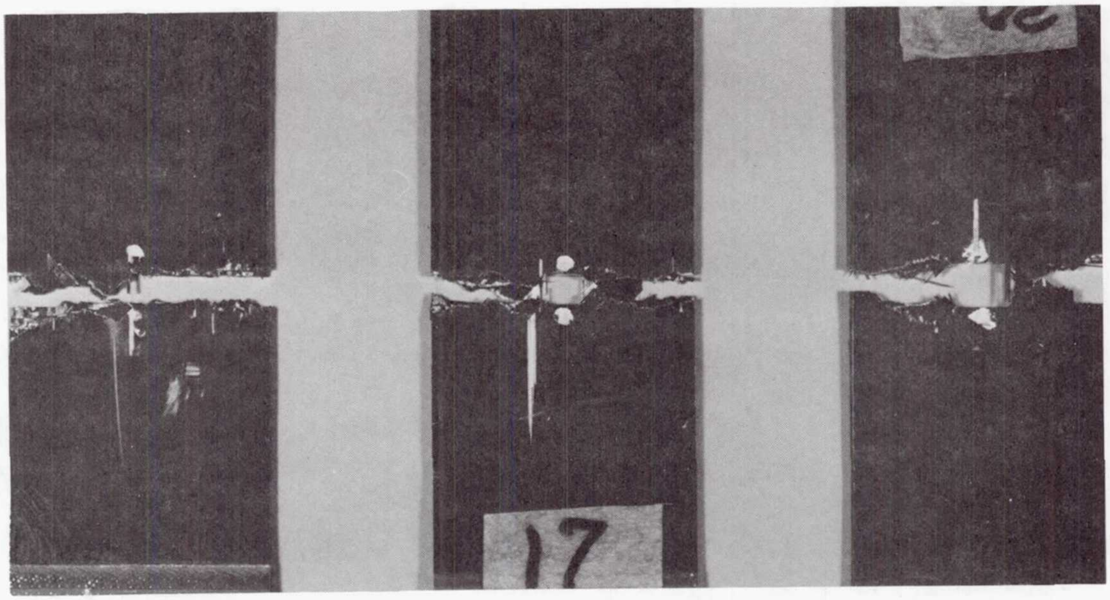

- Specimen L1-6-5
- 1/8 FP slit
- 10^5 cycles
- Residual static

- Specimen L1-2-6
- 3/8 FP slit
- Preload
- Residual static

- Specimen L1-7-14
- 5/8 FP slit
- 1.5 x 10^6 cycles
- Residual static

Figure E-3. Laminate L1 Test Specimens Containing a Full-Penetration Slit

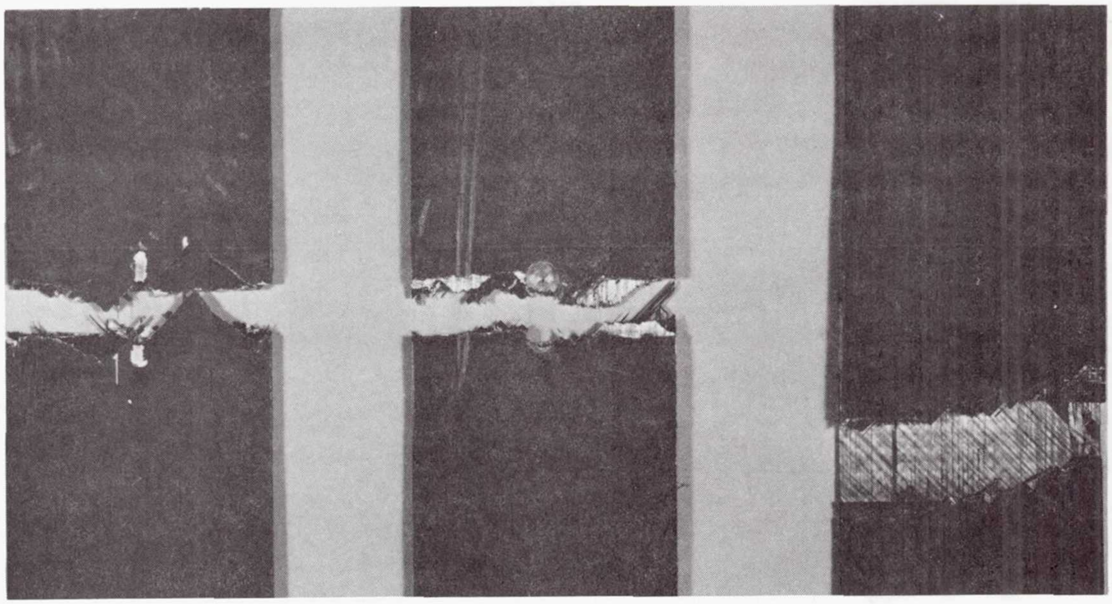

• Specimen L1-1-5	• Specimen L1-1-10	• Specimen L1-1-13
• 1/8 HP hole	• 3/8 HP hole	• 5/8 HP hole
	• Preload	
• Static	• Residual static	• Static

Figure E-4. Laminate L1 Test Specimens Containing a Half-Penetration Hole

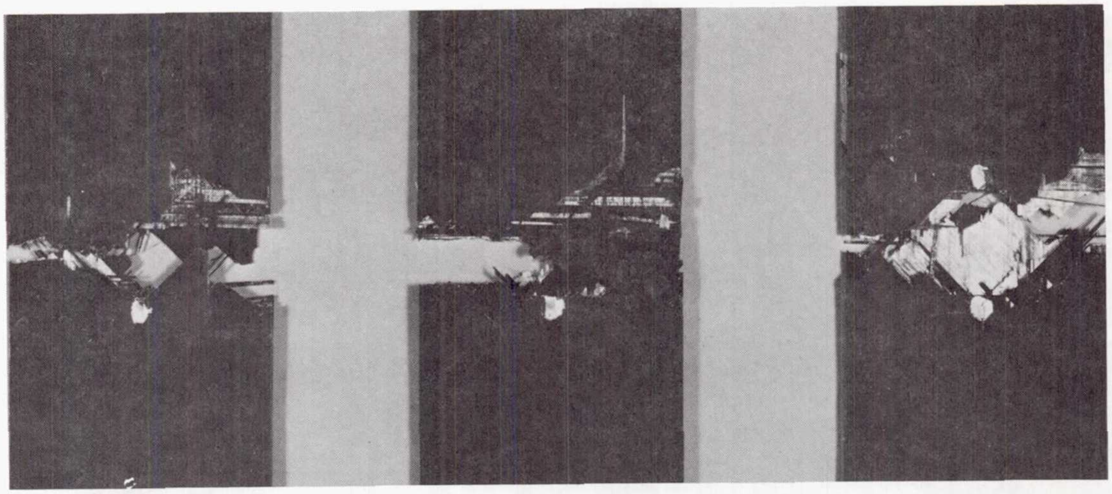

• Specimen L1-2-3	• Specimen L1-2-8	• Specimen L1-2-11
• 1/8 HP slit	• 3/8 HP slit	• 5/8 HP slit
	• Preload	
• Static	• Residual static	• Static

Figure E-5. Laminate L1 Test Specimens Containing a Half-Penetration Slit

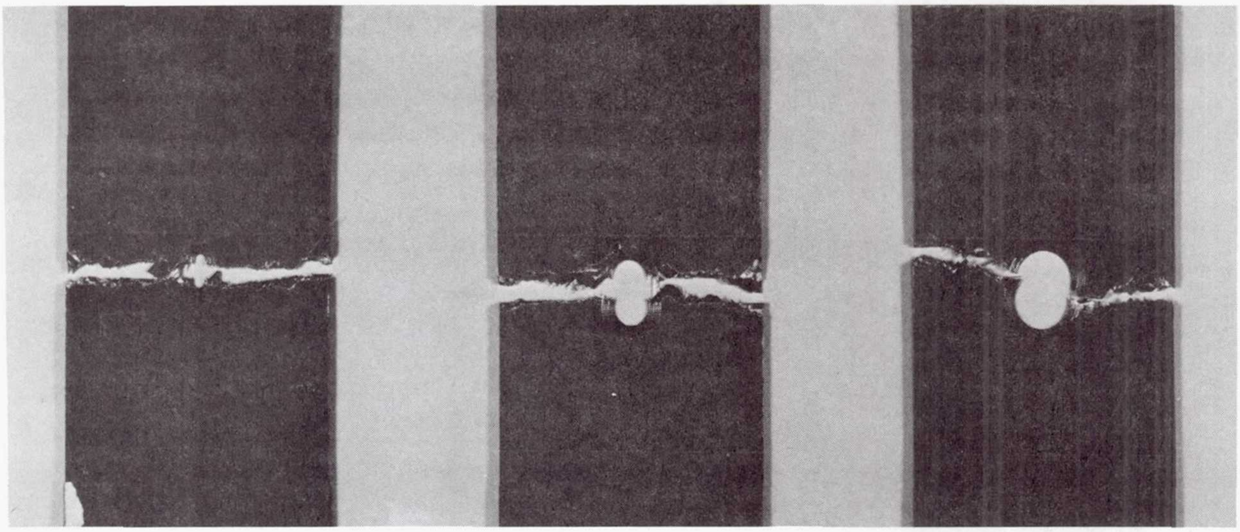

• Specimen L1-8-7	• Specimen L1-3-2	• Specimen L1-8-12
• 1/8 CSK hole	• 3/8 CSK hole	• 5/8 CSK hole
• 10^3 cycles	• Preload	• 1.5×10^6 cycles
• Residual static	• Residual static	• Residual static

Figure E-6. Laminate L1 Test Specimens Containing a Hole With a Full-Depth Countersink

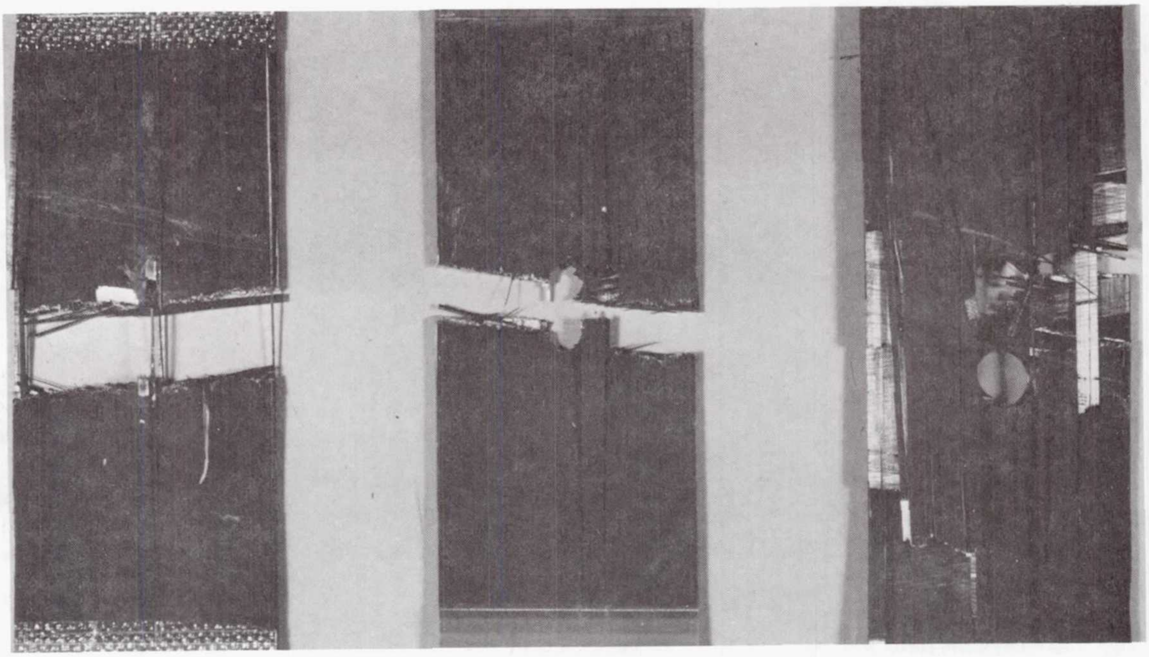

- Specimen L2-1-25
- 1/8 FP hole
- 1.5 x 10^6 cycles
- Residual static

- Specimen L2-1-6
- 3/8 FP hole
- Preload
- Residual static

- Specimen L2-1-29
- 5/8 FP hole
- 1.5 x 10^6 cycles
- Residual static

Figure E-7. Laminate L2 Test Specimens Containing a Full-Penetration Hole

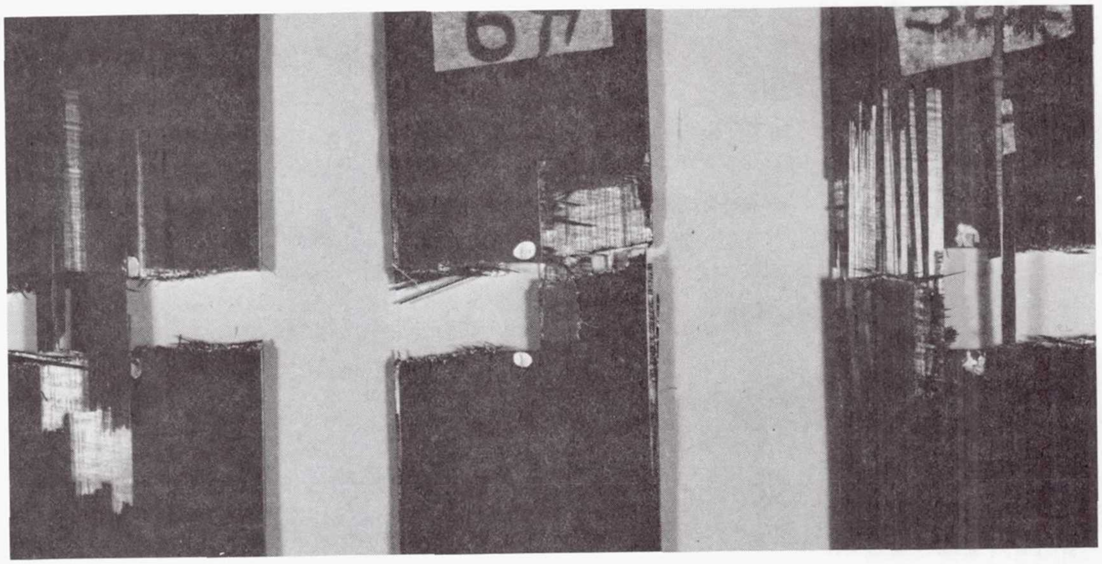

• Specimen L2-1-10	• Specimen L2-1-14	• Specimen L2-1-42
• 1/8 FP slit	• 3/8 FP slit	• 5/8 FP slit
• Preload	• Preload	• 10^3 cycles
• Residual static	• Residual static	• Residual static

Figure E-8. Laminate L2 Test Specimens Containing a Full-Penetration Slit

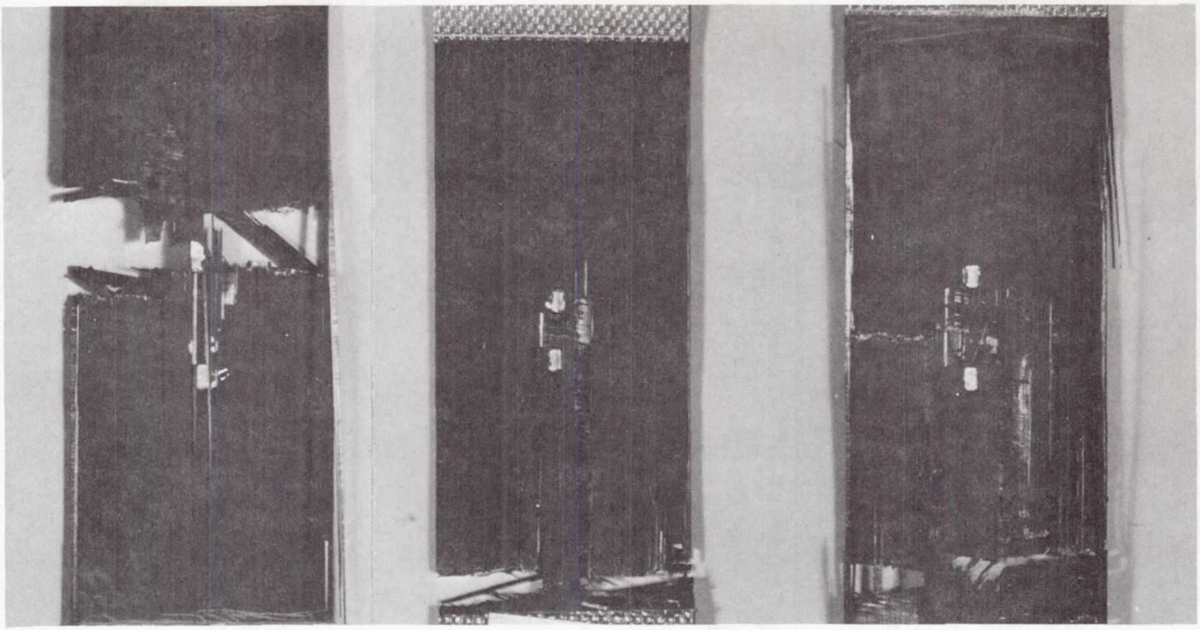

• Specimen L2-1-35	• Specimen L2-1-16	• Specimen L2-1-19
• 1/8 FP slit	• 3/8 HP slit	• 5/8 HP slit
• Preload		
• 1.5×10^6 cycles	• Preload	
• Residual static	• Residual static	• Static

Figure E-9. Laminate L2 Test Specimens Containing a Full- or Half-Penetration Slit

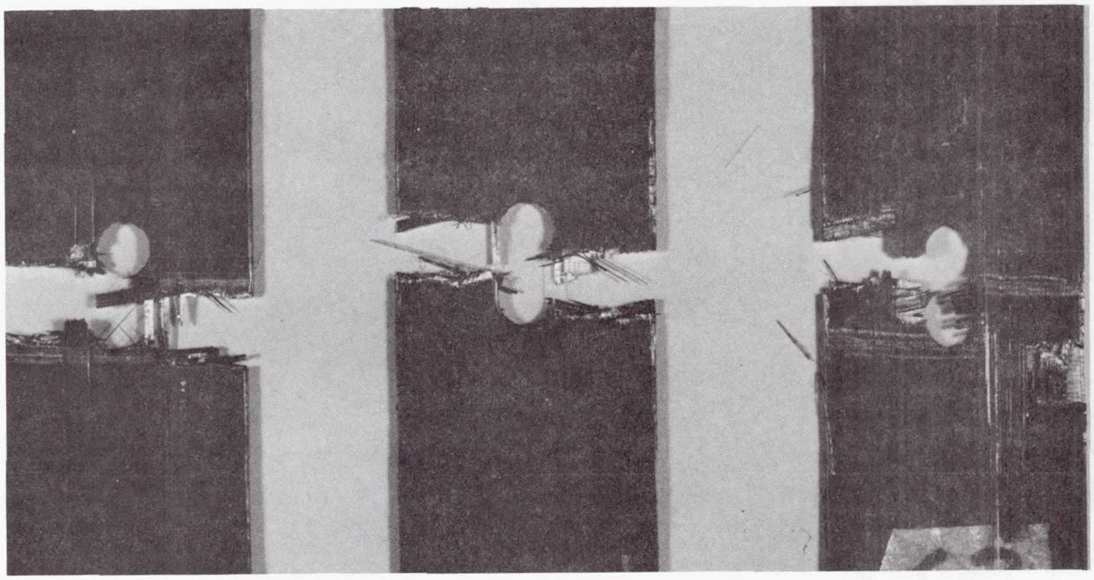

• Specimen L2-2-3	• Specimen L2-3-1	• Specimen L2-4-2
• 345 kPa/(50 lb/in^2) cure	• 172 kPa(25 lb/in^2 cure	• 86 kPa(12.5 lb/in^2) cure
• 1.5 x 10^6 cycles		
• Residual static	• Static	• Static

Figure E-10. Laminate L2 Test Specimens Cured With Low Autoclave Pressure

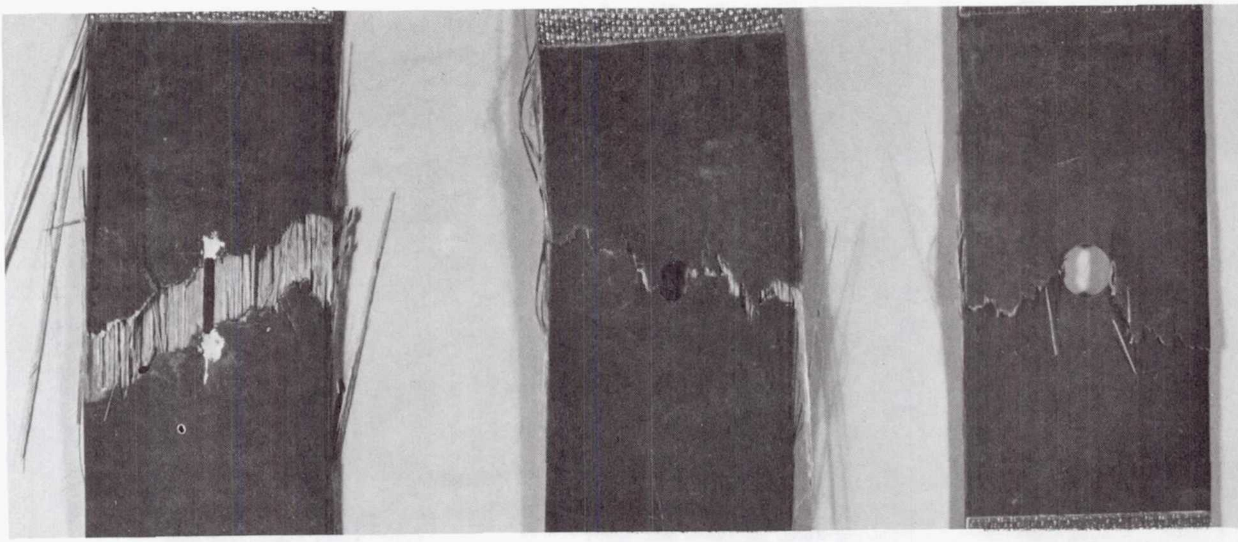

- Specimen L3-1-28
- 1/8 FP hole
- Preload
- 10^3 cycles
- Residual static

- Specimen L3-1-29
- 3/8 FP hole
- 1.5×10^6 cycles
- Residual static

- Specimen L3-1-7
- 5/8 FP hole
- Static

Figure E-11. Laminate L3 Test Specimens Containing a Full-Penetration Hole

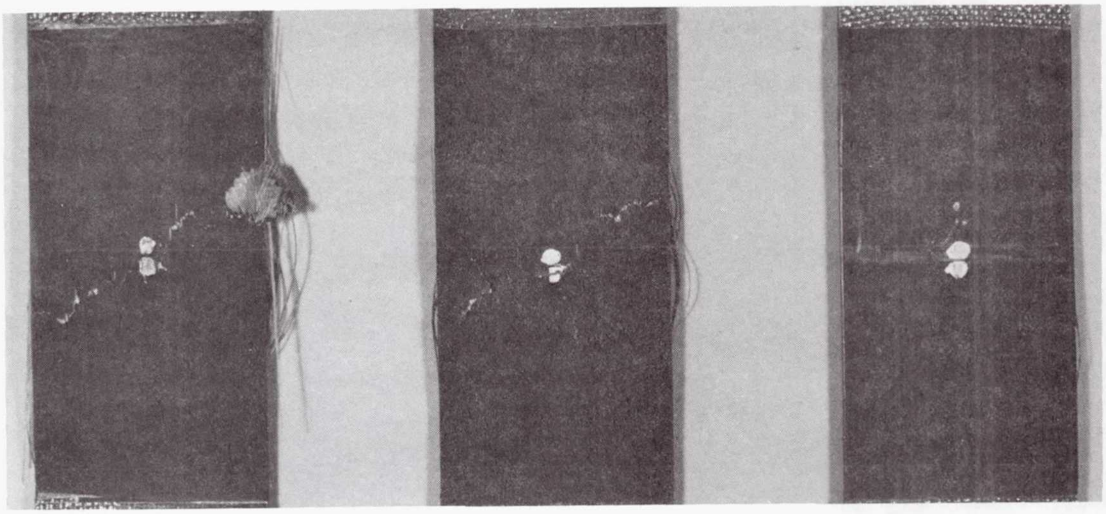

- Specimen L3-1-40
- 1/8 FP slit
- 10^3 cycles
- Residual static

- Specimen L3-1-14
- 3/8 FP slit
- Preload
- Residual static

- Specimen L3-1-17
- 5/8 FP slit
- Static

Figure E-12. Laminate L3 Test Specimens Containing a Full-Penetration Slit

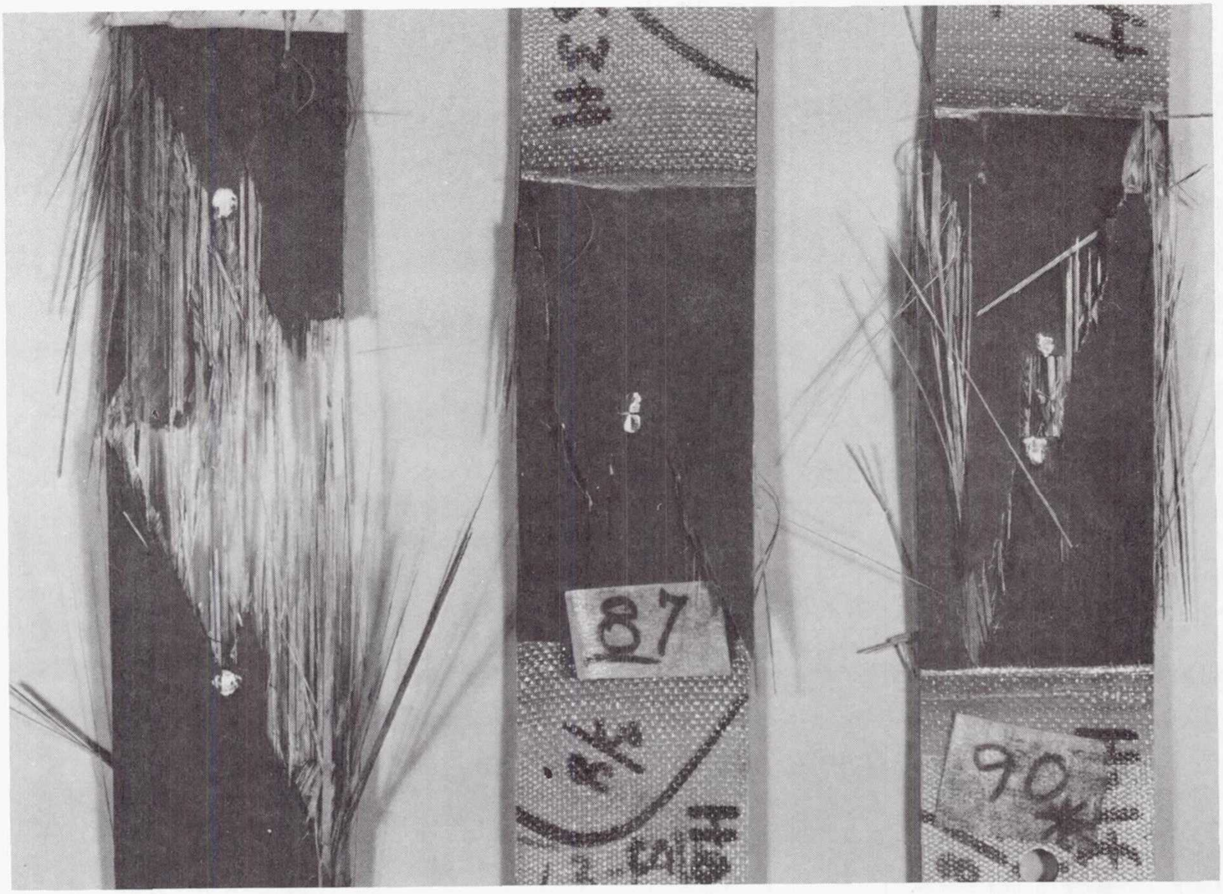

• Specimen L3-1-44	• Specimen L3-1-15	• Specimen L3-1-60
• 1/8 HP slit	• 3/8 HP slit	• 5/8 HP slit
• 10^3 cycles		• 10^3 cycles
• Residual static	• Static	• Residual static

Figure E-13. Laminate L3 Test Specimens Containing a Half-Penetration Slit

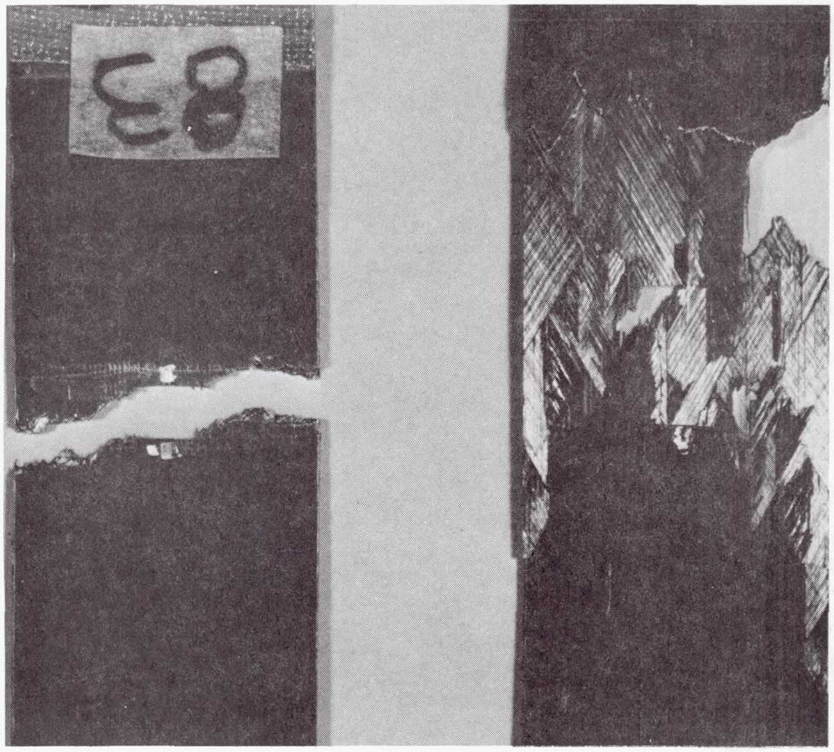

- Specimen L3-2-5
- 5/8 FP slit
- Preload
- Residual static

- Specimen L3-2-6
- 5/8 HP slit
- Static

Figure E-14. All-Graphite Laminate L3 Test Specimens Containing a Full- and a Half-Penetration Slit

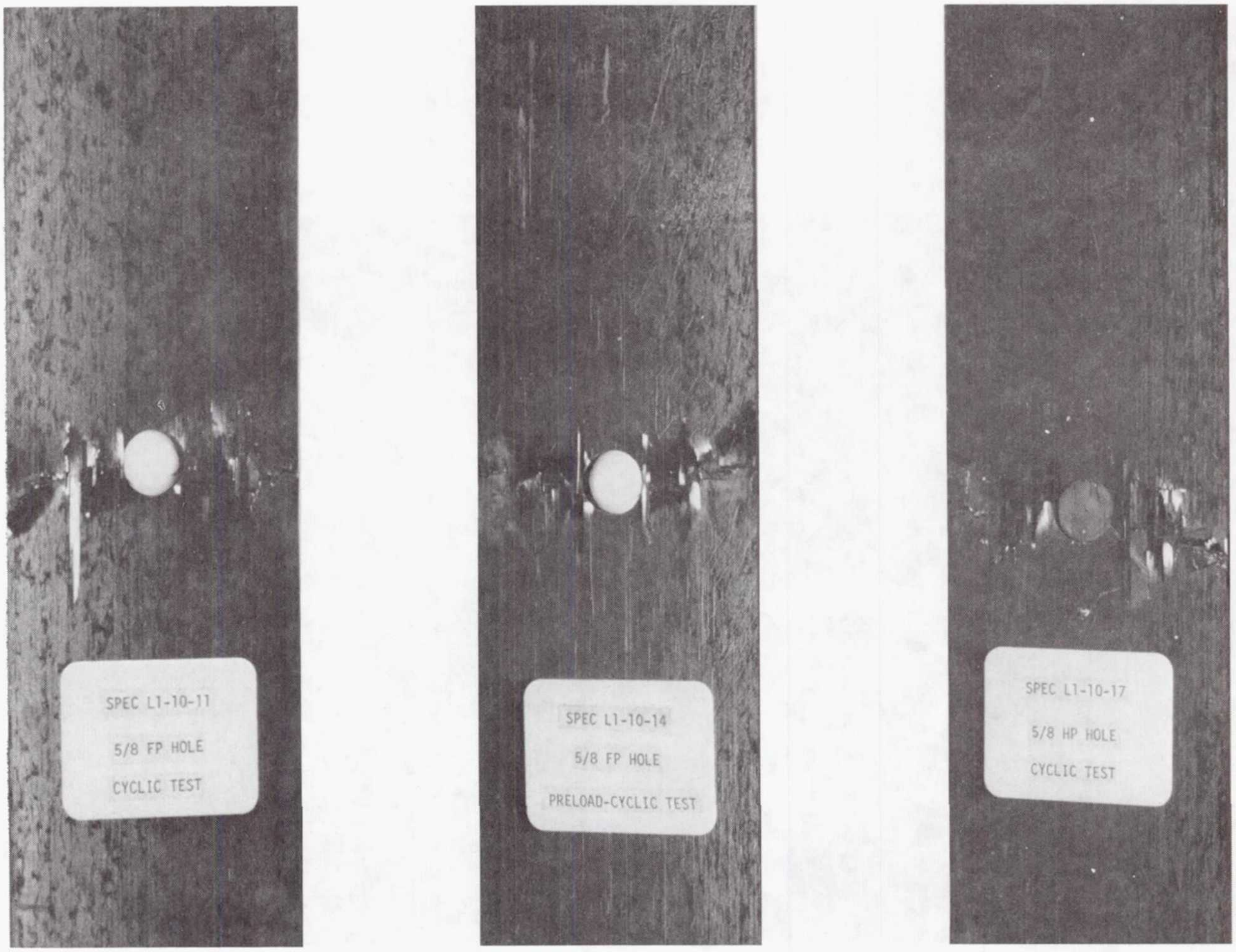

- 7,300 cycles
- Fatigue Failure

- 22,800 cycles
- Fatigue failure

- 3,100 cycles
- Fatigue failure

Figure E-15. Tension-Compression Fatigue (R = –1.0) Laminate L1 Test Specimens Containing a Full- and a Half-Penetration Hole

FINAL REPORT DISTRIBUTION LIST, CR-135403

NAS3-19709

"EVALUATION OF FLAWED COMPOSITE STRUCTURE
UNDER STATIC AND CYCLIC LOADING"

Advanced Research Projects Agency
Washington, D.C. 20525

Attn: Library

Advanced Technology Center, Inc.
LTV Aerospace Corporation
P.O. Box 6144
Dallas, TX 75222

Attn: D. H. Petersen
W. J. Renton

Air Force Flight Dynamics Laboratory
Wright-Patterson Air Force Base, OH 45433

Attn: G. P. Sendeckyj (FBC)
R. S. Sandhu

Air Force Materials Laboratory
Wright-Patterson Air Force Base, OH 45433

Attn: H. S. Schwartz (LN)
T. J. Reinhart (MBC)
G. P. Peterson (LC)
E. J. Morrisey (LAE)
S. W. Tsai (MBM)
N. J. Pagano
J. M. Whitney (MBM)

Air Force Office of Scientific Research
Washington, D.C. 20333

Attn: J. F. Masi (SREP)

Air Force Office of Scientific Research
1400 Wilson Boulevard
Arlington, VA 22209

Air Force Advanced Systems Division
Wright-Patterson Air Force Base, OH 45433

Attn: C. F. Tiffany

AFOSR/NA
Bolling Air Force Base, D.C. 20332

Attn: W. J. Walker

Babcock & Wilcox Company
Advanced Composites Department
P.O. Box 419
Alliance, OH 44601

Attn: P. M. Leopold

Bell Helicopter Company
P.O. Box 482
Ft. Worth, TX 76101

Attn: H. Zinberg

The Boeing Company
Vertol Division
Morton, PA 19070

Attn: R. A. Pinckney
E. C. Durchlaub

Battelle Memorial Institute
Columbus Laboratories
505 King Avenue
Columbus, OH 43201

Attn: E. F. Rybicki
L. E. Hulbert

Brunswick Corporation
Defense Products Division
P.O. Box 4594
43000 Industrial Avenue
Lincoln, NE 68504

Attn: R. Morse

Commander
Naval Air Systems Command
U.S. Navy Department
Washington, D.C. 20360

Attn: M. Stander, AIR-43032D

Commander
Naval Ordnance Systems Command
U.S. Navy Department
Washington, D.C. 20360

Attn: B. Drimmer, ORD-033
M. Kinna, ORD-033A

Cornell University
Department Theoretical & Applied Mechanics
Thurston Hall
Ithaca, NY 14853

Attn: S. L. Phoenix

Defense Metals Information Center
Battelle Memorial Institute
Columbus Laboratories
505 King Avenue
Columbus, OH 43201

Department of the Army
U.S. Army Aviation Materials Laboratory
Ft. Eustis, VA 23604

Attn: I. E. Figge, Sr.
Library

Department of the Army
U.S. Army Aviation Systems Command
P.O. Box 209
St. Louis, MO 63166

Attn: R. Vollmer, AMSAV-A-UE

Department of the Army
Plastics Technical Evaluation Center
Picatinny Arsenal
Dover, NJ 07801

Attn: H. E. Pebly, Jr.

Department of the Army
Watervliet Arsenal
Watervliet, NY 12189

Attn: G. D'Andrea

Department of the Army
Watertown Arsenal
Watertown, MA 02172

Attn: A. Thomas

Department of the Army
Redstone Arsenal
Huntsville, AL 35809

Attn: R. J. Thompson, AMSMI-RSS

Department of the Navy
Naval Ordnance Laboratory
White Oak
Silver Springs, MD 20910

Attn: R. Simon

Department of the Navy
U.S. Naval Ship R&D Laboratory
Annapolis, MD 21402

Attn: C. Hersner, Code 2724

Director
Deep Submergence Systems Project
6900 Wisconsin Avenue
Washington, D.C. 20015

Attn: H. Bernstein, DSSP-221

Director
Naval Research Laboratory
Washington, D.C. 20390

Attn: Code 8430
I. Wolock, Code 8433

Drexel University
32nd and Chestnut Streets
Philadelphia, PA 19104

Attn: P. C. Chou

E. I. duPont DeNemours & Company
duPont Experimental Station
Wilmington, DE 19898

Attn: C. H. Zweben

Fiber Science, Inc.
245 East 157th Street
Gardena, CA 90248

Attn: E. Dunahoo

General Dynamics
P.O. Box 748
Ft. Worth, TX 76100

Attn: M. E. Waddoups
Library

General Dynamics/Convair
P.O. Box 1128
San Diego, CA 92112

Attn: J. L. Christian

General Electric Company
Evendale, OH 45215

Attn: C. Stotler
R. Ravenhall
R. Stabrylla

General Motors Corporation
Detroit Diesel-Allison Division
Indianapolis, IN 46244

Attn: M. Herman

Georgia Institute of Technology
School of Aerospace Engineering
Atlanta, GA 30332

Attn: L. W. Rehfield

Grumman Aerospace Corporation
Bethpage, Long Island, NY 11714

Attn: S. Dastin
J. B. Whiteside

Hamilton Standard Division
United Aircraft Corporation
Windsor Locks, CT 06096

Attn: W. A. Percival

Hercules, Inc.
Allegheny Ballistics Laboratory
P.O. Box 210
Cumberland, MD 21053

Attn: A. A. Vicario

Hughes Aircraft Company
Culver City, CA 90230

Attn: A. Knoell

Illinois Institute of Technology
10 West 32nd Street
Chicago, IL 60616

Attn: L. J. Broutman

IIT Research Institute
10 West 35th Street
Chicago, IL 60616

Attn: I. M. Daniel

Jet Propulsion Laboratory
4800 Oak Grove Drive
Pasadena, CA 91103

Attn: Library

Lawrence Livermore Laboratory
P.O. Box 808, L-421
Livermore, CA 94550

Attn: T. T. Chiao
E. M. Wu

Lehigh University
Institute of Fracture & Solid Mechanics
Bethlehem, PA 18015

Attn: G. C. Sih

Lockheed-Georgia Company
Advanced Composites Information Center
Department 72-14, Zone 402
Marietta, GA 30060

Attn: T. M. Hsu

Lockheed Missiles and Space Company
P.O. Box 504
Sunnyvale, CA 94087

Attn: R. W. Fenn

Lockheed-California
Burbank, CA 91503

Attn: J. T. Ryder
K. N. Lauraitis
J. C. Ekvall

McDonnell Douglas Aircraft Corporation
P.O. Box 516
Lambert Field, MS 63166

Attn: J. C. Watson

McDonnell Douglas Aircraft Corporation
3855 Lakewood Boulevard
Long Beach, CA 90810

Attn: L. B. Greszczuk

Material Sciences Corporation
1777 Walton Road
Blue Bell, PA 19422

Attn: B. W. Rosen

Massachusetts Institute of Technology
Cambridge, MA 02139

Attn: F. J. McGarry
J. F. Mandell
J. W. Mar

NASA-Hugh L. Dryden Flight Research Center
P.O. Box 273
Edwards, CA 93523

Attn: Library

NASA-George C. Marshall Space Flight Center
Huntsville, AL 35812

Attn: C. E. Cataldo, EH01
Library
C. E. Lifer, EP41

NASA-Goddard Space Flight Center
Greenbelt, MD 20771

Attn: Library

NASA-Langley Research Center
Hampton, VA 23665

Attn: E. E. Mathauser, MC 188a
R. A. Pride, MC 188a
M. C. Card, MC 230
J. R. Davidson, MC 188E

NASA-Lewis Research Center
21000 Brookpark Road
Cleveland, OH 44135

Attn: Contracting Officer, MS 500-312
Tech. Report Control, MS 5-5
Tech. Utilization, MS 3-19
AFSC Liaison, MS 501-3
Rel. and Quality Assur., MS 500-211
T. W. Orange, MS 49-3
R. F. Lark, MS 49-3
J. C. Freche, MS 49-1
R. H. Johns, MS 49-3
C. C. Chamis, MS 49-3
Library, MS 60-3
G. T. Smith, MS 49-3 (20 copies)

NASA-Lyndon B. Johnson Space Center
Houston, TX 77001

Attn: S. Glorioso, ES5
Library
R. G. Forman, ES5

NASA Scientific and Technical Information Facility
P.O. Box 33
College Park, MD 20740

Attn: Acquisitions Branch (10 copies)

National Aeronautics and Space Administration
Office of Advanced Research & Technology
Washington, D.C. 20546

Attn: M. J. Salkind, Code RWS-3
D. P. Williams, Code RW-3

National Aeronautics and Space Administration
Office of Technology Utilization
Washington, D.C. 20546

National Science Foundation
Engineering Division
1800 G. Street, NW
Washington, D.C. 20540

Attn: Library

Northrop Space Laboratories
3401 West Broadway
Hawthorne, CA 90250

Attn: R. M. Verette
G. C. Grimes

Pratt & Whitney Aircraft
East Hartford, CT 06108

Attn: A. J. Dennis
T. Zupnik

Rockwell International
Los Angeles Division
International Airport
Los Angeles, CA 90009

Attn: L. M. Lackman
D. Y. Konishi

Sikorsky Aircraft Division
United Aircraft Corporation
Stratford, CT 06602

Attn: Library

Southern Methodist University
Dallas, TX 75275

Attn: R. M. Jones

Southwest Research Institute
8500 Culebra Road
San Antonio, TX 78284

Attn: P. H. Francis

Space & Missile Systems Organization
Air Force Unit Post Office
Los Angeles, CA 90045

Attn: Technical Data Center

Structural Composites Industries, Inc.
6344 N. Irwindale Avenue
Azusa, CA 91702

Attn: R. Gordon

Texas A&M
Mechanics & Materials Research Center
College Station, TX 77843

Attn: R. A. Schapery

TRW, Inc.
23555 Euclid Avenue
Cleveland, OH 44117

Attn: W. E. Winters

Union Carbide Corporation
P.O. Box 6116
Cleveland, OH 44101

Attn: J. C. Bowman

United Technologies Research Center
East Hartford, CT 06108

Attn: R. C. Novak

University of Dayton Research Institute
Dayton, OH 45409

Attn: R. W. Kim

University of Delaware
Mechanical & Aerospace Engineering
Newark, DE 19711

Attn: B. R. Pipes

University of Illinois
Department of Theoretical & Applied Mechanics
Urbana, IL 61801

Attn: S. S. Wang

University of Oklahoma
School of Aerospace Mechanical & Nuclear Engineering
Norman, OK 73069

Attn: C. W. Bert

University of Wyoming
College of Engineering
University Station Box 3295
Laramie, WY 82071

Attn: D. F. Adams

U.S. Army Materials & Mechanics Research Center
Watertown Arsenal
Watertown, MA 02172

Attn: E. M. Lenoe
D. W. Oplinger

V.P.I. and S.U.
Department of Engineering Mechanics
Blacksburg, VA 24061

Attn: R. H. Heller
H. J. Brinson
C. T. Herakovich